

# **Improving Sensitivity, Robustness, and Stability of Beer Flavor Analysis by Novel GC-MS/MS Assays**

vorgelegt von

**M. Sc.**

**Johanna Dennenlöhr**

an der Fakultät III – Prozesswissenschaften  
der Technischen Universität Berlin  
zur Erlangung des akademischen Grades

Doktor der Ingenieurwissenschaften

- Dr.-Ing. -

genehmigte Dissertation

Promotionsausschuss:

Vorsitzender: Prof. Dr. Peter Neubauer

Gutachter: Prof. Dr. Juri Rappsilber

Gutachter: Dr.-Ing. Nils Rettberg

Tag der wissenschaftlichen Aussprache: 06. September 2021

Berlin 2021

# Acknowledgements

This thesis has been made possible by the support, mentoring, and friendship of several people to whom I would like to express my gratitude.

First of all, I would like to thank my supervisor Dr.-Ing. Nils Rettberg, for your valuable suggestions and support anytime I needed it. I learned a lot during our collaboration and I highly appreciate your great contribution to improve the quality of our papers.

Special thanks go to Prof. Dr. Juri Rappsilber for examining my thesis as well as Prof. Dr. Peter Neubauer for his willingness to chair the dissertation committee.

A significant part of the success of this work is due to Dr. Sarah Thörner. You introduced me to the fundamentals of method development and the scientific exchange with you deepened my interest.

I would also like to thank my other colleagues from the Special Analyses Department for the great working atmosphere and the many entertaining conversations over lunch. Especially I am grateful to Christian Schubert for your help with the maintenance of the GC-MS/MS and your open ear for all my questions around beer, Laura Knoke for sharing ideas, and Dr. Aneta Manowski for your helpful support in chemical issues.

Finally, I want to thank my husband Marco, for your love and your tireless support during my journey to the PhD.

## Abstract

In bioanalytics, the aim is to monitor or identify biological processes. The analytical tools employed depend on nature and concentration of the respective target analytes, as well as the matrix and system under investigation. In beer production, sometimes referred to as humankind's oldest biotechnology, the goal is to produce a beverage with consistent flavor, which is the result of hundreds of volatiles present in the beverage. In order to quantify flavor compounds in beer and brewing samples, targeted HS-SPME-GC-MS assays are most common. However, with the multiplicity of compounds present in brewing samples, the low concentration and reactivity of key aroma compounds, beer flavor analysis remains challenging. In order to improve beer flavor analysis, and in particular to increase sensitivity, robustness, and stability, three novel HS-SPME-GC-MS/MS assays were introduced and validated.

*Publication A* "Analysis of Selected Hop Aroma Compounds in Commercial Lager and Craft Beers Using HS-SPME-GC-MS/MS" deals with the analysis of 16 selected hop aroma compounds covering the most relevant substance classes (terpenes, terpenoids, esters) commonly associated with hoppy beer flavor. With the industry standard HS-SPME-GC-MS methods, sufficient extraction and enrichment of volatiles requires maximizing sample volume and extraction times that stresses fiber material and limits fiber lifetime. Using tandem-mass spectrometry, sample volumes can be decreased, which reduces the amount of volatiles adsorbed onto the fiber and consequently prolonged the fiber lifetime. This study indicated that the combination of HS-SPME-GC-MS/MS with suitable stable isotope labelled ISTDs provides an assay with excellent stability that is not affected by e.g. fiber-to-fiber variations. The method development focused on the individual steps of MRM optimization and discussed them in detail. Moreover, the advantages of MRM in the reduction of matrix effects were illustrated.

In *Publication B* "Analysis of Selected Staling Aldehydes in Wort and Beer by GC-EI-MS/MS Using HS-SPME with On-Fiber Derivatization", an assay to quantify 15 analytical markers for beer flavor (in)stability was developed. The list of analytes includes lipid oxidation products (e.g., (*E*)-2-nonenal), products of Strecker degradation (e.g., methional), and so-called heat indicators (e.g., furfural). While the established methodology HS-SPME-GC-MS combined to on-fiber derivatization is a good approach regarding a fast sample preparation, the quantification of low abundant aldehydes in GC-MS must be performed in the lowest technically achievable level of quantification. The direct comparison of GC-EI-MS/MS and GC-EI-MS

revealed that due to the lower selectivity of SIM mode the quantification of these low abundant aldehydes by MRM mode is more reproducible. As this method is designed to quantify and monitor staling aldehydes from both wort and fresh as well as aged beers, the assay covers a wide concentration range (0.01-1000 µg/L) and should also provide good long-term stability. Hence, the long-term stability, herein defined as peak area consistency of two ISTDs over 24 weeks, across different beer matrices was determined and evaluated as excellent.

*Publication C* “Analysis of Hop-Derived Thiols in Beer Using On-Fiber Derivatization in Combination with HS-SPME and GC-MS/MS” is the most complex of the three assays. This relates to the fact that thiols appear in ng/L levels and are very prone to oxidation. In order to achieve quantification via GC-MS, time-consuming multi-step sample preparation procedures, which in some cases involve the handling of mercury containing solvents, are used. By taking advantage of the noise filtering by MRM mode and by using an automated on-fiber derivatization approach, the sample preparation requires minimal manual handling, which improves analysis quality as shown by validation. Whilst in the two above-mentioned publications method development was performed in a stepwise procedure, this method development used a central composite design. Validation of the optimized assay proves its sensitivity (limits of quantification below the sensory threshold of 4MMP, 3MH, and 3MHA) while being more rapid than any of the previously published methods.

In conclusion, the three developed HS-SPME-GC-MS/MS assays improved throughput, robustness, and sensitivity of beer flavor analysis. The improved detection sensitivity and selectivity offered by use of triple quadrupole GC-MS/MS resulted in prolonged fiber lifetimes and improved HS-SPME calibration consistency for hop aroma analysis, more reproducible results for low-abundant staling aldehydes as well as excellent long-term stability of the assay. Additionally, the required sensitivity for thiol quantification without extensive sample preparation was achieved. The publications demonstrate that the use of HS-SPME-GC-MS/MS in beer flavor analysis is highly beneficial, thus probably encouraging brewing chemists to adapt these published methodologies.

## Zusammenfassung

In der Bioanalytik besteht das Ziel darin, biologische Prozesse zu überwachen oder zu identifizieren. Die eingesetzten Analyseverfahren hängen von der Art und Konzentration der jeweiligen Zielanalyten sowie von der Matrix und dem zu untersuchenden System ab. Bei der Bierherstellung, die mitunter als die älteste Biotechnologie der Menschheit bezeichnet wird, ist es das Ziel, ein Getränk mit konstantem Geschmack herzustellen, der das Ergebnis hunderter im Getränk vorhandener volatiler Substanzen ist. Um Aromastoffe in Bier- und Brauereiprozessproben zu quantifizieren, werden meist *targeted* HS-SPME-GC-MS Assays eingesetzt. Aufgrund der Vielzahl von Verbindungen, die in Brauereiprozessproben vorhanden sind, der geringen Konzentration und der Reaktivität bedeutender Aromastoffe bleibt die Aromaanalytik von Bier eine Herausforderung. Um die Bieraromaanalytik zu verbessern und insbesondere die Empfindlichkeit, Robustheit und Stabilität zu erhöhen, wurden drei innovative HS-SPME-GC-MS/MS Assays entwickelt und validiert.

Die *Publikation A* "Analysis of Selected Hop Aroma Compounds in Commercial Lager and Craft Beers Using HS-SPME-GC-MS/MS" beschreibt die Analyse von 16 ausgewählten Hopfenaromastoffen, die die wichtigsten Substanzklassen (Terpene, Terpenoide, Ester) abdecken und die gemeinhin mit einem hopfenbetonten Bieraroma verbunden sind. Die branchenüblichen HS-SPME-GC-MS Methoden erfordern für eine ausreichende Extraktion und Anreicherung von flüchtigen Bestandteilen eine Maximierung des Probenvolumens und der Extraktionszeiten, was das Fasermaterial belastet und die Lebensdauer der Fasern begrenzt. Durch den Einsatz der Tandem-Massenspektrometrie können die Probenvolumina verringert werden, sodass die Menge der an der Faser adsorbierten volatilen Substanzen reduziert und die Lebensdauer der Faser folglich verlängert wird. Im Rahmen dieser Studie konnte nachgewiesen werden, dass die Kombination von HS-SPME-GC-MS/MS und geeigneter, stabil isotoopenmarkierter ISTDs einen Assay mit hervorragender Stabilität gewährleistet, der beispielsweise nicht durch Faser-zu-Faser-Schwankungen beeinflusst wird. Die Methodenentwicklung hat sich auf die einzelnen Schritte der MRM-Optimierung fokussiert und diese detailliert erläutert. Außerdem wurden die Stärken des MRM-Modus hinsichtlich der Reduzierung von Matrixeffekten dargestellt.

In der *Publikation B* "Analysis of Selected Staling Aldehydes in Wort and Beer by GC-EI-MS/MS Using HS-SPME with On-Fiber Derivatization" wurde ein Assay zur Quantifizierung von

15 Analyten zur Beurteilung der (In-)Stabilität des Bieraromas entwickelt. Die Analytliste umfasst Lipid-Oxidationsprodukte (z. B. (*E*)-2-Nonenal), Produkte des Strecker-Abbaus (z. B. Methional) und so genannte Hitze-Indikatoren (z. B. Furfural). Während die bestehende Messmethodik, HS-SPME-GC-MS in Verbindung mit *on-fiber* Derivatisierung, ein guter Ansatz hinsichtlich einer schnellen Probenvorbereitung ist, muss gleichwohl die Quantifizierung von gering konzentrierten Aldehyden mittels GC-MS im untersten technisch zu realisierenden Bereich erfolgen. Der direkte Vergleich von GC-EI-MS/MS und GC-EI-MS zeigte, dass aufgrund der geringeren Selektivität des SIM-Modus der MRM-Modus eine reproduzierbarere Quantifizierung dieser gering konzentrierten Aldehyde ermöglicht. Da diese Methode für die Quantifizierung und Kontrolle von Alterungsaldehyden sowohl aus Würze als auch aus frischen und gealterten Bieren entwickelt wurde, deckt der Assay einen breiten Konzentrationsbereich (0,01-1000 µg/L) ab und sollte zudem eine gute Langzeitstabilität bieten. Daher wurde die Langzeitstabilität, hier definiert als Beständigkeit der Peakflächen zweier ISTDs über 24 Wochen, in verschiedenen Biermatrixen ermittelt und als ausgezeichnet bewertet.

Die *Publikation C* "Analysis of Hop-Derived Thiols in Beer Using On-Fiber Derivatization in Combination with HS-SPME and GC-MS/MS" ist der komplexeste der drei Assays. Dies liegt daran, dass Thiole in Konzentrationen von wenigen ng/L vorliegen und sehr anfällig für Oxidation sind. Um eine Quantifizierung mittels GC-MS zu erreichen, werden zeitaufwändige, mehrstufige Verfahren zur Probenvorbereitung eingesetzt, die in manchen Fällen den Einsatz von quecksilberhaltigen Lösungsmitteln beinhalten. Durch die Ausnutzung der Rauschfilterung im MRM-Modus und durch die Verwendung eines automatisierten *on-fiber* Derivatisierungsansatzes erfordert die Probenvorbereitung nur einen minimalen manuellen Aufwand, wodurch die Qualität der Analyse erhöht wird, wie die Validierungsergebnisse belegen. Während in den beiden zuvor genannten Publikationen die Methodenentwicklung in einem schrittweisen Verfahren erfolgte, wurde bei dieser Methodenentwicklung ein Central Composite Design eingesetzt. Die Validierung des optimierten Assays bestätigte seine Sensitivität (Bestimmungsgrenze unterhalb der sensorischen Schwelle von 4MMP, 3MH und 3MHA) und zugleich seine Schnelligkeit im Vergleich zu allen zuvor veröffentlichten Methoden.

Zusammenfassend betrachtet, verbesserten die drei entwickelten HS-SPME-GC-MS/MS Assays den Durchsatz, die Robustheit und die Empfindlichkeit der Bieraromaanalytik. Die verbesserte Nachweisempfindlichkeit und Selektivität, die durch den Einsatz eines Triple-Quadrupol GC-MS/MS ermöglicht wurde, führte zu höheren Lebensdauern der Fasern und zu einer verbesserten Konstanz der Kalibrierung mittels HS-SPME bei der Hopfenaromen Analyse, zu

reproduzierbareren Ergebnissen von gering konzentrierten Alterungsaldehyden sowie zu einer hervorragenden Langzeitstabilität des Assays. Zusätzlich wurde für die Thiolquantifizierung die erforderliche Sensitivität ohne aufwändige Probenvorbereitung erreicht. Die Veröffentlichungen verdeutlichen, dass der Einsatz von HS-SPME-GC-MS/MS in der Aromaanalytik von Bier sehr lohnenswert ist, wodurch Brauereichemiker dazu angeregt werden dürften die veröffentlichten Methoden entsprechend zu nutzen.

# Table of Contents

<b>Abstract</b> .....	<b>i</b>
<b>Zusammenfassung</b> .....	<b>iii</b>
<b>List of Abbreviations</b> .....	<b>vii</b>
<b>1 Aspects of Beer Stability and their Analysis</b> .....	<b>1</b>
1.1 Basic Stability Parameters of Beer .....	2
1.2 Flavor and Flavor Stability.....	4
1.2.1 Impact of Hops on Beer Flavor.....	4
1.2.2 Aging Related Off-Flavors.....	7
1.3 Methods of Beer Flavor Analysis.....	8
1.3.1 Isolation.....	10
1.3.2 Separation .....	13
1.3.3 Detection.....	14
1.3.4 Quantification .....	15
1.4 Research Objectives.....	16
<b>2 Publication A: Hop Aroma Compounds</b> .....	<b>18</b>
<b>3 Publication B: Staling Aldehydes</b> .....	<b>46</b>
<b>4 Publication C: Hop-Derived Thiols</b> .....	<b>70</b>
<b>5 Closing Discussion</b> .....	<b>92</b>
5.1 Bound Aroma Compounds.....	93
5.1.1 Glycosidic Aroma Compounds in Hops.....	94
5.1.2 S-cysteinylated and S-glutathionylated Thiol Precursors .....	96
5.1.3 Cysteinylated Aldehydes.....	99
5.2 Analytical Aspects.....	103
5.2.1 Further Development of Hop-Derived Thiol Quantification .....	103
5.2.2 HS-SPME – not the End of the Road yet.....	104
<b>References</b> .....	<b>106</b>
<b>Appendix</b> .....	<b>117</b>
List of Publications.....	117
Conference Contributions.....	118

## List of Abbreviations

### A

AEDA	aroma extract dilution analysis
ASBC	American Society of Brewing Chemists
ATP	adenosine triphosphate

### C

CAR	carboxen
CCD	central composite design
CHARM	combined hedonic aroma response measurement
CID	collision-induced dissociation
Cys3MH	3- <i>S</i> -cysteinyl-hexan-1-ol
Cys4MMP	4- <i>S</i> -cysteinyl-4-methylpentan-2-one
Cys-BEN	2-phenylthiazolidine-4-carboxylic acid
Cys-FUR	2-(furan-2-yl)-1,3-thiazolidine-4-carboxylic acid
Cys-HEX	2-pentylthiazolidine-4-carboxylic acid
Cys-2MB	2-(secbutyl)thiazolidine-4-carboxylic acid
Cys-3MB	2-isobutylthiazolidine-4-carboxylic acid
Cys-2MP	2-isopropylthiazolidine-4-carboxylic acid
Cys-MET	2-(2-(methylthio)ethyl)thiazolidine-4-carboxylic acid
Cys-PAA	2-benzylthiazolidine-4-carboxylic acid

### D

DMS	dimethyl sulfide
DVB	divinylbenzene

### E

EBC	European Brewery Convention
ECD	electron capture detector
EI	electron impact

### F

FID	flame ionization detection
-----	----------------------------

### G

G3MH	3- <i>S</i> -glutathionyl-hexan-1-ol
G4MMP	4- <i>S</i> -glutathionyl-4-methylpentan-2-one
GC	gas chromatography
GC×GC	two-dimensional gas chromatography
GC-MS	gas chromatography-mass spectrometry
GC-MS/MS	gas chromatography-tandem mass spectrometry
GC-O	gas chromatography-olfactometry
GC-O-MS	gas chromatography-olfactometry-mass spectrometry

### H

HPLC	high performance liquid chromatography
------	--

HS	headspace
HS-SPME	headspace solid-phase microextraction
<b>I</b>	
IPA	India Pale Ale
ISTD	internal standard
ITEX	in-tube extraction
IT-SPME	in-tube SPME
<b>L</b>	
LC	liquid chromatography
LC-MS/MS	liquid chromatography-tandem mass spectrometry
LLE	liquid-liquid extraction
LOD	limit of detection
LOQ	limit of quantification
<b>M</b>	
2-MBIB	2-methylbutyl isobutyrate
3MH	3-mercaptohexan-1-ol
3MHA	3-mercaptohexylacetate
4MMP	4-mercapto-4-methylpentan-2-one
MEBAK	Central European brew-technical analysis commission
MRM	multiple reaction monitoring
MS	mass spectrometry
MS/MS	tandem mass spectrometry
m/z	mass to charge ratio
<b>N</b>	
NaCl	sodium chloride
NCI	negative chemical ionization
NEIPA	New England India Pale Ale
NMR	nuclear magnetic resonance
<b>O</b>	
OAV	odor activity value
OFD	on-fiber derivatization
<b>P</b>	
PCR	polymerase chain reaction
PDMS	polydimethylsiloxane
PFB	2,3,4,5,6-pentafluorobenzyl
PFBBr	2,3,4,5,6-pentafluorobenzyl bromide
PFBHA	<i>O</i> -(2,3,4,5,6-pentafluorobenzyl)hydroxylamine
PFBO	<i>O</i> -(2,3,4,5,6-pentafluorobenzyl)hydroxylamine oxime
PFPD	pulsed flame photometric detector
<b>S</b>	
SAFE	solvent assisted flavor evaporation
SBSE	stir bar sorptive extraction
SCD	sulfur chemiluminescence detector
SDE	simultaneous distillation extraction

SIDA	stable isotope dilution analysis
SIM	selected ion monitoring
SPDE	solid-phase dynamic extraction
SPE	solid-phase extraction
SPME	solid-phase microextraction
<b>T</b>	
TEA	triethylamine
<b>U</b>	
UPLC-PDA	ultra performance liquid chromatography-photo diode array
UHPLC-MS	ultra high performance liquid chromatography-mass spectrometry
<b>V</b>	
4VP	4-vinylpyridine

# 1 Aspects of Beer Stability and their Analysis

In biotechnology, biological materials are converted by fermentation using specific microorganisms or enzymes. By means of these controlled bioreactions, complex products can be generated that would be difficult or significantly more costly to produce by chemical synthesis. An example of such a process is beer production, which is probably mankind's oldest biotechnology.<sup>1</sup> The four key ingredients are: water, malt, hops (*Humulus lupulus* L.), and yeast. Put simply, to make the raw material components of the grain (e.g., barley, wheat) accessible to the yeasts, starch and protein degrading enzymes must first be formed or activated during steeping and germination. During malting, the enzymatic bioconversion starts and continues during mashing until the fermentable components (maltose, free amino acids) are dissolved. In brewing, hops are added to introduce bitterness and aroma. The wort is boiled, whereas a number of physical and chemical processes take place (e.g., isomerization of hop compounds, coagulation and precipitation of tannin-protein complexes, sterilization of wort). During anaerobic fermentation, the fermentable sugars from the malt are converted by yeasts to ethanol and carbon dioxide. Furthermore, flavor-active substances are produced as by-products. In order to acquire its final taste, the green beer post-ferments during maturation.

By monitoring the raw materials, intermediate and end-products, microbiological, chemical-physical, and sensory properties of the beer are controlled to produce a beverage that is characterized by stability in four categories: microbiological, colloidal, foam, and flavor stability. Together they determine beer shelf-life and are used to assess beer quality. Reinforced by the increasing popularity of craft breweries, interpretation and reinterpretation of different beer types lead to numerous different beer styles to meet each person's individual flavor preferences. Therefore, the consumer associates high beer quality with both sufficient stability of the beer during the shelf life, which is usually six to twelve months, and with a desirable taste. Beer is a fresh product, but unfortunately most consumers do not consider it as such. It is beyond the brewer's control what happens to the beer in the time after packaging and before consumption, which is why increased demands are placed on flavor stability. Hops have a prominent importance during the brewing process and have a decisive influence on all four stability parameters. Although hops are used in quite different quantities than malt (25-30 kg/hL for malt versus hundreds of g/hL for hops), they provide the unique flavor typical for beer, even in non-alcoholic beers.<sup>2</sup> Comparing the public perceptions of wine and beer, the hop harvests are

also subject to annual variations, but unlike wine, consumers expect a consistent hoppy flavor in beers over the different “vintages”. This requires an in-depth understanding of this key raw material, its composition, and the changes of aroma compounds during the brewing process. In order to better comprehend the complex impact of hops on various aspects of beer quality, the four categories of stability will be discussed in more detail below, with a focus on flavor and flavor stability together with the corresponding analytical tools to investigate them.

### 1.1 Basic Stability Parameters of Beer

Microbiological stability is the basic requirement for obtaining a safe product and prolonging the shelf life of beer. Contamination with bacteria, wild yeasts, or fungi deteriorates product quality in various ways.<sup>3</sup> The most potential contaminants originate from raw materials and insufficiently cleaned vessels and pipes. Given the low pH of beer, the high ethanol content, the anaerobic environment, the low nutrient level, the carbonation, and antimicrobial active compounds of the hops, microbiological growth is suppressed.<sup>3</sup> Despite this, most of the contaminants induces off-flavors or with increased propagation the formation of haze. For instance, lactic acid bacterial contamination in the storage or finishing tanks leads to the production of diacetyl and causes an unpleasant buttery off-flavor, which significantly affects the flavor stability.<sup>4</sup> Wild yeast contamination of the pitching yeast can lead to various off-flavors (e.g., *Debaromyces*, *Pichia*, and *Williopsis* species cause yeasty or estery off-flavors).<sup>5</sup> Fermentation problems may also be caused by competing with the culture yeast for nutrients or even actively suppressing them by releasing killer toxins.<sup>5</sup> In contrast, barley infected with fungi from the *Fusarium* genus can cause gushing and/or the release of mycotoxins.<sup>3</sup> To detect, quantify, and identify possible contamination for quality control purposes different physical (e.g., turbidometry), biochemical (e.g., ATP bioluminescence), and molecular methods (e.g., PCR analytics) have been developed.<sup>6-8</sup> By strict cleaning routines together with pasteurization or sterile filtration of the finished beer, the risk of microbiological contaminations are minimized.

According to consumer expectations, haziness in Lager or Pilsner beer styles is primarily caused by microbiological contamination. Therefore, haziness is considered as defect or as a potential health threat regardless of the origin of the turbidity. Colloidal stability is therefore an important quality parameter for brilliant, clear beers. Different types of non-biological haze exist, including permanent haze, reversible chill haze, and haze caused by other substances (e.g., polysaccharides, calcium oxalate, silica).<sup>9</sup> Colloidal haze formation is mainly driven by the

interaction of polypeptides and polyphenols. The polyphenol-protein complexes of chill haze remain soluble and dissolve at increasing temperatures. When the soluble polyphenol-protein complexes convert to insoluble complexes and covalent attachments are developed, permanent haze is formed.<sup>10</sup> The polypeptides associated with haze appear to be derived from barley hordeins (major storage proteins), while the polyphenols originate from barley and hops.<sup>9,11</sup> To determine the turbidity tendency, various methods such as forcing tests and precipitative tests were developed, validated, and finally published as a standardized method in publications of the Central European brew-technical analysis commission (MEBAK 2.14.2.1), European Brewery Convention (EBC 9.29, EBC 9.41), or American Society of Brewing Chemists (ASBC Beer-27). In order to ensure colloidal stability, many stabilization treatments are established. In general, a stabilization agent (e.g., silica, polyvinylpolypyrrolidone) is added to the beer, which binds to its specific turbidity precursor, and the resulting complexes are removed by filtration.<sup>9</sup>

Along with color and clarity, foam is one of the first characteristics that consumers notice while serving and drinking a beer out of a glass. Depending on consumer preference, different combinations and levels of the following qualities are regarded as excellent foam quality: stability, quantity, lacing (glass adhesion), whiteness, creaming, and strength.<sup>12</sup> However, not only visual aspects are crucial for the foam quality. In addition, the mouthfeel is decisively influenced by the degree of carbonation as well as stability and structure of the foam, which in turn depends on foam physics.<sup>12,13</sup> In analytical foam measurement, the parameter stability has become the most important quality feature to be evaluated, since the other quality parameters are only relevant if a stable foam is present.<sup>11</sup> Similar to colloidal stability, standardized methods have been introduced for foam stability, usually using a NIBEM or Steinfurth foam stability tester (EBC 9.42.1, EBC 9.42.2). Foam stability is influenced by a variety of factors such as raw material selection and process control during brewing, resulting in a foam quality specific to the beer style. Simply put, foam stability is largely the interaction of the quality and quantity between malt foam positive proteins (e.g., lipid transfer protein 1, protein Z) and the selection of hop acids.<sup>12,14</sup> Nevertheless, other factors that cannot be controlled by the brewer, such as dispensing the beer as well as the cleanliness, shape, and material of the glass, ultimately affect the foam stability.

## 1.2 Flavor and Flavor Stability

Flavor is caused by the individual and specific interaction between olfactory, gustatory, and trigeminal (e.g., astringent, sparkling) perception.<sup>15</sup> In complex matrices such as beer, it is difficult to relate one particular volatile compound to a specific flavor, as usually several compounds causes a specific flavor impression. Nevertheless, flavor stability is the key quality feature of beer, as flavor is the most important characteristic for brand recognition and overall consumer acceptance. Thus, brewers aim to produce beverages with a reproducible and sufficiently stable beer flavor, which is the result of hundreds of volatiles determined by a series of interacting production processes. This parameter is challenging, firstly because of the large variety of aroma components and the associated need to make a selection of suitable aroma components of interest. Secondly, flavor stability requires the simultaneous analysis of two complex processes: stability represented as batch-to-batch consistency as well as stability towards the formation of a stale character during aging.

Although malt is the most important raw material in terms of quantity, it is not the raw material that significantly affects beer flavor in the majority of beers. That is mainly due to the fact that the volatile components such as alcohols, aldehydes, fatty acids, furans, ketones, phenols, pyrazines, and sulphur compounds formed by the process of malt kilning are lost during boiling or fermentation.<sup>16</sup> Some exceptions are beers brewed with specialty malts. The caramel, chocolate, coffee, and nut-like attributes of a Porter are due to the addition of highly roasted, dark malts. On the other hand, the smoking of malt introduces the characteristic smoked, bacon-like aroma into Rauchbier.

### 1.2.1 Impact of Hops on Beer Flavor

The raw material that contributes significantly to the character of the final beer is hops. By variation of this main ingredient and the technical parameters of the brewing process, a diverse range of beer flavors are achieved, since hops are mainly responsible for the addition of bitterness and the characteristic hoppy aroma.<sup>15</sup> The main constituents responsible for the flavor of beer are stored in the lupulin glands of the female hop cone: hop resins and hop oil. The total resin fraction comprises 10–30% of the total weight of dried hops and is further divided in soft and hard resins.<sup>17</sup> Among the soft resins,  $\alpha$ -acids are most important constituents as they

are the precursors of the key compounds responsible for the bitterness in the later brewing process.

Depending on the variety, cultivation area, and harvest year, the total content of hop oil of dried hop cones is 0.2-3%.<sup>15</sup> There are probably more than 1000 hop oil compounds, of which approximately 500 substances have been identified so far.<sup>18</sup> These are considered as the primary source of hop-derived aroma. Although many hop-derived aroma compounds are present in beer at subthreshold concentrations, they are relevant for the overall hop aroma profile due to additive, synergistic or suppression effects.<sup>19</sup> For instance, traces of citronellol and geraniol interact synergistically to enhance the flavor impression of linalool.<sup>20</sup> According to Sharpe and Laws<sup>21</sup> hop oil compounds are classified into three categories: hydrocarbons (40-80%, e.g., monoterpenes, sesquiterpenes), oxygenated compounds (~30%, e.g., terpene alcohols, esters, ketones), and sulfur-containing compounds (~1%, e.g., thiols, sulfides, thioesters). As the description of the exact chemical composition exceeds the scope of this introduction and has already been discussed in detail,<sup>15,16,21-23</sup> selected hop oil compounds are presented hereafter.

The most abundant component of hop oil is the monoterpene myrcene (resinous), which is also the sensorial dominant component in fresh hop cones.<sup>24</sup> In much lower quantities (at least 100 times less)  $\alpha$ - and  $\beta$ -pinene (piney), as well as limonene (citrus) are present in hop oil. Further major components of hop oil are the sesquiterpenes  $\alpha$ -humulene (medicinal) and  $\beta$ -caryophyllene (clove). Nevertheless, most of the hydrocarbons evaporate during boiling after a conventional hop dosage (kettle hopping) or are removed during separation processes in brewing. Besides monoterpenes and sesquiterpenes, carboxylic acid esters are quantitatively the third largest substance group in hop oil (~15%). Quantitatively, 2-methylbutyl isobutyrate (2-MBIB, fruity) belongs to the primary hop-derived ester in beer.<sup>25</sup> It was even recently shown that 2-MBIB is one of the most abundant hop-derived volatiles in ales.<sup>26</sup> The concentration of 2-MBIB in the finished beer ( $\mu\text{g/L}$  range) depends on the used hop variety. Varieties such as the DE-Hüll Melon, US-Mosaic, and NZ-Southern Cross contain relatively high amounts of 2-MBIB.<sup>25</sup> However, the majority of flavor active esters are fermentation-derived (e.g., ethyl acetate, isoamyl acetate, ethyl hexanoate). In the group of terpene alcohols, linalool is of particular importance. In various studies<sup>27-29</sup> it has been shown that linalool (floral) significantly contributes to the hop aroma in beer as it withstands the process to the finished beer and exceeds its threshold ( $<10 \mu\text{g/L}$ ). Because of the observed correlation between the hoppy flavor intensity and the linalool concentration,<sup>30-32</sup> this analyte is often used to estimate the overall

hoppy flavor. Another potent odor-active compound with a similarly low threshold represents geraniol (rose-like). During fermentation, various biotransformations by lager and ale yeasts occur: geraniol is primarily transformed to citronellol (citrus) and to a lesser extent into linalool, whereas linalool and nerol (floral, citrus) are isomerized to  $\alpha$ -terpineol (lilac-like).<sup>33</sup> Sulfur compounds (e.g., dimethyl trisulfide, S-methylthiohexanoate) are often responsible for a number of unpleasant odors (onion-like, cheesy, cooked vegetable) in beer.<sup>27,34</sup> In contrast, certain United States, Australian, or New Zealand hop varieties (e.g., Citra, Simcoe, Cascade) contain thiols like 4-mercapto-4-methylpentan-2-one (4MMP, blackcurrant-like) and 3-mercaptohexan-1-ol (3MH, grapefruit-like),<sup>35-37</sup> which have a large impact on beer aroma due to their thresholds in the ng/L range. Beer hopped with these varieties is characterized by a positive, tropical flavor, which is highly desired in hop forward beer styles. The thiol 3-mercaptohexylacetate (3MHA, passion fruit-like) is formed by yeast from 3MH during fermentation.<sup>38,39</sup>

The final hop-derived beer flavor is influenced by numerous factors such as the hop variety used, the harvest date, and yeast metabolism.<sup>20,35,40,41</sup> However, the impact of different hopping regimes (e.g., timing, quantity, temperature) on either a more bitter or hoppy flavor profile is probably among the best researched, but is still not fully understood.<sup>15,17,42</sup> To introduce bitterness, hop varieties declared as bitter and high alpha hops ( $\alpha$ -acid levels of approx. 10-20%) are usually added at the beginning of wort boiling (kettle hopping). During wort boiling, the native, non-bitter  $\alpha$ -acids isomerize to water-soluble iso- $\alpha$ -acids, the main contributor to beer bitterness. Among other factors, boiling time, boiling temperature, and pH of the wort determine the solubility of  $\alpha$ -acids and consequently the isomerization rate.<sup>15</sup> Hops also contain  $\beta$ -acids, which are degraded during wort boiling to less significant bitter-tasting products.<sup>43</sup> In addition, a volatilization of unwanted flavors (e.g., dimethyl sulfide, DMS) is targeted, but this simultaneously leads to the evaporation of most hoppy aroma compounds from the wort.<sup>15,31,44</sup> To achieve increased hop aroma, aroma hops (usually  $\alpha$ -acid levels of <10%) are added at the end of wort boiling or in the whirlpool (late hopping) in an additional hop dosage to preserve volatile aroma compounds. At temperatures below 100 °C, the isomerization of  $\alpha$ -acids into iso- $\alpha$ -acids is limited and the extraction of hop aroma compounds is enhanced.<sup>31</sup> Another method to brew hop forward beer styles is dry hopping. For this type of hop dosage, a cold extraction (4-20 °C) with significantly high hopping rates (100-6000 g/hL) takes place during fermentation or in the green beer.<sup>45</sup> The hop aroma of late and dry hopped beers vary significantly.<sup>25</sup> The relatively low temperatures during dry hopping further reduce thermal

degradation and loss of volatile aroma compounds. The dry-hop character is determined by hop quality. Processing conditions, including agricultural factors, harvest date and growing region, have a significant influence on hop oil content and composition.<sup>41,45</sup> Additionally, it was shown that the perception of hop aroma is also influenced by fermentation technology and the concentration of fermentation by-products.<sup>32</sup>

Considering all of the presented factors relating to the composition of hop aroma compounds in the final beer, flavor stability is difficult to achieve. It is obvious that dry-hopped beers are facing greater problems in achieving consistent flavor stability, which is due to the higher hop dosages. Hop inhomogeneity, dissolved oxygen concentration, and the volume of the dry hopping treatment are the major factors affecting the reproducibility of dry-hop aroma in beer.<sup>46</sup> Especially considering that these styles meanwhile represent a considerable market share,<sup>45</sup> flavor consistency is of great relevance for breweries.

### 1.2.2 Aging Related Off-Flavors

The second aspect that is essential for achieving flavor stability is the prevention of flavor changes caused by the increased stale flavor during storage. Depending on the storage conditions (e.g., temperature, light), transformation processes lead to a decrease of desired hop aroma compounds and simultaneously to an increase of negative associated flavors. Thus, lightly hopped beers are affected to a greater extent, as the increasing off-flavors can be masked worse than in hop forward beer styles.<sup>19,47,48</sup> Since Lager style beers are the best-selling products and distributed worldwide, sufficiently stable beer flavor is a major concern for many breweries to meet consumer expectations.

The reaction pathways of stale flavor generation are diverse and likewise not entirely explored.<sup>49,50</sup> It is proven that increased concentration of aldehydes, esters, and sulfur containing compounds are associated to an aged flavor profile. Lipid oxidation products (alkanals, (*E*)-2-alkenals, (*E,E*)-2,4-alkadienals)) and Strecker aldehydes (2-methylpropanal, 2-methylbutanal, 3-methylbutanal, methional, benzaldehyde, phenylacetaldehyde) primarily contribute to flavor defects during storage.<sup>47,49</sup> In addition, furfural is considered as a suitable marker for heat-induced beer aging.<sup>51</sup> Aging related off-flavors vary between beer styles. For instance, (*E*)-2-nonenal, whose distinct cardboard flavor is perceptible at sub- $\mu\text{g/L}$  levels, is a major indicator for aged Lager beers.<sup>49</sup>

Unlike colloidal or foam stability, no standardized methods for flavor stability exist. Analytical assays investigating compounds responsible for hoppy flavor or stale characteristics have to overcome certain challenges. In both cases, the analytes of interest are present in low concentrations (ng/L to  $\mu\text{g/L}$  levels). Depending on the beer style studied, the composition of the beers differs significantly. Especially, the analysis of trace compounds is affected by other beer matrix compounds (e.g., co-elution). Additionally, compounds with a carbonyl or thiol function are very reactive, which have to be taken into account during sample preparation. Nevertheless, the quantification of hop-derived volatiles and stale aroma compounds is essential both from a practical quality perspective in breweries as well as for research purposes.

### 1.3 Methods of Beer Flavor Analysis

In principle, there are two approaches to analytical work: targeted (analysis of defined analytes or analyte groups) and untargeted (global analysis of all analytes in a sample). In order to obtain a better understanding of the correlation of volatile and nonvolatile compounds in beer with both the ingredients used as well as the compositional changes during malting, brewing, and storage, targeted and untargeted metabolomic studies were performed. Metabolomics is the analysis of all metabolic products, usually with a molecular mass between 50 and 1200 Da. The characteristic metabolite profile of a sample is defined as set of all detected metabolites. Depending on the particular issue, gas chromatography (GC) based separation methods are used for volatile metabolites and liquid chromatography (LC) or nuclear magnetic resonance (NMR) based analysis techniques are chosen for the nonvolatile fraction of beer metabolites. The systems are coupled to high-resolution mass spectrometers to determine the monoisotopic mass. By comparison to reference spectra from standards or a database, the monoisotopic mass confirms the identity of compounds. Metabolite profiling involves biostatistical methods in order to identify specific relevant metabolites by comparison of metabolite profiles of different samples. For instance, beer metabolomics has been used to investigate the effects of barley genotypes on sensory attributes and metabolic profiles,<sup>52</sup> to determine the effects of storage conditions and brewing techniques on flavor stability,<sup>53,54</sup> and to study the yeast purine metabolism of late and dry hopped beers.<sup>55</sup> In summary, beer metabolomics potentially provides new insights into the effect of volatile and nonvolatile compounds, especially when the biological mechanism is not yet fully understood and/or not all target analytes have been identified.

From a technical point of view, the untargeted approach using gas chromatography-olfactometry (GC-O) is less demanding. GC-O is commonly used to detect potent odor compounds from food and beverages in order to assign certain volatile substances to a specific flavor. For an improved identification of odor compounds, GC-O is often combined with a mass spectrometer (GC-O-MS). Crucial for the quality of data collected by GC-O is both an optimal separation of the volatile compounds and for the sensory evaluation a properly trained assessor. Therefore, one of the drawbacks of this analysis technique is that trace compounds could co-elute with other substances, making the correct matching between the detected aroma and the correct compound difficult even with GC-O-MS. Furthermore, the sensitivity of the human assessor fluctuates and may vary over time, health status, and mood.<sup>56</sup> GC-O is not only applied for screenings, rather it is used for dilution to threshold methods (e.g., aroma extract dilution analysis (AEDA), combined hedonic aroma response measurement (CHARM)) to evaluate the odor potency of a compound. For this purpose, serial dilutions are performed and GC-O was used to examine for the highest dilution at which the odor is still detected. As a result, odor thresholds have already been identified for a large number of volatile compounds in beer.<sup>29,35,57,58</sup> By quantifying these odor-active components, the individual ratio of concentration to odor threshold can be calculated. The resulting odor activity value (OAV) is an index of how probably a volatile substance affects the flavor profile.

By studying OAVs and flavor thresholds<sup>59,60</sup> the key compounds that contribute significantly to the characteristic hop aroma or staling flavor have already been identified, so that a targeted approach for quantification is more reasonable. The advantage of targeted quantification is that by limiting the number of analytes, the quantification is more accurate through suitable calibration procedures. Using internal standards (ISTDs), instrument variations were normalized. Furthermore, the choice of the measurement mode influence the signal-to-noise ratio when using an MS detector, which increases the analytical performance.

During method development, suitable procedures and parameters for the four steps isolation, separation, detection, and quantification needs to be defined. The following section is a brief description of the approaches relevant in beer flavor analysis.

### 1.3.1 Isolation

An effective isolation and enrichment of the volatile analytes from the complex beer matrix is important for the quality of the whole assay, as it influences the performance of all further steps. In case of poor isolation of the volatiles of interest, the separation performance of the column becomes insufficient and the signals of minor aroma compounds are covered by high concentrated volatiles (e.g., alcohols, esters), resulting in an inaccurate or impossible quantification. Furthermore, an incomplete sample clean up leads to the injection of the nonvolatile sample compounds into analytical instruments. In case of gas chromatography-mass spectrometry (GC-MS), the performance of GC column and ion source will be reduced.<sup>22</sup> At the same time, isolation is the most challenging step as, depending on the extraction method, it may require complex sample preparation, which is time-consuming and error-prone considering the extent of manual handling.<sup>61</sup>

In 1964, Likens and Nickerson firstly introduced a method for isolation of hop oil from beer.<sup>62</sup> The simultaneous distillation extraction (SDE), also known by the name “Likens and Nickerson” method, involves the simultaneous steam distillation and the extraction of volatiles into a solvent in a special distillation unit.<sup>62</sup> Even though the published workflow was reasonable at this time regarding the exhaustive isolation of the volatile fraction, numerous alternative isolation procedures for aroma analysis in beer have been introduced.<sup>63-66</sup> Solid-phase extraction (SPE), liquid-liquid extraction (LLE), as well as solvent assisted flavor evaporation (SAFE) were mainly used before the widespread availability of so-called microextraction methods. The thermal load causing artefact formation is omitted for SPE, LLE, and SAFE. However, as for SDE, solvents, comparably large sample volumes, and time-consuming sample preparations are required, that inhibits a high sample throughput.

For a solvent-less sample preparation, the liquid organic solvent is replaced by a gas or a solid sorbent. The main advantage of this approach besides environmental aspects is the ability of the extractant to either renew itself in case of headspace extraction or to be regenerated for a couple of hundreds of extractions when a solid sorbent is used.<sup>67</sup> A simple isolation technique is static headspace (HS) sampling, where an aliquot of the headspace is directly injected into the GC. However, HS-sampling approaches are insufficient for minor volatiles in beer due to their limited sensitivity.<sup>28</sup> In addition to static methods, dynamic extraction methods were developed such as HS-trap and purge and trap, which were adapted for the analysis of flavor compounds in beer.<sup>68,69</sup>

In volatile beer flavor analysis nowadays, headspace solid-phase microextraction (HS-SPME) is a frequently used extraction technique.<sup>25,28,70,71</sup> SPME was first published in 1989 to facilitate sample preparation by introducing a versatile single step extraction/introduction method.<sup>72</sup> This solvent-free microextraction technique allows simultaneous sampling, extraction, selective enrichment, and sample introduction to an analytical instrument. Thus, it complies with the requirements for rapid, automated, solvent-free, and sensitive sample preparation. The extractant consists of a 1-2 cm long fiber inside a syringe that is coated with various single or mixed polymer materials. The fiber coatings differ in polarity, thickness, length, as well as their affinity for absorption or adsorption processes, affecting the selectivity towards an analyte.<sup>70,73,74</sup> SPME is used either directly into the liquid sample or in the headspace of the vial, the latter being recommended for volatile analytes. Furthermore, the absent contact with the liquid sample prevents the degradation of the fiber coating and reduces matrix influences.<sup>75</sup> HS-SPME includes three steps: incubation, extraction, and desorption. During incubation, the separation of volatile compounds from the non-volatile sample matrix to the headspace above is forced, which is influenced by numerous parameters (e.g., temperature, time, agitation rate, and NaCl addition). When the SPME fiber is exposed to the headspace, the extraction to the fiber coating starts immediately. It is completed as soon as the concentration of the volatiles have reached an equilibrium between the fiber coating and the sample matrix, which is dependent on their relative distribution coefficients.<sup>72</sup> Therefore maximum sensitivity is achieved under equilibrium conditions. Nevertheless, often pre-equilibrium conditions are used to achieve high sample throughput, as the use of an autosampler guarantees repeatable extraction conditions for an accurate quantification.<sup>76</sup> During thermal desorption the analytes were transferred into the GC inlet. A comprehensive review on the optimization parameters during method development of SPME was written by Risticvic et al.<sup>76</sup> Briefly, optimization of SPME parameters is difficult, as generally with methods involving several analytes, since conditions promoting the extraction of one target analyte might suppress the extraction of others. The main drawback of HS-SPME methods is the sensitivity toward any changes in extraction condition.<sup>75</sup> While most instrument parameters (e.g., incubation and extraction time, temperature) are kept constant using an autosampler, complex sample compositions may cause matrix effects that cannot be influenced and affect the extraction efficiency of each analyte individually. To account for this limitation, suitable quantification procedures have to be selected for HS-SPME (see 1.3.4 Quantification). Due to the syringe design, the volume of SPME coating is limited, resulting in limited extraction capacity for some applications.

To overcome the limited extraction capacity, stir bar sorptive extraction (SBSE)<sup>77</sup> was developed in 1999 and has been successfully applied for beer flavor analysis.<sup>42,44,78</sup> For SBSE, a coated stir bar is added to the liquid sample for stirring and extraction. Due to the diffusion into a sorption phase volume up to 100 times larger, the equilibrium time increases compared to HS-SPME.<sup>77</sup> Until now, the variety of commercially available stir bar layers (polydimethylsiloxane, ethylene glycol/silicone) is much smaller compared to fiber coatings. The major drawback of SBSE is the limited automation after extraction. The preparation of the stir bars for thermal desorption or liquid desorption requires additional manual steps. In addition, the direct analysis of solids (e.g., malt, hops) is not provided, whereas HS-SPME enables a flexible implementation. This flexibility is particularly advantageous for process monitoring and quality control.<sup>22</sup> By using HS-SPME, the development of certain volatile compounds from hops to beer could be observed.

Since the introduction of SPME over 30 years ago, numerous new microextraction techniques have been developed and studies have been conducted to demonstrate the improvements over conventional SPME techniques. Most new developments targeted the limited sorption capacity and fiber fragility of SPME. To name just a few examples of needle-based microextraction techniques besides SPME: in-tube SPME (IT-SPME, 1997),<sup>79</sup> solid-phase dynamic extraction (SPDE, 2001),<sup>80</sup> in-tube extraction (ITEX, 2008),<sup>81</sup> and SPME Arrow (2016).<sup>67,82</sup> IT-SPME is often applied especially for use with on-line HPLC. SPDE and ITEX have been applied to a wide range of different analytes in various matrices, including the analysis of volatile compounds in beer samples.<sup>83,84</sup> Introduced in 2016, the SPME Arrow is a comparatively new microextraction technique and combines the advantages of SPME and SBSE. SPME Arrow is characterized by a higher mechanical robustness due to the 2-3 times larger external diameter of the septum piercing needle. Through an arrow shaped tip, the force required to penetrate septa is reduced, which further increases the mechanical stability.<sup>85</sup> SPME Arrow provides an approximately 10 times larger sorption phase volume compared to SPME fiber.<sup>82</sup> Up to now, no SPME Arrow application for beer flavor analysis has been published, although it seems to be a promising and powerful extraction technique for the analysis of potent odor-active trace compounds in beer. Recently an application for the quantification of cannabis-derived terpenes that are about 1000 times higher than in beer samples was published.<sup>86</sup> However, the higher extraction efficiency has been demonstrated in other food and beverage applications by comparative studies between HS-SPME and SPME Arrow sampling.<sup>87-89</sup>

### 1.3.2 Separation

As in beer flavor analysis, primarily volatile or low molecular weight compounds need to be separated, GC is the ideal analytical instrument. There are few LC approaches for volatile compounds that previously used special derivatization reagents adapted for LC (e.g., analysis of thiols).<sup>90</sup> The aim in both cases is the chromatographic separation of the mixture into individual analytes, ideally baseline separated. A good separation performance is necessary for a reliable identification and quantification of the peaks. To optimize GC separation, numerous factors have to be considered such as the choice of stationary phase (material, column length, diameter, film thickness), GC temperature program, and the gas flow. Generally, the polarity of the stationary phase is selected to be as similar as possible to the polarity of the analytes. For hop aroma compounds, which are very heterogeneous regarding their polarity (nonpolar hydrocarbons vs. polar terpene alcohols), both nonpolar phase (e.g., 5% phenyl 95% dimethylpolysiloxane) and polar phases (e.g., polyethylene glycol) are used.<sup>25,42,44</sup> However, a co-elution of aroma components with very similar chromatographic properties (e.g., boiling point, polarity) cannot always be prevented. In these cases, a reliable identification and quantification of the co-eluting compounds is ensured either by a mass-selective detector or by the application of two-dimensional GC (GC×GC). In GC×GC separation, two different stationary phases (usually nonpolar and polar) are connected sequentially by a cryogenic modulator. At the end of the first column, the eluent is retained and concentrated by the modulator before being pulsed onto the second column for further separation. For particular issues, such as the separation of enantiomers (e.g., (R)- and (S)-linalool), the installation of a chiral column can be necessary either as main column<sup>91</sup> or as second dimension in a GC×GC application.<sup>28,29</sup> However, the improved separation performance of the GC×GC is dependent on the trouble-free continuous operation of the technically highly complex interactions at the modulator. Alternating cryofocusing and thermal desorption require permanent and perfect synchronization, which is technically difficult to realize so far but essential for high throughput analysis.

### 1.3.3 Detection

GC with flame ionization detection (FID) is a simple and robust technique that enables a reliable quantification of high concentrated and separated compounds. Substance identification is based on matching retention times of analytes and reference standard on a polar and nonpolar column. As GC-FID is a widely used technique in brewery laboratories, there are several standard methods (e.g., ASBC Beer-48, EBC 9.39). Another non mass-selective detector is the electron capture detector (ECD). However, the ECD is rarely used in beer flavor analysis.<sup>92</sup> Sulfur selective detectors such as pulsed flame photometric detector (PFPD) or sulfur chemiluminescence detector (SCD) are used, for example, to determine DMS in beer (ASBC Beer-44). However, these detectors are not suitable for sulfur trace compounds (e.g., 4MMP) in complex matrices such as beer, as interferences by other sulfur compounds cause error in identification and quantification.

Overcoming these detection problems by using a sensitive and mass-selective detector, GC coupled to quadrupole MS has become the primary technique in the analysis of hop-derived aroma compounds in beer.<sup>25,42,44,68</sup> Using the quadrupoles in different modes, GC-MS enables accurate qualitative and quantitative analysis. In scan mode, the identification of unknown substances by comparison to reference spectra from standards or a database is provided. While GC-MS in selected ion monitoring (SIM) mode is used to measure a few characteristic ions of each analyte, which improves the detection sensitivity of quantification.

An improvement of the single quadrupole MS was the introduction of triple quadrupole instruments, also known as tandem MS (MS/MS). For MS/MS, operation in different modes is also possible. Besides the scan and SIM mode, the multiple reaction monitoring (MRM) mode is the key feature and most commonly used for the quantification of trace compounds. In MRM, the quadrupoles 1 and 3 of MS/MS instruments work in SIM programs, whereas quadrupole 2 is used for collision-induced dissociation (CID). By means of CID, the precursor ions of quadrupole 1 undergo further fragmentation and the resulting fragment ions (product ions) are then separated in quadrupole 3. A set of precursor and product ions is called MRM transition. MRM transitions are more specific than the characteristic ions detected in SIM, which enhances the signal-to-noise-ratio and sensitivity of MRM based assays.<sup>22</sup> LC-MS/MS is established in various fields of research including brewing science.<sup>93,94</sup> In contrast, GC-MS/MS is not widely used in beer flavor analysis, even though the advantages of MRM indicate the potential of GC-MS/MS for more sensitive analysis of trace compounds in beer.

### 1.3.4 Quantification

There are various quantification procedures and the selection of the appropriate protocol should be based on the desired quality of the results, the sample composition, the instrumental setup, and practical aspects such as availability of suitable ISTDs.

To investigate only the distribution of major hop volatiles, such as in the standardized hop oil analysis (e.g., ASBC Hops-17) relative quantification is sufficient. Accordingly, the obtained result is a percentage contribution of a single compound to the total chromatographic area. Relative quantification does not require any further calibration measurements, but its accuracy is limited regarding trace concentrated volatiles.<sup>22</sup> The combination with equilibrium extraction techniques for sample preparation is not possible.<sup>22</sup>

However, if the objective of quantification is the determination of concentrations, external or internal calibration protocols have to be chosen. Both involve the generation of calibration curves (plot of instrumental response versus concentration) using reference standards with known concentrations. In external calibration, calibration curves are obtained by separate measurements of differently concentrated reference standards. External calibration is the ideal approach for analytical assays that require only minimal sample preparation, as stable measurement conditions are essential to ensure reliable results. In addition, the composition of the sample and standard matrix must be as similar as possible for good accuracy.<sup>22</sup> Otherwise, matrix effects occur resulting in over- or underestimation. Possible matrix effects are considered by a matrix-matched calibration or the standard addition method. The major drawback of standard addition is high expenditure of time, as a separate calibration is required for each sample respectively matrix.

Internal calibration is the best choice if the sample matrix is expected to affect the analyte signal (peak area) or if variations cannot be excluded during sample preparation (e.g., fiber aging, fiber-to-fiber variations). In internal calibration, a substance that is physically and chemically similar to the analyte, but not originally included in the sample, is added with a constant concentration to the samples at the beginning of sample preparation. Thus, the ISTD is subject to the same procedure as the analytes of interest and potential losses during sample preparation or systemic errors affect both ISTD and sample, which ensures the robustness of the quantification.<sup>22</sup> Especially in combination with a selective isolation technique (e.g., HS-SPME, SBSE) the quality of quantification depends on the conditions during calibration and analysis

being as similar as possible. Therefore, a matrix-matched calibration is also recommended for an internal calibration protocol.<sup>61</sup>

A subtype of internal calibration is the widely used stable isotope dilution analysis (SIDA).<sup>29,68,95</sup> Based on the quantification of trace aroma compounds it was proven that the most suitable ISTD is the isotopically labelled analogue of the analyte.<sup>28</sup> The limited selection of commercially available stable isotope labeled standards and the high acquisition costs are drawbacks of SIDA.<sup>96</sup> It is worth mentioning that SIDA can only be applied in combination with a mass-selective detector, due to the (partial) co-elution of the ISTD and its unlabeled isotopologue. Depending on the heterogeneity of the analytes, physical-chemically different ISTDs in different concentration ranges should be used for quantification.<sup>61</sup> The selection of appropriate analyte-ISTD pairings are principally established considering the retention time or structural similarity. The quantification of trace compounds in complex matrices such as beer should preferably be performed with SIDA, especially in combination with selective isolation techniques. Briefly, HS-SPME coupled with suitable ISTDs enables analytical assays with excellent stability.<sup>28,61</sup>

#### 1.4 Research Objectives

Beer flavor and flavor stability are the most demanding quality aspects in the brewery. The aim of this thesis is to develop and test improved analytical assays for important but challenging beer aroma compounds. The introduction of novel HS-SPME-GC-MS/MS assays can help to understand which raw material-related or technological factors have positive or negative influences on the overall beer aroma. Within the scope of this thesis, the following three objectives are to be achieved:

1. The first aim is to develop a HS-SPME-GC-MS/MS based methodology for the quantification of selected hop aroma compounds in beer, covering a wide concentration range. It is intended to ensure that this method is applied to lightly hopped Lagers as well as highly dry-hopped beers. To reach this objective, suitable stable isotope standards will first be synthesized and characterized. Furthermore, possible advantages of MRM in beer flavor analysis will be investigated. Common SPME-related drawbacks (e.g., short fiber-lifetimes, poor calibration consistency) need to be examined for their validity regarding the novel HS-SPME-GC-MS/MS method.

2. Currently, HS-SPME-GC-MS methods with on-fiber derivatization (OFD) are widely used for the detection of undesired aged aroma compounds. Part two of this thesis aimed to develop an OFD-HS-SPME-GC-MS/MS assay for more sensitive and stable quantification of staling aldehydes in wort and beer. In order to verify this, a comparative study of the newly developed assay with the OFD-HS-SPME-GC-EI-MS approach will be performed. To reliably monitor flavor changes during beer aging, the assay requires an excellent long-term stability.
3. The objective of the third part is to develop an OFD-HS-SPME-GC-MS/MS approach for simple thiol analysis from beer. To date, there is no established method available for the quantification of 4MMP, 3MH, and 3MHA in beer matrix that reaches the required sensitivity without a time-consuming sample preparation, the use of solvents, or mercury-containing reagents. In order to reliably quantify thiols at ng/L levels in a complex matrix such as beer, a suitable optimization of many OFD-HS-SPME and MRM parameters are required to achieve this objective.

## 2 Publication A

# Analysis of Selected Hop Aroma Compounds in Commercial Lager and Craft Beers Using HS-SPME-GC-MS/MS

### Summary

The development of a HS-SPME-GC-MS/MS based analytical assay as well as the synthesis of d<sub>5</sub>-linalool, d<sub>2</sub>-myrcene, and d<sub>6</sub>-citronellol for the quantification of 16 selected hop aroma compounds is presented. The validated method was shown to be applicable to both lightly hopped Lager beers and hop forward beer styles such as IPA. It has been demonstrated that using MRM mode, sample volumes can be decreased, which extends the fiber lifetime due to the reduced amount of volatiles adsorbed onto the fiber. In combination with suitable ISTDs, the assay provides excellent stability that is not affected by e.g. fiber-to-fiber variations. Considering that GC-MS/MS is not yet widely used in beer analysis, the individual steps of MRM optimization were discussed in detail.

**Author Contributions:** J.D. developed and validated analytical assay, performed analytics, analyzed and visualized data, conceptualized paper, wrote and edited paper; S.T. supported in method development and validation; A.M. performed synthesis and NMR measurements; N.R. interpreted data, conceptualized paper, reviewed and edited paper

## **Publication A**

**Dennenlöhner, J; Thörner, S; Manowski, A; Rettberg, N. Analysis of Selected Hop Aroma Compounds in Commercial Lager and Craft Beers Using HS-SPME-GC-MS/MS. *J. Am. Soc. Brew. Chem.* 78(1), 16–31, 2020.**

This is an Accepted Manuscript of an article published by Taylor & Francis in Journal of the American Society of Brewing Chemists on 18 November 2019, available online: <https://www.tandfonline.com/doi/10.1080/03610470.2019.1668223>.

# Analysis of Selected Hop Aroma Compounds in Commercial Lager and Craft Beers Using HS-SPME-GC-MS/MS

Johanna Dennenlöhr, Sarah Thörner, Aneta Manowski, and Nils Rettberg<sup>1</sup>

Research Institute for Beer and Beverage Analysis, Versuchs- und Lehranstalt für Brauerei in Berlin (VLB) e.V., Seestr. 13, 13353 Berlin, Germany

<sup>1</sup>Corresponding author. E-mail: n.rettberg@vlb-berlin.org; phone: +49 30 45080106.

## Abstract

In recent years, hop aroma emerged as a key quality characteristic of popular beer styles. Accordingly, the instrumental analysis of hop derived odorants in beer advanced as a must have analytical technique for research and quality control purposes. Still, the analysis of hop aroma compounds is challenging. Substance concentrations might strongly vary depending on the beer style, matrix effects might hinder reliable quantification, and SPME-GC-MS based protocols are suspected to lack (long-term) stability. The current paper describes the validation and application of a headspace solid-phase microextraction (HS-SPME) – gas chromatography (GC)– tandem mass spectrometry (MS/MS) method for analysis of 16 selected hop aroma compounds in beer. To enable rapid and reliable quantification of selected terpenes, terpenoids, and esters across a wide working range (1 - 1000 µg/L) instrumental parameters were optimized and three stable isotope labeled standards, namely d<sub>5</sub>-linalool, d<sub>2</sub>-myrcene, and d<sub>6</sub>-citronellol, were synthesized and characterized by nuclear magnetic resonance (NMR) spectroscopy. Extensive method validation and routine application proves the excellent selectivity, sensitivity, and robustness of the method in all relevant matrices such as light hopped lagers and dry-hopped ales.

**Keywords:** beer flavor, hop aroma, HS-SPME-GC-MS/MS, tandem mass spectrometry, terpenes

## Introduction

Hoppy beer flavor is a complex phenomenon that relates to the transfer of hop oil constituents from hops into wort or beer, as well as multiple (bio-) chemical modifications some of these volatiles undergo throughout the brewing process. In brief, the occurrence of hoppy characteristics in beer depends on numerous factors such as hop variety, the amount of hops added, the type of hop product used, and on the timing of the hop dosage. Whereas lager beers are usually produced by adding a single hop dosage during the boil, many hop forward beer styles

such as India pale ales (IPAs) are created by adding multiple and preferably late hop dosages. In these beer styles, hops are added towards the end of the boil, to the whirlpool, and to the green and/or bright beer (dry hopping). Dry hopping might be a static or dynamic process in which contact times can range from several hours up to several days. Depending on the hopping regime, the concentration of hop-derived odorants in beer differs significantly.<sup>1,2</sup> Subtle or distinct hop aroma is present in pilsner or pale lager style beer. Here, the concentration of any hop-derived volatile hardly exceeds concentrations of 10 µg/L. In contrast to this,

many popular dry-hopped beers contain high levels of hop aroma compounds, concentrations of some compounds reach several hundred ppb or low ppm range.

Today, hop aroma is a key quality characteristic of many popular beer styles and reproducible aromas (batch-to-batch consistency) is a concern of many brewers. Scientifically, there exists considerable interest in gaining a global understanding of hoppy beer flavor by linking results of instrumental analysis with sensory. In addition to the complexity hop aroma itself, the analysis of hop derived volatiles in beer remains challenging to researchers and quality management staff in breweries.<sup>1</sup> Up to today, there exists no validated EBC, ASBC, or BCOJ standard method for hop aroma compounds in beer. Instead, there exist multiple analytical tools and routes for hop aroma analysis.<sup>1</sup> One of the most frequently employed assays is HS-SPME coupled to GC-MS.<sup>3,4</sup> HS-SPME is a suitable alternative to other time consuming, extraction and enrichment procedures such as simultaneous distillation extraction (SDE)<sup>5</sup> and appears to be more flexible than other modern micro extraction techniques such as stir-bar-sportive extraction (SBSE). Even though HS-SPME has many advantages (e.g. automation, no need for harmful solvents), there exist technical limitations associated to its nature of being a so-called “non-exhaustive equilibrium extraction technique”. When applied for quality control purposes, robust quantification of key analytes over long periods is required and changes in the extraction system (fiber aging or fiber-to-fiber variation) as well as matrix interferences challenge the analyst. In order to assure analytical consistency (required to prove product consistency), suitable calibration routines using internal standards are required.<sup>6</sup> A proper internal standard, which is chemically similar to the analyte of interest, keeps the quantification robust, as changes in extraction conditions (and different matrices) affect the standard and the analyte in a similar fashion. Internal standards, in combination with GC-MS,

especially stable isotope standards fulfil the demands of modern quality control systems.<sup>7,8</sup> However, some analytes are not commercially available in isotopically labelled form, or are prohibitively expensive.

### **Gas chromatography-tandem mass spectrometry**

Today, GC-MS is employed to investigate multiple beer flavor related questions. It is sometimes used in untargeted profiling, but more importantly for quantitative analysis. Decreasing instrument prices led to the fact that quadrupole GC-MS found its way into many well-equipped brewery laboratories. Here, they are used for analysis of fermentation by products, vicinal diketones, staling aldehydes, and hop aroma compounds. Recent technical progress yielded a new generation of GC-MS instruments, namely GC triple quadrupole (QQQ) instruments, also called GC tandem MS or GC-MS/MS. MS/MS instruments are generally made up by coupling of mass spectrometers, in triple quadrupole instruments three quadrupoles are interfaced. By using these quadrupoles in different modes, either molecular structures can be elucidated or sets of defined analytes can be quantified. For trace level quantification, the most common MS/MS experiment is the so-called multiple reaction monitoring (MRM). In MRM, precursor ions are separated by their mass-to-charge ratio ( $m/z$ ) and are then subjected to collision-induced dissociation (CID). By CID, the precursor ions undergo further fragmentation, the resulting fragment ions (product ions) are then separated and detected in a second stage of mass spectrometry. The quadrupoles 1 and 3 of a triple quadrupole instruments work in (coordinated) selected ion monitoring programs, whereas quadrupole 2 is used for CID. A set of precursor and product ions is called (MRM) transition and at least two transitions per target compound are commonly examined. The peak area resulting from the “quantitative transition” is used for quantification, whereas the peak area of the

“qualitative transition” is used to confirm compound identity. MRM mode enhances the signal to noise ratio and consequently the sensitivity and selectivity of analytical methods.<sup>9,10</sup> Whereas interfacing of triple quadrupole mass spectrometers with liquid chromatography is established in various fields of research including brewing science, GC-MS/MS is not. This is due to the fact that GC-MS/MS instruments are rather costly and the performance of GC single quadrupole instruments meet the requirements of many analysts. However, it is important to note that GC-MS/MS is beneficial in the analysis of low concentrated compounds in complex matrices and offers substantial advantages over single quadrupole GC-MS.<sup>11,12</sup>

### **Aim of the current paper**

The work described in the current paper aimed to develop and validate HS-SPME-GC-MS/MS based methodology for quantification of selected hop aroma compounds in beer. The method to be developed aimed to cover a wide concentration range (1-1000 µg/L) and to be applicable to all relevant matrices ranging from light lagers to highly dry-hopped beer. The methodology should include the compilation of a practical calibration routine, as well as the synthesis and characterization of suitable stable isotope standards for quantification of key analytes. The application of the method to a large sample set aimed to prove its versatility and stability, as well as to underline advantages of GC-MS/MS based beer flavor analysis.

## **Experimental**

### **Chemicals**

α-pinene (98 %), β-pinene (99 %), myrcene (>95 %), limonene (97 %), linalool oxide (mixture of 54% *cis*-isomers and 46% *trans*-isomers) (>97 %), linalool (97 %), citronellol (99 %), nerol (97 %), geraniol (98 %), geranyl acetate (>95 %), β-caryophyllene (>95 %), α-humulene (96 %), and caryophyllene oxide (>98,5 %) were

obtained from Sigma-Aldrich (Steinheim, Germany). α-terpineol (>98 %) was purchased from Merck (Darmstadt, Germany) and 2-methylbutyl isobutyrate (>95 %) from aromaLAB (Planegg, Germany). From all above listed compounds, the analyte mixture was prepared in ethanol (myrcene was previously dissolved in ethyl acetate). Ethanol absolute, ethyl acetate and sodium chloride (NaCl) were of analytical grade and were purchased from Th. Geyer (Berlin, Germany).

Chemicals and solvents listed in *Internal standard synthesis and characterization* were purchased from Sigma-Aldrich, Merck, VWR (Dresden, Germany), and abcr (Karlsruhe, Germany). For NMR, deuteriochloroform (CDCl<sub>3</sub>) (99.8 atom % D) was purchased from Roth (Karlsruhe, Germany), deuterium oxide (D<sub>2</sub>O) (99.96 atom % D) was purchased from VWR, and d<sub>6</sub>-benzene (C<sub>6</sub>D<sub>6</sub>) (99.6 atom % D) was purchased from Sigma-Aldrich.

### **Internal standard synthesis and characterization**

Three stable isotope labeled standards (ISTD), namely d<sub>2</sub>-myrcene, d<sub>5</sub>-linalool, and d<sub>6</sub>-citronellol were synthesized and characterized (purity and stability) by means of GC-EI-MS and NMR spectroscopy.

D<sub>2</sub>-myrcene was selected because myrcene is the most abundant monoterpene of hop essential oil.<sup>13</sup> As it is a nonpolar analyte, its transfer into beer but also its analysis is challenging. Several in-house investigations have shown that myrcene binds comparatively strongly to the DVB/CAR/PDMS fiber and a quantification via a polar ISTD leads to false results (too high concentrations). As the second ISTD d<sub>5</sub>-linalool was selected. Its unlabeled isotopologue linalool is considered as a key aroma compound of hops and hoppy beer.<sup>13,14</sup> Also, in contrast to myrcene, it is a more polar compound. To enable reliable quantification of citronellol, nerol, and geraniol, which have related structures (nerol and geraniol are configuration isomers) and similar retention behavior,

$d_6$ -citronellol was synthesized. Compared to nerol and geraniol, citronellol has a higher molecular weight. This has the practical advantage that the precursor ions of

$d_6$ -citronellol do not overlap with any other precursor ions. Figure 1 shows the GC-EI mass spectra of the three ISTD and their corresponding unlabeled analogues.

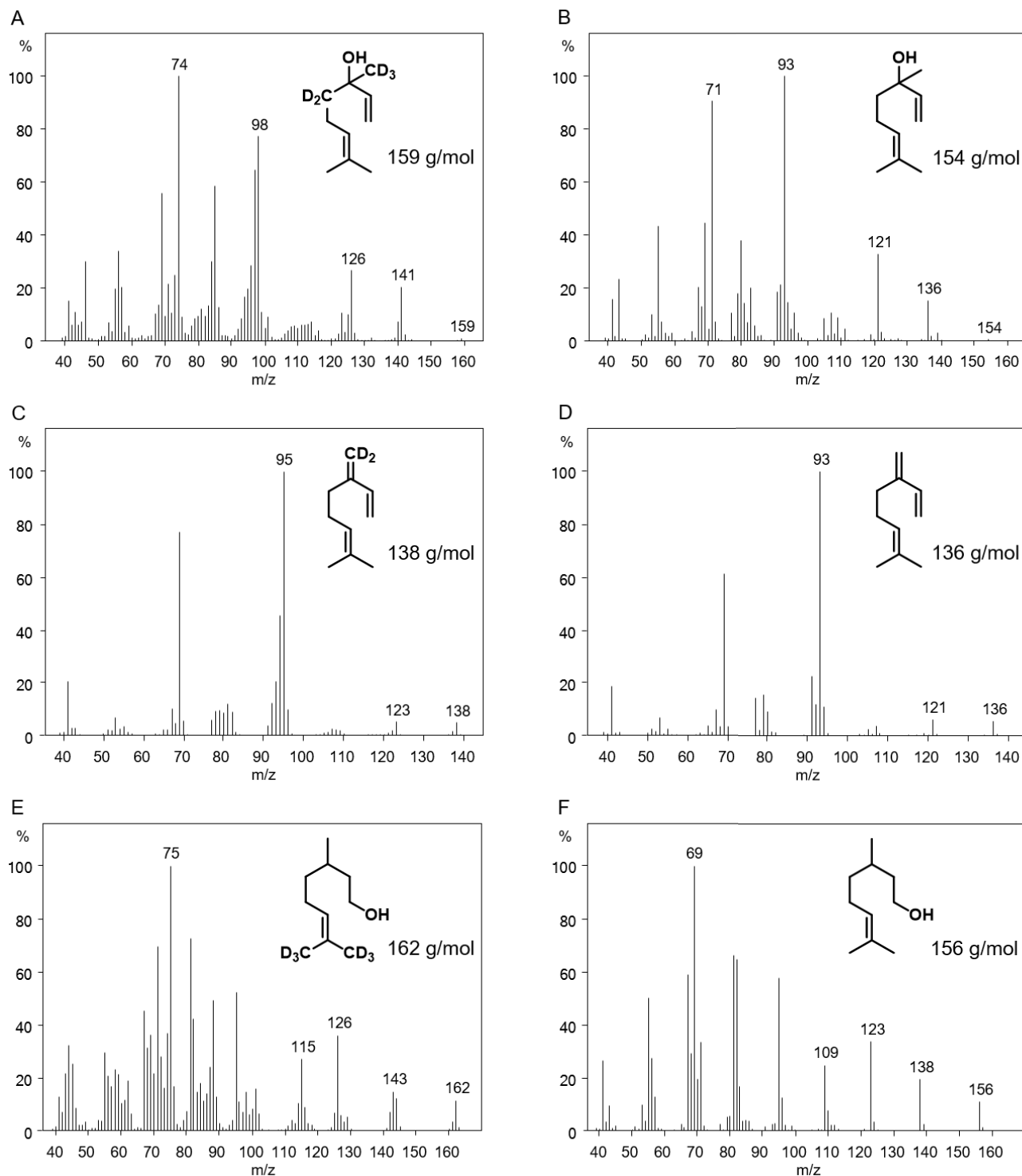


**Figure 1. Electron impact mass spectra of  $d_5$ -linalool (A), linalool (B),  $d_2$ -myrcene (C), myrcene (D),  $d_6$ -citronellol (E), and citronellol (F). The intensity relative to the base peak is plotted against the mass-to-charge ratio (m/z). Labeled ions show a mass shift indicating the presence of deuterium labels.**

NMR spectra were recorded in  $\text{CDCl}_3$ ,  $\text{D}_2\text{O}$ , and  $\text{C}_6\text{D}_6$  using a Bruker Avance II 400 ( $^1\text{H}$ , 400 MHz) spectrometer at room temperature. The chemical shifts ( $\delta$ ) were referenced versus residual solvent shifts in parts per million (ppm). The coupling constants ( $J$ ) are reported in Hertz (Hz). Signal multiplicities are indicated as follows: singlet (s), doublet (d), triplet (t), quartet (q), multiplet (m) and broad (br).

**D<sub>5</sub>-linalool.** The GC-MS spectrum of linalool (Figure 1B) shows two predominant fragment ions,  $m/z=93$  (base peak) and  $m/z=71$ . Since the most intensive fragment ions contain either the methyl group or the methylene group in  $\alpha$ -position to hydroxyl group, the deuteration was introduced in these positions. The fully labeled methyl group and methylene group in  $\alpha$ -position to hydroxyl group lead to the corresponding labeled fragment ions,  $m/z=98$  and  $m/z=74$ . Figure 2 shows exemplary the fragmentation of  $d_5$ -linalool in the MRM mode. The product ions of  $d_5$ -linalool are determined by submitting both most abundant precursor

ions ( $m/z=74$  and  $m/z=98$ ) to CID. *Rac*-3,7-[10,10,10- $^2\text{H}_3$ ]dimethyl-1,6-[4,4- $^2\text{H}_2$ ]octadien-3-ol ( $d_5$ -linalool) was synthesized according to the method of Kreck et al.<sup>15</sup> yielding 65 % over two steps, which was 60 % more than the yield based on the literature. In brief, the reaction involved a hydrogen/deuterium exchange of a ketone precursor (6-methyl-5-hepten-2-one, 1.000 g, 7.92 mmol) in basic medium by sodium methanolate to 6-methyl-5-[1,1,1,3,3- $^2\text{H}_5$ ]hepten-2-one (0.816 g, 6.22 mmol, 79 % yield). Subsequent Grignard reaction of 6-methyl-5-[1,1,1,3,3- $^2\text{H}_5$ ]hepten-2-one (0.538 g, 4.10 mmol) with vinylmagnesium chloride obtained  $d_5$ -linalool (0.539 g, 3.38 mmol, 82 % yield).

$^1\text{H}$ -NMR (400 MHz,  $\text{CDCl}_3$  with one drop of  $\text{D}_2\text{O}$ , 25 °C):  $\delta$  (ppm) = 5.91 (dd,  $J$  = 17.4, 10.8 Hz, 1H, H-2), 5.21 (dd,  $J$  = 17.4, 1.3 Hz, 1H, H-1 $_{trans}$ ), 5.12 (t,  $J$  = 7.2 Hz, 1H, H-4), 5.06 (dd,  $J$  = 10.8, 1.3 Hz, 1H, H-1 $_{cis}$ ), 2.06–1.95 (m, 2H, H-3), 1.68, 1.60 (d,  $J$  = 1.0 Hz and br s, 2 x 3H, H-5 and H-6).

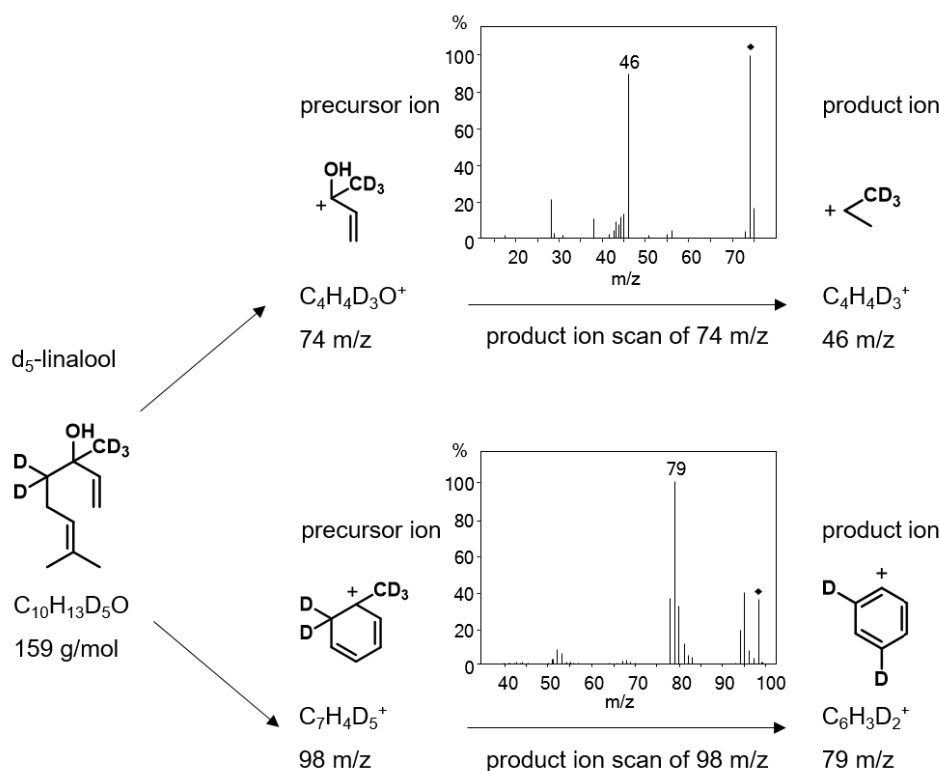


**Figure 2.** Possible fragmentation pattern of  $d_5$ -linalool for the selected transitions 74→46 m/z and 98→79 m/z.

**D<sub>2</sub>-myrcene.** For the synthesis of d<sub>2</sub>-myrcene, the deuteration was intended to be introduced at the 3-methylene position, which is part of the base peak forming ions (m/z=93). Labeling was reached by orthoester Johnson-Claisen rearrangement, 2-methyl-3-butene-2-ol and triethylacetate were converted with catalytic acetic acid to ethyl 5-methyl-4-hexenoate. 5-Methyl-4-hexenoic acid was prepared by saponification of ethyl 5-methyl-4-hexenoate. The ketone 7-methyl-1,6-octadiene-3-one is formed in a Grignard reaction of vinylmagnesium bromide with the Weinreb amide of 5-methyl-4-hexenoic acid. By Wittig reaction of 7-methyl-1,6-octadiene-3-one and d<sub>3</sub>-methyltriphenylphosphonium iodide, d<sub>2</sub>-myrcene is obtained in 6 to 10 % yield, which is acceptable in the lab-scale.

<sup>1</sup>H-NMR (400 MHz, C<sub>6</sub>D<sub>6</sub>, 25 °C): δ (ppm) = 6.37 (dd, *J* = 17.6, 10.9 Hz, 1H, H-2), 5.22–5.17 (m, 1H, H-5), 5.21 (dd, *J* = 17.6, 1.1 Hz, 1H, H-1*trans*), 4.97 (dd, *J* = 10.8, 1.1 Hz, 1H, H-1*cis*), 2.27–2.18 (m, 4H, H-3 and H-4), 1.65, 1.51 (2 x br s, 2 x 3H, H-6 and H-7).

**5-Methyl-4-hexenoic acid.** For the orthoester Johnson-Claisen rearrangement, 2-methyl-3-butene-2-ol (4.000 g, 46.44 mmol), triethyl orthoacetate (22.603 g, 139.32 mmol), and a catalytic amount of acetic acid (0.279 g, 4.64 mmol, 10 mol%) were placed in a tabletop autoclave at 180 °C (18-20 bar) for 14.5 h. After dilution of the reaction mixture in diethyl ether (75 mL), the organic layer was washed with saturated NaHCO<sub>3</sub> solution and brine, dried over Na<sub>2</sub>SO<sub>4</sub>, filtered, and the solvents were evaporated in vacuo. The crude ethyl 5-methyl-4-hexenoate was dissolved in methanol (165 mL), 6.25 M aqueous NaOH solution (40 mL) was added, and the solution was heated under reflux for 14.5 h. The methanol was subsequently removed in vacuo, water (50 mL) was added, and the aqueous layer was extracted three times with diethyl ether (the organic layers were disposed). Afterwards the aqueous layer was acidified using diluted hydrochloric acid and extracted four times with diethyl ether. The combined organic extracts were washed with brine, dried over Na<sub>2</sub>SO<sub>4</sub>, filtered, and

concentrated in vacuo to yield crude 5-methyl-4-hexenoic acid (5.022 g, 39.18 mmol, 84 % yield over two steps).

***N*-Methoxy-*N*-methyl-5-methyl-4-hexenamamide (Weinreb amide of 5-methyl-4-hexenoic acid).** To a stirred solution of 5-methyl-4-hexenoic acid (4.356 g, 33.99 mmol) in chloroform (75 mL), triethylamine (4.74 mL, 34.00 mmol) was added, followed by a slow addition of pivaloyl chloride (3.80 mL, 30.85 mmol). After stirring for 4 h at room temperature it was cooled to 0 °C where *N,O*-dimethylhydroxylamine hydrochloride (3.315 g, 33.99 mmol) and a catalytic amount of 4-(dimethylamino)pyridine were added. Then triethylamine (12.31 mL, 88.32 mmol) was slowly added (1 mL/min). The reaction mixture was stirred for 2 h at 0 °C, washed with water, and extracted with chloroform. The organic extract was washed with 0.4 M sulfuric acid, water, and 10 % Na<sub>2</sub>CO<sub>3</sub> solution, dried over Na<sub>2</sub>SO<sub>4</sub>, filtered, and concentrated in vacuo. The purification by column chromatography yielded the Weinreb amide of 5-methyl-4-hexenoic acid (2.520 g, 14.72 mmol, 48 % yield).

**7-Methyl-1,6-octadiene-3-one.** For the Grignard reaction, a solution of the Weinreb amide of 5-methyl-4-hexenoic acid (1.234 g, 7.206 mmol) in absolute diethyl ether (25 mL) was cooled to 0 °C and stirred under nitrogen atmosphere. To this solution, 1.6 M solution of vinylmagnesium chloride in tetrahydrofuran (6.8 mL, 10.81 mmol) was added over 20 min and stirred for 30 min at 0 °C. Afterwards the reaction mixture was stirred at room temperature for 1.5 h, washed with 0.5 M sulfuric acid. The aqueous layer was extracted twice with diethyl ether. The combined organic extracts were washed with water, saturated NaHCO<sub>3</sub>, and brine, dried over Na<sub>2</sub>SO<sub>4</sub>, filtered, and finally concentrated in vacuo. The purification by column chromatography yielded 7-methyl-1,6-octadiene-3-one (0.927 g, 6.707 mmol, 93 % yield).

**[<sup>2</sup>H<sub>3</sub>]Methyl(triphenyl)phosphonium iodide (d<sub>3</sub>-methyltriphenylphosphonium iodide).** The deuterated starting material was prepared

from  $d_3$ -methyl iodide (4.566 g, 31.50 mmol), which was added dropwise to a stirred solution of triphenylphosphine (7.500 g, 28.59 mmol) in acetone (35 mL). The suspension was stirred for 45 min, then cooled to  $-20\text{ }^\circ\text{C}$ . The resulting white precipitate,  $d_3$ -methyltriphenylphosphonium iodide, was recovered by filtration and dried at  $80\text{ }^\circ\text{C}$  (11,003 g, 27.02 mmol, 95 % yield).

**7-Methyl-3- $^{2}\text{H}_2$ methylene-1,6-octadiene ( $d_2$ -myrcene).** For the Wittig reaction, a suspension of  $d_3$ -methyltriphenylphosphonium iodide (3.939 g, 9.67 mmol) in absolute tetrahydrofuran (64 mL) was prepared under nitrogen atmosphere and cooled to  $0\text{ }^\circ\text{C}$ . To this suspension, 1.6 M *n*-butyllithium in *n*-hexane (5.58 mL, 8.93 mmol) was added over 18 min and stirred for 30 min at  $0\text{ }^\circ\text{C}$ . 7-methyl-1,6-octadiene-3-one (1.028 g (collected from several approaches of the previously described procedures), 7.44 mmol) in absolute tetrahydrofuran (6.50 mL) was added over 7 min. After stirring for another 10 min at  $0\text{ }^\circ\text{C}$ , the reaction mixture was warmed to room temperature over 35 min. The reaction mixture was diluted with diethyl ether (6 mL), water (25 mL) was added, and the layers were separated. The aqueous layer was extracted two more times with diethyl ether and the combined organic layers were washed with brine, dried over  $\text{Na}_2\text{SO}_4$ , filtered, and concentrated in vacuo ( $40\text{ }^\circ\text{C}$ , 300 mbar). *n*-Pentane (15 mL) was added onto the residue, the precipitated triphenylphosphine oxide was filtered off, washed with *n*-pentane, and concentrated in vacuo again. The purification by column chromatography yielded  $d_2$ -myrcene (105.3 mg, 0.76 mmol, 10 % yield).

**$D_6$ -citronellol.** The general strategy for labelling of open-chain terpene-alcohols, here  $d_6$ -citronellol, is taken from Sen and Garvin.<sup>16</sup> It leads to a  $d_6$ -labelling on the two terminal methyl groups that are part of the prenyl structure motive of these molecules. The  $d_6$ -labeled citronellol was synthesized from the corresponding unlabeled

compound. After the hydroxyl group has been protected as triisopropylsilyl (TIPS) ether, the terminal isopropylidene group of unlabeled citronellol is split off chemically and selectively. To achieve this, the terminal isopropylidene group of the *O*-TIPS-citronellol needed to react in two steps with AD-mix- $\alpha$  or  $\beta$  (1,2-diol generation) and finally with sodium metaperiodate in a methanol/water mixture (diol scission). The deuterated alkyl bromide precursor  $d_7$ -2-bromopropane is converted in a tabletop autoclave to the corresponding phosphonium salt ( $d_7$ -isopropyltriphenylphosphonium bromide). Then the isopropylidene group was reintroduced in a Wittig reaction of 4-methyl-6-[(triisopropylsilyloxy]hexanal and  $d_7$ -isopropyltriphenylphosphonium bromide. The last step was the deprotection of the triisopropylsilyl group with tetra-*n*-butyl ammonium fluoride (TBAF) in tetrahydrofuran, obtaining selectively terminally hexadeuterated  $\beta$ -citronellol in 57 % overall yield.

$^1\text{H-NMR}$  (400 MHz,  $\text{CDCl}_3$  with one drop of  $\text{D}_2\text{O}$ ,  $25\text{ }^\circ\text{C}$ ):  $\delta$  (ppm) = 5.09 (t,  $J = 7.2\text{ Hz}$ , 1H, H-7), 3.72–3.62 (m, 2H, H-1), 2.08–1.90 (m, 2H, H-6), 1.65–1.63 (m, 2H, H-2 and H-3), 1.43–1.30 (m, 2H, H-2' and H-5), 1.24–1.13 (m, 1H, H-5'), 0.90 (d,  $J = 6.6\text{ Hz}$ , 3H, H-4).

**Triisopropyl[(3,7-dimethyl-6-octen-1-yl)oxy]silane (*O*-TIPS-citronellol).** For the introduction of TIPS protecting group,  $\beta$ -citronellol (3.39 mL, 18.45 mmol), 4-dimethylaminopyridine (2.426 g, 21.49 mmol), and imidazole (0.219 g, 3.21 mmol, 20 mol%) were dissolved in absolute *N,N*-dimethylformamide (40 mL). Triisopropylsilyl chloride (3.42 mL, 16.04 mmol) was added slowly and the reaction mixture was stirred for 20 h at room temperature. The suspension was diluted with water (100 mL) and extracted with *n*-pentane. The combined organic layers were washed with 5 % citric acid and water, dried over  $\text{Na}_2\text{SO}_4$ , filtered, and concentrated in vacuo. The purification by column chromatography provided the *O*-TIPS

protected citronellol (4.734 g, 15.14 mmol, 94 % yield).

*2,6-Dimethyl-8-[(triisopropylsilyl)oxy]octane-2,3-diol (1,2-diol)*. For the dihydroxylation of the alkene, *O*-TIPS-citronellol (7.508 g (from several approaches), 24.02 mmol) was dissolved in *tert*-butanol/water (1:1, 192 mL), methanesulfonamide (2.331 g, 24.51 mmol) was added to the stirred solution, and finally an excess of AD mix (40 g) was added. The orange-yellow suspension was left to stir at room temperature for 28 h. The reaction mixture was diluted with water (300 mL) and extracted with ethyl acetate. To the aqueous layer, solid Na<sub>2</sub>SO<sub>3</sub> (20 g) was added and it was extracted three times with ethyl acetate. The combined organic extracts were washed with a solution of 10 % trisodium citrate dehydrate, dried over Na<sub>2</sub>SO<sub>4</sub>, filtered, and concentrated in vacuo. Then *n*-pentane (100 mL) was added, the precipitate was filtered off, and the solution was concentrated in vacuo yielding 1,2-diol (8.085 g, 23.32 mmol, 97 % yield), which was used without further purification.

*4-Methyl-6-[(triisopropylsilyl)oxy]hexanal*. To a stirred solution of the 1,2-diol (7.977 g, 23.01 mmol) in methanol (180 mL), sodium metaperiodate (5.180 g, 24.22 mmol) dissolved in water (70 mL) was added and stirred for 9 h at room temperature. The reaction mixture was diluted with water (250 mL) and extracted two times with petroleum ether. The combined organic extracts were dried over Na<sub>2</sub>SO<sub>4</sub>, filtered, and concentrated in vacuo. The crude product was purified by column chromatography to obtain 4-methyl-6-[(triisopropylsilyl)oxy]-hexanal (5.872 g, 20.49 mmol, 89 % yield).

*2-[<sup>2</sup>H<sub>7</sub>]Propanyl(triphenyl)phosphonium bromide (d<sub>7</sub>-isopropyltriphenylphosphonium bromide)*. The deuterated starting material was prepared in a tabletop autoclave. The triphenylphosphine (7.904 g, 30.13 mmol) was dissolved in toluene (50 mL), d<sub>7</sub>-2-bromopropane (3.4 mL, 36.16 mmol) was added, and the reaction mixture was left to stir for 72 h at 160 °C (8 bar). The resulting

salt was dissolved in methanol and concentrated in vacuo. Ethyl acetate was added, d<sub>7</sub>-isopropyltriphenylphosphonium bromide was crashed with a glass rod, filtered off, washed with ethyl acetate, and dried at 80 °C (11.585 g, 29.53 mmol, 98 % yield).

*Triisopropyl[(3-methyl-7-[<sup>2</sup>H<sub>3</sub>]methyl-6-[8,8,8-<sup>2</sup>H<sub>3</sub>]octen-1-yl)oxy]silane (O-TIPS-d<sub>6</sub>-β-citronellol)*. For the Wittig reaction, d<sub>7</sub>-isopropyltriphenylphosphonium bromide (4.441 g, 11.32 mmol) was suspended in absolute tetrahydrofuran (55 mL) under nitrogen atmosphere. After cooling to 0 °C, a solution of 1.6 M methyllithium in diethyl ether (6.97 mL, 11.15 mmol) was slowly added and stirred for 30 min at 0 °C under nitrogen atmosphere. Then a solution of 4-methyl-6-[(triisopropylsilyl)oxy]hexanal (2.494 g, 8.70 mmol) in absolute tetrahydrofuran (5 mL) was added slowly. The reaction mixture was warmed to room temperature and stirred for 30 min. The suspension was transferred in a separating funnel with ethyl acetate (50 mL) and water (100 mL) and the layers were separated. The aqueous layer was extracted one more time with ethyl acetate and the combined organic layers were dried over Na<sub>2</sub>SO<sub>4</sub>, filtered, and concentrated in vacuo. To the residue, *n*-pentane (50 mL) was added, the precipitated triphenylphosphanoxide was filtered off, washed with a small amount of *n*-pentane, and concentrated in vacuo again. The purification by column chromatography yielded *O*-TIPS-d<sub>6</sub>-β-citronellol (2.173 g, 6.82 mmol, 78 % yield).

*3-Methyl-7-[<sup>2</sup>H<sub>3</sub>]methyl-6-[8,8,8-<sup>2</sup>H<sub>2</sub>]octen-1-ol (d<sub>6</sub>-citronellol)*. For the removal of the protecting group, *O*-TIPS-d<sub>6</sub>-citronellol (0.884 g, 2.77 mmol) was dissolved in absolute tetrahydrofuran (7 mL). A solution of 1.0 M TBAF in tetrahydrofuran (5 mL, 5.00 mmol) was added, before the reaction mixture was left to stir for 20 h at room temperature. The reaction mixture was added into a mixture of diethyl ether (25 mL) and 6 % NaH<sub>2</sub>PO<sub>4</sub>·2H<sub>2</sub>O solution (25 mL). The layers were separated and the aqueous layer

was extracted two more times with diethyl ether. The combined organic layers were dried over Na<sub>2</sub>SO<sub>4</sub>, filtered, and concentrated in vacuo. The purification by column chromatography provided d<sub>6</sub>-citronellol (0.415 g, 2.56 mmol, 92 % yield).

### Beer samples

Within this study more than 200 beer samples, mostly lager beers or dry-hopped ales, were analyzed. Whereas most of the dry-hopped ales originated from the USA and Germany, lager beers were either from European, Asian or African countries.

### Sample preparation

Beer samples (20 mL) were transferred in a 50 mL Schott flask. The flask was loosely sealed by a screw cap and placed in a refrigerator (4°C) for 30 min. This procedure was chosen to reduce the carbon dioxide level in beer in order to ensure bubble-free and accurate pipetting of small volumes. After decarbonization two replicates each consisting of 1 mL sample, 0.4 ± 0.1 g NaCl, and 20 µL of an ethanolic ISTD solution (d<sub>2</sub>-myrcene, d<sub>5</sub>-linalool and d<sub>6</sub>-citronellol each 5 mg/L) were transferred into 10 mL headspace vials. The vials were sealed with magnetic screw caps (silicone/PTFE septum) and were then placed on the GC-autosampler.

### Matrix matched calibration and quantification

Calibration was carried out according to the so-called standard addition method. This method requires a base beer with low concentrations of the respective target analytes. For this purpose, a pilsner beer produced by a large-scale industrial brewery was chosen. The beer has consistent levels of 2-4 µg/L for myrcene, linalool, α-terpineol, and geraniol; other hop-derived volatiles are absent. To record calibration curves, 1 mL aliquots of this decarbonated base beer were mixed with 0.4 g ± 0.1 g NaCl, and 20 µL of ISTD solution in 10 mL headspace vials. This mixture was then spiked by adding the analyte mixture at concentration levels of 1,

2, 5, 10, 20, 50, and 100 µg/L plus a blank (pilsner beer 0 µg/L added). For dry-hopped products, three additional calibration points (200, 500, and 1000 µg/L) were added. After spiking with the ethanolic analyte mixture, an ethanol content of 5-7.5 % is obtained in the individual calibration points. This corresponds to the ethanol range in commonly found in beer.

The area ratios of the blank (pilsner beer) to ISTD, which represents the concentration of the existing hop aroma compound in the base beer, were subtracted for each analyte from every calibration point. The fitted area ratios were then plotted against the concentration ratio of analyte against ISTD and in a linear model, curve slope and y intercept were calculated. Since the calibration is a matrix calibration, the concentration of the analyte has been corrected by the value calculated for an area of zero ( $C_{\text{area } 0}$ ). This ensures that the concentration of the analytes is zero, if there is no analyte peak detected in the samples.

The four monoterpenes α-pinene, β-pinene, myrcene, and limonene are quantified using d<sub>2</sub>-myrcene. d<sub>5</sub>-linalool was used to quantify linalool, 2-methylbutyl isobutyrate, *cis*-linalool oxide, *trans*-linalool oxide, α-terpineol, caryophyllene, α-humulene, and caryophyllene oxide. In principle, the analyte ISTD pairs were assigned considering the retention time or structural similarity. Since an ISTD for the last three analytes is either not available for purchase or is very difficult to synthesize, they are also quantified using d<sub>5</sub>-linalool. Recovery tests and the coefficient of determination of the calibration function have shown that d<sub>5</sub>-linalool is the more suitable ISTD than the later eluting d<sub>6</sub>-citronellol. D<sub>6</sub>-citronellol is used as ISTD for citronellol, nerol, geraniol, and geranyl acetate.

### MRM setup and optimization

The selection of suitable precursor and product ions, as well as the optimization of the CID collision energy to obtain selective transitions with sufficient intensities was

**Table I. Multiple reaction monitoring transitions and retention times of 16 selected hop aroma compounds as well as the three stable isotope labeled standards (bold) used for quantification.**

Compound	Quantitative transition [m/z]	Qualitative transition [m/z]	Retention time [min]*+-	Dwell time [ms]	Quantification by
$\alpha$ -pinene	93→77	121→93	4.42	130	d <sub>2</sub> -myrcene
$\beta$ -pinene	93→77	121→93	5.02	130	d <sub>2</sub> -myrcene
<b>d<sub>2</sub>-myrcene</b>	95→78	123→94	5.14	100	-
myrcene	93→77	121→93	5.16	100	d <sub>2</sub> -myrcene
2-methylbutyl isobutyrate	71→43	70→55	5.49	130	d <sub>5</sub> -linalool
limonene	93→77	121→93	5.73	130	d <sub>2</sub> -myrcene
<i>cis</i> -linalool oxide	94→79	111→93	6.37	130	d <sub>5</sub> -linalool
<i>trans</i> -linalool oxide	94→79	111→93	6.59	130	d <sub>5</sub> -linalool
<b>d<sub>5</sub>-linalool</b>	74→46	98→79	6.68	100	-
linalool	71→43	93→77	6.72	100	d <sub>5</sub> -linalool
$\alpha$ -terpineol	93→77	59→31	8.09	130	d <sub>5</sub> -linalool
<b>d<sub>6</sub>-citronellol</b>	75→44	126→81	8.49	100	-
citronellol	123→81	138→95	8.55	100	d <sub>6</sub> -citronellol
nerol	93→77	121→93	8.58	100	d <sub>6</sub> -citronellol
geraniol	93→77	69→41	8.93	130	d <sub>6</sub> -citronellol
geranyl acetate	93→77	69→41	10.67	130	d <sub>6</sub> -citronellol
$\beta$ -caryophyllene	93→77	133→105	11.30	130	d <sub>5</sub> -linalool
$\alpha$ -humulene	93→77	147→105	11.74	130	d <sub>5</sub> -linalool
caryophyllene oxide	93→77	133→105	13.34	130	d <sub>5</sub> -linalool

\* The average RT is plotted. The shift over two years and with two different columns is  $\pm 0.06$  min.

performed manually. In order to enable unambiguous substance identification, the retention time and the characteristic fragment ions of each hop aroma compound and ISTD were examined individually by a precursor ion scan ( $m/z=29$  to  $m/z=250$ ). Product ions scans were carried out by selecting suitable  $m/z$  precursor ions, whereas one ion was selected for quantification and a second for qualification. MRM transitions that showed selective and characteristic  $m/z$  and provide a high abundance were chosen.

To optimize respective MRM signal intensities, collision energies of 1, 3, 5, 7, 10, 15, and 20 were tested by fivefold and randomized measurements. The final value for collision energy for all analytes is 10 eV. The dwell time was set to record 15-20 data points across each peak (Table I).

### HS-SPME-GC-MS/MS method

**Instrument specifications.** GC-MS/MS analysis was performed on an Agilent Technologies 7890B gas chromatograph interfaced to a 7000C Triple Quadrupole mass spectrometer (Agilent, Santa Clara, CA, USA). This GC-MS/MS setup was equipped with a Gerstel MPS 2XL sampler (GERSTEL, Mühlheim an der Ruhr, Germany) for automated HS-SPME sampling. Agilent MassHunter WorkStation - Qualitative Analysis software (ver. B.07.00) was used for data analysis.

**HS-SPME sampling.** Extraction of volatiles by HS-SPME was reached using a 50/30  $\mu\text{m}$  DVB/CAR/PDMS (Supelco, St. Louis, MO, USA) fiber that was preconditioned according to the manufacturer's instructions. This triple-phase fiber coating with mixed polarity was chosen because many studies have

shown that volatile compounds in beer adsorb well to it.<sup>17,18</sup> For HS-SPME optimization relevant incubation and extraction conditions were varied. Therefore NaCl additions (without, 0.2, and 0.4 g), incubation times (3.5, 5.5, 7.5, 9.5, and 11.5 min), extraction times (3.5, 5.5, 7.5, 9.5, and 11.5 min), and temperatures (40, 45, 50, 55, 60, 65, 70, and 75 °C) were tested.

Final HS-SPME parameters were as follows: the samples were initially incubated at 60 °C and agitated at 500 rpm for 7.5 min. HS-SPME extraction was carried out in 7.5 min at 60 °C with an agitation rate of 500 rpm. The fiber was desorbed for 1 min at 250 °C in the injection port operated in split mode with a split ratio 1:20 (Multimode Inlet System, Agilent) equipped with a 0.75 mm i.d. Ultra Inert SPME Liner (Agilent). To prevent analyte carryover, the SPME fiber was conditioned for 4 min at 250 °C after each extraction.

**GC analysis.** The GC analysis was carried out on a HP-5MS UI column (30 m x 0.25 mm i.d. x 0.25 µm film thickness, Agilent) using helium (99.999 %, AIR LIQUIDE, Düsseldorf, Germany) as mobile phase. The following temperature program was found being optimal: 50 °C raised to 190 °C at a rate of 10 °C/min, followed by a final ramp to 300 °C at 70 °C/min (1 min hold), giving a 16.5 min run time.

**Mass spectrometry.** The MS transfer line temperature was set to 320 °C. Ionization was performed in electron impact (EI) mode at 70 eV, ion source and MS quadrupole temperatures were 230 °C and 150 °C. In the collision cell, the quench gas (helium) was adjusted to a flow of 2.25 mL/min and the collision gas (nitrogen, purity 99.999 %, Air Liquide) to a flow rate of 1.5 mL/min. The gain value for each time segment was set from 0.1 to 10 to adapt to the different response factor of each analyte and to reach a minimum area of approximately 1000 for the smallest calibration point.

### Method validation

The method was validated by determining its linearity (Mandel's fitting test,  $R^2$ ), the limit of detection (LOD), the limit of quantification (LOQ), the accuracy (% Recovery: spiking 5 and 100 µg/L), the measurement precision (%RSD: six fold determination), the laboratory precision (%RSD: different days and analysts), and the robustness (%RSD: measurement of a randomly picked sample at the beginning, in the middle, and at the end of the batch of approx. 20 samples). LOD and LOQ were determined according to the ASBC method for low-level detection.<sup>19</sup> They are defined as  $LOD = \bar{x}_B + 3\sigma$  and  $LOQ = \bar{x}_B + 10\sigma$  ( $\bar{x}_B$ - mean signal of replicate reagent blanks (N = 6),  $\sigma$ - standard deviation of the blank).

### Multivariate analysis

In order to simplify and summarize the results of beer analysis, principal component analysis (PCA) using XLSTAT 2019 (Addinsoft, Long Island, NY, USA) was applied. By reducing the dimensions of the original analysis data matrix, differences between lager and dry-hopped beers but also differences between the beers of each group is well represented. At the same time, the relative contribution of each variable (here the hop aroma compound determined by GC-MS/MS) to this differentiation is described.

## Results and Discussion

### Analyte selection

Amongst multiple of hop-derived volatiles commonly present in commercial beer, 16 volatiles were selected for quantitative analysis. Unlike in GC-MS applications were semi quantification of unknowns (or tentatively identified compounds) is sometimes based on integration of total ion current (TIC) signals, GC-MS/MS in MRM mode requires the availability of pure reference standards for MRM optimization. As there exists no general agreement on a list

of volatiles that suitably describes hop aroma in beer<sup>1</sup> the molecules quantified in published studies differ.<sup>20,21</sup> Consequently, the selection of target compounds for GC-MS/MS analysis was based on the following aims:

- include the primary compounds of hop oil (myrcene,  $\alpha$ -humulene,  $\beta$ -caryophyllene)
- cover the most relevant substance classes commonly associated to hoppy beer flavor (terpenes, terpenoids, and esters)
- capture the most potent (non-thiol) hop derived aroma compounds in beer (linalool, geraniol, and citronellol)
- select substances that are described to correlate with hop related flavors (floral, citrus, fruity, spicy or herbal) in beer
- include markers that enable monitoring of yeast enzyme activity / biotransformation (citronellol)
- trace brewhouse or hop storage induced oxidation of hop derived compounds (linalool oxides and caryophyllene oxides) that correlate with kettle hop flavor

The final analyte selection is shown in Table I and is further discussed below (*Application to beer samples*).

### Method development

**Gas chromatography.** GC optimization was carried out pragmatically, i.e. the temperature gradient aimed to provide baseline separation of the target compounds in a minimized runtime. The temperature gradient described above (50 °C raised to 190 °C at a rate of 10 °C/min, then final ramp to 300 °C at 70 °C/min with 1 min hold time), has a total GC runtime of 16.5 minutes and provided separated peaks for the majority of compounds. As shown in Table I, stable isotope standards (d<sub>2</sub>-myrcene, d<sub>5</sub>-linalool, and d<sub>6</sub>-citronellol) and their respective unlabeled isotopologues (myrcene, linalool, and citronellol) co-elute. Due to the small shift in molecular mass d<sub>2</sub>-myrcene and myrcene show very similar retention on the given column, whereas the existence of five (d<sub>5</sub>-linalool) respectively six deuterium atoms (d<sub>6</sub>-citronellol) causes a detectable

forward shift of both peaks compared to unlabeled linalool and citronellol. Usually, co-elution of analyte and stable isotope standards can be resolved by mass spectrometry, whereas co-elution of unlabeled target analytes can be challenging. In the given chromatographic setup (HP-5MS UI column) the peaks of nerol, citronellol, and d<sub>6</sub>-citronellol overlap and cannot be sufficiently separated by temperature gradient adjustment. Thus, selection of suitable MRM transitions for qualification and quantification (see below) was of prime importance. Considering the GC runtime of 16.5 minutes, as well as additional 3.5 minutes for cool down of the GC oven, the overall duration between two injections is 20 minutes. This setup enables the analysis of three samples per hour and is therefore very appropriate for a routine method employed on a daily basis. Compared to other published assays<sup>4</sup> that target a similar number of analytes this means a reduction of analysis time of more than 50%.

**MRM optimization.** Because of their comparably low flavor thresholds most hop-derived aroma compounds contribute to beer flavor at ppb levels. Whereas terpene analysis by GC-MS can become increasingly difficult at low analyte levels (e.g. in light lagers), GC-MS/MS easily provides the required sensitivity and specificity. Tandem mass spectrometry provides three major parameters that enable an optimized detection across a wide working range and help to overcome challenges in hop aroma analysis:

- 1) Selection of suitable precursor and product ions for MRM minimizes matrix effects and resolves co-elution related issues.
- 2) Selection of suitable CID collision energies for each MRM maximizes the product ion yield.
- 3) Manipulation of the detector gain in MRM time segments amplifies small signals (one time segment might contain multiple MRMs).

By selecting suitable MRM transitions, random signal fluctuations (noise) can be reduced and lower LOD and LOQ can be reached. Although MRM peak areas are smaller than TIC or SIM areas peaks, they commonly appear with considerably increased signal-to-noise ratio. By using MRM, interferences caused by omnipresent, noisy mass traces or coelutions with abundant matrix constituents (e.g. higher aliphatic alcohols or acids) are reduced.<sup>22</sup> By this, the chromatographic performance that might rapidly decrease by injection of complex samples into a system is discharged by adding a second mass spectrometric dimension. This is helpful as the appearance of some matrix compounds (e.g. fronting peaks for octanoic acid or decanoic acid on non-polar GC phases) is a function of matrix and column age and might impair GC-SIM-MS analysis.<sup>6,23</sup>

MRM optimization involves a stepwise evaluation of suitable precursor and product ions. The selection of precursor ions was primarily subject to two factors: On the one hand, the selection aimed to find substance or substance group specific ions with high  $m/z$  that allow further fragmentation by CID. On the other hand, ions with high abundance are required in order to obtain a suitable current of product ions. In some cases, additional considerations are required in order to assure spectral overlap of co-eluting target compounds or target compounds with stable isotope standards do not cause any interferences (see below). In GC-EI-MS, the highest  $m/z$  of a pure compound results from the molecular ion. This  $m/z$  is surely the most selective, but its low abundance (typically <5%) is disadvantageous (Figure 1). In the given case the molecular weight of the sixteen target compounds ranges between 136 g/mol (myrcene) and 220 g/mol (caryophyllene oxide), whereas the selected precursor ions of the qualifier and quantifier MRMs range between  $m/z=59$  and  $m/z=147$ . With exception of 2-methylbutyl isobutyrate, the remaining target compounds are terpenes or terpenoids. Resulting from their structural

similarity, their GC-EI-MS fragmentation patterns are related. Monoterpene EI-MS spectra (e.g. of myrcene, limonene,  $\alpha$ -pinene, and  $\beta$ -pinene) are characterized by a base peak with  $m/z=93$ . The ion with  $m/z=121$  is the most abundant fragment ion with  $m/z>100$ . Consequently, ions with  $m/z=93$  and  $m/z=121$  ions are either used as quantitative or qualitative MRM transition for the aforementioned compounds (Table I). For the stable isotope labelled myrcene ( $d_2$ -myrcene), the corresponding fragments were chosen. Due to the incorporation of two deuterium labels at suitable structural elements of the molecule, fragmentation produces ions with  $m/z=95$  and  $m/z=123$ . The mass spectra of the two sesquiterpenes  $\alpha$ -humulene and  $\beta$ -caryophyllene are similar to those of the monoterpenes. Thus  $m/z=93$  is used as the precursor ion for the quantitative MRM transition. Additionally, there exist two characteristic fragment ions with  $m/z=133$  ( $\beta$ -caryophyllene) and  $m/z=147$  ( $\alpha$ -humulene). As both ions appear in approx. 25-40% of base peak intensity they were selected as MRM precursor ions (qualitative transition). Since the mass spectra of caryophyllene oxide and  $\beta$ -caryophyllene are similar, the exact same precursor and product ion pairs were selected (Table I). The mass spectra of the four isomeric monoterpenoids linalool,  $\alpha$ -terpineol, nerol, geraniol, as well as those of citronellol and geranyl acetate are more complex. There exist multiple differences in the intensities of major fragment ions. Still, in most cases, except linalool and citronellol,  $m/z=69$ ,  $m/z=93$ ,  $m/z=121$  are abundant and are therefore used in MRMs for  $\alpha$ -terpineol, geraniol, and geranyl acetate (Table I). As  $d_6$ -citronellol, citronellol, and nerol overlap, the selection of suitable MRM transitions was more complicated.  $m/z=69$ , which is used as qualitative transition for geraniol and geranyl acetate is abundant in both mass spectra (nerol and citronellol). As both compounds coelute,  $m/z=69$  cannot be used for either qualification or quantification. For nerol, terpene specific fragments of  $m/z=93$  and  $m/z=121$  were chosen. Both are absent in

citronellol, which exclusively contains one double bond at C6 position instead of two in C6 and C1 (linalool) or C6 and C2 (nerol, geraniol) position. Only one corresponding fragment  $m/z=123$  is used for citronellol, since the other corresponding fragment  $m/z=95$  also occurs in the isotope labeled analogue ( $d_6$ -citronellol). Instead, the fragment  $m/z=138$  was chosen for citronellol.  $D_6$ -citronellol is quantified using the base peak forming precursor ions  $m/z=75$  (six deuterium labels) and qualified using  $m/z=126$  (three deuterium labels). With  $m/z=71$  and  $m/z=70$  the two most abundant fragment ion of 2-methylbutyl isobutyrate were used in MRM. The configurational isomers *cis*-linalool oxide and *trans*-linalool oxide have almost the same mass spectra, therefore  $m/z=94$  and  $m/z=111$  were chosen for both.  $M/z=94$  and  $m/z=111$  represent either the second or third most abundant precursor ions and they are more specific than the ion with  $m/z=59$  (base peak). In linalool  $m/z=71$  and  $m/z=93$  appear as abundant precursor ions and are therefore used for MRM. In  $d_5$ -linalool the ions with  $m/z=74$  (three deuterium labels) and the ion with  $m/z=98$  (five deuterium labels) were chosen as precursor ions. In accordance to the description given for  $d_2$ -myrcene, incorporation of deuterium labels at suitable structural elements is vital when combining GC-MS/MS and stable isotope dilution assays. The proposed MS/MS fragmentation pattern of  $d_5$ -linalool is shown in Figure 2.

After suitable precursor ions were selected, they were subjected to product ion scan experiments. Whereas all precursor ions are formed by EI ionization at 70 eV, variation of CID energy in the collision cell (quadrupole 2) is used to manipulate CID product ion spectrum and yield of individual product ions. As a rule of thumb, in LC-MS/MS large precursor ions require high CID energies, whereas small precursor ions sufficiently form product ions at lower energies.<sup>24</sup> In the current study the selected precursor ions ranged between  $m/z=59$  to  $m/z=147$ , and can therefore be considered as relatively small ions. Therefore, the first product ion

scans were performed at a collision energy of 5 eV to determine suitable product ions. In order to optimize product ion yield, the collision energy was tested in a stepwise procedure using 1, 3, 5, 7, 10, 15, and 20 eV. The product ion yields were evaluated by integration of the quantitative and qualitative MRM signal intensities and averaged. Table II shows the percentage in relation to the maximum area of the respective analyte. An empty circle represents values less than 20 %, a quarter filled circle represents values greater than or equal to 20 % and less than 40 %, a half-filled circle represents values greater than or equal to 40 % and less than 60 %, a three quarters filled circle represents values greater than or equal to 60 % and less than 80 %, and a filled circle represents values greater than or equal to 80 %. Most of the analytes have an optimum of intensity at collision energies between 5 and 15 eV. Terpene characteristic MRM transitions, which are used several times for different analytes (e.g.  $93 \rightarrow 77$ ,  $121 \rightarrow 93$ ), have their optimum reproducibility in a similar range. For the sake of simplicity, CID collision energy was set to 10 eV, since there existed no intensity problems. At this collision energy, 33 of 38 transitions tested showed relative signal intensities of greater than or equal to 80 % (almost half were at their optimum) and three transition give intensities of less than 80 % but greater than or equal to 60 %. The qualifier MRMs for *cis/trans*-linalool oxide ( $111 \rightarrow 93$ ) were exceptions, since their optimal collision energy was at 3 eV and at 10 eV they had relative intensities of less than 60 %.

As suitable MRM transitions were evaluated the method was fine-tuned by detector gain adjustment. Even though gain adjustment capabilities are available in both GC-MS and GC-MS/MS, they are rarely used in optimization. Still, using detector gain can provide a number of advantages (i.e. better compound response stability, better correspondence between instruments)<sup>25</sup> but most importantly it is a simple approach to adjust the working range of MS detection. The principle of detector gain is that ion signals

Table II. Influence of collision energy (CE) on signal intensity of quantitative and qualitative MRM transitions. CE of 1, 3, 5, 7, 10, 15, and 20 eV were each tested in five repetitions and averaged. The values are normalized in relation to the maximum area of the respective analyte [%]. The circles represent the percentage share, a filled circle indicates a value greater than or equal to 80 %, an empty circle indicates a value less than 20 %.

Compound	[m/z]	CE 1	CE 3	CE 5	CE 7	CE 10	CE 15	CE 20
$\alpha$ -pinene	93→77*	○ 21	○ 26	○ 52	● 69	● 100	● 98	● 85
	121→93	● 77	● 66	● 100	● 97	● 97	○ 38	○ 16
$\beta$ -pinene	93→77*	○ 22	○ 28	○ 55	● 73	● 100	● 98	● 78
	121→93	● 69	● 63	● 97	● 99	● 100	○ 43	○ 17
<b>d<sub>2</sub>-myrcene</b>	95→78*	○ 22	○ 28	○ 54	● 70	● 98	● 100	● 85
	123→94	● 66	● 66	● 100	● 99	● 94	○ 49	○ 22
myrcene	93→77*	○ 26	○ 33	○ 57	● 72	● 100	● 99	● 79
	121→93	● 70	● 71	● 96	● 95	● 100	○ 51	○ 26
2-methylbutyl isobutyrate	71→43*	● 99	● 81	● 100	● 92	● 83	○ 41	○ 17
	70→55	○ 57	● 60	● 91	● 97	● 100	○ 54	○ 21
limonene	93→77*	○ 20	○ 25	○ 46	● 61	● 100	● 96	● 86
	121→93	○ 52	○ 51	○ 77	● 83	● 100	○ 64	○ 42
<i>cis</i> -linalool oxide	94→79*	○ 50	● 70	● 83	● 94	● 100	● 80	○ 46
	111→93	● 96	● 100	● 88	○ 72	○ 46	○ 15	○ 4
<i>trans</i> -linalool oxide	94→79*	○ 51	● 70	● 84	● 94	● 100	● 80	○ 46
	111→93	● 96	● 100	● 89	○ 74	○ 47	○ 15	○ 4
<b>d<sub>5</sub>-linalool</b>	74→46*	○ 54	● 73	● 85	● 97	● 100	○ 78	○ 57
	98→79	○ 20	○ 32	○ 46	○ 64	● 90	● 100	● 82
linalool	71→43*	○ 53	● 73	● 87	● 98	● 100	● 86	○ 62
	93→77	○ 20	○ 32	○ 46	○ 63	● 85	● 100	○ 77
$\alpha$ -terpineol	93→77*	○ 18	○ 30	○ 43	○ 60	● 84	● 100	○ 78
	59→31	○ 38	○ 55	○ 74	● 89	● 100	● 89	○ 58
<b>d<sub>6</sub>-citronellol</b>	75→44*	● 66	● 85	● 95	● 100	● 97	○ 65	○ 36
	126→81	○ 26	○ 76	● 87	● 95	● 100	○ 76	○ 51
citronellol	123→81*	● 60	● 80	● 91	● 100	● 99	○ 75	○ 42
	138→95	● 72	● 87	● 88	● 100	● 88	○ 67	○ 38
nerol	93→77*	○ 19	○ 31	○ 41	○ 62	○ 75	● 100	○ 71
	121→93	○ 56	○ 77	● 82	● 100	● 81	○ 61	○ 22
geraniol	93→77*	○ 17	○ 29	○ 37	○ 51	○ 69	● 100	○ 71
	69→41	● 70	● 94	● 98	● 100	● 95	● 83	○ 40
geranyl acetate	93→77*	○ 16	○ 25	○ 39	○ 54	○ 74	● 100	○ 79
	69→41	● 64	● 83	● 100	● 94	● 98	○ 79	○ 42
$\beta$ -caryophyllene	93→77*	○ 24	○ 32	○ 53	○ 70	● 92	● 100	○ 73
	133→105	○ 45	○ 51	○ 75	● 89	● 100	● 92	○ 61
$\alpha$ -humulene	93→77*	○ 18	○ 25	○ 43	○ 59	● 85	● 100	● 80
	147→105	○ 55	○ 63	● 84	● 92	● 100	● 99	● 86
caryophyllene oxide	93→77*	○ 18	○ 28	○ 43	○ 59	● 85	● 100	○ 72
	133→105	○ 44	○ 60	○ 77	● 89	● 100	● 87	○ 55

\* Quantitative transition

○ < 20 %, ○ 20 and < 40 % ○ 40 and < 60 % ○ 60 and < 80 %, and ● ≥ 80 %.

are directly proportional to the gain setting of the MS acquisition method. Increasing the gain by factor two results a signal amplification of factor two, increasing the gain by factor five results in a five-fold signal amplification and so forth. The Agilent 7000C Triple Quadrupole mass spectrometer used in this study allows gain factor adjustment in a range of 0.1 – 100 (relative to tuning result). Depending on the amount of ions transferred into the MS detector, high gain can result in flat-topped peaks (poor quantification capabilities at higher concentrations), whereas low gain can result in low detector response and sensitivity. It is worth mentioning that an increase in gain does not affect the S/N ratio and high signal amplification might reduce detector lifetime. In the current method, the gain value for each MRM time segment was set individually ranging from 0.1 to 10. Gain adjustment aimed to obtain a minimum peak area of approx. 1000 counts for the smallest calibration point (1 µg/L) and a maximum peak area of approx. 1000000 for the highest calibration point (1000 µg/L). Analytes showing a high response (e.g. humulene) were suppressed by choosing a gain of 0.1,

analytes with low response (e.g. caryophyllene oxide) were amplified by choosing gain of 10. Consequently, gain optimization allowed the consideration of analyte specific response factors and is regarded as advantageous for multi methods covering a wide working range. From an analyst's point of view, data evaluation is facilitated, because all target analytes exhibit related peak areas at a given concentration level.

**HS-SPME sampling.** GC gradient optimization yielded a total GC runtime (separation and cool down) of approx. 20 min. In order to develop an effective and rapid routine method, the total duration of the HS-SPME protocol was also set to 20 min. Allowing 1 min of fiber desorption and 4 min of conditioning per run, 15 min remained available for sample incubation and HS-SPME extraction. Optimization of HS-SPME in multi methods is difficult, because conditions promoting the extraction of one analyte might suppress the extraction of others. In brief, there exist optimal conditions for each analyte (Table III) and optimization therefore aims to obtain good recovery of compounds

**Table III. Optimal HS-SPME extraction conditions for maximal area. A DVB/CAR/PDMS fiber was used. The agitation speed was set at 500 rpm and desorption time was 1 min.**

Compound	Time [min]		Temperature [°C]	Salt [g]
	Incubation	Extraction		
α-pinene	11.5	3.5	40	0
β-pinene	9.5	5.5	40	0
myrcene	11.5	3.5	40	0
2-methylbutyl isobutyrate	11.5	3.5	40	0
limonene	11.5	3.5	40	0
<i>cis</i> -linalool oxide	*	*	75	0.4
<i>trans</i> -linalool oxide	*	*	75	0.4
linalool	*	*	50	0.4
α-terpineol	3.5	11.5	70	0.4
citronellol	3.5	11.5	70	0.4
nerol	3.5	11.5	75	0.4
geraniol	3.5	11.5	75	0.4
geranyl acetate	5.5	9.5	60	*
β-caryophyllene	11.5	3.5	40	0
α-humulene	*	*	40	0
caryophyllene oxide	3.5	11.5	65	0.4

\* Variation of the parameter has no effect on the analyte.

being present in low concentration, showing a low recovery in the analytical system, or both. In the current study, optimization was performed by variation of incubation and extraction time, temperature, as well by salt addition at three concentration levels. The optimization was preformed stepwise, potential interactions between the different treatments were not considered. As expected, the tested incubation and extraction times (inc./ex.: 3.5/11.5, 5.5/9.5, 7.5/7.5, 9.5/5.5, and 11.5/3.5 min) indicated no uniform trend for all analytes. Since there existed no intensity problems at low analyte concentrations (1 µg/L) the incubation and extraction period were distributed equally allowing 7.5 min for each treatment. The evaluation of different extraction and incubation temperatures (40, 45, 50, 55, 60, 65, 70, and 75 °C) showed that volatiles with higher boiling points were more efficiently extracted at higher temperatures, whereas the recovery of more volatile and non-polar compounds decreased with rising temperatures. These observations are consistent with other studies published for beer, hop oil or wine.<sup>26,27</sup> With regard to the

high response of myrcene, which is due to its high volatility and low polarity, the temperature was finally set to 60 °C aiming to reduce/suppress myrcene adsorption onto the fiber. Afterwards, analyses with 0.4 g (saturated solution) and 0.2 g NaCl per 1 mL beer were performed and results were compared to those of samples without salt added. The NaCl addition influenced the extraction in three ways. First, for all nonpolar compounds and 2-methylbutyl isobutyrate the extraction yield decreased with salt addition. Second, no effect was observed for geranyl acetate. Third, the extraction of the remaining polar compounds was positively influenced by salt addition due to the “salting-out” effect. Comparing the salt addition of 0.2 and 0.4 g, the higher amount leads to slightly higher peak areas for the aforementioned polar analytes (data not shown). Since salt addition improved the extraction efficiency for half of the analytes, the NaCl addition was set to 0.4 g per 1 mL beer. The positive effect of salt addition on the recovery of certain volatiles correspond with published studies.<sup>4,28</sup>

**Table IV. Results for statistical parameters of method validation: linearity (range, R<sup>2</sup>, Mandel fitting test), limit of detection and quantification (LOD, LOQ), %recovery, and measurement precision.**

Compound	Linearity			LOD <sup>a</sup> / LOQ <sup>b</sup> [µg/L]	%Recovery	Precision <sup>c</sup> [%RSD]
	Range [µg/L]	R <sup>2</sup>	Mandel			
α-pinene	1–100	>0.99	linear	0.02/ 0.08	117–119	5.6
β-pinene	1–100	>0.99	linear	0.01/ 0.05	116–119	7.0
myrcene	1–1000	>0.99	linear	0.20/ 0.67	86–98	5.3
2-methylbutyl isobutyrate	1–1000	>0.99	linear	0.03/ 0.09	94–112	7.3
limonene	1–1000	>0.99	linear	0.10/ 0.33	92–109	6.6
<i>cis</i> -linalool oxide	1–100	>0.99	linear	0.10/ 0.35	103–116	5.4
<i>trans</i> -linalool oxide	1–100	>0.99	linear	0.11/ 0.35	103–116	7.5
linalool	1–1000	>0.99	linear	0.19/ 0.63	97–100	1.7
α-terpineol	1–500	>0.99	linear	0.10/ 0.35	106–119	5.2
citronellol	1–500	>0.99	linear	0.18/ 0.61	84–88	3.4
nerol	1–100	>0.99	linear	0.11/ 0.36	80–87	5.4
geraniol	1–1000	>0.99	linear	0.03/ 0.09	85–93	5.4
geranyl acetate	1–100	>0.99	linear	0.10/ 0.33	80–110	8.1
β-caryophyllene	1–1000	>0.99	linear	0.03/ 0.09	81–102	6.0
α-humulene	1–1000	>0.99	linear	0.07/ 0.23	81–96	6.4
caryophyllene oxide	1–100	>0.99	linear	0.02/ 0.07	96–114	5.7

<sup>a</sup> LOD =  $\bar{x}_B + 3\sigma$  ( $\bar{x}_B$ - mean signal of replicate reagent blanks (N = 6),  $\sigma$ - standard deviation of the blank)

<sup>b</sup> LOQ =  $\bar{x}_B + 10\sigma$

<sup>c</sup> Measurement precision (sixfold determination)

### Method validation

In order to confirm that the established analytical procedure is well suitable for its intended use, an extensive method validation was performed (Table IV). In the calibration range the overall assay consisting of HS-SPME sample preparation and GC-MS/MS analysis showed an excellent linearity ( $R^2 > 0.99$ ) in the Mandel fitting test. Both, LOD and LOQ, were below  $0.7 \mu\text{g/L}$  for all analytes, which is well below the flavor thresholds of the selected compounds. Based on these findings a concentration of  $1 \mu\text{g/L}$  was defined as the lower end of the working range for all analytes. The recovery rates of the individual odorants were determined at concentration levels of  $5 \mu\text{g/L}$  and  $100 \mu\text{g/L}$ , respectively. Recoveries ranged from 80-120 %, which was judged fully acceptable. Light volatile terpenes (e.g.  $\alpha$ -pinene and  $\beta$ -pinene) tended to have high recoveries, whereas high boiling point terpenes (e.g.  $\alpha$ -humulene and  $\beta$ -caryophyllene) tended to have lower recoveries. The measurement precision, 6 fold repeat analysis of a sample, showed an  $\text{RSD} < 10 \%$ . Table IV gives a detailed overview of the results of method validation. Laboratory precision (duplicates of samples measured on different days, and duplicates analyzed by different analysts) and robustness (measurement at the beginning and end of the batch) were as well either less than 10 %RSD or equal to 10 %RSD (data not shown).

### Stability of calibration

Even though HS-SPME has many advantages (easy to use, solvent-less, etc.) analysts consider the stability of HS-SPME (calibration) a major issue. In contrast to extraction techniques, e.g. liquid-liquid extraction, the extractant (SPME-fiber) is reused multiple times. During extraction and desorption the fiber is subjected to heating and cooling, to mechanical (agitation) and chemical stress. Thus, (rapid) loss of adsorptive capacity (fiber aging or fiber abrasion) is frequently cited as major disadvantage of HS-SPME.<sup>7,29</sup> In order to

obtain low LOD and LOQ, many analysts that use GC-MS or less sensitive detectors for aroma analysis aim to maximize the extraction of volatiles from sample onto SPME, hence into the chromatographic system. Practically, sample volume and extraction temperature are maximized, and extraction times are expanded.<sup>30,31</sup> We suppose that those procedures stress the fiber material and therefore cause (very) limited fiber lifetimes. As a course of fiber aging signal intensities decrease and fibers need to be replaced quickly (50 injections). This is not only causing efforts for manual handling, and costs for the fibers, but also requires extensive re-calibration protocols. Through the use of GC-MS/MS, sensitivity is not a problem when aiming to quantify compounds at ppb levels. As described above, LOQs of  $1 \mu\text{g/L}$  are easily reached for all analytes even though small sample volumes are employed for analysis (1 mL in 10 mL HS-Vial). Small sample volumes leave considerable headspace and prevent liquid from splashing onto the fiber while agitating the vials during extraction. According to our experience, this protects the fiber and eliminates analytical inconsistencies. By using small sample volumes, the concentration of volatiles (matrix and target compounds) in the headspace above the sample is reduced. Consequently, the amount of volatiles adsorbed onto fiber is reduced. With the given instrument sensitivity this is considered very beneficial, as fiber lifetime can be prolonged. In order to monitor long-term fiber performance, evaluation of the peak areas of the internal standard(s) areas of the matrix matched calibration are suitable. As the standard is always added at the exact same concentration and the same base beer was used, peak area variation must result from the analytical system. In the given HS-SPME-GC-MS/MS setup, the quantifier ion peak of  $d_5$ -linalool spiked at a concentration of  $100 \mu\text{g/L}$  yielded 54735 counts using a brand new but conditioned fiber. Repeat analysis of the same base beer spiked with  $100 \mu\text{g/L}$   $d_5$ -linalool after 60, 80, 110, 240, and 380 injections yielded areas that ranged

between 85% and 101% of the initial area. After 450 injections, the respective peak area was found to be approx. 70% of the initial value, whereas it was reduced to 50% after 650 injections. This observation reveals that under the given conditions 500 extraction-desorption cycles (or more) per fiber are possible without a reduction in analysis quality. In an extreme case this is by factor ten more than we ourselves have observed in SPME GC-FID assays or, for example, fivefold more than Stashenko and Martínez recommend.<sup>29</sup> In summary, these findings show reduced fiber aging corresponds with small sample volumes.

In addition to extended fiber lifetime GC-MS/MS methodology showed excellent calibration consistency. Over a twelve-month period, in which the mass spectrometer was cleaned, GC column was replaced, and four different DVB/CAR/PDMS fibers were used, fourteen randomly picked linalool calibration curves were recorded (Supplementary Figure 1). It was observed that the linear calibration functions were very constant as the slope varies between 1.51 and 1.90. This evidences the combination HS-SPME-GC-MS/MS coupled with suitable ISTD provides an assay with excellent stability. The results also display that under the conditions used herein fiber-to-fiber variations and their influence

on quantification is insignificant. In summary, we have not observed instability or inconsistency of calibration reported in literature in the trials presented here in. Under the given conditions, we even propose to minimize efforts for calibration, e.g. replace daily full calibration with analysis of one or two selected control points.

### Application to beer samples

The optimized method was applied for routine analysis of more than 200 commercial beer samples (lager beer, dry-hopped beer) as well as green beer, hop teas, and wort samples. All samples were analyzed in duplicates. When verifying that the pair of results from each the duplicate match, the mean value of both measurements was calculated. As long as the difference between mean value and each of the single results were less than 10 %, the mean value was judged to be valid. Despite some of the given analyte dependent (see discussion above) and laboratory operation related variations observed, deviations were well below 10%. The quantity of repeat measurement was approx. 3%. In addition, the deviation for all analytes was comparable in the above listed matrices, which highlights the versatility of the methodology.

**Table V: Concentration range of approx. 100 dry-hopped beer samples.**

Analyte	Minimum [ $\mu\text{g/L}$ ]	Median [ $\mu\text{g/L}$ ]	Maximum [ $\mu\text{g/L}$ ]
$\alpha$ -pinene	<1.0	<1.0	5.5
$\beta$ -pinene	<1.0	<1.0	28.9
myrcene	2.6	23.4	2126.1*
2-methylbutyl isobutyrate	<1.0	50.5	584.4
limonene	<1.0	4.1	669.5
<i>cis</i> -linalool oxide	<1.0	7.8	46.6
<i>trans</i> -linalool oxide	<1.0	6.6	36.2
linalool	17.2	166.3	2035.0*
$\alpha$ -terpineol	9.2	20.3	213.0
citronellol	1.6	13.4	142.1
nerol	<1.0	4.9	99.7
geraniol	4.9	20.9	756.0
geranyl acetate	<1.0	<1.0	59.2
$\beta$ -caryophyllene	<1.0	<1.0	443.0
$\alpha$ -humulene	<1.0	2.6	764.1
caryophyllene oxide	<1.0	<1.0	34.7

\* Outside the calibration range

In order to obtain an overview of the distribution of the individual analytes in different beers and to discuss the analyte selection, results are summarized in two groups: lager beer (Supplementary Table I) and dry-hopped beer (Table V). In lager beers the maximum concentrations of most analytes were below 20  $\mu\text{g/L}$  and many medians were below 6  $\mu\text{g/L}$  or below the LOQ (<1.0  $\mu\text{g/L}$ ). The only exceptions were linalool and myrcene which were found in maximum concentrations of 115.8 and 146.8  $\mu\text{g/L}$ , respectively. As expected, the medians of all analytes are equal respectively higher in the dry-hopped beers compared to lager beers, but also the concentration ranges differ widely within a group (see minimum and maximum concentration). This can be clearly seen in the case of myrcene and linalool, which differ by a factor of 2000 (not detectable vs. >2000ppb). In no other analysis of beer flavor compounds do concentrations of relevant analytes fluctuate so broadly. The wide concentration ranges of selected analytes in dry-hopped beers is explained by the great diversity in hops (variety and quantity) and the exact procedure (temperature, time, yeast present) used. Generally, the range of myrcene and linalool found in various beer styles is enormous. The maximum concentrations for myrcene between 1300 and 2100  $\mu\text{g/L}$  were measured in so-called New England IPAs (NEIPAs), which were well ahead of the concentrations of the next two strongly hopped IPAs, which were between 750 and 900  $\mu\text{g/L}$ . The maximum values of linalool, 2-methylbutyl isobutyrate, caryophyllene, humulene, geranyl acetate,  $\alpha$ -pinene, and  $\beta$ -pinene were also measured in a NEIPA. The highest limonene concentration of almost 670  $\mu\text{g/L}$  was found in a beer that was flavored with tangerine peel. Without fruit peel addition, the maximal concentration of limonene was 160  $\mu\text{g/L}$ . The range of geraniol varies range comparable to that of myrcene and linalool. As expected, the geraniol concentrations were particularly high in dry-hopped beers, which were labelled to contain certain hop varieties

(e.g. Cascade, Mosaic, Bravo, Citra, and Amarillo). Even though in the results summarized herein  $\alpha$ - and  $\beta$ -pinene concentrations are very low these analytes are of relevance in beers brewed with hemp, herbs, or spices, such as Gose or Wit beer, which contains coriander. In addition, we have observed  $\alpha$ - and  $\beta$ -pinene being present at higher levels in beers that were treated with wood chips (data not shown).

In order to visualize differences within the lager beers and the dry-hopped beers (Figure 3) and in order to identify correlations between the selected target compounds, PCA was used. The first two principal components explain 65 % of the variation in the data set, whereas PC1 accounts for 44 % and PC2 accounts for 21 %. The biplot (Figure 3A) reveals that PC1 is well linked with linalool, whereas myrcene, nerol, 2-methylbutyl isobutyrate, and geraniol are also dominant features in PC1. Citronellol, *cis*- and *trans*-linalool oxide,  $\alpha$ -humulene,  $\beta$ -caryophyllene, and  $\alpha$ -pinene contribute most to PC2. The Pearson correlation matrix (data not shown) depicts that among the selected analytes only *cis*-linalool oxide and *trans*-linalool oxide (0.991) as well as caryophyllene and humulene (0.983) strongly correlate. Therefore it remains to be discussed whether it is sufficient or not to measure only one of the two analytes.

Moving from left to right across PC1 Figure 3B shows that lager beers cluster on the left side near the center, with increasing analyte concentration dry-hopped beers spread in two directions: which is driven by either citronellol or myrcene concentrations. In order to verify similarities by grouping, the beers of cluster 1 were examined more closely. All beers of cluster 1 are NEIPAs that are characterized by high concentrations of hop-derived metabolites. These beers are located near to the loadings of analytes that have their maximum values in this beer variety (4<sup>th</sup> quadrant). The double IPAs of cluster 2 are separated from the other dry-hopped beers. These samples represent a storage trial in which a similar product was repeatedly

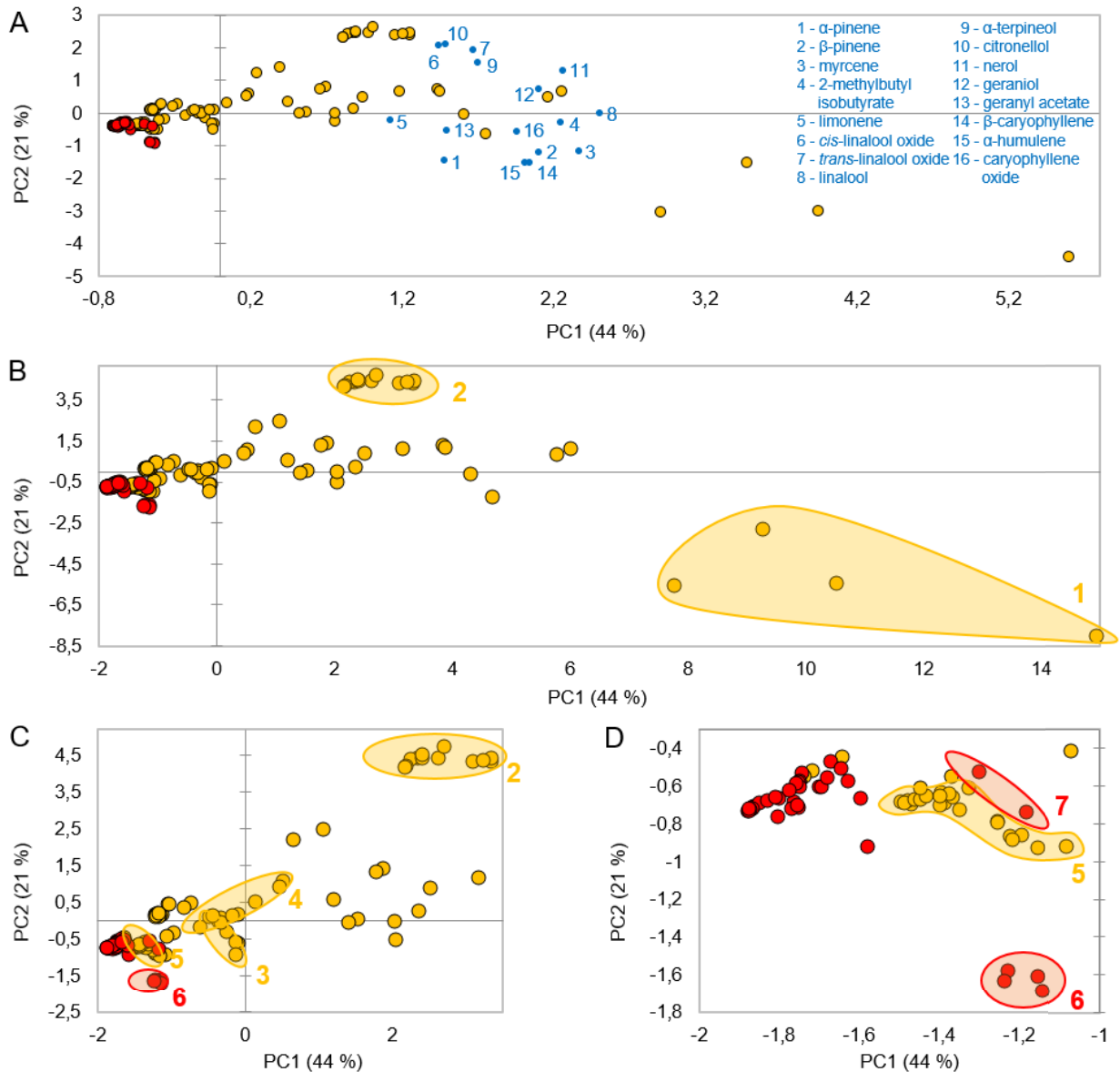


**Figure 3.** Principal component analysis (PCA) for lager beers (red dots, Supplementary Table I) and dry-hopped beers (yellow dots, Table V) including the concentration of the 16 hop aroma analytes. PC1 vs. PC2 explaining 65 % of the variation in the data. The Biplot (A) shows the loading of each analyte (blue numbers) on PC1 and PC2 and their contribution to beer samples clustering. Plot (B) shows an overview of all scores of the PCA. Plot (C) and (D) are zoomed in for better identification of clusters. The numbers refer to different clusters: 1, New England IPAs (NEIPAs); 2, storage trial of double IPAs; 3, dry-hopped with different amount Cascade hops; 4, dry-hopped with different amount of unknown hops; 5, storage trial of lightly hopped beers; 6, same lager beer brand brewed in different breweries; 7, hoppy pilsner.

tested over a 6-month period. Figure 3C and Figure 3D are enlarged views to resolve cluster 3-7. The beers of cluster 3 and 4 were experimental single hop IPAs in which hop variety and dry-hop dosage have been varied. Beers that were produced at higher dry-hopping rates show a drift within the cluster. In cluster 5, there are beers with a very subtle dry-hop aroma cluster close to the lager

beers. Within the lager beers, two separate clusters were observed. Cluster 6 shows beer samples of the same brand brewed in four different breweries. The “hoppy pilsner” samples of cluster 7 were clearly separated from the main group of lager beers. Even though the beer was not advertised/labelled as being dry-hopped, the analyte concentrations suppose a hop addition to

cold side beer. In summary, the PCA shows that the selected analytes allow beer styles to be easily distinguished and enable the differentiation of beers with different hopping regimes.

## Conclusions

A rapid HS-SPME-GC-MS/MS method to quantify 16 selected hop aroma compounds in beer was developed and successfully validated. The method development primarily included the synthesis and characterization of three stable isotope labelled standards, the optimization of SPME sampling as well as MRM method development. Since GC-MS/MS is not yet widely used in beer analysis the MRM method development was discussed in detail and the benefits of MRM were demonstrated. Most importantly, MRM resolves matrix effects such as overlapping peaks of chemically similar (target) compounds. On the one hand, this is regarded as beneficial in the case of analysis of massively hopped beers (signal overlap caused by high concentrations of some hop derived volatiles). On the other hand, it also supports the reliable detection of traces of hop volatiles in lagers. In the latter case, MRM provides the ability to select product ions with low noise or high S/N, which is a substantial advantage over GC-SIM-MS that is limited to abundant, but sometimes noisy and unspecific fragment ions. By minimizing co-elution problems the use of rapid GC methods, 16.5 minutes in this case, is possible. The analysis of small sample volumes (1 mL) extended SPME fiber lifetime and yielded excellent long-term stability, both aspects are usually regarded as major SPME-related drawbacks. By extensive method validation and application to beer samples, the benefits of the three ISTD was highlighted. For the first time, the synthesis and characterization of d<sub>2</sub>-myrcene and d<sub>6</sub>-citronellol was described. Both standards (and d<sub>5</sub>-linalool) are proposed as primary standards for hop aroma analysis by either GC-MS or GC-MS/MS. They represent

important polar and non-polar hop aroma compounds and elute at the beginning, middle and end of the chromatogram. In the current paper, the working range was adjusted to the concentration of hop aroma compounds practically found in different beer styles, we did not target to reach the lowest technically possible LOD and LOQ. Instrument sensitivity and selectivity qualify GC-MS/MS for other more challenging beer flavor related topics such as staling aldehyde or thiol analysis.

## Additional information

### Acknowledgements

The authors like to thank Dr. Sven Hanelt for developing the strategy for d<sub>6</sub>-citronellol synthesis and Prof. Juri Rappsilber (Technische Universität Berlin) for providing access to the NMR instruments. The skilled assistance of Laura Knoke, Christian Schubert, and Christopher Bergtholdt is greatly acknowledged.

### Declaration of interest statement

The authors declare no conflict of interest.

### Funding details

The SPME-GC-MS/MS instrument used in this study was funded by the German Federal Ministry for Economic Affairs and Energy (grant number 49IZ180038).

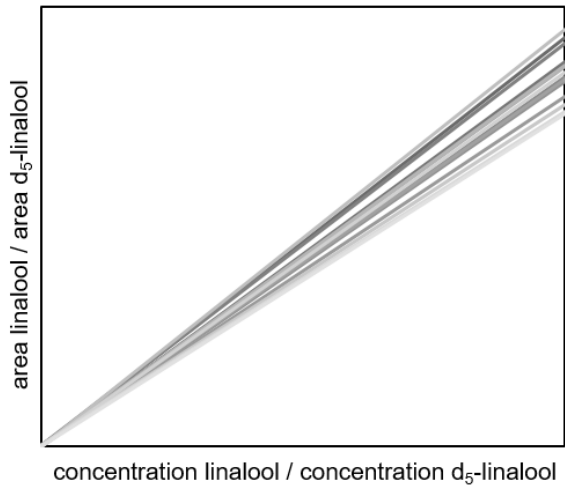
## Literature Cited

1. Rettberg, N; Biendl, M; Garbe, L. Hop Aroma and Hoppy Beer Flavor: Chemical Backgrounds and Analytical Tools-A Review. *J. Am. Soc. Brew. Chem.* 76(1), 1–20, 2018.
2. Sharp, DC; Qian, Y; Shellhammer, G; Shellhammer, TH. Contributions of Select Hopping Regimes to the Terpenoid Content and Hop Aroma Profile of Ale and Lager Beers. *J. Am. Soc. Brew. Chem.* 75(2), 93–100, 2017.

3. Forster, A; Gahr, A. On the Fate of Certain Hop Substances during Dry Hopping. *BrewingSci.* 66(7/8), 93–103, 2013.
4. Hao, J; Dong, J; Yin, H; Yan, P; Ting, PL; Li, Q; Tao, X; Yu, J; Chen, H; Li, M. Optimum Method of Analyzing Hop Derived Aroma Compounds in Beer by Headspace Solid-Phase Microextraction (SPME) with GC/MS and Their Evolutions During Chinese Lager Brewing Process. *J. Am. Soc. Brew. Chem.* 72(4), 261–270, 2014.
5. Likens, ST; Nickerson G. B. Detection of Certain Hop Oil Constituents in Brewing Products. *Proc. Am. Soc. Brew. Chem.* 22(1), 5–13, 1964.
6. Rettberg, N. Instrumental Analysis of Hop Aroma in Beer: On the Challenges of Transforming a Research Application into a QC Tool. International Brewers Symposium on Hop Flavor and Aroma in Beer, Corvallis, OR, USA, 2017.
7. Steinhaus, M; Fritsch, HT; Schieberle, P. Quantitation of (R)- and (S)-Linalool in Beer Using Solid Phase Microextraction (SPME) in Combination with a Stable Isotope Dilution Assay (SIDA). *J. Agric. Food Chem.* 51(24), 7100–7105, 2003.
8. Siebert, TE; Smyth, HE; Capone, DL; Neuwöhner, C; Pardon, KH; Skouroumounis, GK; Herderich, MJ; Sefton, MA; Pollnitz, AP. Stable isotope dilution analysis of wine fermentation products by HS-SPME-GC-MS. *Anal. Bioanal. Chem.* 381(4), 937–947, 2005.
9. Cavaliere, B; Macchione, B; Sindona, G; Tagarelli, A. Tandem mass spectrometry in food safety assessment: The determination of phthalates in olive oil. *J. Chromatogr. A.* 1205(1-2), 137–143, 2008.
10. Hjelmeland, AK; Collins, TS; Miles, JL; Wylie, PL; Mitchell, AE; Ebeler, SE. High-Throughput, Sub ng/L Analysis of Haloanisoles in Wines Using HS-SPME with GC-Triple Quadrupole MS. *Am. J. Enol. Vitic.* 63(4), 494–499, 2012.
11. Wang, P; Yu, W; Qiu, Y; Liu, Y; Rong, M; Deng, H. Levels of Nine Volatile N-Nitrosamines in Chinese-Style Sausages as Determined by Quechers-Based Gas Chromatography-Tandem Mass Spectrometry. *Ann. Public Health Res.* 3(4), 1049–1055, 2016.
12. Aszyk, J; Kubica, P; Woźniak, MK; Namieśnik, J; Wasik, A; Kot-Wasik, A. Evaluation of flavour profiles in e-cigarette refill solutions using gas chromatography-tandem mass spectrometry. *J. Chromatogr. A.* 1547, 86–98, 2018.
13. Steinhaus, M; Schieberle, P. Comparison of the Most Odor-Active Compounds in Fresh and Dried Hop Cones (*Humulus lupulus* L. Variety Spalter Select) Based on GC-Olfactometry and Odor Dilution Techniques. *J. Agric. Food Chem.* 48(5), 1776–1783, 2000.
14. Fritsch, HT; Schieberle, P. Identification Based on Quantitative Measurements and Aroma Recombination of the Character Impact Odorants in a Bavarian Pilsner-type Beer. *J. Agric. Food Chem.* 53(19), 7544–7551, 2005.
15. Kreck, M; Püschel, S; Wüst, M; Mosandl, A. Biogenetic Studies in *Syringa vulgaris* L.: Synthesis and Bioconversion of Deuterium-Labeled Precursors into Lilac Aldehydes and Lilac Alcohols. *J. Agric. Food Chem.* 51(2), 463–469, 2003.
16. Sen, SE; Garvin, GM. Synthesis of (2E,6E)-[10-<sup>3</sup>H]farnesol and (2E,6E)-[10-<sup>3</sup>H]farnesal for insect dehydrogenase studies. *J. Lab. Comp. and Radiopharm.* 36(11), 1063–1069, 1995.
17. Riu-Aumatell, M; Miró, P; Serra-Cayuela, A; Buxaderas, S; López-Tamames, E. Assessment of the aroma profiles of low-alcohol beers using HS-SPME-GC-MS. *Food Res. Int.* 57, 196–202, 2014.
18. Silva, GC da; Silva, AAS da; Silva, LSN da; Godoy, Ronoel Luiz de O; Nogueira, LC; Quitério, SL; Raices, Renata S L. Method development by GC-ECD and HS-SPME-GC-MS for beer volatile analysis. *Food Chem.* 167, 71–77, 2015.
19. ASBC Technical Committee. Limits of Detection and Determination. Statistical Analysis-2. In: Sedin D, editor. ASBC Methods of Analysis, 14th edn. St. Paul, MN, USA: ASBC, 2011.

20. Takoi, K; Tokita, K; Sanekata, A; Usami, Y; Itoga, Y; Koie, K; Matsumoto, I; Nakayama, Y. Varietal Difference of Hop-Derived Flavour Compounds in Late-Hopped/Dry-Hopped Beers. *BrewingSci.* 69(1/2), 1–7, 2016.
21. Schmidt, C; Biendl, M. Headspace Trap GC-MS analysis of hop aroma compounds in beer. *BrewingSci.* 69(1/2), 9–15, 2016.
22. Patel, K; Fussell, RJ; Hetmanski, M; Goodall, DM; Keely, BJ. Evaluation of gas chromatography–tandem quadrupole mass spectrometry for the determination of organochlorine pesticides in fats and oils. *J. Chromatogr. A.* 1068(2), 289–296, 2005.
23. Koserske, J; Thörner, S; Rettberg, N. Rapid quantification of major hop aroma compounds in beer by static headspace GC-MS. ASBC Annual Meeting, Fort Myers, FL, USA, 2017.
24. Lange, V; Picotti, P; Domon, B; Aebersold, R. Selected reaction monitoring for quantitative proteomics: a tutorial. *Mol. Syst. Biol.* 4(222), 1–14, 2008.
25. Prest, H; Hom, B. A Quick-Start Guide to Optimizing Detector Gain for GC/MSD. Agilent Technologies, Inc., 2013. <https://www.agilent.com/cs/library/technicaloverviews/public/5991-2105EN.pdf>. Accessed 1 March 2019.
26. Gonçalves, J; Figueira, J; Rodrigues, F; Câmara, JS. Headspace solid-phase microextraction combined with mass spectrometry as a powerful analytical tool for profiling the terpenoid metabolomic pattern of hop-essential oil derived from Saaz variety. *J. Sep. Sci.* 35(17), 2282–2296, 2012.
27. Setkova, L; Risticovic, S; Pawliszyn, J. Rapid headspace solid-phase microextraction-gas chromatographic-time-of-flight mass spectrometric method for qualitative profiling of ice wine volatile fraction. I. Method development and optimization. *J. Chromatogr. A.* 1147(2), 213–223, 2007.
28. Jiang, W; Wang, D; Wu, Y; Lin, Z; Wang, L; Wang, L; Huangfu, J; Pavlovic, M; Dostalek, P. Analysis of Monoterpenol Isomers in Hops and Beers: Comparison of Methods with a Chiral Column and a Nonchiral Column. *J. Am. Soc. Brew. Chem.* 75(2), 149–155, 2017.
29. Stashenko, EE; Martínez, JR. Sampling volatile compounds from natural products with headspace/solid-phase micro-extraction. *J. Biochem. Biophys. Methods.* 70(2), 235–242, 2007.
30. Yang, X; Peppard, T. Solid-Phase Microextraction for Flavor Analysis. *J. Agric. Food Chem.* 42(9), 1925–1930, 1994.
31. Zhang, Z; Pawliszyn, J. Headspace Solid-Phase Microextraction. *Anal. Chem.* 65(14), 1843–1852, 1993.

## Supplemental online material



**Supplementary Figure 1. Linear calibration curves of linalool over 1 year. The 14 measurements were done with 4 different DVB/CAR/PDMS fibers. The slope varies between 1.51 and 1.90.**

**Supplementary Table I. Concentration range of approx. 50 lager beer samples.**

<b>Analyte</b>	<b>Minimum [µg/L]</b>	<b>Median [µg/L]</b>	<b>Maximum [µg/L]</b>
α-pinene	<1.0	<1.0	3.2
β-pinene	<1.0	<1.0	2.2
myrcene	2.4	5.6	146.8
2-methylbutyl isobutyrate	1.1	2.1	3.5
limonene	<1.0	<1.0	6.3
<i>cis</i> -linalool oxide	<1.0	<1.0	3.3
<i>trans</i> -linalool oxide	<1.0	<1.0	2.5
linalool	5.0	16.5	115.8
α-terpineol	2.1	5.7	18.6
citronellol	1.5	5.8	17.1
nerol	<1.0	1.1	7.2
geraniol	<1.0	5.3	14.1
geranyl acetate	<1.0	<1.0	5.2
β-caryophyllene	<1.0	<1.0	1.9
α-humulene	<1.0	<1.0	6.7
caryophyllene oxide	<1.0	<1.0	3.3

### 3 Publication B

## Analysis of Selected Staling Aldehydes in Wort and Beer by GC-EI-MS/MS Using HS-SPME with On-Fiber Derivatization

#### Summary

A HS-SPME-GC-MS/MS assay using OFD with PFBHA for the quantification of 15 selected staling aldehydes is introduced and validated. Due to its wide concentration range (0.01-1000 µg/L), the method can be applied to fresh Lager beers as well as to aged beer samples or wort. During method development, special focus was placed to ISTD selection, MRM design, and long-term stability. The long-term stability was evaluated as excellent, which is essential for the practical applicability for tracking beer aging. By a comparative study of GC-EI-MS/MS and GC-EI-MS, it was shown that the quantification of low abundant aldehydes by MRM mode is more reproducible.

**Author Contributions:** J.D. developed and validated analytical assay, performed analytics, analyzed and visualized data, conceptualized paper, wrote and edited paper; S.T. supervised research project; J.M. reviewed paper; N.R. interpreted data, conceptualized paper, reviewed and edited paper

## **Publication B**

**Dennenlöhner, J; Thörner, S; Maxminer, J; Rettberg, N. Analysis of Selected Staling Aldehydes in Wort and Beer by GC-EI-MS/MS Using HS-SPME with On-Fiber Derivatization. *J. Am. Soc. Brew. Chem.* 78(4), 284–298, 2020.**

This is an Accepted Manuscript of an article published by Taylor & Francis in Journal of the American Society of Brewing Chemists on 18 August 2020, available online: <https://www.tandfonline.com/doi/10.1080/03610470.2020.1795478>.

# Analysis of Selected Staling Aldehydes in Wort and Beer by GC-EI-MS/MS Using HS-SPME with On-Fiber Derivatization

Johanna Dennenlöhr, Sarah Thörner, Jörg Maxminer, and Nils Rettberg<sup>1</sup>

Research Institute for Beer and Beverage Analysis, Versuchs- und Lehranstalt für Brauerei in Berlin (VLB) e.V., Seestr. 13, 13353 Berlin, Germany

<sup>1</sup>Corresponding author. E-mail: n.rettberg@vlb-berlin.org; phone: +49 30 45080106.

## Abstract

Quantification of staling aldehydes from wort and beer requires sensitive instrumental analysis. In the brewing industry this is for the most part accomplished by GC-MS using headspace solid-phase microextraction (HS-SPME) and on-fiber derivatization (OFD) with *O*-(2,3,4,5,6-pentafluorobenzyl)hydroxylamine (PFBHA). With respect to lipid oxidation products (e.g. (*E*)-2-nonenal and minor Strecker aldehydes (e.g. methional), the sensitivity of GC-EI-MS might not be sufficient to ensure reliable quantification and long-term stability regarding method performance. To overcome these problems, an elaborate gas chromatography-electron impact-tandem mass spectrometry (GC-EI-MS/MS) methodology was implemented. GC-EI-MS/MS improved sensitivity and reduced matrix effects resulting from overlapping PFBHA-oximes (PFBOs). It enabled reliable quantification of 15 selected aldehydes in different matrices (wort, beer) across a wide concentration range (0.01 - 1000 µg/L). Extensive method validation and long-term stability testing proved excellent method performance. Lastly, direct comparison of GC-EI-MS/MS and GC-EI-MS revealed that the quantification of low abundant aldehydes via GC-EI-MS/MS is more reproducible and that lower limits of quantification were achieved.

**Keywords:** beer aging, mass spectrometry, on-fiber derivatization, SPME, staling aldehydes

## Introduction

Flavor is the main quality characteristic of beer and it is important for brand recognition and identification. In order to meet consumer expectations, the desire of any brewer is to achieve reproducible and sufficiently stable beer flavor. Since the conditions of distribution, storage at the point of sale, and handling by the customer are beyond control of the brewer, intensive research attempts to improve intrinsic beer flavor stability. Beer, as manufactured, is not in an equilibrium state and many chemical reactions occur in the packaged product. Simply put, compositional changes result in a loss of fresh

beer flavor and the appearance of an undesired stale character. Given the complexity of beer flavor stability and the wealth of significant literature published the interested reader might refer to *Baert et al.*<sup>1</sup> or *Vanderhagen et al.*<sup>2</sup> for comprehensive reviews.

One of the well-established observations during beer staling is the increase of aldehydes. Aldehydes are primarily formed during malting and wort production. During fermentation, the majority is either reduced to their corresponding alcohols, or bound to bisulfite or cysteine. The bound aldehydes, called bisulfite or cysteine adducts, are

non-volatile and not flavor-active. Some of these aldehyde-adducts are removed from beer by downstream processing, the ones present in packaged beer might be a source of beer instability. The release of odor active aldehydes from non-volatile adducts during beer aging is today considered the primary source of aldehydes in finished products.<sup>3-5</sup>

In consideration of above stated publications, it is reasonable to summarize that lipid oxidation products (alkanals, (*E*)-2-alkenals, (*E,E*)-2,4-alkadienals), Strecker aldehydes (2-methylpropanal, 2-methylbutanal, 3-methylbutanal, methional, benzaldehyde, phenylacetaldehyde), and furfural are suitable analytical markers for beer aging.<sup>1,2,6</sup>

The major analytical challenges in aldehyde quantification from beer relate to their low concentration (ng/L to µg/L levels), the reactivity of their carbonyl function, their low molecular weight, and in some cases to their volatility. In recent years, the use of HS-SPME-GC-MS with on-fiber derivatization (OFD) using *O*-(2,3,4,5,6-pentafluorobenzyl)hydroxylamine hydrochloride (PFBHA, in some publications also abbreviated PFBOA) has become increasingly popular.<sup>1,4,7-11</sup> In HS-SPME-OFD, the SPME fiber is first loaded with the derivatization reagent PFBHA. Secondly, this PFBHA preconditioned fiber is used to simultaneously extract and derivatize aldehydes from the headspace of a wort or beer sample. The reaction of PFBHA with aldehydes forms PFBHA-oximes (PFBOs). All aldehydes, besides formaldehyde, produce two isomers (*syn/anti* PFBO). Depending on the chromatographic conditions applied, these isomers might be baseline separated, or partly or completely co-eluting. In case isomers are baseline separated this results in a bisection of the peak area that reduces the signal intensity per peak. This influences the signal-to-noise ratio, which becomes relevant when aiming to quantify low concentrated aldehydes such as (*E*)-2-nonenal.

The first application of HS-SPME OFD with PFBHA for gaseous formaldehyde analysis by

GC-FID was published in 1998.<sup>12</sup> In 2003 *Vesely et al.*<sup>7</sup> showed that this technique combined with GC-EI-MS is suitable for staling aldehyde analysis in beer. Even though the published workflow was reasonable at that time, multiple modifications of the original method have been published and are now used in the industry. Six selected examples are summarized in Table I. Even though all cited studies use OFD with PFBHA and HS-SPME coupled to quadrupole GC-MS, there exists considerable variation in the execution of this assay. To allow a comparison of setup and to estimate the performance of each analytical assay, Table I contains the ionization mode, the main calibration and validation parameters (if provided by the authors). Please note that different approaches to calculate the limit of quantification (LOQ) were applied (Table I). As can be seen by comparison of the methods by *Saison et al.*<sup>8</sup> and *Ortiz*<sup>9</sup>, both calibrated in beer matrix using similar methods of LOQ calculation, the use of negative chemical ionization (NCI) is an effective measure to increase sensitivity of aldehyde-PFBO detection for almost all analytes. Nevertheless, underivatized beer volatiles such as acids, terpenes, esters or alcohols are preferably analyzed using electron impact (EI) ionization. This is due to its efficiency to ionize and fragment small molecules that yields library-searchable mass spectra. Given that a brewer commonly aims to analyze a broader range of volatiles, GC-NCI-MS requires either the replacement of the ion source prior to aldehyde analysis, the use of ion sources that can operate EI and NCI (not commonly available), or a second GC-MS. All studies referenced in Table I use quadrupole mass spectrometers operated in selected ion monitoring (SIM) mode. SIM is used to improve detection selectivity and sensitivity. *Andrés-Iglesias et al.*<sup>11</sup> and *Vesely et al.*<sup>7</sup> built their methods on EI-SIM with  $m/z=181$ , only. In EI-MS  $m/z=181$  is the most prominent ion of all aldehyde-PFBOs and choosing this ion gives maximum signal intensity. However, selectivity is reduced and quantification might be impaired by

Table I. Overview of selected published methods for staling aldehyde analysis in beer.<sup>a</sup>

Ionization	Matrix calibration	Internal Standard	Analyte	LOQ [ $\mu\text{g/L}$ ]	Range [ $\mu\text{g/L}$ ]	Reference
EI	5 vol% ethanol solution, pH 4.5	N/A (external)	3MB	N/A	0.1-50	<i>Vesely et al.</i> <sup>7</sup>
			FUR	N/A	0.1-50	
			MET	N/A	0.1-50	
			PAA	N/A	0.1-50	
			E2N	N/A	0.01-5	
EI	beer	500 $\mu\text{g/L}$ 4-fluorobenzaldehyde	3MB	4.754 <sup>b</sup>	5-300	<i>Saison et al.</i> <sup>8</sup>
			FUR	9.304 <sup>b</sup>	10-600	
			MET	0.862 <sup>b</sup>	0.2-12	
			PAA	7.758 <sup>b</sup>	0.9-54	
			E2N	0.027 <sup>b</sup>	0.02-1.2	
NCI	beer	0.023 $\mu\text{g/L}$ 3-fluorobenzaldehyde	3MB	1.2 <sup>c</sup>	1.0-20	<i>Ortiz</i> <sup>9</sup>
			FUR	2.7 <sup>c</sup>	15-390	
			MET	2.8 <sup>c</sup>	0.5-16	
			PAA	2.1 <sup>c</sup>	2.0-50	
			E2N	0.03 <sup>c</sup>	0.03-0.6	
EI	5 vol% ethanol solution, pH 4.5	30 $\mu\text{g/L}$ 3-methyl-2-butenal/ 3 $\mu\text{g/L}$ d <sub>6</sub> -benzaldehyde <sup>e</sup>	3MB	0.30 <sup>d</sup>	0.3-50	<i>Carrillo et al.</i> <sup>10</sup>
			FUR	5.20 <sup>d</sup>	5-300	
			MET	1.00 <sup>d</sup>	1.0-20	
			PAA	0.76/0.55 <sup>d,e</sup>	0.6-20	
			E2N	0.05 <sup>d</sup>	0.05-0.25	
NCI	beer	20 $\mu\text{g/L}$ d <sub>10</sub> -2-methylbutanal/ 2 $\mu\text{g/L}$ d <sub>6</sub> -benzaldehyde		N/A	N/A	<i>Baert et al.</i> <sup>4</sup>
EI	N/A	526 $\mu\text{g/L}$ 3-fluorobenzaldehyde		N/A	N/A	<i>Andrés-Iglesias et al.</i> <sup>11</sup>

<sup>a</sup> In all studies, OFD with PFBHA and HS-SPME combined with GC-MS were used. PDMS/DVB fibers were used with the exception of *Andrés-Iglesias et al.*, who used a DVB/CAR/PDMS fiber.

<sup>b</sup> LOQ = 10 $\sigma$  ( $\sigma$  - standard deviation of fresh pilsner beer).

<sup>c</sup> LOQ = 10 $\sigma$ /S ( $\sigma$  - standard deviation of blank beer, S - slope of calibration curve).

<sup>d</sup> LOQ =  $\bar{x}_B + 10\sigma$  ( $\bar{x}_B$  - mean signal of replicate reagent blanks (n = 10),  $\sigma$  - standard deviation of blank solution).

<sup>e</sup> d<sub>6</sub>-benzaldehyde used on a trial basis for PAA.

LOQ – limit of quantification, EI – electron impact, NCI – negative chemical ionization, 3MB – 3-methylbutanal, FUR – furfural, MET – methional, PAA – phenylacetaldehyde, E2N – (*E*)-2-nonenal, N/A – not available

co-elution of unknown aldehyde- or ketone-PFBOs. The problems associated with m/z=181 are discussed below (*MRM setup and optimization* section) and they are surely the reason why other researchers (Table I) added additional (aldehyde) characteristic ions to their methods. The most important modification to the method published by

*Vesely et al.*<sup>7</sup> is the introduction of internal standards (ISTDs). ISTDs are part of all published methods, excluding the one published by *Vesely et al.*<sup>7</sup>, compiled in Table I. The most common ISTDs are either fluorobenzaldehyde or isotopically labeled benzaldehyde (d<sub>6</sub>-benzaldehyde). Due to its high boiling point (BP~179°C, 1 atm),

$d_6$ -benzaldehyde is frequently combined with a second (low boiling point) aldehyde such as 3-methyl-2-butenal (BP~134°C, 1 atm) or  $d_{10}$ -2-methylbutanal (BP~92°C, 1 atm). In case two ISTDs are used, these are added at two different concentrations. Finally, calibration is performed either in model solutions (e.g. 5 vol% ethanol/water solution, pH 4.5) or preferably in fresh beer.

### Motivation and aim of the current study

HS-SPME-GC-MS with OFD currently appears to be the most suitable option for staling aldehyde analysis. Still, reliable quantification of aldehydes present in the sub- $\mu\text{g/L}$  range is difficult to achieve.<sup>13</sup> In flavor analysis, analysts generally aim to achieve a LOQ well below the flavor threshold of the respective target compound. For aldehydes such as (*E*)-2-nonenal and (*E,E*)-2,4-decadienal with flavor thresholds of ~0.03  $\mu\text{g/L}$  respectively ~0.11  $\mu\text{g/L}$ ,<sup>6</sup> concentrations in beer are commonly close to or even below the LOQ of OFD-HS-SPME-GC-EI-MS methods. In line with brewer's desire to lower the aldehyde levels in beer, brewing chemists aim to develop analysis methods that are more sensitive. One possible measure to improve analytical sensitivity is the use of tandem mass spectrometry (MS/MS). The applicability and advantages of GC-EI-MS/MS in beer flavor analysis were described recently.<sup>14,15</sup> Up to today, only *Schmarr et al.*<sup>16</sup> (use of OFD-HS-SPME-GC-IT-MS/MS) and *Schmidt et al.*<sup>17</sup> (GC-EI-MS/MS after liquid extraction) reported the use of GC-MS/MS for aldehyde analysis in beer. Still, to our best knowledge, there exists no validated and published methodology using OFD and HS-SPME-GC-EI-MS/MS for quantification of staling aldehydes in wort and beer. Given the importance of aldehydes to beer flavor and the challenges associated to their analysis, the aim of the current study was to introduce and fully validate an OFD-HS-SPME-GC-EI-MS/MS method. Assay long-term stability, defined as peak area consistency of two ISTDs over 24 weeks, was evaluated across different beer matrices. In

consideration of the motivation for aldehyde analysis (track beer aging), long-term stability is considered as a key factor, which, for our surprise, is commonly not considered in scientific studies. Finally, in order to benchmark the performance offered by GC-EI-MS/MS, a comparative study with GC-EI-MS was performed.

## Experimental

### Chemicals

The chemicals 2-methylpropanal (99%), pentanal (97.5%), hexanal (98%), furfural (98%), heptanal (95%), octanal (99%), benzaldehyde (99%), nonanal (95%), and decanal (98%) were obtained from Sigma-Aldrich (Steinheim, Germany). 2-methylbutanal (95%), methional (98%), phenylacetaldehyde (95%), and (*E*)-2-nonenal (97%) were purchased from Alfa Aesar (Heysham, Great Britain). 3-methylbutanal (99%) and (*E,E*)-2,4-decadienal (95%) were obtained from J&K Scientific GmbH (Pforzheim, Germany). Based on the expected concentration range, the analyte mixture was prepared in ethanol and was composed as follows: 2 mg/L for pentanal, heptanal, octanal, nonanal, (*E*)-2-nonenal, decanal, and (*E,E*)-2,4-decadienal; 5 mg/L for hexanal; 25 mg/L for 2-methylbutanal, methional, and benzaldehyde; 50 mg/mL for 2-methylpropanal and 3-methylbutanal; 100 mg/mL for phenylacetaldehyde; 200 mg/mL for furfural. All solutions were stored at -20°C. Uniformly labeled  $d_{12}$ -hexanal (CAS No. 1219803-74-3, 96%, Sigma-Aldrich) and benzene ring labeled  $d_5$ -phenylacetaldehyde (CAS No. 879549-73-2, 95%, aromaLAB, Planegg, Germany) were used as internal standards. *O*-(2,3,4,5,6-pentafluorobenzyl)hydroxylamine hydrochloride (PFBHA, 99%) was purchased from Sigma-Aldrich, ethanol absolute and sodium chloride (NaCl) were of analytical grade and were purchased from Th. Geyer (Berlin, Germany). Deionized water was used for dilution of wort samples and PFBHA.

### Beer and wort samples

Within this study, three different sample sets were analyzed: The first sample set used for calibration range adjustment, consisted of 75 samples in total. It contained a range of 60 Lager, Pale Ale, IPA, and non-alcoholic beer samples. The samples varied in age, as commercially available. In addition, 15 wort samples (pre- and post-boil) of different gravities were included. The second sample set used to investigate GC-EI-MS/MS long-term stability included one Lager 5.0% ABV, one Pale Ale 5.4% ABV, one IPA 8.2% ABV, and one non-alcoholic beer 0.4% ABV. Sample selection aimed to cover different alcohol contents as well as a range of aldehyde levels in the fresh product (see section *Long-term method stability and influence of ethanol content on peak areas* for furfural concentrations of the fresh products). These samples were subjected to a storage trial with a total duration of 24 weeks, in which containers of all four beers were stored at 4°C and 20°C. During this period, the samples were repeatedly analyzed. Additionally, forced aged samples (shaken at 20°C for 24 h on a horizontal shaker (100 rpm), then held at 40°C for 4 days) were analyzed. The third sample set

that was used for comparison of the GC-EI-MS/MS (multiple reaction monitoring, MRM) and GC-EI-MS (SIM) methods consisted of four different commercially available Lagers with 5.0% ABV.

### Sample preparation

Beer samples (~20 mL) were transferred in 50 mL laboratory glass bottles. The bottles were loosely sealed with a screw cap and placed in a refrigerator (4°C, 30 min) to remove excess carbon dioxide. After this decarbonization step, two replicates each consisting of 3 mL sample, 1.0 ± 0.1 g NaCl, and 15 µL of an ethanolic ISTD solution (d<sub>12</sub>-hexanal at 1 mg/L, d<sub>5</sub>-phenylacetaldehyde at 10 mg/L) were transferred into 10 mL amber headspace vials. The resulting concentration of d<sub>12</sub>-hexanal was 5 µg/L and of d<sub>5</sub>-phenylacetaldehyde was 50 µg/L. The vials were sealed with magnetic screw caps (silicone/PTFE septum) and were then placed onto a cooled GC-autosampler tray (5°C). Homogenized wort samples were diluted 1 to 10 with deionized water (0.3 mL wort/ 2.7 mL water) and processed accordingly, skipping the decarbonization step.

**Table II. Calibration ranges of 15 selected staling aldehydes as well as the assignment of analyte-ISTD pairs.**

Compound	Range [µg/L]	Quantification by
2-methylpropanal	0.25–250	d <sub>12</sub> -hexanal
2-methylbutanal	0.125–50	d <sub>12</sub> -hexanal
3-methylbutanal	0.25–100	d <sub>12</sub> -hexanal
pentanal	0.01–2	d <sub>12</sub> -hexanal
hexanal	0.025–5	d <sub>12</sub> -hexanal
furfural	1–1000	d <sub>5</sub> -phenylacetaldehyde
heptanal	0.01–2	d <sub>12</sub> -hexanal
methional	0.125–50	d <sub>12</sub> -hexanal
octanal	0.01–2	d <sub>12</sub> -hexanal
benzaldehyde	0.125–25	d <sub>5</sub> -phenylacetaldehyde
phenylacetaldehyde	0.5–100	d <sub>5</sub> -phenylacetaldehyde
nonanal	0.1–4	d <sub>12</sub> -hexanal
(E)-2-nonenal	0.01–2	d <sub>5</sub> -phenylacetaldehyde
decanal	0.01–2	d <sub>12</sub> -hexanal
(E,E)-2,4-decadienal	0.01–2	d <sub>5</sub> -phenylacetaldehyde

### Calibration

Calibration was carried out according to the standard addition method. This method requires a (base) beer with preferably low concentrations of the respective target analytes. For this purpose, a fresh Lager (5.0% ABV) produced by a large-scale industrial brewery was collected immediately after packaging and stored cold (2°C). To record calibration curves 3 mL aliquots of this decarbonated base beer were mixed with 1.0 g ± 0.1 g NaCl, and 15 µL of ISTD solution in 10 mL amber headspace vials. This mixture was then spiked with the diluted analyte mixture. The calibration was performed at seven levels across the calibration ranges given in Table II. The calibration for wort samples was done accordingly, whereas a 1 to 20 diluted wort (0.15 mL wort/ 2.85 mL water) was used as base wort. For aldehyde quantification, the peak areas of the two aldehyde-PFBOs (*syn/anti*) were summed. Exceptions from this were nonanal- and decanal-PFBOs, which were not chromatographically resolved. The area ratios of the blank (Lager) to ISTD, which represents the concentration of aldehydes in the base beer, were subtracted from every calibration point. The fitted area ratios were then plotted against the concentration ratio of analyte against ISTD and in a linear model, curve slope and y intercept were calculated. The concentration of each analyte was finally corrected by the value calculated for an area of zero ( $C_{\text{area } 0}$ ). The analyte-ISTD pairs are shown in Table II.

### Method development: MRM setup and optimization

Retention time and the characteristic fragment ions of analyte and internal standard PFBOs were examined individually by precursor ion scans ( $m/z=29$  to  $m/z=400$ ). Product ion scans were then carried out by selecting suitable precursor ions, whereas one ion was selected for quantification and a second for qualification purposes. MRM transitions that showed

characteristic  $m/z$  and provide a high abundance, were chosen. To optimize MRM signal intensities collision energies of 5, 10, 15, 20, 25, and 30 eV were tested by fivefold measurements. The final value for collision energy for the analytes is listed in Table III. The dwell time was set to record 15-20 data points across a peak (recommended by the instrument manufacturer).

### Method development: Definition HS-SPME conditions and optimization of GC separation

In order to identify suitable conditions for HS-SPME OFD and for GC separation, published studies (Table I) were reviewed. GC optimization aimed the separation of target aldehyde-PFBOs with minimal GC runtime. Practically, optimization was performed by measuring a spiked sample using different GC programs, starting with an initial temperature of 40°C (in accordance to Ortiz<sup>9</sup>). The initial temperature was then adjusted in steps of 10°C, examining 50°C, 60°C, 70°C, and 80°C. To evaluate the influence of a shortened runtime, aldehydes were quantified and resulting data sets were compared.

### Method development: Assignment of analyte-ISTD pairs and calibration range adjustment

In order to establish appropriate analyte-ISTD pairings and a suitable calibration range, 75 samples (Lager, Pale Ale, IPA, non-alcoholic beer, and wort) were analyzed. Here, the upper limits of calibration range were set at 500 µg/L for furfural, 100 µg/L for Strecker aldehydes, 10 µg/L for lipid oxidation products with exception of (*E*)-2-nonenal, whose upper limit was 5 µg/L. In contrast to the final method, all analytes were quantified using both ISTDs and the smallest calibration point was defined as LOQ (1.25 µg/L for furfural, 0.5 µg/L for Strecker aldehydes, 0.05 µg/L for lipid oxidation products with exception of 0.025 µg/L for (*E*)-2-nonenal).

**Table III. Multiple reaction monitoring transitions and retention times of 15 selected staling aldehydes as well as the two stable isotope labeled standards (bold) used for quantification.**

Compound	Quantitative transition [m/z]	Qualitative transition [m/z]	Retention time [min] <sup>a</sup>	Collision energy [eV]
2-methylpropanal	195→145	250→208	4.78/ 4.79	15
2-methylbutanal	181→161	239→181	5.59/ 5.64	25
3-methylbutanal	181→161	239→181	5.73/ 5.80	25
pentanal	239→181	181→161	6.17/ 6.22	25
<b>d<sub>12</sub>-hexanal</b>	243→181	126→62	7.19/ 7.23	15
hexanal	239→181	114→55	7.30/ 7.35	15
furfural	291→181	181→161	7.79/ 8.04	25
heptanal	181→161	239→181	8.60/ 8.64	25
methional	252→181	102→74	9.16/ 9.21	15 <sup>b</sup> / 10 <sup>c</sup>
octanal	181→161	239→181	10.09/ 10.12	25
benzaldehyde	301→181	181→161	10.45/ 10.57	25
<b>d<sub>5</sub>-phenylacetaldehyde</b>	122→94	96→68	11.34/ 11.46	15
phenylacetaldehyde	117→90	91→65	11.37/ 11.51	15
nonanal	181→161	239→181	11.72	25
( <i>E</i> )-2-nonenal	250→181	181→161	12.79/ 13.00	15 <sup>b</sup> / 25 <sup>c</sup>
decanal	181→161	239→181	13.43	25
( <i>E,E</i> )-2,4-decadienal	276→181	181→161	16.12/ 16.23	15 <sup>b</sup> / 25 <sup>c</sup>

<sup>a</sup> The average retention time of *anti*- and *syn*-isomer is plotted. The shift over two years on two different columns is ±0.08 min.

<sup>b</sup> Collision energy for quantitative transition.

<sup>c</sup> Collision energy for qualitative transition.

### Final HS-SPME-GC-EI-MS/MS method

GC-EI-MS/MS analysis was performed on an Agilent Technologies 7890B gas chromatograph interfaced to a 7000C Triple Quadrupole mass spectrometer (Agilent, Santa Clara, CA, USA). This GC-EI-MS/MS setup was equipped with a Gerstel MPS 2XL sampler (Gerstel, Mühlheim an der Ruhr, Germany) for automated HS-SPME sampling. Agilent MassHunter Workstation Software- Qualitative Analysis (ver. B.07.00) and Quantitative Analysis (ver. B.07.01) were used for data analysis. OFD was performed as follows: Per batch one 10 mL headspace vial for derivatization was prepared by addition of 1 mL aqueous PFBHA solution (6 g/L) to 2 mL deionized water. The vial was then sealed and placed in the derivatization position of the agitator. OFD was reached using a 65 µm PDMS/DVB (Supelco, St. Louis, MO, USA) fiber that was preconditioned

according to the manufacturer's instructions. The PDMS/DVB fiber coating was chosen due to its ability to retain the derivatization reagent and for its affinity to PFBHA derivatized compounds.<sup>12</sup> The HS-SPME parameters were as follows: The fiber was placed in the headspace of the vial containing the derivatizing reagent at 50 °C and agitated at 250 rpm (agitator on 60 sec, agitator off 2 sec) for 10 min. Simultaneously, the sample vial was incubated in the agitator to enrich aldehydes in the headspace above the liquid beer sample. OFD was then carried out in the HS of the sample vial for 30 min at 50 °C with an agitation rate of 250 rpm. The fiber was desorbed for 3 min at 240 °C in the injection port operated in split mode with a split ratio of 1:20 (Multimode Inlet System, Agilent) equipped with a 0.75 mm i.d. Ultra Inert SPME Liner (Agilent). To prevent analyte carryover the SPME fiber was conditioned for

5 min at 240 °C after each extraction. The GC analysis was carried out on a HP-5MS UI column (30 m x 0.25 mm i.d. x 0.25 µm film thickness, Agilent) using helium (99.999 %, Air Liquide, Düsseldorf, Germany) as the mobile phase. The following temperature program was used: 80 °C raised to 150 °C at a rate of 15 °C/min, increased to 220 °C at 5 °C/min, followed by a final ramp to 300 °C at 50 °C/min (5 min hold), giving a 25.27 min run time. The MS transfer line temperature was set to 320 °C. Ionization was performed by electron impact (EI) at 70 eV, ion source and MS quadrupole temperatures were set to 230 °C and 150 °C. In the collision cell, the quench gas (helium) was adjusted to a flow of 2.25 mL/min and the collision gas (nitrogen, 99.999 %, Air Liquide) to a flow rate of 1.5 mL/min. The detector gain for each time segment was set from 0.1 to 25 to adapt to the different response factor of each analyte and to reach a minimum area of approximately 1000 for the smallest calibration point.

#### HS-SPME-GC-EI-MS/MS method validation and assessment of long term stability

The HS-SPME-GC-EI-MS/MS method was validated by determination of linearity (Mandel's fitting test<sup>18</sup>,  $R^2$ ), limit of detection (LOD), LOQ, accuracy (%Recovery<sup>18</sup>), measurement precision (%RSD: six fold determination), laboratory precision (%RSD: different days and analysts), and robustness (%RSD: measurement of a randomly picked sample at the beginning, in the middle, and at the end of the batch with 25 samples). LOD and LOQ were determined according to the ASBC method for low-level detection.<sup>19</sup> They are defined as  $LOD = \bar{x}_B + 3\sigma$  and  $LOQ = \bar{x}_B + 10\sigma$  ( $\bar{x}_B$ - mean signal of replicate reagent blanks ( $n = 6$ ),  $\sigma$ - standard deviation of blank beer). The %Recovery of the individual aldehydes were determined at concentration levels of 0.4 µg/L and 1 µg/L referring to pentanal, heptanal, octanal, nonanal, (*E*)-2-nonenal, decanal, and (*E,E*)-2,4-decadienal, respectively at 1 µg/L and 2.5 µg/L for hexanal, 5 µg/L and 12.5 µg/L for 2-methylbutanal, methional, and benzaldehyde, 10 µg/L and 25 µg/L for

2-methylpropanal and 3-methylbutanal, 20 µg/L and 50 µg/L for phenylacetaldehyde, and 40 µg/L and 100 µg/L for furfural.

In order to evaluate the long-term stability of the OFD-HS-SPME-GC-EI-MS/MS method, four different beers (Lager, Pale Ale, IPA, and non-alcoholic beer) were used. Over a period of 24 weeks, these beers were repeatedly analyzed, not to observe the development of aldehydes during aging, but to monitor the changes in the peak areas of  $d_{12}$ -hexanal- and  $d_5$ -phenylacetaldehyde-PFBOs. To assess the quality of the long-term stability, the peak areas of the two ISTDs and the peak area ratios were plotted. The long-term stability is verified by consistent peak area counts and largely unchanged ratio of the two ISTDs.

#### HS-SPME-GC-EI-MS method

GC-EI-MS analysis was performed on a Shimadzu GCMS-QP2010 Plus (Shimadzu Corporation, Kyoto, Japan) equipped with a Gerstel MPS 2XL sampler. Shimadzu LabSolutions Software (ver. 2.70) were used for data analysis. OFD and GC analysis were performed with the exact same parameters as for the HS-SPME-GC-EI-MS/MS method (see above). The only differences compared to GC-EI-MS/MS were the split ratio (1:2) and the SPME Liner (0.75 mm i.d., Restek Corporation, Bellefonte, PA, USA). The analysis was performed in SIM mode. Here, the precursor ions of the MRM were used and the event time was 0.3 s for every analyte or analyte/ISTD respectively. Ionization was performed in electron impact (EI) mode at 70 eV and ion source temperature was 230 °C. Gain values were not adjusted, as this is not recommended by the instrument manufacturer.

## Results and Discussion

In the following chapters, the individual steps of method development are discussed in chronological order. One should not be confused this order partly differs from the final analysis procedure described above. In brief, method development started with the

selection of suitable internal standards. Second, MRM optimization for analytes and standards were performed. Third, GC and HS-SPME conditions were defined. Fourth, analyte-ISTD pairs were assigned and calibration range was adjusted.

### ISTD selection

As described above, published OFD-HS-SPME-GC-MS methods (Table I), use different approaches for quantification. In HS-SPME sampling, which is a non-exhaustive extraction technique, analyte extraction is influenced by the composition of a sample. Therefore, in an ideal world, calibration should be performed individually for each sample. As this is not practically feasible the choice of suitable internal standards is vital.<sup>20</sup> Suitable means that an ISTD should be chemically similar to the analyte of interest, but must not be present in the sample. It should then be added at a concentration level close to the expected analyte concentration. Taken together, this ensures potential changes in extraction conditions affect standard and analyte in a similar fashion.<sup>20</sup> In order to fulfill these demands, the current method uses two ISTDs, namely  $d_{12}$ -hexanal and  $d_5$ -phenylacetaldehyde. This choice ensures that low and high boiling point analytes are properly covered. Four of the 15 analytes elute prior to the  $d_{12}$ -hexanal-PFBOs, which elute at approximately 162 °C. The next six of 15 analytes elute between the  $d_{12}$ -hexanal-PFBOs and the  $d_5$ -phenylacetaldehyde-PFBOs, which elute at approximately 183 °C. The remaining five analytes elute after the  $d_5$ -phenylacetaldehyde-PFBOs, resulting in a trisection of the 15 target analytes (Table III). Staling aldehydes appear in different concentration ranges and are also subject to changes as beer ages. Whereas lipid oxidation products are usually present around levels of 1 µg/L and lower, Strecker aldehydes and furfural in beer range between 1 and 200 µg/L respectively 500 µg/L. Hence,  $d_{12}$ -hexanal was selected as ISTD because it represents the group of alkanals and  $d_5$ -phenylacetaldehyde was selected, as it is a

Strecker aldehyde. The concentrations, at which both ISTDs are added ( $d_{12}$ -hexanal 5 µg/L and  $d_5$ -phenylacetaldehyde 50 µg/L), represent a reasonable compromise with respect to the ISTD-standards pairs (Table II). As can be seen from method validation and long-term stability (see below), the ISTDs work well. In addition, both ISTDs are commercially available from multiple suppliers and can be purchased in high purity for a reasonable price.

### MRM setup and optimization

This step of method development is more elaborate compared to GC-MS. This is due to the fact that two sets of ions, namely precursor and product ions are required and product ion yield optimization by collision-induced dissociation (CID) might be laborious. As mentioned introductory, the most abundant (precursor) ion formed by EI of all aldehyde-PFBOs is  $m/z=181$ . This ion, the pentafluorobenzyl ion (Figure 1), is formed by bond breakage of the methyl-oxygen bond.  $M/z=181$  is also formulated as fivefold fluoro-substituted tropylium ion resonance structure.<sup>21</sup> It is a common fragment ion for all aldehyde-PFBOs and does therefore not contain any information about the nature of the aldehyde. The second most abundant ion of PFBOs depends on the structure of the aldehyde. Figure 1 shows the main fragmentation patterns of alkanal-, (*E*)-2-alkenal-, and (*E,E*)-2,4-alkadienal-PFBOs. As illustrated, the second most abundant ion derived from alkanal-PFBOs is  $m/z=239$  formed by McLafferty rearrangement. For (*E*)-2-alkenals, the second most abundant ion is characterized by  $m/z=250$ . The formation of this ion, according to *Loidl-Stahlhofen*<sup>22</sup>, is triggered by ionization of the double bond system (hydride migration) followed by cleavage of the C-C bond between C-2 and C-3. For (*E,E*)-2,4-alkadienals the second most abundant fragment ion is characterized by  $m/z=276$ .<sup>23</sup>  $M/z=276$  represents a N-O-CH<sub>2</sub>-pentafluorobenzyl substituted pyridinium ion.<sup>24</sup> In product ion scan experiments  $m/z=161$  was determined as the main

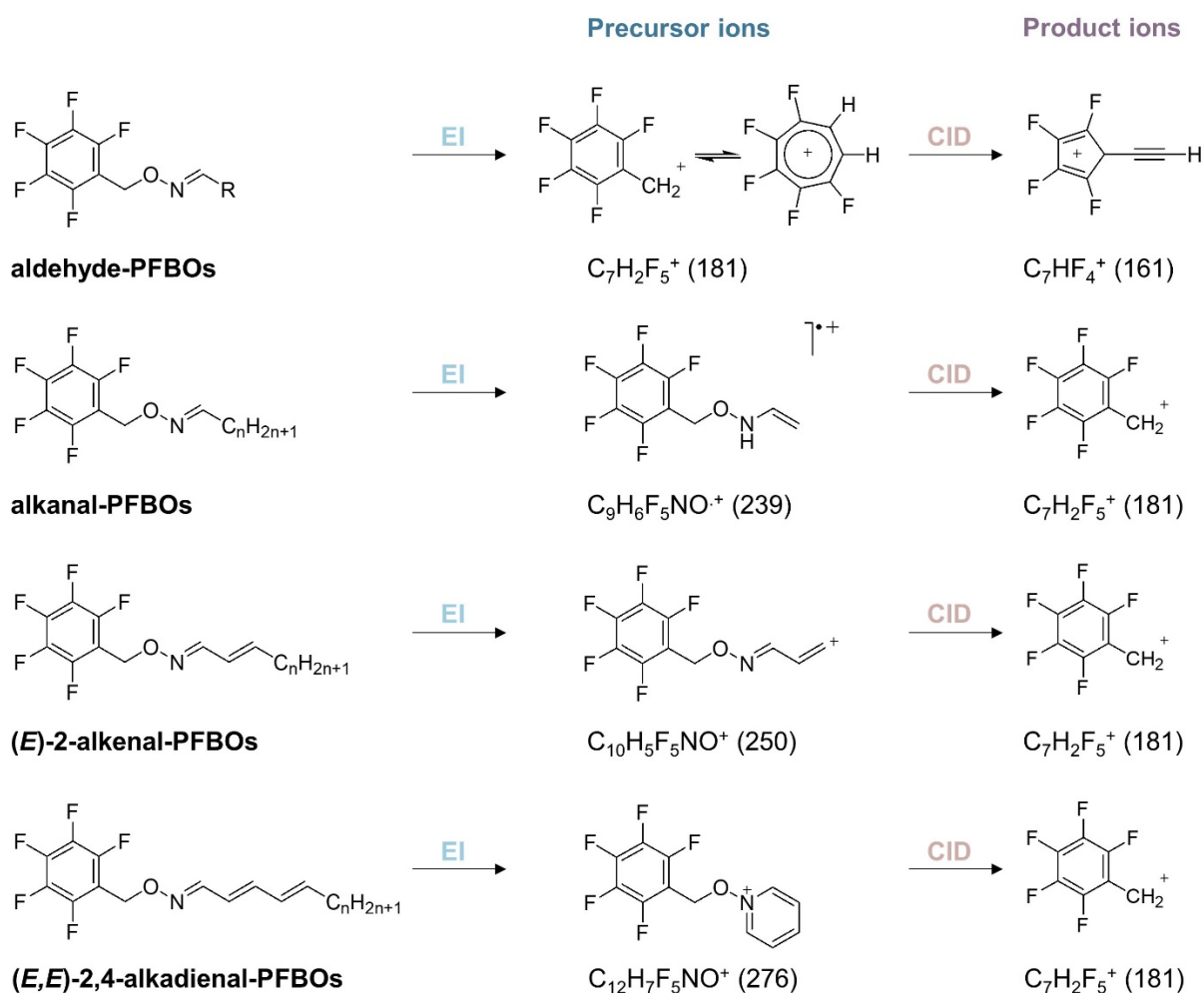


**Figure 1. Schematic representation of electron impact (EI) and collision-induced dissociation (CID) fragmentation of aldehyde-PFBOs for the selected transitions 181→161 m/z, 239→181 m/z, 250→181 m/z, and 276→181 m/z.**

product ion of  $m/z=181$ , whereas  $m/z=181$  was determined as the main product ion of  $m/z=239$ ,  $m/z=250$ , and  $m/z=276$ . Ng *et al.*<sup>21</sup> proposed a structure of  $m/z=161$  after the loss of HF. For furfural- and benzaldehyde-PFBOs the second most abundant ion ( $m/z=291$  and  $m/z=301$  respectively) results from the molecular ion and were used for quantitative MRM transition. Exceptions were methional- and 2-methylpropanal-PFBOs as well as the analytes with a corresponding ISTD (hexanal and phenylacetaldehyde), for which the precursor ion with  $m/z=181$  cannot be used for different reasons. In the case of methional- and 2-methylpropanal-PFBOs, standard addition to a fresh base beer did not result in a linear calibration in lower concentrations. This observation might be explained by the

presence of unknown aldehyde- or ketone-PFBOs that interfere with both target analytes. Hence, for 2-methylpropanal-PFBOs  $m/z=195$  and  $m/z=250$  were chosen as precursor ions, and  $m/z=145$  respectively  $m/z=208$  were chosen as product ions (Table III).  $M/z=195$  and  $m/z=250$  were simply the two next most abundant ions without interferences. For methional-PFBOs, ion selection was more complicated. The second most abundant ion ( $m/z=61$ ) is rather unspecific, same accounts for its product ions. Therefore, the third ( $m/z=102$ ) and fourth ( $m/z=75$ ) abundant ions appeared as suitable candidates.  $M/z=102$  yields product ions with  $m/z=74$ , which was then set as qualitative transition. Unfortunately, observation for  $m/z=75$  was similar as described for  $m/z=61$ . Thus,  $m/z=252$  (fifth

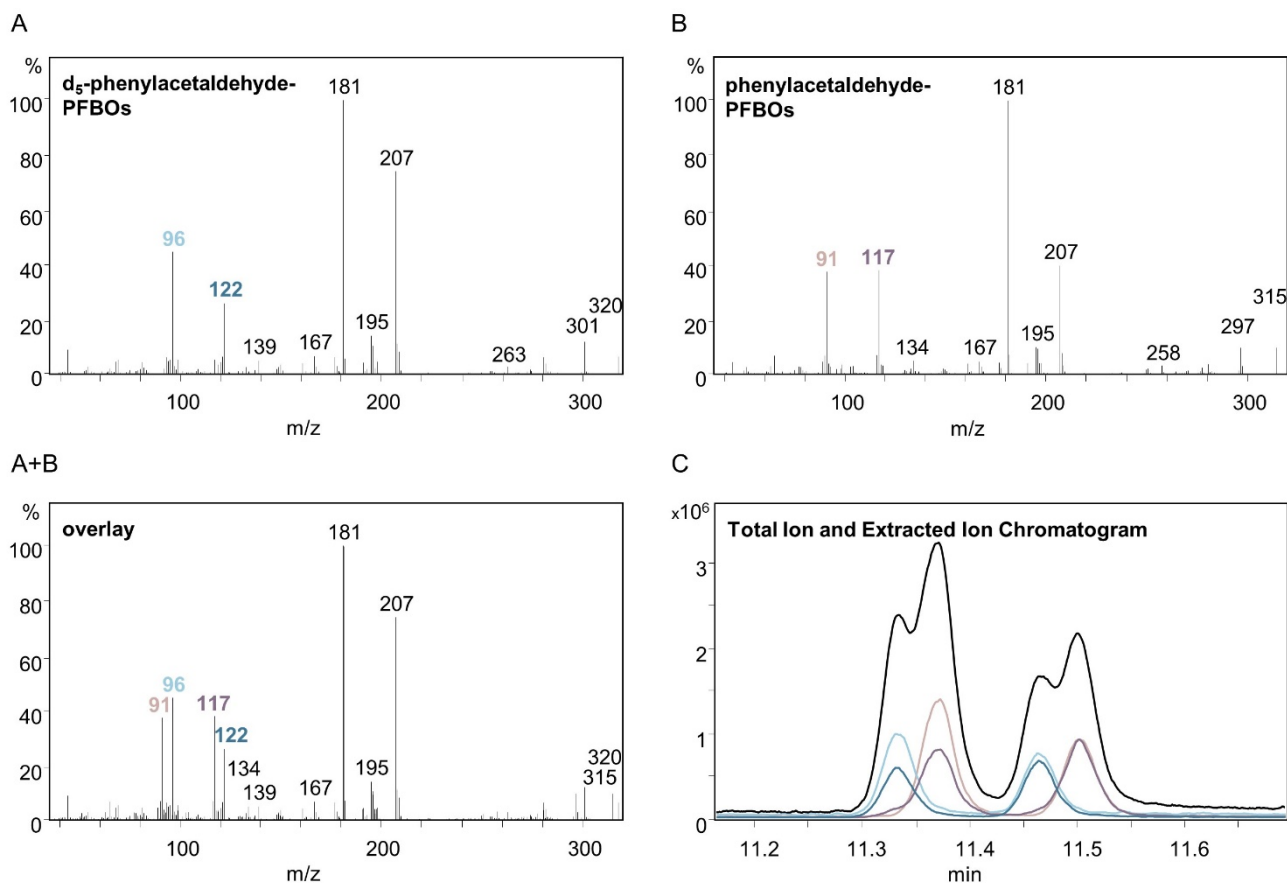


**Figure 2.** Electron impact mass spectra of  $d_5$ -phenylacetaldehyde (A), phenylacetaldehyde (B), an overlay of both spectra (A+B), and a chromatogram of a beer sample showing the ( $d_5$ -)phenylacetaldehyde-PFBO region (C). For A and B, the intensity relative to the base peak is plotted against the mass-to-charge ratio (m/z) while for C, the total ion current is plotted against the retention time. In Figure 2C, the first two overlapping peaks of the total ion current (black line) result from *anti*- $d_5$ -phenylacetaldehyde- and *anti*-phenylacetaldehyde-PFBOs, peaks three and four from *syn*- $d_5$ -phenylacetaldehyde- and *syn*-phenylacetaldehyde-PFBOs. The extracted ion chromatograms of the precursor ions are marked in colored lines.

abundant ion) was selected for the quantitative transition for methional. When selecting MRM for ISTDs ( $d_{12}$ -hexanal and  $d_5$ -phenylacetaldehyde) and their unlabeled isotopologues, it was considered that both compounds co-elute and that abundant fragment ions such as m/z=181 and m/z=207 are present in analyte- and ISTD-PFBOs. In order to distinguish between analyte- and ISTD-PFBOs, specific MRMs are required. Those can be identified by simple comparison of both mass spectra. Figure 2C (black line) shows an extract of a total ion chromatogram illustrating the co-elution of  $d_5$ -phenylacetaldehyde- and phenylacetaldehyde-PFBOs. As one can see, the chromatogram shows four peaks. Since for this type of GC column, the *anti*-isomer elutes before the *syn*-isomer<sup>25</sup>, the first two

overlapping peaks result from *anti*- $d_5$ -phenylacetaldehyde- and *anti*-phenylacetaldehyde-PFBOs, peaks three and four from *syn*- $d_5$ -phenylacetaldehyde- and *syn*-phenylacetaldehyde-PFBOs. Figure 2A and Figure 2B show the mass spectra of  $d_5$ -phenylacetaldehyde- and phenylacetaldehyde-PFBOs, whereas Figure 2A+B represent an overlay of both mass spectra. Figure 2A+B illustrates the spectral overlap between analyte and corresponding ISTD. As can be seen abundant fragment ions match. Differentiation of phenylacetaldehyde- and  $d_5$ -phenylacetaldehyde-PFBOs is granted by ions with m/z=91, m/z=117, m/z=315 and m/z=96, m/z=122, m/z=320 respectively. M/z=315 and m/z=320, representing the molecular ions of phenylacetaldehyde- and  $d_5$ -phenylacetaldehyde-PFBOs, are low

abundant. This is why  $m/z=122$  and  $m/z=96$  are the most suitable fragment ions for  $d_5$ -phenylacetaldehyde-PFBOs and  $m/z=117$  and  $m/z=91$  are the most suitable fragment ions for phenylacetaldehyde-PFBOs. Figure 2C (colored lines) illustrates the extracted ion chromatograms for these four mass traces and the baseline separation of the *anti/syn*-isomers of  $d_5$ -phenylacetaldehyde- and phenylacetaldehyde-PFBOs. For hexanal, the second analyte with corresponding ISTD, the McLafferty fragment was chosen with  $m/z=239$  for hexanal-PFBOs respectively  $m/z=243$  for  $d_{12}$ -hexanal-PFBOs. For qualitative transitions, the fragments  $m/z=114$  for hexanal-PFBOs and the isotopically labeled  $m/z=126$  for  $d_{12}$ -hexanal-PFBOs were used.

The determination of suitable MRM transitions was then followed by optimization of the collision energy in a stepwise procedure (5, 10, 15, 20, 25, and 30 eV). The yield of each product ion (34 ions in sum) was evaluated by integration of the quantitative and qualitative MRM signal intensities (data not shown). The selected collision energies ranged between and 10 and 25 eV and are depicted in Table III. Compared to a previous study, in which most of the analytes had an optimum of intensity at collision energies of 5-15 eV<sup>14</sup>, the collision energies used herein are commonly higher. This is likely due to the structure and high molecular weight of aldehyde-PFBOs.

### Definition HS-SPME conditions and optimization of GC separation

In respect to HS-SPME sampling with OFD, multiple published studies are available (cf. Table I). However, only *Saison et al.*<sup>8</sup> and *Ortiz*<sup>9</sup> published complete parameter sets that could be tested and adapted. The final parameters for HS-SPME with OFD (described in the section *Final HS-SPME-GC-EI-MS/MS method*) are in line with the ones published by *Ortiz*<sup>9</sup>, with a shortened extraction time as described by *Saison et al.*<sup>8</sup>. We have favored a reduced extraction time to increase sample throughput and to match duration of HS-SPME sampling and GC runtime. As this hybrid showed a suitable performance, no efforts for further optimization were undertaken.

In respect to the GC temperature program, modifications were introduced. Previously published methods have long overall runtimes, as temperature gradients started at 40 °C<sup>7,9-11</sup>, 50 °C<sup>4,16</sup>, or 60 °C<sup>8</sup>. As aldehyde levels in the spiked sample using 40°C, 50°C, 60°C, 70°C, and 80°C did not differ significantly (data not shown), the GC temperature program was shortened by setting the initial temperature to 80 °C. By doing so, the GC runtime was reduced to 25.27 min, allowing interlacing of sample preparation and separation. From a quality perspective, a fast assay is advantageous as it reduces a potential increase/formation of reactive analytes during sample holding times.

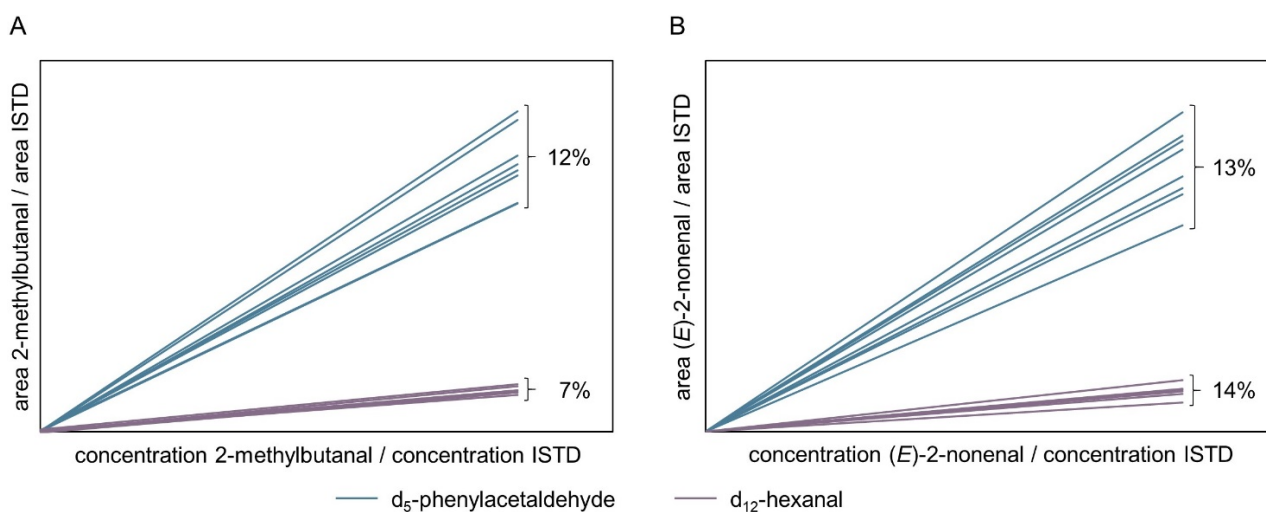


**Figure 3. Calibration curves of 2-methylbutanal (A) and (E)-2-nonenal (B) using either  $d_5$ -phenylacetaldehyde (blue) or  $d_{12}$ -hexanal (purple) as ISTD.**

### Assignment of analyte-ISTD pairs and calibration range adjustment

To establish appropriate analyte-ISTD pairings and a suitable calibration range, 75 samples (Lager, Pale Ale, IPA, non-alcoholic beer, and wort) were analyzed. After analysis of this sample set, including eight recalibrations, the linearity of calibration ( $R^2$ ) was judged fully acceptable by both ISTDs ( $>0.99$ ). Thus, the criterion of linearity could not be applied for the selection of most suitable analyte-ISTD pairs. In order to identify the most suitable analyte-ISTD pairs, we compared the slopes of the calibration graphs. While little variation in slope over time means analyte and standard behave very similar, larger variations indicate that the analyte-standard system is likely affected by changes in instrument performance and fiber aging.<sup>26</sup>

As an example, the calibration curves of 2-methylbutanal (Figure 3A) and (*E*)-2-nonenal (Figure 3B) are given using *d*<sub>5</sub>-phenylacetaldehyde as well as *d*<sub>12</sub>-hexanal as ISTD. The Strecker aldehyde

2-methylbutanal provides with *d*<sub>12</sub>-hexanal significantly more stable slopes of the calibration curves than with the Strecker ISTD *d*<sub>5</sub>-phenylacetaldehyde. (*E*)-2-nonenal on the other hand shows a more stable slope by using *d*<sub>5</sub>-phenylacetaldehyde as ISTD. Thus, the originally intended ISTD-analyte (based on structural similarity or retention time) was partly adjusted and the final analyte-ISTD pairings are listed in Table II.

The next focus was set on the adaptation of a suitable calibration range. For this purpose, the measured minimum and maximum concentrations (preliminary method) practically found in each of 60 beers of different beer styles and 15 wort samples were used (Table IV). At this point, the results might not be discussed in detail, however it is obvious that aldehyde concentrations are beer style specific. While aldehyde levels in Lager tend to be low, non-alcoholic beer and wort are characterized by high aldehydes levels. For all 60 beer samples, the selected upper limit of the calibration range corresponded to the maximum value. As

**Table IV. Concentration ranges of aldehydes in different matrices.<sup>a</sup>**

Compound	Lager [ $\mu\text{g/L}$ ] <sup>b</sup>	Pale Ale and IPA [ $\mu\text{g/L}$ ]	Non-alcoholic beer [ $\mu\text{g/L}$ ]	Wort [ $\mu\text{g/L}$ ]
2-methylpropanal	8.84–95.2	5.16–44.1	12.2–182.1	37.3–1541
2-methylbutanal	1.68–26.2	1.27–7.76	2.11–79.2	9.2–1245
3-methylbutanal	3.91–63.7	4.30–28.8	8.49–189.5	39.2–1654
pentanal	0.13–0.68	0.09–0.48	0.13–0.95	2.8–32.3
hexanal	0.38–1.86	0.26–1.54	0.25–2.19	8.5–133.6
furfural	29.5–356.9	1.50–31.1	26.9–601.0	85.4–2646
heptanal	0.08–0.69	0.06–0.38	0.10–0.69	1.4–5.9
methional	1.02–39.0	2.21–24.8	1.00–67.2	27.5–359.6
octanal	0.07–0.56	0.06–2.01	<0.05–0.15	1.1–3.5
benzaldehyde	<0.5–2.78	<0.5–1.8	<0.5–3.44	5.4–53.3
phenylacetaldehyde	6.91–95.9	8.33–37.7	5.10–80.8	70.8–295.6
nonanal	0.13–1.15	0.13–5.38	0.10–0.38	3.8–12.1
( <i>E</i> )-2-nonenal	0.07–0.34	<0.025–0.12	<0.025–0.14	0.3–1.9
decanal	<0.05–0.26	0.06–0.22	<0.05–0.29	<0.5–7.9
( <i>E,E</i> )-2,4-decadienal	<0.05–0.06	<0.05	<0.05	<0.5–4.1

<sup>a</sup> To estimate a suitable calibration range beer and wort samples (in total 75) were analyzed using the preliminary method. Hence, the minimum concentrations given in this table do not correspond with the LOQ of the final validated method.

<sup>b</sup> Fresh and aged samples.

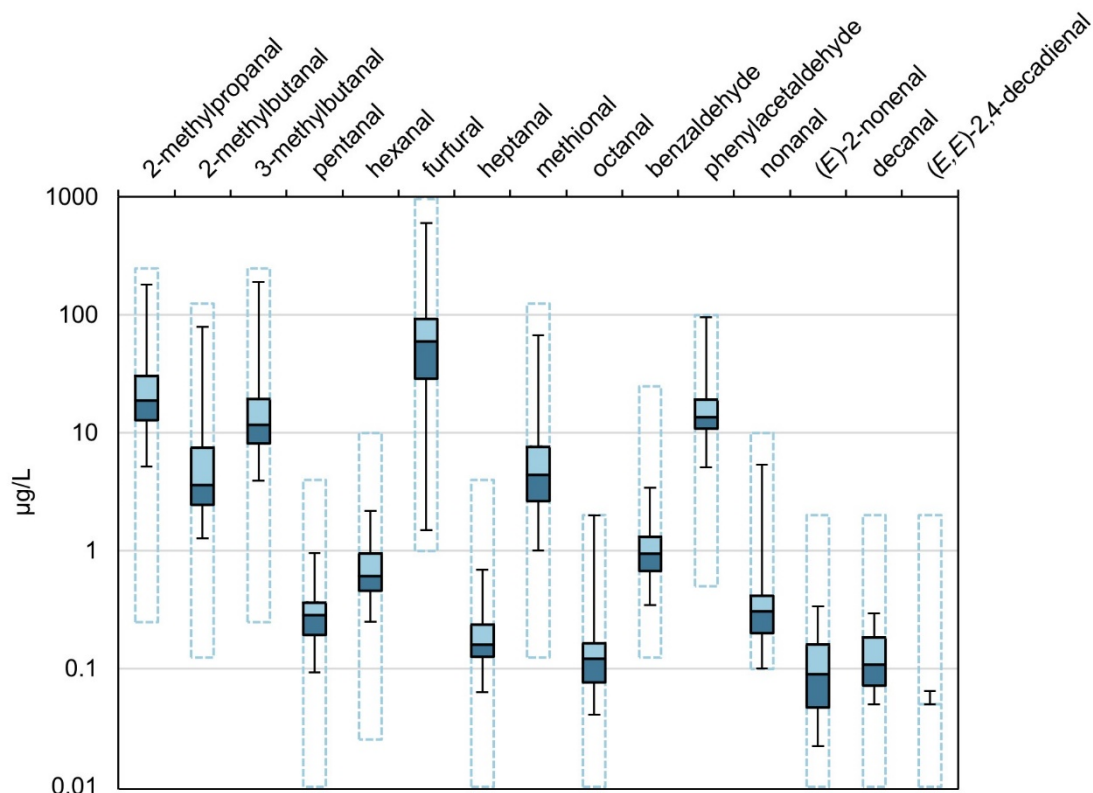


**Figure 4. Boxplots (logarithmic scale) summarizing the dataset from staling aldehyde analysis of 60 beer samples measured for calibration range adjustment. Minimal and maximal concentrations for each aldehyde are indicated by the whiskers. The light blue boxes stand for the third quartile (middle value between the highest concentration and the median concentration), the dark blue boxes for the first quartile (middle value between the lowest concentration and the median concentration), and the black line separating these two boxes stands for the median concentration. The final calibration ranges appear as light blue dashed lines, which are also listed in Table II.**

described in the section *Method development: Assignment of analyte-ISTD pairs and calibration range adjustment*, the smallest calibration point was also defined as LOQ. By doing so, the concentrations of some aldehydes (e.g. *(E,E)*-2,4-decadienal) were below the LOQ. Since it was technically possible to calibrate in an even lower range, the working range was adjusted to achieve the final method (see Table II). Figure 4 summarizes the data from each of the 60 beers of different style (Table IV) in a boxplot chart, the newly defined calibration ranges appear as blue dashed lines. As the concentration ranges of the individual aldehydes differ significantly, the boxplots are based on a logarithmic scale. The wort samples were excluded from Figure 4 since their aldehyde level is significantly higher than that of beer samples. By simply replacing 3 mL beer with 3 mL wort, the

method is too sensitive. Hence, different modifications such as dilution of the wort samples and split ratio adjustment were tested (data not shown). Finally, a dilution (1:10) with deionized water was found most suitable. It is advantageous that both beer and wort samples can be quantified with one measurement method.

#### Method validation

In order to confirm that the established method is well suited for its intended use, extensive method validation was performed. The results of method validation are summarized in Table V. In brief, OFD-HS-SPME-GC-EI-MS/MS analysis showed an excellent linearity ( $R^2 > 0.99$ ) in the Mandel fitting test. The LOD and LOQ were also well below the flavor thresholds of the selected compounds and below those of published methods (Table I). Recoveries

**Table V. Statistical parameters of method validation: linearity (range, R<sup>2</sup>, Mandel fitting test), limit of detection and quantification (LOD, LOQ), %recovery, and measurement precision.**

Compound	Linearity			LOD <sup>a</sup> / LOQ <sup>b</sup> [µg/L]	%Recovery <sup>c</sup>	Precision [%RSD]
	Range [µg/L]	R <sup>2</sup>	Mandel			
2-methylpropanal	0.25–250	>0.99	linear	0.021/ 0.072	87–96	2.4 <sup>d</sup> / 5.7 <sup>e</sup> / 3.2 <sup>f</sup>
2-methylbutanal	0.125–125	>0.99	linear	0.018/ 0.059	89–94	2.3 <sup>d</sup> / 4.0 <sup>e</sup> / 3.8 <sup>f</sup>
3-methylbutanal	0.25–250	>0.99	linear	0.064/ 0.214	98–108	2.3 <sup>d</sup> / 5.0 <sup>e</sup> / 4.0 <sup>f</sup>
pentanal	0.01–4	>0.99	linear	0.001/ 0.005	94–105	4.5 <sup>d</sup> / 4.8 <sup>e</sup> / 3.4 <sup>f</sup>
hexanal	0.025–10	>0.99	linear	0.003/ 0.009	98–99	4.0 <sup>d</sup> / 2.5 <sup>e</sup> / 3.4 <sup>f</sup>
furfural	1–1000	>0.99	linear	0.111/ 0.371	88–93	5.5 <sup>d</sup> / 5.5 <sup>e</sup> / 7.2 <sup>f</sup>
heptanal	0.01–4	>0.99	linear	0.001/ 0.004	100–103	3.9 <sup>d</sup> / 3.5 <sup>e</sup> / 3.9 <sup>f</sup>
methional	0.125–125	>0.99	linear	0.030/ 0.100	103–118	9.2 <sup>d</sup> / 7.1 <sup>e</sup> / 2.2 <sup>f</sup>
octanal	0.01–2	>0.99	linear	0.003/ 0.010	90–107	4.9 <sup>d</sup> / 7.2 <sup>e</sup> / 8.2 <sup>f</sup>
benzaldehyde	0.125–25	>0.99	linear	0.052/ 0.173	83–88	4.9 <sup>d</sup> / 1.7 <sup>e</sup> / 8.1 <sup>f</sup>
phenylacetaldehyde	0.5–100	>0.99	linear	0.129/ 0.432	105–107	1.6 <sup>d</sup> / 3.4 <sup>e</sup> / 4.0 <sup>f</sup>
nonanal	0.1–10	>0.99	linear	0.024/ 0.081	97–117	7.0 <sup>d</sup> / 12.1 <sup>e</sup> / 6.6 <sup>f</sup>
( <i>E</i> )-2-nonenal	0.01–2	>0.99	linear	0.003/ 0.009	81–98	5.1 <sup>d</sup> / 5.2 <sup>e</sup> / 6.0 <sup>f</sup>
decanal	0.01–2	>0.99	linear	0.003/ 0.010	94–96	8.3 <sup>d</sup> / 2.4 <sup>e</sup> / 6.3 <sup>f</sup>
( <i>E,E</i> )-2,4-decadienal	0.01–2	>0.99	linear	0.001/ 0.003	80–85	2.6 <sup>d</sup> / 2.5 <sup>e</sup> / 3.8 <sup>f</sup>

<sup>a</sup> LOD =  $\bar{x}_B + 3\sigma$  ( $\bar{x}_B$ - mean signal of replicate reagent blanks (n = 6),  $\sigma$ - standard deviation of blank beer)

<sup>b</sup> LOQ =  $\bar{x}_B + 10\sigma$

<sup>c</sup> Mean %Recovery (n = 3) at two concentration levels.

<sup>d</sup> Measurement precision (n = 6).

<sup>e</sup> Laboratory precision at two days (n = 6).

<sup>f</sup> Laboratory precision for two analysts (n = 6).

ranged from 80-118%, with (*E,E*)-2,4-decadienal trending low (80-85%) and methional trending high (103-118%). For hexanal and phenylacetaldehyde the recoveries were 98-99% and 105-107%, which is likely explained by the fact d<sub>12</sub>-hexanal and d<sub>5</sub>-phenylacetaldehyde were used as ISTDs. The measurement precision, 6 fold repeat analysis of a single sample, showed an RSD < 10% for all analytes, while 10 out of 15 analytes varied less than 5 %RSD (Table V). Methional (9.2 %RSD) was the compound that was analyzed with the lowest measurement precision. Laboratory precision, defined as relative standard deviation (%RSD) obtained from repeat analysis of a sample on different days by different analysts, was also < 10 %RSD for all analytes except nonanal (12.1 %RSD). The

good match between laboratory precision and measurement precision underlines excellent method applicability. Robustness, i.e. the repeat analysis of a sample at the beginning, in the middle, and at the end of a batch of 25 samples, was < 10 %RSD for all analytes with the exception of methional (13.2 %RSD). Methional is the only sulfur-containing aldehyde tested. It is chemically reactive, which is a probable explanation for higher variations in both measurement precision and robustness testing. In sum, method validation confirmed the method is very suitable for aldehydes analysis.

#### **Long-term method stability and influence of ethanol content on peak areas**

In many cases, staling aldehyde analysis accompanies long-term storage trials aiming

to monitor chemical and sensory changes of beer during shelf life. Thus, a consistent high analytical performance, herein referred as the long-term method stability, is of prime importance. In brewery quality control laboratories, daily method performance checks are carried out by analysis of a “standard beer”. In addition to instrument calibration, this ensures collection of reliable data. While this works well for parameters that are not affected by the age of a sample (e.g. ethanol content in beer), the significance of this approach in staling aldehyde analysis can be questioned. As there (unfortunately) exists no entirely stable beer, alternative approaches to validate long-term stability are required. In GC methods that use two ISTDs, ISTD peak area and ISTD peak area ratio are a suitable measures to monitor system (in)stability.<sup>15,26</sup> In order to assess long-term stability of the OFD-HS-SPME-GC-EI-MS/MS method, four beers covering a wide range of alcohol contents and a wide range of

aldehyde levels in fresh and aged product (data not shown) were tested. To illustrate the chemical variation within the set of four beer samples, the alcohol and furfural concentration are stated hereafter: The first product was a domestic Lager with 5.0% ABV and a furfural level of 2.31 µg/L in the fresh product. Product 2 and 3 were ales that contained 5.4% ABV (Pale Ale) and 8.2% ABV (IPA). The fresh Pale Ale contained 1.30 µg/L furfural, the IPA 2.93 µg/L. The last product analyzed was a non-alcoholic beer with 0.4% ABV and a furfural level of 40.14 µg/L in the fresh product. The focus of this repeated analysis was not to track the evolution of aldehydes upon aging, but to monitor the peak area evolution of d<sub>12</sub>-hexanal- and d<sub>5</sub>-phenylacetaldehyde-PFBOs. Figure 5 summarizes the results obtained from the long-term stability trial. It shows four groups of each 22 stacked bars that represent the four different beer samples. Each of the 22 stacked bars labelled with A-V represent the

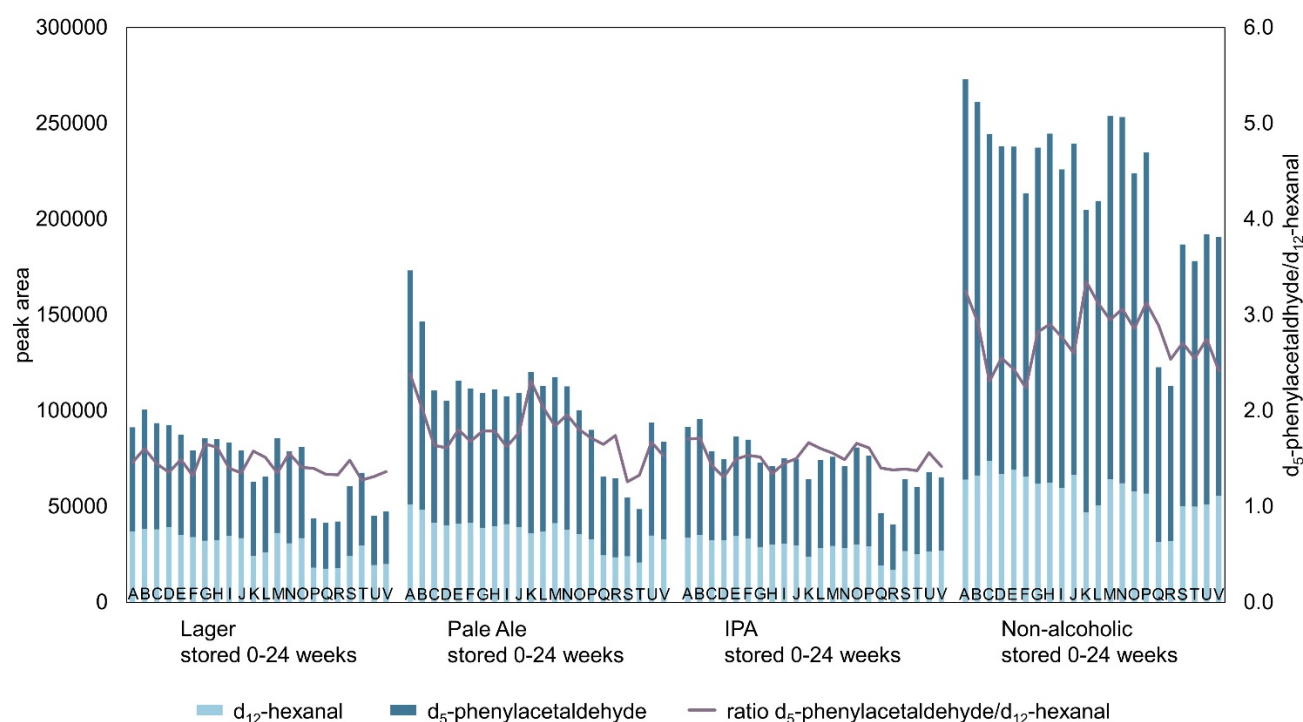


**Figure 5. Evolution of peak areas (d<sub>5</sub>-phenylacetaldehyde- and d<sub>12</sub>-hexanal-PFBOs) and peak area ratio (d<sub>5</sub>-phenylacetaldehyde/d<sub>12</sub>-hexanal PFBOs) determined by repeat analysis of four beer samples. The selected beers (non-alcoholic, Lager, Pale Ale, and IPA) were analyzed at 7 time points: A+B represent the fresh product, C+D represent 2 weeks, E+F represent forced aged samples, G+H represent 4 weeks, I+J represent 8 weeks, K+L represent 12 weeks, M+P represent 18 weeks, Q+R represent 24 weeks of storage. Bar charts indicate the peak area of the respective ISTD and lines plot the ratio between standard pairs.**

peak areas of d<sub>5</sub>-phenylacetaldehyde spiked at 50 µg/L and d<sub>12</sub>-hexanal spiked at 5 µg/L obtained from a single injection. The purple line illustrates the ratio of both peak areas, which was calculated by dividing the peak area of d<sub>5</sub>-phenylacetaldehyde-PFBOs by the peak area of d<sub>12</sub>-hexanal-PFBOs. The trial had a total duration of 24 weeks, during this period the OFD-HS-SPME-GC-EI-MS/MS analysis was executed at seven sampling points. The bar charts A+B in Figure 5 were recorded in the fresh product, C-D were recorded after 2 weeks, E+F represent forced aged samples, G-J were recorded after 4 weeks, K+L were recorded after 8 weeks, M-P were recorded after 12 weeks, Q+R were recorded after 18 weeks, whereas the bar charts S-V were recorded after 24 weeks storage.

When repeatedly applying a method to a sample over period of months or weeks, method long-term stability is verified by consistently (high) peak areas of the ISTDs and most importantly by their ratio. While total peak areas might be affected by instrumental changes (e.g. ion source cleaning, column replacement and fiber replacement) the ratio should remain constant. As one can see from Figure 5, the ISTD peak areas vary to some extent (refer to bars Q+R in Figure 5) while the peak area ratios remained largely unchanged. Under consideration of all measurements (22 injections for each product), the ratio of d<sub>5</sub>-phenylacetaldehyde/d<sub>12</sub>-hexanal varied less than 15%. As the structural differences of both ISTDs are set in relation to the structural differences within the group of the 15 target analytes, both ISTDs are chemically different (boiling point, linear vs. aromatic). Hence, one can conclude that the practical long-term analytical variation of OFD-HS-SPME-GC-EI-MS/MS is < 15%. While validation parameters such as the measurement or laboratory precision refer to experiments performed within a short time frame, long-term stability testing is surely of more practical relevance. With the peak area ratio of two chemically different compounds added to different samples in known concentrations

having a variation of < 15%, storage induced aldehyde changes of ≥ 15% can practically be judged significant.

As a side effect of this trial, the sample set was also useful to evaluate matrix effects concerning SPME extraction. Figure 5 illustrates that the ISTD areas in the non-alcoholic beer (0.4% ABV) were consistently higher compared to those found in the three conventional beers (5.0% - 8.2% ABV). While the peak areas of d<sub>12</sub>-hexanal-PFBOs tended to be slightly elevated (10-15%), peak areas of d<sub>5</sub>-phenylacetaldehyde-PFBOs reached up to ~300%. This observation attributes to the low ethanol concentration in the non-alcoholic beer and corresponds with observations from wort analysis. Ethanol is the primary volatile of beer and reduced ethanol levels are known to favor the extraction of high boiling point volatiles such as d<sub>5</sub>-phenylacetaldehyde. Driven by the increased extraction of d<sub>5</sub>-phenylacetaldehyde, the ratio of d<sub>5</sub>-phenylacetaldehyde/d<sub>12</sub>-hexanal changed, it is significantly higher in the non-alcoholic beer compared to the other beers tested. When comparing the peak areas and the peak area ratio of d<sub>5</sub>-phenylacetaldehyde/d<sub>12</sub>-hexanal in the conventional products, no correlation of ISTD areas and ethanol exists (Figure 5). Variations in the peak area ratios amongst the Lager, the Pale Ale, and the IPA might be explained by minor compositional factors (e.g. fermentation by-product spectrum, concentration of hop-derived volatiles, overall concentration of aldehydes). Practically, the shift in the peak area ratio of the two internal standards illustrates how ethanol or presumably other compositional factors might influence aldehyde quantification. While the matrix has comparably little effect on the extraction of volatiles with lower boiling points (here d<sub>12</sub>-hexanal with BP ~130°C, 1 atm), higher boiling point compounds (here d<sub>5</sub>-phenylacetaldehyde with BP ~195°C, 1 atm) are strongly affected. This in mind, one could suggest to differentiate between calibration procedures for non-alcoholic and conventional beer samples, or even to

calibrate each beer individually. With respect to the differences observed amongst the non-alcoholic beer and the conventional beers, calibration routine adjustment is an option when aiming for an accurate analysis of staling aldehydes in non-alcoholic beer. However, considering the minimal differences between the Lager, the Pale Ale, and the IPA, a beer style specific calibration does not appear meaningful when two ISTDs are used. By using one ISTD with a low and one ISTD with a high boiling point, suitable analyte-ISTD pairs can be defined and extraction related matrix effects are reduced. In the case where external calibration is performed or a single ISTD is used, beer style specific calibration appears unavoidable/reasonable.

#### **Comparison of final GC-EI-MS/MS and GC-EI-MS method**

Finally, to demonstrate and benchmark the benefits of GC-EI-MS/MS in aldehyde analysis, a comparative study with GC-EI-MS was performed. For this, the analysis parameters of the optimized GC-EI-MS/MS method were transferred onto a single quadrupole GC-EI-MS instrument. The MRM precursor ions of GC-EI-MS/MS served as selected ions of GC-EI-MS, yielding a SIM method with similar performance compared to published studies (Table I). The comparison of GC-EI-MS/MS (MRM) and GC-EI-MS (SIM) was then based on running a calibration followed by the analysis of four different Lager samples. All samples were run in parallel, whereby both instruments were equipped with new SPME-fibers. When comparing SIM and MRM chromatograms, peak areas, calibration curves, and final results of quantification, multiple differences were observed. Many of these observations directly relate to technical aspects of (tandem) mass spectrometry, but a detailed discussion is beyond the scope of this paper. With respect to analysis data, the comparative study yielded three major findings: First, the analytical consistency judged by the %RSD of a triplicate analysis varied between the methods (Figure 6).

Second, both methods applied to the exact same sample lead to different results, whereas these differences relate to the nature of the target analyte. Third, in terms of LOQ, MRM is superior to SIM. Figure 6 shows the concentrations of six selected aldehydes, namely (*E*)-2-nonenal, hexanal, nonanal, methional, phenylacetaldehyde, and furfural derived from MRM (GC-EI-MS/MS) and SIM (GC-EI-MS) analysis. The error bars represent the %RSD, which was calculated from the mean value and the standard deviation obtained from triplicate analysis of each beer. When using GC-EI-MS/MS, the %RSD was below 10% for all aldehydes tested. In the best case, quantification of 2-methylpropanal in beer %RSD was 1.4%. GC-EI-MS analysis resulted in %RSDs usually greater than 10%. More precisely, 39 out of 60 triplicates (4 samples tested for 15 analytes = 60 triplicates) ranged between 10.1% and 45.0%RSD. For the six aldehydes shown in Figure 6 these deviations are visualized by error bars, which tend to be small for MRM and large for SIM. Obviously, the most critical analytes were (*E*)-2-nonenal (Figure 6A) and methional (Figure 6D). In the case of (*E*)-2-nonenal %RSD ranged from 27 to 39%, in the case of methional %RSD ranged from 23 to 45%. With the given variation, the informative value of this analysis is questionable. When comparing the aldehyde concentrations determined by SIM and MRM, higher values for almost all compounds were obtained by the SIM method. Setting the MRM result to 100%, the quantification via SIM yielded an average overestimation of 30%. In the example of (*E*)-2-nonenal quantification via SIM resulted in concentrations ranging up to 50% higher compared to MRM. Very similar observations were made for hexanal (Figure 6B), but also for 2-methylbutanal and phenylacetaldehyde (Figure 6E). Overall, furfural (Figure 6F) showed the best match between both methods. The concentration of furfural in beer was considerably higher compared to those of all other aldehydes tested. Differences between the results from both methods can be explained by the nature of the

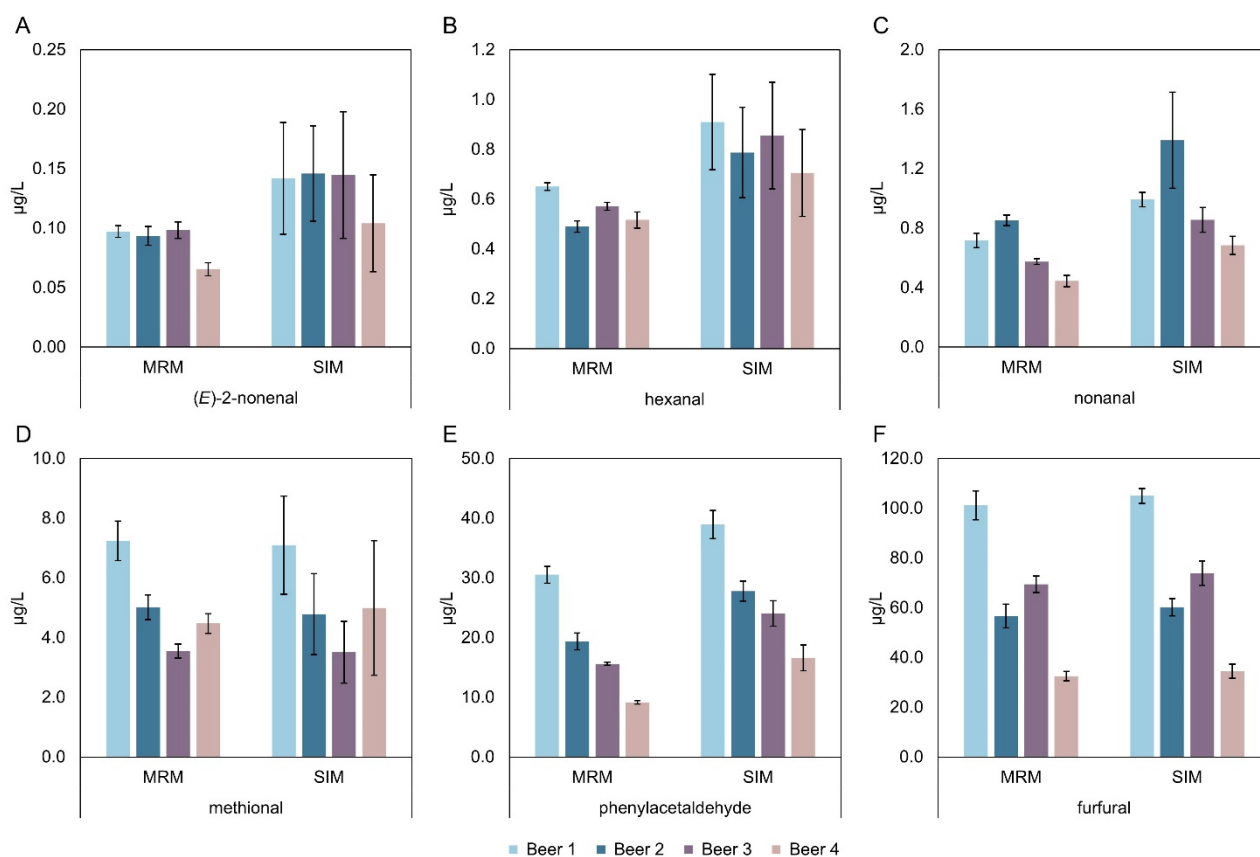


**Figure 6. Concentrations of six selected aldehydes ((E)-2-nonenal (A), hexanal (B), nonanal (C), methional (D), phenylacetaldehyde (E), and furfural (F)) derived from comparative analysis by GC-EI-MS/MS (MRM) and GC-EI-MS (SIM). The four Lager were measured in triplicate. The color-coded bar charts illustrate the mean value of each triplicate, while the error bars indicate the %RSD.**

OFD protocol with PFBHA and the noise filtering by MRM. A major advantage of OFD with PFBHA is that volatiles with a carbonyl function are efficiently derivatized and resulting PFBOs are detected sensitively. The disadvantage is that the primary ions formed during PFBO fragmentation (EI) are specific for the group of PFBOs (Figure 1) but do not necessarily allow unambiguous assignment of individual aldehyde- or ketone-PFBOs. In simple words, the presence of minor aldehydes and ketones in beer produces multiple uncharacterized PFBOs. Even though most PFBOs might only result in a noisy baseline, this appears to be sufficient to interfere with the quantification of low concentrated target compounds such as (E)-2-nonenal. Given by the nature of SIM, these matrix effects are more pronounced compared to MRM and might have greater effects on quantification (increased values). When aiming to quantify linear aldehydes, e.g. heptanal, octanal, or decanal, noise might

hinder the achievement of suitable LOQs. In the given study SIM mode sensitivity was insufficient in the lower calibration range (0.01-0.04  $\mu\text{g/L}$ ), whereas this was easily achieved using MRM. In summary, the performance of GC-EI-MS appeared acceptable for aldehydes present in  $\mu\text{g/L}$  levels (e.g. Strecker aldehydes and furfural). Due to its lack of sensitivity and specificity, it is not generally recommended when aiming for quantification of linear alkanals and alkenals. Doubtless, more reproducible results are achieved using GC-EI-MS/MS, which is due to the superior selectivity of MRM.

## Conclusion

An OFD-HS-SPME-GC-EI-MS/MS method for staling aldehyde analysis was introduced and successfully validated. The final method is demonstrably able to cover a wide

concentration range that enables an application to all relevant matrices ranging from fresh Lager beer (low aldehyde levels) to wort (high aldehyde levels). During method development, special attention was paid to ISTD selection and MRM design. Both aspects are crucial as they greatly influence method performance. To benchmark the advantages of GC-EI-MS/MS (MRM) in staling aldehydes analysis of beer, comparative measurements with GC-EI-MS (SIM) were carried out. In summary, aldehyde levels determined by GC-EI-MS/MS were lower compared to those found by GC-EI-MS. Reproducibility, especially for low concentrated staling aldehydes, was improved when using GC-EI-MS/MS. Both differences between GC-EI-MS/MS and GC-EI-MS relate to the noise filtering by MRM. In order to underline the practical applicability and value of this OFD-HS-SPME-GC-EI-MS/MS method for long-running experiments (e.g. storage trials), the long-term stability was comprehensively investigated. Overall, OFD-HS-SPME in combination with GC-EI-MS/MS technique was proven to be powerful when targeting reactive and low molecular weight compounds like aldehydes. In respect of the sensitivity achieved, OFD-HS-SPME-GC-EI-MS/MS technology might be adapted to other, even more challenging target analytes such as thiols.

## Additional information

### Funding details

This research received partial funding by the German Federal Ministry for Economic Affairs and Energy. Data presented herein is part of the project MF150164, the GC-MS/MS instrument is part of grant number 49IZ180038.

## Literature Cited

1. Baert, JJ; Clippeleer, J de; Hughes, PS; Cooman, L de; Aerts, G. On the Origin of Free and Bound Staling Aldehydes in Beer. *J. Agric. Food Chem.* 60(46), 11449–11472, 2012.
2. Vanderhaegen, B; Neven, H; Verachtert, H; Derdelinckx, G. The chemistry of beer aging – a critical review. *Food Chem.* 95(3), 357–381, 2006.
3. Bustillo Trueba, P; Clippeleer, J de; Van der Eycken, Erik; Guevara Romero, Juan Sebastian; Rouck, G de; Aerts, G; Cooman, L de. Influence of pH on the Stability of 2-Substituted 1,3-Thiazolidine-4-Carboxylic Acids in Model Solutions. *J. Am. Soc. Brew. Chem.* 76(4), 272–280, 2018.
4. Baert, JJ; Clippeleer, J de; Jaskula-Goiris, B; Opstaele, F van; Rouck, G de; Aerts, G; Cooman, L de. Further Elucidation of Beer Flavor Instability: The Potential Role of Cysteine-Bound Aldehydes. *J. Am. Soc. Brew. Chem.* 73(3), 243–252, 2015.
5. Suda, T; Yasuda, Y; Imai, T; Ogawa, Y. Mechanisms for the development of Strecker aldehydes during beer aging. 31st European Brewery Convention Congress, Venice, Italy, 2007.
6. Saison, D; Schutter, DP de; Uyttenhove, B; Delvaux, F; Delvaux, FR. Contribution of staling compounds to the aged flavour of lager beer by studying their flavour thresholds. *Food Chem.* 114(4), 1206–1215, 2009.
7. Vesely, P; Lusk, L; Basarova, G; Seabrooks, J; Ryder, D. Analysis of Aldehydes in Beer Using Solid-Phase Microextraction with On-Fiber Derivatization and Gas Chromatography/Mass Spectrometry. *J. Agric. Food Chem.* 51(24), 6941–6944, 2003.

8. Saison, D; Schutter, DP de; Delvaux, F; Delvaux, FR. Optimisation of a complete method for the analysis of volatiles involved in the flavour stability of beer by solid-phase microextraction in combination with gas chromatography and mass spectrometry. *J. Chromatogr. A*. 1190(1-2), 342–349, 2008.
9. Ortiz, RM. Analysis of Selected Aldehydes in Packaged Beer by Solid-Phase Microextraction (SPME)–Gas Chromatography (GC)–Negative Chemical Ionization Mass Spectrometry (NCIMS). *J. Am. Soc. Brew. Chem.* 73(3), 266–274, 2015.
10. Carrillo, G; Bravo, A; Zufall, C. Application of Factorial Designs To Study Factors Involved in the Determination of Aldehydes Present in Beer by On-Fiber Derivatization in Combination with Gas Chromatography and Mass Spectrometry. *J. Agric. Food Chem.* 59(9), 4403–4411, 2011.
11. Andrés-Iglesias, C; Nešpor, J; Karabín, M; Montero, O; Blanco, CA; Dostálek, P. Comparison of carbonyl profiles from Czech and Spanish lagers: Traditional and modern technology. *LWT - Food Sci. Technol.* 66, 390–397, 2016.
12. Martos, PA; Pawliszyn, J. Sampling and Determination of Formaldehyde Using Solid-Phase Microextraction with On-Fiber Derivatization. *Anal. Chem.* 70(11), 2311–2320, 1998.
13. Ortiz, RM; Kellner, V; Qian, M; Stenerson, K; Cornell, J. Measurement of Volatile Aldehydes in Beer by Solid-Phase Microextraction-Gas Chromatography/Mass Spectrometry. *J. Am. Soc. Brew. Chem.* 69(4), 304–305, 2011.
14. Dennenlöhner, J; Thörner, S; Manowski, A; Rettberg, N. Analysis of Selected Hop Aroma Compounds in Commercial Lager and Craft Beers Using HS-SPME-GC-MS/MS. *J. Am. Soc. Brew. Chem.* 78(1), 16–31, 2020.
15. Rettberg, N. Instrumental Analysis of Hop Aroma in Beer: The Challenges of Transforming a Research Application into a QC Tool. In: Shellhammer TH, Lafontaine S, editors. *Hop Flavor and Aroma: Proceedings of the 2nd International Brewers Symposium*, 1st edn. St. Paul, MN, USA: ASBC-MBAA, 2020. pp. 11–24.
16. Schmarr, H; Potouridis, T; Ganß, S; Sang, W; Köpp, B; Bokuz, U; Fischer, U. Analysis of carbonyl compounds via headspace solid-phase microextraction with on-fiber derivatization and gas chromatographic-ion trap tandem mass spectrometric determination of their O-(2,3,4,5,6-pentafluorobenzyl)oxime derivatives. *Anal. Chim. Acta.* 617(1-2), 119–131, 2008.
17. Schmidt, C; Biendl, M; Lagemann, A; Stettner, G; Vogt, C; Dunkel, A; Hofmann, T. Influence of Different Hop Products on the cis/trans Ratio of Iso- $\alpha$ -Acids in Beer and Changes in Key Aroma and Bitter Taste Molecules during Beer Ageing. *J. Am. Soc. Brew. Chem.* 72(2), 116–125, 2014.
18. Funk, W; Dammann, V; Donnevert, G. *Qualitätssicherung in der Analytischen Chemie*, 2nd edn., Weinheim: Wiley-VCH Verlag GmbH & Co. KGaA, 2005.
19. ASBC Technical Committee. Limits of Detection and Determination. Statistical Analysis-2. In: Sedin D, editor. *ASBC Methods of Analysis*, 14th edn. St. Paul, MN, USA: ASBC, 2011.
20. Steinhaus, M; Fritsch, HT; Schieberle, P. Quantitation of (R)- and (S)-Linalool in Beer Using Solid Phase Microextraction (SPME) in Combination with a Stable Isotope Dilution Assay (SIDA). *J. Agric. Food Chem.* 51(24), 7100–7105, 2003.
21. Ng, K; Lau, YR; Weng, L; Yeung, K; Chan, C. ToF-SIMS and computation analysis: Fragmentation mechanisms of polystyrene, polystyrene-d5, and polypentafluorostyrene. *Surf. Interface Anal.* 50(2), 220–233, 2018.

22. Loidl-Stahlhofen, A. Untersuchungen zur Genese von alpha-Hydroxyaldehyden. Thesis. Universität Bayreuth, Bayreuth, Germany, 1994.
23. Schmarr, H; Sang, W; Ganß, S; Fischer, U; Köpp, B; Schulz, C; Potouridis, T. Analysis of aldehydes via headspace SPME with on-fiber derivatization to their O-(2,3,4,5,6-pentafluorobenzyl)oxime derivatives and comprehensive 2D-GC-MS. *J. Sep. Sci.* 31(19), 3458–3465, 2008.
24. Spiteller, G; Kern, W; Spiteller, P. Investigation of aldehydic lipid peroxidation products by gas chromatography–mass spectrometry. *J. Chromatogr. A.* 843(1-2), 29–98, 1999.
25. Selley, ML; Bartlett, MR; McGuiness, JA; Hapel, AJ; Ardlie, NG. Determination of the lipid peroxidation product trans-4-hydroxy-2-nonenal in biological samples by high-performance liquid chromatography and combined capillary column gas chromatography-negative-ion chemical ionisation mass spectrometry. *J. Chromatogr.* 488(2), 329–340, 1989.
26. Thörner, S; Dennenlöhner, J; Rettberg, N. Critical assessment of calibration strategies for effective beer flavor analysis by solid-phase microextraction (SPME). 37th Congress of the European Brewery Convention, Antwerp, Belgium, 2019.

## 4 Publication C

# Analysis of Hop-Derived Thiols in Beer Using On-Fiber Derivatization in Combination with HS-SPME and GC-MS/MS

### Summary

The development and application of a HS-SPME-GC-MS/MS approach using OFD with PFBBr for the quantification of 4MMP, 3MH, and 3MHA in beer is presented. Special attention was paid to fast sample preparation and moderate time of analysis due to the low concentration and the high reactivity of the thiols. An experimental design approach was used for optimization of OFD-HS-SPME and MRM parameters to increase method sensitivity in a minimum number of experiments. Method validation proved the required sensitivity of the presented analytical assay for thiol analysis in the ng/L range.

**Author Contributions:** J.D. developed and validated analytical assay, planned experimental design, performed analytics, analyzed and visualized data, conceptualized paper, wrote and edited paper; S.T. supervised research project, reviewed paper; N.R. supervised research project, interpreted data, conceptualized paper, reviewed and edited paper

## **Publication C**

**Dennenlöhner, J; Thörner, S; Rettberg, N. Analysis of Hop-Derived Thiols in Beer Using On-Fiber Derivatization in Combination with HS-SPME and GC-MS/MS. *J. Agric. Food Chem.* 68(50), 15036–15047, 2020.**

Including Supporting information

# Analysis of Hop-Derived Thiols in Beer Using On-Fiber Derivatization in Combination with HS-SPME and GC-MS/MS

Johanna Dennenlöhner, Sarah Thörner, and Nils Rettberg\*



Cite This: *J. Agric. Food Chem.* 2020, 68, 15036–15047



Read Online

ACCESS |



Metrics & More



Article Recommendations



Supporting Information

**ABSTRACT:** The quantitation of the hop varietal thiols 4-mercapto-4-methyl-2-pentanone (4MMP), 3-mercapto-1-hexanol (3MH), and 3-mercaptohexylacetate (3MHA) from beer is challenging. This primarily relates to their low concentration (ng/L levels) and their reactivity. Published assays for thiol quantitation from beer include complex and/or time-consuming sample preparation procedures involving manual handling and use reagents that are harmful because they contain mercury. To facilitate thiol analysis from beer, the current article is concerned with the implementation of an automated headspace solid-phase microextraction (HS-SPME) on-fiber derivatization (OFD) approach using 2,3,4,5,6-pentafluorobenzyl bromide followed by gas chromatography-tandem mass spectrometry (GC-MS/MS). Optimization of HS-SPME and MRM conditions was based on a central composite design approach. The final OFD-HS-SPME-GC-MS/MS method yielded limits of quantitation below the sensory thresholds of 4MMP, 3MH, and 3MHA. Method validation and application on beers brewed with German, Australian, and US hops, as well as with added fruits displayed excellent method performance.

**KEYWORDS:** beer, central composite design, HS-SPME-GC-MS/MS, on-fiber derivatization, thiols

## INTRODUCTION

Hop aroma in beer relates to the quality and quantity of hop dosage, the point of addition, and the overall brewing technology applied.<sup>1</sup> While terpenes, terpenoids, esters, and ketones are the most abundant volatile compounds in hops and are also very abundant hoppy beer, thiols quantitatively account for a minor fraction in both.<sup>2,3</sup> However, because of their remarkably low odor thresholds in beer [1.5 ng/L for 4-mercapto-4-methyl-2-pentanone (4MMP), 5 ng/L for 3-mercaptohexylacetate (3MHA), and 55 ng/L for 3-mercapto-1-hexanol (3MH)],<sup>4,5</sup> thiols impact beer quality. Thiols can accumulate above their thresholds if brewers use hop varieties (e.g., Apollo, Cascade, Citra, and Simcoe) that are rich in thiols and thereby impart the fruity odors associated with blackcurrant (4MMP), grapefruit (3MH), and passion fruit (3MHA), which are highly desired in beers such as IPAs. Given the increasing demand for hop forward beer styles and the contribution of thiols to hoppy beer flavor, there is considerable demand for thiol analysis in the brewing industry. Although published methodologies are available, they strongly differ in assay complexity, manual handling, solvent usage, instrumentation, and method performance as, for example, indicated by limit of quantitation (LOQ) or limit of detection (LOD) for the target compounds.<sup>6</sup>

Thiol extraction from beer by *p*-hydroxymercurybenzoate has first been reported by Vermeulen et al.<sup>7</sup> and Kishimoto et al.<sup>5,8</sup> The GC-PFPD and GC-MS analysis of Vermeulen et al.<sup>7</sup> was not sensitive enough to quantitate 4MMP and 3MH, so both compounds were tentatively detected by GC-O. A similar sample preparation combined with GC × GC-MS as described by Kishimoto et al.<sup>5,8</sup> reached the required sensitivity for 3MH and 3MHA but not for 4MMP quantitation (LOQ was 4.0

ng/L). Later, Reglitz et al.<sup>9</sup> isolated 4MMP from beer by using mercurated agarose gel followed by GC × GC-TOFMS analysis, which enabled the quantitation of 4MMP at levels of 1 ng/kg. 3MH and 3MHA were not targeted in their study. Several alternative methods were developed in order to avoid the usage of harmful mercury-containing reagents: Takazumi et al.<sup>10</sup> used an offline silver-ion solid-phase extraction clean-up in combination with GC-MS/MS analysis (LOD: 1.4 ng/L 4MMP, 1.9 ng/L 3MH, 3.7 ng/L 3MHA). Ochiai et al.<sup>11</sup> developed a solvent-less approach using stir bar sorptive extraction (SBSE) with an *in situ* thiol derivatization by ethyl propiolates followed by GC-MS/MS. This method was significantly less sensitive for 3MH than for 4MMP and 3MHA (LODs: 0.20 ng/L 4MMP, 27 ng/L 3MH, 0.19 ng/L 3MHA). An alternative derivatization approach using LC-ESI-HRMS was developed by Vichi et al.<sup>12</sup> Here, ebselen was used as a derivatization reagent and thiols were derivatized and extracted in a single-step protocol. The thiols were detected and quantified as selenium sulfide derivatives using ESI-HRMS. By doing so, Vichi et al.<sup>12</sup> achieved very low LOQs (0.05 ng/L 4MMP, 3MH, and 3MHA). However, to the best of our knowledge, the method has not been used to further study beer quality.

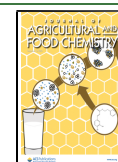
Because thiols contribute to the distinct aroma of certain wines (e.g., Sauvignon Blanc), a wealth of (analytical) research

**Received:** October 2, 2020

**Revised:** November 17, 2020

**Accepted:** November 17, 2020

**Published:** December 4, 2020



has also been carried out in relation to viticulture and oenology.<sup>13–16</sup> Interestingly, Mateo-Vivaracho et al.<sup>17</sup> developed an apparently straightforward approach for thiol quantitation in wine which includes headspace solid-phase microextraction (HS-SPME) on-fiber derivatization (OFD) using 2,3,4,5,6-pentafluorobenzyl bromide (PFBBBr) followed by GC-NCI-MS. Herein, the SPME fiber is preconditioned with PFBBBr before it is then used to simultaneously extract and derivatize thiols from the headspace above the wine sample by converting them into 2,3,4,5,6-pentafluorobenzyl (PFB) thiol derivatives. Even though this protocol appears simple, its sensitivity (LODs: 50 ng/L 4MMP, 300 ng/L 3MH) does not meet the requirements for thiol analysis from beer.

As reflected by the complexity of the assays summarized above, the particular challenges in thiol analysis from beer relate to their presence in ultratrace concentrations and their high reactivity (oxidation, dimerization<sup>18</sup>). Hence, the aim of the current paper was to facilitate thiol analysis from beer by developing an automated, solvent-less method for quantitation of 4MMP, 3MH, and 3MHA. By reviewing published assays and based on experience with similar analytical tasks,<sup>19</sup> OFD-HS-SPME in combination with GC-MS/MS appeared to be a promising approach. As method development and optimization in multianalyte methods can be laborious, an experimental design approach (response surface methodology), was used to increase method sensitivity in a minimum number of experiments.<sup>20,21</sup> Finally, method validation and application to beers brewed with German, Australian, and US hops, as well as with added fruits were used to prove the versatility of the method.

## MATERIALS AND METHODS

**Chemicals.** 4MMP (98%) was purchased from Alfa Aesar (Heysham, Great Britain), 3MH (99%) from J&K Scientific GmbH (Pforzheim, Germany), and 3MHA (95%) from Fluorochem (Hadfield, United Kingdom). As internal standards, uniformly labeled *d*<sub>10</sub>-4MMP (95%, product no. 2093, aromaLAB, Planegg, Germany) and *d*<sub>5</sub>-3MH (95%, product no. 2255, aromaLAB) were used. The deuterium labels in *d*<sub>5</sub>-3MH were located at C5 and C6. The derivatization reagent PFBBBr (99%) and triethylamine (TEA, 99%) were purchased from Sigma-Aldrich (Steinheim, Germany); ethanol absolute and sodium chloride (NaCl) were of analytical grade and were purchased from Th. Geyer (Berlin, Germany). HPLC-grade water (Th. Geyer) was used for dilution of PFBBBr and beer matrix.

**Beer Samples.** Within this study, commercially available dry-hopped ales packaged in 0.33 L cans or bottles were analyzed. The sample set included six different beer styles containing 13 beers brewed with German, Australian, and US hops: Single Hopped India Pale Ale (DE-SHIPA), Pale Ale (DE-PA), Hoppy Lager (AU/US-HL), India Pale Ale (US-IPA), Double IPA (US-DIPA), and New England IPA (US-NEIPA). The beers were selected based on the hop varieties stated on their labels, whereas hop varieties that are, according to Reglitz and Steinhaus,<sup>22</sup> rich in 4-MMP were favored in the selection. In addition, three beers (US-IPA 4, US-IPA 5, US-DIPA 2) with added fruits, whose aroma (e.g., grapefruit) is largely characterized by the thiols, were examined. The DE-SHIPA, served as a negative control. This single hopped beer was produced using German Huell melon hops that is known to contain low levels of 4MMP.<sup>22</sup> For calibration, a non-dry-hopped Lager beer (5.0% ABV) packaged in 0.5 L bottles was used.

**Method Development: GC and MRM Setup.** The goal of GC optimization was to achieve PFB-thiol derivative separation with minimal GC runtime. For this, spiked samples were measured using different GC programs, starting with an initial temperature of 60 °C (in accordance to Mateo-Vivaracho et al.<sup>17</sup>), which was then increased stepwise to 70, 80, and 90 °C. To evaluate the influence of a

shortened runtime, thiols were quantified and data sets were compared. Retention times and characteristic fragment ions of PFBBBr-derivatized analytes and internal standards were examined by precursor ion scans (*m/z* 29 to *m/z* 400). Product ion scans were then carried out by selecting suitable *m/z* precursor ions, whereas one ion was selected for quantitation and a second for qualification (Table 2). The optimization of ionization and collision energy was performed during experimental design (see below). The dwell time was set to record 15–20 data points across a peak as recommended by the instrument manufacturer.

**Method Development: OFD Setup and Matrix Dilution.** To minimize oxidative losses of 4MMP, 3MH, and 3MHA during sampling, OFD-SPME was matched with the GC runtime. The OFD-HS-SPME approach of Mateo-Vivaracho et al.<sup>17</sup> was modified, whereby an alkali as a reaction accelerator was added directly to the sample vial. To examine the effect of alkali addition and peak area stability over time, eight aliquots of the abovementioned Lager beer were spiked with 250 ng/L 4MMP, 250 ng/L *d*<sub>10</sub>-4MMP, 2500 ng/L 3MH, and 2500 ng/L *d*<sub>5</sub>-3MH. To four of the eight vials, TEA (1 μL) was added. Each one duplicate, with and without TEA added, was then measured at the beginning and end of a sample batch with 13.5 h overall runtime. Samples were held on a cooled autosampler (5 °C) until OFD. The effects of matrix dilution on the linearity and signal intensity of the calibration were tested. For this purpose, different calibration matrices were examined: 5 vol % hydroethanolic solution, Lager beer, and Lager beer diluted with a 2.5 vol % hydroethanolic in ratios of 1:1/1:2/1:3.

**Method Development: Experimental Design.** For the optimization of SPME and MRM, a central composite design (CCD) was used. The dependent variable was peak area maximization, which was tested by variation of six independent variables: extraction temperature, derivatization time, extraction time, NaCl addition, collision energy, and ionization energy. Design Expert software (ver. 12.0.3.0, Stat-Ease, Minneapolis, MN, USA) was applied to design and to evaluate the experiment. The ranges and levels of the six independent variables are listed in Table 1.

**Table 1. Experimental Levels for the Independent Variables of CCD with  $\alpha = 1.56508$  Resulted in 88 Runs<sup>a</sup>**

parameter	unit	$-\alpha$	-1	0	+1	$+\alpha$
temperature	°C	30	37	50	63	70
derivatization time	min	0.20	1.07	2.60	4.13	5.00
extraction time	min	1.00	6.24	15.50	24.76	30.00
NaCl addition	g	0.0	0.4	1.0	1.6	2.0
collision energy	eV	0.1	4	10	16	20
ionization energy	eV	10	24	48	71	85

<sup>a</sup>The measurements were performed in five blocks (four factorial blocks with two center points each, one axial block with four center points).

The factor ranges of the CCD were entered in terms of alphas (distance of each axial point to the center). As more than five factors (*k*) were examined, the so-called “practical approach” was chosen with  $\alpha = k^{1/4} = 6^{1/4} = 1.56508$ , resulting in a rotatable design. As minimum ( $-\alpha$ ), either the technically minimal possible (temperature, NaCl addition, collision energy, ionization energy) or reasonable value (derivatization and extraction time > 0 min) was defined. The maximum ( $\alpha$ ) was defined in accordance with previously published OFD approaches.<sup>19</sup> Because the CCD resulted in an experiment with 86 measurements, the experiment was divided into five blocks with 88 runs in total including 12 center points. By doing so, a maximum of 18 samples were prepared simultaneously and each block was measured within less than 8 h. For practical reasons, the optimization measurements were always performed in order of ascending incubation temperature. The experiments were carried out using 10 mL amber headspace vials containing 1.5 mL decarbonated Lager beer and 1.5 mL 2.5 vol % hydroethanolic solution. This liquid was

then spiked with thiols and ISTDs. The resulting thiol concentrations in beer were 150 ng/L 4MMP, 150 ng/L 3MHA, 1500 ng/L 3MH, 250 ng/L  $d_{10}$ -4MMP, and 1500 ng/L  $d_5$ -3MH. 1  $\mu$ L TEA was added to each vial prior to sealing. In addition, the following parameters were defined: PFBBBr concentration (2  $\mu$ L of PFBBBr in 3 mL HPLC-grade water), 250 rpm stirring speed, and desorption at 250 °C for 1 min. Until analysis, the vials were placed on a cooled GC-autosampler tray (5 °C). The results of the CCD were evaluated by analysis of variance (ANOVA) to determine the level of significance ( $p$ -value  $\leq 0.05$ ). To determine the optimal factor settings for maximal peak areas, desirability functions were applied. Finally, the design models were validated by comparing the predicted values with the mean  $\pm$  confidence interval at the 95% probability level of data obtained in an independent confirmative experiment ( $n = 3$ ).

**Sample Preparation.** Cooled beer samples (4 °C,  $\sim$ 20 mL) were transferred in 50 mL laboratory glass bottles. The bottles were flushed with nitrogen, loosely sealed with a screw cap, and placed in a refrigerator (4 °C) to gently remove excess carbon dioxide, which hinders accurate pipetting of small volumes. Even though beer samples will contain residual carbon dioxide, they are referred to as "decarbonated beer" herein. After 30 min stand time in the refrigerator, two replicates each consisting of 1.5 mL sample were transferred into 10 mL amber headspace vials prepared with 1.2  $\pm$  0.1 g NaCl and 1.5 mL 2.5 vol % hydroethanolic solution (1:1 matrix dilution). Then, 37.5  $\mu$ L of an ethanolic ISTD solution ( $d_{10}$ -4MMP at 0.01 mg/L,  $d_5$ -3MH at 0.06 mg/L) and 1  $\mu$ L TEA was added. The vials were sealed with magnetic screw caps (silicone/PTFE septum) and were then placed onto a cooled GC-autosampler (5 °C).

**Calibration and Quantitation.** To record calibration curves, 10 mL amber headspace vials were prepared with 1.2 g  $\pm$  0.1 g NaCl, before 1.5 mL aliquots of decarbonated Lager beer, 1.5 mL 2.5 vol % hydroethanolic solution, and 37.5  $\mu$ L of ISTD solution were added. The vials were then spiked with different volumes of the ethanolic analyte mixture in order to achieve thiol concentrations of 1, 2.5, 5, 10, 25, and 100 ng/L 4MMP and 3MHA, respectively, and 10, 25, 50, 100, 250, and 1000 ng/L 3MH in beer. One additional unspiked vial was used to estimate the blank value. Finally, 1  $\mu$ L TEA was added to each vial prior to sealing. The analyte/ISTD area ratios of the blank were subtracted from the analyte/ISTD ratio of every calibration point. The fitted area ratios were then plotted against the analyte/ISTD concentration ratios and the curve slope was calculated in a linear model.

**HS-SPME-GC-MS/MS Method. Instrument Specifications.** GC-MS/MS analysis was performed on an Agilent Technologies 7890B gas chromatograph interfaced to a 7000C Triple Quadrupole mass spectrometer (Agilent, Santa Clara, CA, USA). This GC-MS/MS setup was equipped with a Gerstel MPS 2XL sampler (Gerstel, Mühlheim an der Ruhr, Germany) for automated HS-SPME sampling. Agilent MassHunter Workstation Software—Qualitative Analysis (ver. B.07.00) was used for data analysis.

**HS-SPME Sampling with OFD.** A 10 mL headspace vial for derivatization was prepared by addition of 2  $\mu$ L of PFBBBr to 3 mL HPLC-grade water. The vial was then sealed and placed in the derivatization position of the agitator. OFD was reached using a 65  $\mu$ m PDMS/DVB (Supelco, St. Louis, MO, USA) fiber that was preconditioned according to the manufacturer's instructions. The PDMS/DVB fiber coating was chosen because of its ability to retain the derivatization agent and for its affinity to PFBBBr-derivatized compounds.<sup>17,23</sup> The HS-SPME parameters were as follows: the fiber was placed in the headspace of the vial containing PFBBBr at 55 °C and agitated at 250 rpm (agitator on 10 s, agitator off 1 s) for 2 min. Simultaneously, the sample vial was incubated in the agitator to enrich thiols in the headspace above the liquid beer sample. OFD was then carried out in the HS of the sample vial for 15 min at 55 °C with an agitation rate of 250 rpm. The fiber was desorbed for 1 min at 250 °C in the injection port operated in split mode with a split ratio of 1:2 (Multimode Inlet System, Agilent) equipped with a 0.75 mm i.d. Ultra Inert SPME Liner (Agilent). To prevent analyte carryover, the SPME fiber was conditioned for 2 min at 250 °C after each extraction.

**GC Analysis.** The GC analysis was carried out on a HP-5MS UI column (30 m  $\times$  0.25 mm i.d.  $\times$  0.25  $\mu$ m film thickness, Agilent) using helium (99.999%, Air Liquide, Düsseldorf, Germany) as the mobile phase. The following temperature program was used: 90 °C raised to 230 °C at a rate of 10 °C/min, followed by a final ramp to 300 °C at 70 °C/min, giving a 15 min run time.

**Mass Spectrometry.** The MS transfer line, ion source, and MS quadrupole temperature were set to 320, 230, and 150 °C, respectively. Ionization was performed by EI at 67 eV for ( $d_{10}$ -)4MMP, 74 eV for ( $d_5$ -)3MH, and 60 eV for 3MH. In the collision cell, the quench gas (helium) was adjusted to a flow of 2.25 mL/min and the collision gas (nitrogen, 99.999%, Air Liquide) to a flow rate of 1.5 mL/min. The detector gain for each time segment was set at 60 (maximum amplification factor recommended by the instrument manufacturer).

**Method validation.** The OFD-HS-SPME-GC-MS/MS method was validated by determination of linearity,<sup>24</sup> LOD,<sup>25</sup> LOQ,<sup>25</sup> measurement precision,<sup>24</sup> accuracy,<sup>24</sup> and ruggedness.<sup>26</sup> Linearity, LOD, and LOQ were calculated from the calibration curve, while measurement precision, accuracy, and ruggedness were determined by analysis of spiked US-IPA 6. LOD and LOQ were determined according to the ASBC method for low-level detection and are defined as  $LOD = \bar{x}_B + 3\sigma$  and  $LOQ = \bar{x}_B + 10\sigma$  ( $\bar{x}_B$ —mean signal of replicate blanks ( $n = 6$ ),  $\sigma$ —standard deviation of the blank). For determination of measurement precision, US-IPA 6 was spiked with 25 ng/L 4MMP, 125 ng/L 3MHA, and 250 ng/L 3MH. Spiking and analysis were done in sixfold repeat and the % RSD was calculated. The accuracy was assured by determining the recovery (%) of the three thiols at two spike levels. For this purpose, US-IPA 6 was spiked with 5 ng/L and 25 ng/L 4MMP, 25 ng/L and 125 ng/L 3MHA, and 50 ng/L and 250 ng/L 3MH. These spiked samples were prepared and analyzed in triplicate. For ruggedness testing, the effect of sample stand times was determined by repeated measurements of a spiked sample at the beginning, middle, and end of a batch. This batch consisted of 21 sequential measurements, which equals 7.5 h in total. The beer sample used was again US-IPA 6; spiking levels corresponded to those used to determine the measurement precision. Ruggedness on two different days was determined by triplicate analysis of a corresponding sample. In addition, ruggedness for two analysts was determined. Here, US-IPA 6 was spiked with 5 ng/L 4MMP, 25 ng/L 3MHA, and 50 ng/L 3MH, measured, and evaluated in triplicate by each analyst.

## RESULTS AND DISCUSSION

**Method Development. GC and MRM Setup.** The aim of GC optimization was to provide baseline separation of the target compounds in a minimized runtime. The GC temperature gradient of Mateo-Vivaracho et al.<sup>17</sup> started at 60 °C and had a runtime of 25 min. As thiol levels in the spiked sample using 60, 70, 80, and 90 °C did not differ significantly (data not shown), the GC temperature program was shortened by setting the initial temperature to 90 °C and increasing the temperature gradient. By doing so, the GC runtime was reduced to 15 min, which increases the sample throughput. As shown in Figure 1G,  $d_5$ -3MH and its unlabeled isotopologue partly co-elute whereas the existence of ten deuterium ions in  $d_{10}$ -4MMP causes a detectable forward shift compared to unlabeled 4MMP. This observation was made with all temperature gradients tested. In order to achieve the required sensitivity for thiol quantitation in the ng/L range, tandem mass spectrometry was applied. In EI-MS of PFB-thiol derivatives, the ion with  $m/z$  181 is very abundant and in most cases, with exception of 3MHA, it even represents the base peak (Figure 1A–E). The ion with  $m/z$  181, the pentafluorobenzyl ion, is formed by bond breakage of the methyl–sulfur bond. As in other PFB-containing systems,<sup>19</sup>  $m/z$  181 is also formulated as a fivefold fluoro-substituted

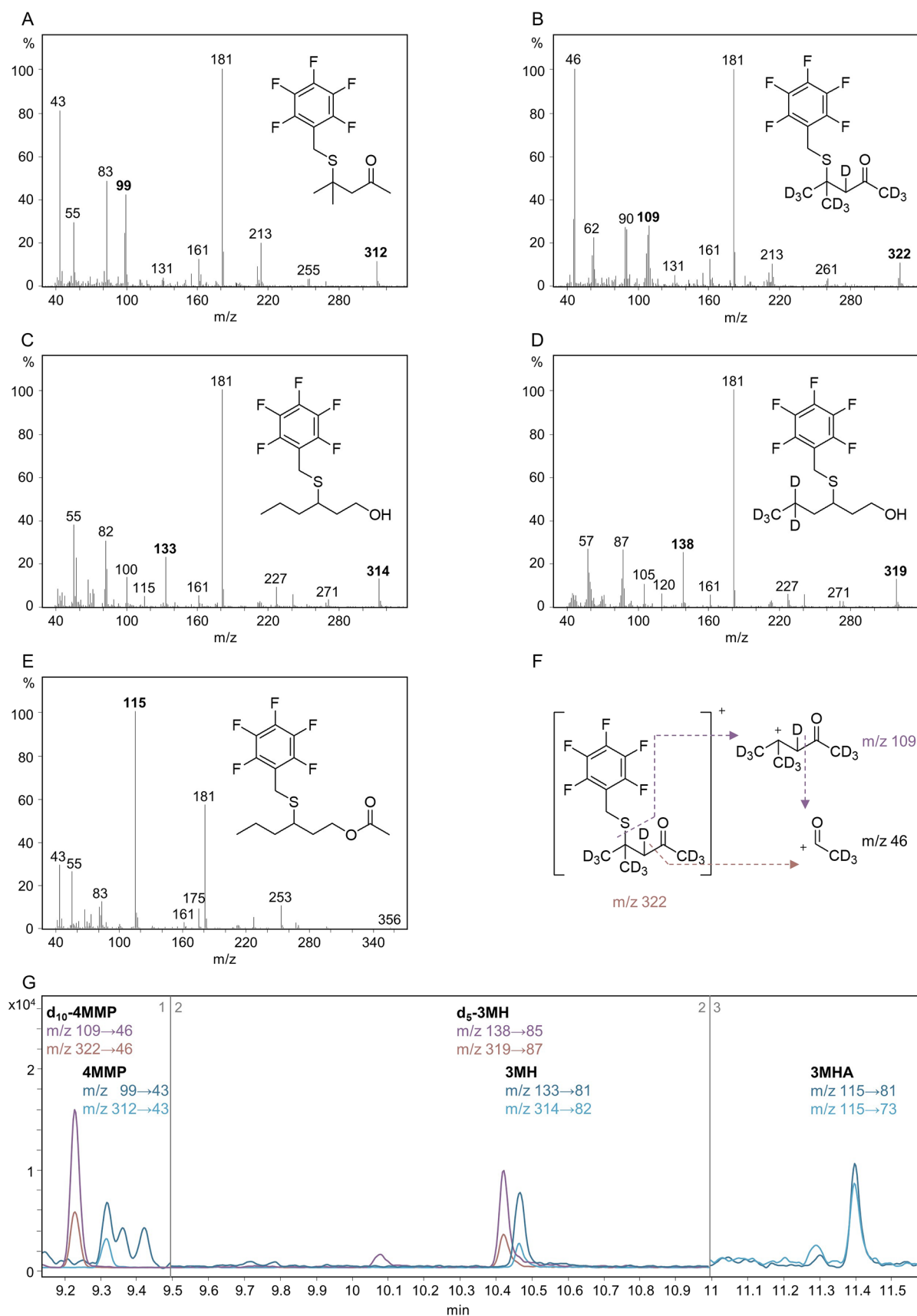


**Figure 1.** Electron impact mass spectra of PFBBr-derivatized 4MMP (A),  $d_{10}$ -4MMP (B), 3MH (C),  $d_5$ -3MH (D), and 3MHA (E), fragmentation of the PFB- $d_{10}$ -4MMP derivative (F), as well as the MRM chromatogram of a beer spiked with 100 ng/L 4MMP and 3MHA, 250 ng/L  $d_{10}$ -4MMP, 1000 ng/L 3MH, and 1500 ng/L  $d_5$ -3MH (G). For (A–E), the intensity relative to the base peak is plotted against the mass-to-charge ratio ( $m/z$ ), while for (G), the selected MRMs are plotted against the retention time.

tropylium ion resonance structure.<sup>27</sup> However,  $m/z$  181 is a common fragment ion for all (beer) volatiles undergoing OFD with PFBBR and therefore contains no specific information required for thiol identification. Hence, for the PFB-3MHA derivative, the most abundant fragment ion ( $m/z$  115) was chosen as the precursor ion and  $m/z$  81 and  $m/z$  73 were chosen as product ions, respectively. Because the four next most abundant ions ( $m/z$  181,  $m/z$  43,  $m/z$  55, and  $m/z$  83) are rather unspecific, the same accounts for its product ions (Figure 1E). On the other hand,  $m/z$  356, representing the molecular ion of PFB-3MHA derivative, is not abundant in sufficient quantities (2.8% of base peak intensity).

When selecting suitable MRM transitions for ISTDs ( $d_{10}$ -4MMP and  $d_5$ -3MH), it was considered that precursor ions carrying deuterium labels were selected. Differentiation of the PFB- $d_{10}$ -4MMP derivatives and their unlabeled isotopologues is granted by ions with  $m/z$  109 and  $m/z$  99, as well as their molecular ions  $m/z$  322 and  $m/z$  312 (Figure 1A,B). The product ion of PFB- $d_{10}$ -4MMP ( $m/z$  46) carries three deuterium labels (Figure 1F). The exact same criteria were applied for the selection of  $m/z$  138 and  $m/z$  319 for the PFB- $d_5$ -3MH derivative and  $m/z$  133 and  $m/z$  314 for the PFB-3MH derivative (Figure 1C,D). The resulting product ions are listed in Table 2. The optimization of collision and ionization energy to obtain MRM transitions with sufficient intensities was performed by CCD (see below).

**Table 2. Multiple Reaction Monitoring Transitions and Retention Times of Three Selected Thiol Compounds as Well As the Internal Standard (Bold) Used for Quantitation**

compound	quantitative transition [ $m/z$ ]	qualitative transition [ $m/z$ ]	retention time [min]	dwell time [ms]
$d_{10}$ -4MMP	109 → 46	322 → 46	9.24	50
4MMP	99 → 43	312 → 43	9.33	50
$d_5$ -3MH	138 → 85	319 → 87	10.43	50
3MH	133 → 81	314 → 82	10.48	50
3MHA	115 → 81	115 → 73	11.41	100

**OFD Setup and Matrix Dilution.** Mateo-Vivaracho et al.<sup>17</sup> showed that the addition of an alkali improved the speed of OFD. During their investigation, it was further observed that the peak areas decreased when samples were stored for longer periods on the cooled autosampler prior to measurement. Hence, both aspects were considered in this method development. The OFD procedure of Mateo-Vivaracho et al.<sup>17</sup> was as follows: the fiber was first loaded with PFBBR and then exposed to the alkali in a second vial, before the actual OFD was performed in the headspace of the sample vial. In their experimental setup, tributylamine has proven to be the most suitable alkali, as it retained well on the fiber because of its higher boiling point (214 °C). In the presented OFD-HS-SPME-GC-MS/MS method, the alkali was added directly into each sample vial to further simplify the assay. Consequently, it appeared more suitable to choose an alkali with a lower boiling point. TEA (boiling point 89 °C) was chosen, and henceforth, 1  $\mu$ L TEA was added to each sample before sealing the vial. By incubating the sample at 55 °C, the majority of TEA was forced into the headspace of the sample vial, where it promoted the OFD by dehydration of the thiol group, as shown in Figure 2. The influence of TEA addition as well as a longer measuring period on the peak areas were investigated

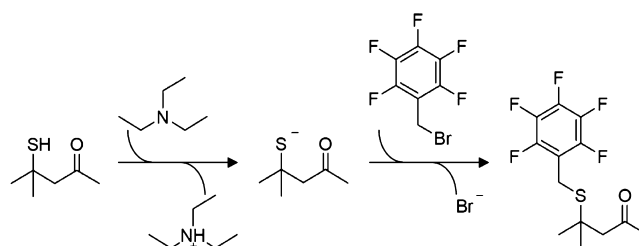


**Figure 2.** Proposed reaction scheme for PFBBR derivatization of 4MMP. TEA activates 4MMP by dehydration of the thiol group. In the subsequent nucleophilic substitution, the thiolate react with PFBBR to result in the PFB-4MMP derivative.

simultaneously. On the one hand, data shown in Figure 3 reveals a 46–57% peak area increase when TEA is added to beer. This confirms that the modified procedure adapted from Mateo-Vivaracho et al.<sup>17</sup> works well. On the other hand, the observation of the decreased peak areas after a longer measuring period was also confirmed with this adapted OFD setup. In manual derivatization procedures, derivatization is one of the first steps of the sample preparation. In contrast, derivatization in the automated OFD approach occurs prior to injection of the sample into GC-MS/MS. As beer is transferred from an oxygen-free environment (bottle or can) into an oxygen-containing atmosphere (GC vial), thiols might partly oxidize. Practically, the peak area decrease of the beer samples sitting on the autosampler at 5 °C for 13.5 h until measurement ranged between 81 and 85% (Figure 3). At this, three things need to be noted: First, the thiol spike levels were comparably high, which was chosen, as the method was not optimized at the point where this trial was performed. Second, the total batch runtime of 13.5 h was caused by the underlying experimental design and, as described below (see Method Validation section), is of limited practical relevance. Third, the decrease of the peak area affected analytes and ISTDs equally (Figure 3). In the experiments performed, the analyte/ISTD ratios varied between 6.5 and 9.6%, which is judged fully acceptable. Ruggedness testing of the optimized method (see Method Validation section) verified that a batch length of 7.5 h, which equals 20 injections or 10 beer samples measured in duplicates, does not negatively influence the quality of the results.

Because initial 4MMP spiking experiments to beer showed no satisfying increase in signal intensities in the range 1–5 ng/L ( $R^2 = 0.24$ ), the OFD approach of Mateo-Vivaracho et al.<sup>17</sup> was adapted to beer samples by matrix dilution experiments. It was observed that calibration in 5 vol % hydroethanolic solution yielded a strong peak area increase compared to calibration in beer. For example, in the case of 4MMP, qualifier and quantifier areas increased by 73–555% compared to the beer matrix (data not shown). Because of significant increased 4MMP peak areas in the lower calibration range, the required sensitivity and linearity were achieved ( $R^2 = 0.99$ ). As calibration in hydroethanolic solution does not sufficiently represent the real sample matrix, we aimed to improve the yield of HS-SPME OFD while preserving the interaction of the matrix components with the analytes. Sufficient peak areas (up to 50% larger  $d_{10}$ -4MMP areas compared to beer matrix) and good linearity in the low calibration range ( $R^2 = 1.00$ ) were achieved by diluting the Lager beer matrix 1:1 with 2.5 vol % hydroethanolic solution. Hence, as described in the final method above, base beer for

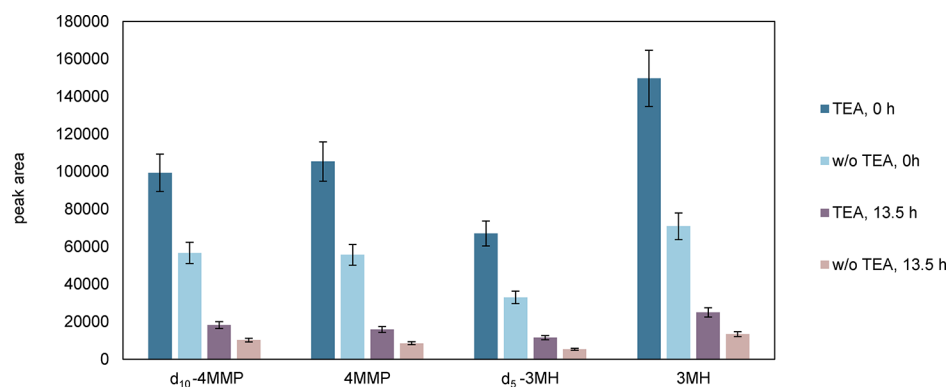


**Figure 3.** Effect on PFB-thiol ( $d_{10}$ -4MMP, 4MMP,  $d_5$ -3MH, and 3MH) derivative peak areas during a runtime of 13.5 h with and without (w/o) TEA addition. The error bars indicate a 10% deviation, which corresponds to the measurement precision of the final method.

**Table 3.** Response Equations in Terms of Coded Factors<sup>a</sup>

	$d_{10}$ -4MMP		4MMP		$d_5$ -3MH		3MH		3MHA	
	109→46	322→46	99→43	312→43	138→85	319→87	133→81	314→82	115→81	115→73
Intercept	26694	4357	17282	3306	9158	1435	14140	1641	146400	198300
A										
B										
C										
D										
E										
F										
A·B										
A·C										
A·D										
A·F										
C·D										
C·E										
C·F										
D·F										
E·F										
A <sup>2</sup>										
B <sup>2</sup>										
C <sup>2</sup>										
D <sup>2</sup>										
E <sup>2</sup>										
F <sup>2</sup>										

<sup>a</sup>The corresponding values are listed in Table S1. The coefficients are plotted in data bars and are proportional to the observed effect. The blue bars indicate factors with a positive effect of the peak area, and the violet bars factors with a negative effect. A—temperature, B—derivatization time, C—extraction time, D—NaCl, E—collision energy, and F—ionization energy

calibration and samples for analysis was diluted (i.e., 1.5 mL of the sample was diluted with 1.5 mL of 2.5 vol % hydroethanolic solution). By doing so, the ethanol content of the samples as well as the matrix load was decreased. It remains speculative to which extent the overall reduction of volatiles in the sample vial or the reduction of nucleophilic volatiles that undergo reaction with PFBBBr, such as other thiols, contribute to this observation.

**Experimental Design.** Evaluation of optimal SPME and MRM parameters in a multicomponent method is difficult. In many cases, the optimal conditions are analyte-specific, which is why optimization aims to achieve good recovery of compounds present in low concentration, showing a low recovery in the analytical system, or both. In the current study, optimization was performed by CCD with the aim to maximize the analyte peak areas to increase method sensitivity. It was consciously performed in the same matrix in which the calibration is performed (see above). As a result, it was

observed whether the variation of the independent variables resulted in an improvement of only the analyte signal and/or the background signal. The dependent variables (responses) obtained for this CCD were 10 peak areas (all quantitative and qualitative MRM transitions) and they were individually correlated using quadratic polynomial equations. As not all of the factors and their interactions resulted in significant model terms ( $p < 0.05$ ), model reductions were used to improve each model. The reduced quadratic models were generated by deleting insignificant model terms ( $p > 0.1$ ) but not those required to support hierarchy. Table S1 provides an overview of the actual and coded factors used for the respective response equation. The equations in terms of actual and coded factors make the same predictions about the respective response, but actual factors are not intended to determine the relative impact of each factor. To highlight the most influential factors, the coded factors are displayed in data bars in Table 3. The coded coefficients are proportional to the

Table 4. ANOVA Results for the Fitting of Data to the Reduced Quadratic Models<sup>a</sup>

source	F-value	p-value	F-value	p-value	F-value	p-value	F-value	p-value	F-value	p-value
	<i>d</i> <sub>10</sub> -4MMP 109 → 46		<i>d</i> <sub>10</sub> -4MMP 322 → 46		4MMP 99 → 43		4MMP 312 → 43		<i>d</i> <sub>5</sub> -3MH 138 → 85	
model	25.54	<0.0001	30.40	<0.0001	18.91	<0.0001	34.71	<0.0001	16.86	<0.0001
A	1.76	0.1887	5.11	0.0270	5.57	0.0212	4.62	0.0353	25.84	<0.0001
B	—	—	—	—	0.56	0.4581	0.07	0.7921	0.58	0.4476
C	26.06	<0.0001	49.36	<0.0001	30.05	<0.0001	60.76	<0.0001	27.80	<0.0001
D	10.51	0.0018	20.16	<0.0001	0.16	0.6928	21.25	<0.0001	13.19	0.0005
E	—	—	20.69	<0.0001	—	—	31.10	<0.0001	0.01	0.9366
F	76.18	<0.0001	209.80	<0.0001	98.95	<0.0001	256.71	<0.0001	47.64	<0.0001
A·B	—	—	—	—	2.77	0.1005	—	—	—	—
A·C	2.95	0.0903	6.36	0.0140	6.56	0.0126	5.09	0.0274	4.97	0.0291
A·D	—	—	—	—	3.30	0.0739	—	—	3.27	0.0752
A·F	—	—	6.13	0.0158	6.61	0.0124	6.30	0.0146	16.28	0.0001
C·D	—	—	5.27	0.0248	—	—	4.77	0.0325	4.42	0.0393
C·E	—	—	3.04	0.0856	—	—	5.20	0.0258	—	—
C·F	16.13	0.0001	41.34	<0.0001	23.10	<0.0001	51.59	<0.0001	16.96	0.0001
D·F	6.92	0.0104	17.94	<0.0001	—	—	17.76	<0.0001	9.50	0.0030
E·F	—	—	11.47	0.0012	—	—	18.69	<0.0001	—	—
A <sup>2</sup>	14.56	0.0003	12.96	0.0006	4.67	0.0341	14.50	0.0003	—	—
B <sup>2</sup>	—	—	—	—	2.91	0.0925	4.57	0.0361	3.60	0.0620
C <sup>2</sup>	6.42	0.0135	5.58	0.0211	6.77	0.0113	9.34	0.0032	—	—
D <sup>2</sup>	15.56	0.0002	12.74	0.0007	6.45	0.0134	17.32	<0.0001	13.58	0.0005
E <sup>2</sup>	—	—	—	—	—	—	—	—	14.17	0.0004
F <sup>2</sup>	23.71	<0.0001	—	—	18.95	<0.0001	—	—	11.43	0.0012
lack of fit	1.17	0.4514	2.49	0.1024	2.11	0.1510	1.86	0.1969	1.43	0.3281
	<i>d</i> <sub>5</sub> -3MH 319 → 87		3MH 133 → 81		3MH 314 → 82		3MHA 115 → 81		3MHA 115 → 73	
model	35.25	<0.0001	21.17	<0.0001	38.53	<0.0001	21.50	<0.0001	27.67	<0.0001
A	56.66	<0.0001	31.51	<0.0001	65.60	<0.0001	0.35	0.5578	0.99	0.3242
B	—	—	0.42	0.5184	—	—	—	—	—	—
C	58.83	<0.0001	31.62	<0.0001	67.66	<0.0001	22.32	<0.0001	26.14	<0.0001
D	23.66	<0.0001	12.43	0.0008	29.18	<0.0001	8.05	0.0060	9.96	0.0024
E	0.12	0.7290	0.92	0.3410	3.50	0.0658	11.10	0.0014	0.07	0.7925
F	134.44	<0.0001	53.07	<0.0001	160.66	<0.0001	45.19	<0.0001	56.35	<0.0001
A·B	—	—	—	—	—	—	—	—	—	—
A·C	10.90	0.0015	6.46	0.0133	10.67	0.0017	—	—	—	—
A·D	3.52	0.0647	—	—	4.60	0.0356	—	—	—	—
A·F	43.15	<0.0001	18.85	<0.0001	50.46	<0.0001	—	—	—	—
C·D	5.78	0.0189	4.33	0.0412	10.76	0.0016	—	—	—	—
C·E	—	—	—	—	—	—	4.24	0.0433	—	—
C·F	44.70	<0.0001	20.21	<0.0001	52.28	<0.0001	13.35	0.0005	16.61	0.0001
D·F	21.09	<0.0001	10.06	0.0023	26.68	<0.0001	5.18	0.0259	6.54	0.0127
E·F	—	—	—	—	4.54	0.0368	12.07	0.0009	—	—
A <sup>2</sup>	—	—	—	—	—	—	14.23	0.0003	20.18	<0.0001
B <sup>2</sup>	—	—	4.03	0.0486	—	—	—	—	—	—
C <sup>2</sup>	—	—	—	—	—	—	2.85	0.0961	6.78	0.0112
D <sup>2</sup>	17.40	<0.0001	16.99	0.0001	12.79	0.0006	11.66	0.0011	16.84	0.0001
E <sup>2</sup>	20.40	<0.0001	21.34	<0.0001	23.62	<0.0001	26.35	<0.0001	18.33	<0.0001
F <sup>2</sup>	—	—	13.25	0.0005	—	—	11.59	0.0011	14.47	0.0003
lack of fit	2.45	0.1064	1.68	0.2424	2.80	0.0769	0.51	0.9278	0.42	0.9682

<sup>a</sup>Bold *p*-values indicate significant terms ( $p < 0.05$ ), and — indicates that the term is not significant ( $p > 0.05$ ) and not necessary for hierarchy. A—temperature, B—derivatization time, C—extraction time, D—NaCl, E—collision energy, and F—ionization energy.

observed effect. The blue bars indicate that an increase of this factor in the respective model equation causes an increased peak area. In contrast, increasing the factor with a violet bar results in a reduced peak area. Consequently, if both colors are displayed in the column, this factor affects the peak areas differently. The factor extraction time and ionization energy were the variables with a significant positive effect ( $p < 0.0001$ ) on all peak areas (Table 4). On the other hand, the factor

derivatization time and collision energy as well as their interactions were in most cases not significant, resulting in a very limited impact on the models (Table 4).

With regard to the setting of a uniform SPME temperature, it was expected that a good compromise is required because the optimum temperature is very different for all thiols (see blue and purple bars, Table 3). For *d*<sub>5</sub>-3MH and 3MH, the higher positive value of the coefficient indicates that the

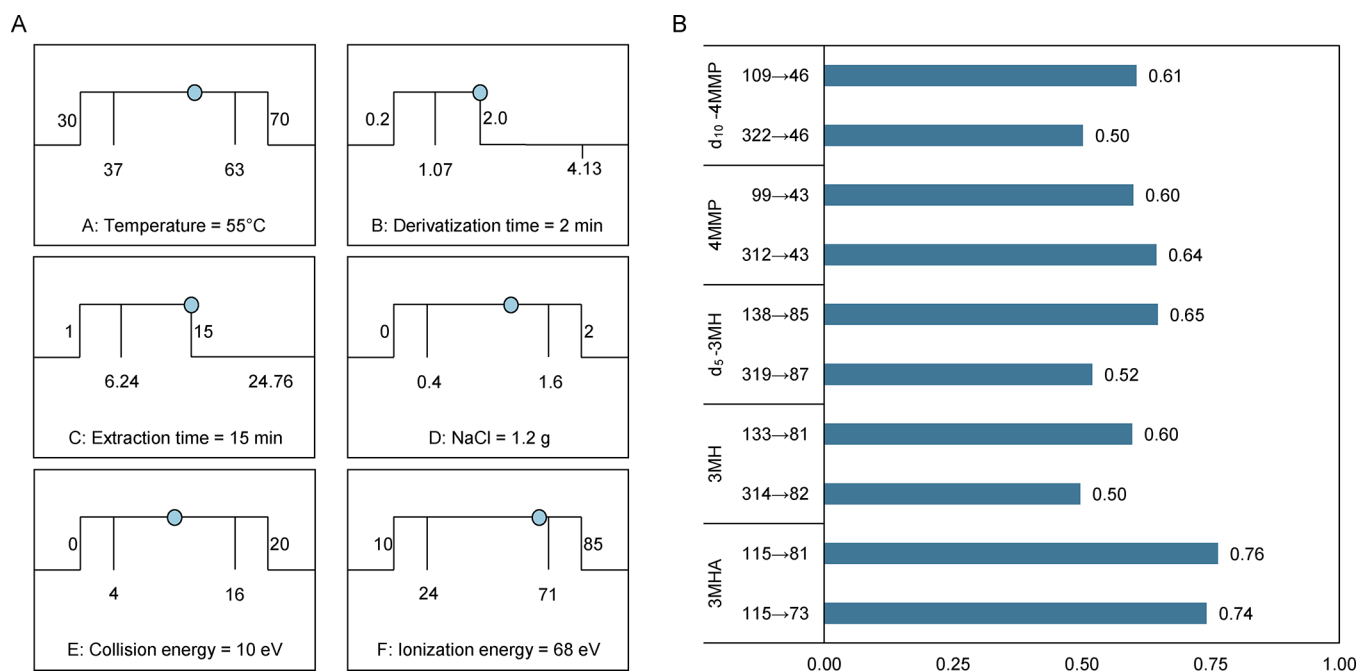


**Figure 4.** Desirability function to maximize the peak area of all MRM transitions. The light blue dots on the ramp function graph mark the factor settings by which all responses reach a maximum peak area (overall combined desirability = 0.615) (A). The bar graphs show the individual desirability for this combination of factor settings (B).

temperature has a more positive effect on the peak area and that the optimum temperature is therefore higher compared to the other thiols. As 3MH (250 °C) has the highest boiling point compared to 4MMP (174 °C) and 3MHA (236 °C), this result was expected considering that volatiles with higher boiling points are extracted more efficiently at higher temperatures.

The statistical evaluation showed that the relationship between experimental data and fitted model is good (difference between predicted  $R^2$  and adjusted  $R^2 < 0.2$ , significant model  $f$ -values, insignificant lack of fit, Table 4). Each model offers good potential for predictions and optimization. The 12 center points that were used to verify the reproducibility of the results discovered no possible block effects, although the CCD had to be measured in five blocks, and for each block, new analyte and ISTD solutions were diluted. The evaluation of the correlation analysis revealed that the dependence between 3MHA ( $m/z$  115 → 81) and  $d_{10}$ -4MMP ( $m/z$  109 → 46) was slightly stronger ( $r = 0.883$ ) than to  $d_5$ -3MH ( $m/z$  138 → 85,  $r = 0.818$ ); hence from then on, 3MHA was quantified via  $d_{10}$ -4MMP. The increased stability of this analyte-ISTD pairing was also demonstrated by the more constant analyte-ISTD ratio of the center points. The % RSD was 12% for 3MHA/ $d_{10}$ -4MMP ratio and 13% for 3MHA/ $d_5$ -3MH, which is fully acceptable. In comparison, the ratio of  $d_{10}$ -4MMP and  $d_5$ -3MH with the respective non-isotopically labeled analyte was 8%, respectively.

To determine the optimal conditions for multiple responses (10 peak areas resulting from three analytes and two standards), desirability function proposed by Derringer and Suich<sup>28</sup> was used to simultaneously optimize a series of quadratic models. Design Expert's numerical optimization software calculates the scale-free value desirability (0–1), that is, the measure of how well the solution met the combined goals for all responses (1 = ideal response value). The overall desirability simplifies the decision regarding the combination

of factor settings, which leads to maximized peak areas. The goal of all factors were set “in range”, whereas for temperature, NaCl, collision energy, and ionization energy, the lower and upper limits corresponds to the minimum and maximum limits ( $\pm\alpha$ ) in Table 1. To allow a high-sample throughput, the upper limit of derivatization and extraction time was set at 2 and 15 min. Because the GC runtime was 15 min and approx. more than 5 min was needed to cool down the column oven, 20 min was available for total fiber utilization. Subtracting desorption time (1 min) and fiber conditioning time (2 min), 17 min remained for the derivatization and extraction steps.

In order to target maximal peak areas, the goal for all responses was set to “maximize”. For the criterion importance (range 1–5), a medium setting was selected by setting “3” for all qualifier MRM transitions. The importance value was raised to “5” for all quantifier MRM transitions because an increase in these peak areas is of primary importance for the method. By considering each individual optimum, Figure 4A shows the factor settings by which all responses reach a maximum peak area (overall combined desirability = 0.615) and Figure 4B depicts the individual desirability for this combination of factor settings. It reveals that the optimum temperature is 55 °C, which is in accordance with Mateo-Vivaracho et al.<sup>17</sup> The optimal conditions for derivatization and extraction time are on the upper limit. If  $+\alpha$  would be allowed as the maximum level for both factors, the optimal condition would be 2.69 min for derivatization time, 30 min for extraction time, and 0.775 for desirability (data not shown). However, as explained above, a moderate decrease in signal intensity is accepted to ensure a higher sample throughput of the highly reactive analytes. Because thiols are polar compounds, they are positively influenced by salt addition because of the “salting out” effect. In this case, the sample is saturated with an addition of 1.2 g NaCl.

While collision energy is a standard parameter of MRM optimization, ionization energy is usually not investigated. This

is because ionization at 70 eV is very efficient and leads to highly reproducible, but fragment-rich mass spectra. However, as under certain conditions, lower ionization energies in some cases contribute positively to a preservation of the molecular or other high  $m/z$  fragment ions;<sup>29</sup> this was of interest for the current study. To determine the optimal ionization energy individually for each time segment, three further numerical optimizations were performed. For this purpose, temperature, derivatization time, extraction time, and NaCl were set “equal to” 55 °C, 2 min, 15 min, or 1.2 g. Only the MRM transitions of one time segment were examined, while the responses of the other two time segments were removed from the optimization. Ionization energies of 10 or 24 eV yielded no peaks, while ionization at 48 eV yielded reasonable signals. The optimal conditions were found to be 67 eV for  $d_{10}$ -4MMP/4MMP, 74 eV for  $d_5$ -3MH/3MH, and 60 eV for 3MHA (Table 5). It

**Table 5. Collision and Ionization Energy Settings Based on Desirability Function for Maximum Peak Area<sup>a</sup>**

compound	[ $m/z$ ]	collision energy [eV]	ionization energy [eV]
$d_{10}$ -4MMP	109 → 46	16	67
	322 → 46	20	67
4MMP	99 → 43	16	67
	312 → 43	20	67
$d_5$ -3MH	138 → 85	10	74
	319 → 87	10	74
3MH	133 → 81	10	74
	314 → 82	9	74
3MHA	115 → 81	9	60
	115 → 73	10	60

<sup>a</sup>The factor settings used to estimate these were set to 55 °C incubation temperature, 2 min desorption time, 15 min extraction time, and addition of 1.2 g NaCl.

should be noted that the mass spectrometer used herein was not equipped with a low-energy electron ionization source. Those ions sources, which are technically modified to increase of sensitivity and robustness, are now commercially available, and one could assume that for certain analytes, for example, PFB-3MHA, they could potentially improve the performance of the assay described herein.

In the final step of optimization, the previously optimized factors were set to their respective settings, while the collision energy was determined individually for each MRM transition. The selected collision energies range between 9 and 20 eV and are depicted in Table 5. Compared to a previous study in which *O*-(2,3,4,5,6-pentafluorobenzyl)hydroxylamine hydrochloride (PFBHA)-derivatized aldehydes displayed an optimum of intensity at collision energies of 10–25 eV,<sup>19</sup> the collision energies used herein are quite similar. This is explained by the fact that PFBBR-derivatized thiols and PFBHA-derivatized aldehydes have comparable molecular weights and their structure is similar. In contrast, non-derivatized hop aroma compounds have optimum intensities at significantly lower collision energies (5–15 eV).<sup>30</sup>

The confirmation of the model after full optimization could not be completely carried out with the Design Expert software. The collision and ionization energies were individually optimized, but Design Expert could only make predictions at uniform collision and ionization energies. Thus, the confirmation could not be made at the optimal settings determined from the analysis. For this reason, the model was

alternatively examined with the factor settings of the best global response (Figure 4A). The confirmative experiment was performed in three replicates employing the identical sample composition as used in CCD. Table 6 shows the good

**Table 6. Results of Confirmative Experiment ( $n = 3$ ) Carried Out at 55 °C Temperature, 2 min Derivatization Time, 15 min Extraction Time, 1.2 g NaCl, 10 eV Collision Energy, and 68 eV Ionization Energy**

response	predicted value	experimental value
$d_{10}$ -4MMP 109 → 46	25 853	32 460
$d_{10}$ -4MMP 322 → 46	5736	6890
4MMP 99 → 43	1088	19 430
4MMP 312 → 43	4157	4291
$d_5$ -3MH 138 → 85	10 100	1365
$d_5$ -3MH 319 → 87	2199	2570
3MH 133 → 81	15 391	13 658
3MH 314 → 82	2621	2459
3MHA 115 → 81	145 820	157 653
3MHA 115 → 73	197 015	190 493

agreement of predicted and the mean of the experimental values indicating the adequacy of the model equation. Based on the above data, the final conditions for thiol analysis in beer were set at 55 °C temperature, 2 min derivatization time, 15 min extraction time, and 1.2 g NaCl, 9–20\* eV collision energy, and 60–74\* eV ionization energy (\*refer to Table 5).

**Method validation.** Method validation was performed in order to confirm that the established analytical procedure is well suited for its intended use. The results of method validation are summarized in Table 7, and the corresponding raw data sets are provided in the Supporting Information. Recoveries ranged from 84 to 108% and precision ranged from 7.0 to 11.3 % RSD. Both results were judged fully acceptable. The calculated LODs and LOQs were below the odor thresholds of the selected compounds and were either better or comparable to those of published methods.<sup>5,10,11</sup> More importantly, the working range (Table 7) in which OFD-HS-SPME-GC-MS/MS analysis showed an excellent linearity ( $R^2 > 0.99$ ) covered 4MMP, 3MH, and 3MHA concentrations below the odor thresholds. The lowest concentration of the working range equals 1 ng/L for 4MMP, 1 ng/L for 3MHA, and 10 ng/L for 3MH (Table 7) and is practically used as LOQ when results are reported (see Table 8). In spiking experiments that were done prior to method optimization, a decrease in analyte and ISTD areas by sample stand times (elapsed time between pipetting a sample and its injection) was observed (see OFD Setup and Matrix Dilution section). This was confirmed by ruggedness testing, but it was also validated that peak area decrease at stand times equal to/below 7.5 h did not negatively affect method performance. Peak areas determined at the beginning, middle, and end of a batch varied by approx. 30%, while the difference between the lowest and highest peak areas was in the range of approx. 50% (see Supporting Information). Still, the % RSD which result from analyte/ISTD area ratios ranged from 7.9% for 3MHA to 10.1% for 4MMP. These satisfying results are explained by the usage of stable isotope-labelled ISTDs, but also by the selective detection using MRM. While stable isotope-labelled ISTDs compensate for area fluctuations, MRM detection results in low noise and the ability to quantitate small signals properly. Ruggedness at the beginning, middle, and end of a batch was

**Table 7. Results for Statistical Parameters of Method Validation: Linearity (Range,  $R^2$ , Mandel Fitting Test), LOD, LOQ, % Recovery, Precision, and Ruggedness**

compound	linearity			LOD <sup>a</sup> /LOQ <sup>b</sup> [ng/L]	% recovery <sup>c</sup>	precision <sup>d</sup> [% RSD]	ruggedness [% RSD]
	range [ng/L]	$R^2$	Mandel				
4MMP	1–100	>0.99	Linear	0.16/0.53	87–95	10.3	10.1 <sup>e</sup> /13.5 <sup>f</sup> /13.9 <sup>g</sup>
3MH	10–1000	>0.99	linear	2.09/6.96	87–108	11.3	8.3 <sup>e</sup> /13.0 <sup>f</sup> /11.3 <sup>g</sup>
3MHA	1–100	>0.99	linear	0.21/0.70	84–95	7.0	7.9 <sup>e</sup> /12.1 <sup>f</sup> /8.9 <sup>g</sup>

<sup>a</sup>LOD =  $\bar{x}_B + 3\sigma$  ( $\bar{x}_B$ —mean signal of replicate reagent blanks ( $n = 6$ ),  $\sigma$ —standard deviation of blank beer). <sup>b</sup>LOQ =  $\bar{x}_B + 10\sigma$ . <sup>c</sup>Mean % recovery ( $n = 3$ ) at two concentration levels. <sup>d</sup>Measurement precision ( $n = 6$ ). <sup>e</sup>Ruggedness determined at the beginning, middle, and end of a batch ( $n = 6$ ). <sup>f</sup>Ruggedness determined on two different days ( $n = 6$ ). <sup>g</sup>Ruggedness determined for two analysts ( $n = 6$ ).

**Table 8. Concentration of 4MMP, 3MH, and 3MHA As Well As the Hop Varieties Used in Thirteen Beer Samples**

beer	4MMP [ng/L]	3MH [ng/L]	3MHA [ng/L]	hop variety
DE-SHIPA	<1.0	<10.0	<1.0	Huell Mellon
DE-PA	<1.0	<10.0	<1.0	Cascade, Centennial, Citra, Saphir, Willamette
AU/US-HL	8.9	11.4	1.0	Galaxy, Mosaic, Topaz
US-IPA 1	8.0	49.5	<1.0	Amarillo, Citra, Comet, El Dorado, Mosaic
US-IPA 2	33.3	16.5	1.0	Amarillo, Cascade, Chinook, Nugget, Mosaic, Simcoe
US-IPA 3	86.1	40.0	<1.0	Citra, Mosaic
US-IPA 4 <sup>a</sup>	6.0	<10.0	<1.0	Amarillo, Citra, Magnum, Mosaic, Simcoe
US-IPA 5 <sup>b</sup>	1.1	244.9	<1.0	Azacca, Galaxy, Millenium
US-IPA 6	6.7	269.8	3.8	Citra, Centennial, Apollo, Ekuanot
US-DIPA 1	39.1	18.6	<1.0	Azacca, Mandarina Bavaria, Mosaic
US-DIPA 2 <sup>c</sup>	75.9	130.4	9.5	Citra, Centennial, Ekuanot, Nugget
US-NEIPA 1	106.6 <sup>d</sup>	37.3	<1.0	Cascade, Citra, Galaxy, Mosaic, Simcoe
US-NEIPA 2	238.9 <sup>d</sup>	119.6	<1.0	Cascade, Citra, Mosaic, Simcoe

<sup>a</sup>Special ingredients: grapefruit and orange. <sup>b</sup>Special ingredients: guava, orange, and passionfruit. <sup>c</sup>Special ingredients: guava and spruce. <sup>d</sup>Outside the calibration range.

comparable to ruggedness determined on two different days (12.1–13.5 % RSD) and to ruggedness determined for two analysts (8.9–13.9 % RSD). All three % RSD from ruggedness testing were comparable to method precision (Table 7), indicating that sample stand times, analyst-to-analyst, and day-to-day variation are of minor importance. Regarding the fact that chemically reactive thiol compounds in ng/L concentrations were tested, the results of the validation are fully acceptable and underline the analytical applicability of the assay. Compared to the methods published earlier (see Introduction), the OFD-HS-SPME-GC-MS/MS method reached the required sensitivity for all three analytes without a time-consuming sample preparation, the use of solvents, or mercury-containing reagents.<sup>5,7–10</sup>

**Application.** The optimized method was then applied for the analysis of commercial beer samples. The thirteen selected samples were analyzed in duplicates, and the mean values are reported in Table 8. Significant concentration differences in the sample set were observed for 4MMP and 3MH. 4MMP ranged from <1.0 to 238.9 ng/L, while 3MH ranged from <10.0 to 269.8 ng/L. The highest 4MMP concentrations were detected in the two US-NEIPA beers. Because of the massive

hop additions used to produce this style of beer, NEIPAs have been called the “hop aroma champion”, and high thiol levels were reported earlier.<sup>31</sup> The 3MHA concentration in all beers tested were close to/below the LOQ (Table 8). US-Double IPA 2 was an exception from this (9.5 ng/L); this beer included guava and spruce additions. High 3MH concentrations were also found in beers to which guavas were added (US-IPA 5, US-Double IPA 2). These results correspond to literature in a way that 3MH and 3MHA were reported as key aroma compounds of guava.<sup>32</sup> However, the 3MHA concentration in beer brewed with guavas, oranges, and passion fruits (US-IPA 5) was below the LOQ, although 3MHA naturally occurs in guavas<sup>32</sup> and passion fruits.<sup>33</sup> Interestingly, the grapefruit-blended US-IPA 4 (Table 8) contained only low thiol levels (6.0 ng/L 4MMP, <10.0 ng/L 3MH, <1.0 ng/L 3MHA), although this beer had a strong grapefruit note and all three thiols impact the characteristic sulfurous grapefruit aroma.<sup>34,35</sup> The latter results raise the need to identify the key aroma compounds of beers with different fruit additions as these gather more and more consumer acceptance. For the sake of completeness, it needs to be mentioned that the two German dry-hopped ales, including the control beer (DE-SHIPA), did not contain quantifiable levels of 4MMP, 3MH, and 3MHA (Table 8). This might be explained by the fact that American Brewers tend to dry-hop more heavily. The distribution of the three thiols measured herein is consistent with the literature.<sup>5,10,11</sup> In general, the 3MHA content of beer is low when compared to 4MMP and 3MH. This relates to the fact that 3MHA is formed from 3MH during fermentation and its concentration is therefore dependent on the hopping regime, fermentation parameters, and yeast strain.<sup>5,36</sup> The distribution of 4MMP and 3MH varies from beer to beer and from publication to publication. While Takazumi et al.<sup>10</sup> and Ochiai et al.<sup>11</sup> detected significantly more 3MH (94–290 ng/L) than 4MMP (<4.6–22 ng/L) in their sample sets, Kishimoto et al.<sup>5</sup> detected higher 4MMP (110–185 ng/L) levels compared to 3MH (40–60 ng/L). In the beers analyzed herein, both analyte ratios were found. For example, in US-IPA 3, the concentration of 4MMP was higher by factor two compared to the concentration of 3MH, while the concentration of 3MH was higher compared to 4MMP in US-IPA 1 and US-IPA 6 (Table 8).

In summary, the developed OFD-HS-SPME-GC-MS/MS method fully meets the requirements of thiol analysis from beer. Once established, the methodology is fast, manual handling is comparably simple, and the sample preparation is solvent-less. By using a CCD, OFD-HS-SPME and MRM parameters were optimized in a minimum number of experiments. Under consideration of thiol reactivity, the usage of stable isotope-labelled standards is vital to cover analyte losses during sample preparation and processing.

Method validation and application to beer samples proved that the method performance is very suitable for the analysis of hoppy beer.

## ■ ASSOCIATED CONTENT

### SI Supporting Information

The Supporting Information is available free of charge at <https://pubs.acs.org/doi/10.1021/acs.jafc.0c06305>.

Calibration curves of 4MMP, 3MH, and 3MHA, response equations as actual and coded factors, and raw data of method validation (PDF)

## ■ AUTHOR INFORMATION

### Corresponding Author

Nils Rettberg – Research Institute for Beer and Beverage Analysis, Versuchs- und Lehranstalt für Brauerei in Berlin (VLB) e.V., 13353 Berlin, Germany; [orcid.org/0000-0002-3667-2007](https://orcid.org/0000-0002-3667-2007); Phone: +49 30 45080106; Email: [n.rettberg@vlb-berlin.org](mailto:n.rettberg@vlb-berlin.org)

### Authors

Johanna Dennenlöhner – Research Institute for Beer and Beverage Analysis, Versuchs- und Lehranstalt für Brauerei in Berlin (VLB) e.V., 13353 Berlin, Germany

Sarah Thörner – Research Institute for Beer and Beverage Analysis, Versuchs- und Lehranstalt für Brauerei in Berlin (VLB) e.V., 13353 Berlin, Germany

Complete contact information is available at: <https://pubs.acs.org/doi/10.1021/acs.jafc.0c06305>

### Funding

This research was funded by the German Federal Ministry for Economic Affairs and Energy under grant numbers 49VF170007 and 49MF200054. The HS-SPME-GC-MS/MS system is part of grant number 49IZ140016.

### Notes

The authors declare no competing financial interest.

## ■ ACKNOWLEDGMENTS

The authors wish to thank Dr. Aneta Manowski, Laura Knoke, and Christian Schubert for their skilled assistance.

## ■ ABBREVIATIONS

3MH, 3-mercapto-1-hexanol; 3MHA, 3-mercaptohexylacetate; 4MMP, 4-mercapto-4-methyl-2-pentanone; CCD, central composite design; HL, hoppy lager; HS, headspace; IPA, India pale ale; LOD, limit of detection; LOQ, limit of quantitation; MRM, multiple reaction monitoring; NaCl, sodium chloride; NEIPA, New England India pale ale; OFD, on-fiber derivatization; PA, pale ale; PFB, 2,3,4,5,6-pentafluorobenzyl; PFBBr, 2,3,4,5,6-pentafluorobenzyl bromide; PFBHA, O-(2,3,4,5,6-pentafluorobenzyl)hydroxylamine hydrochloride; SBSE, stir bar sorptive extraction; SHIPA, single hopped India pale ale; TEA, triethylamine; w/o, without

## ■ REFERENCES

- (1) Rettberg, N.; Biendl, M.; Garbe, L.-A. Hop Aroma and Hoppy Beer Flavor: Chemical Backgrounds and Analytical Tools—A Review. *J. Am. Soc. Brew. Chem.* **2018**, *76*, 1–20.
- (2) Lafontaine, S.; Varnum, S.; Roland, A.; Delpech, S.; Dagan, L.; Vollmer, D.; Kishimoto, T.; Shellhammer, T. Impact of harvest

maturity on the aroma characteristics and chemistry of Cascade hops used for dry-hopping. *Food Chem.* **2019**, *278*, 228–239.

- (3) Steinhaus, M.; Schieberle, P. Transfer of the potent hop odorants linalool, geraniol and 4-methyl-4-sulfanyl-2-pentanone from hops into beer. *Proceedings of the 31st EBC Congress, Venice, Italy*; Fachverlag Hans Carl: Nürnberg, Germany, 2007; pp 1004–1011.

- (4) Kishimoto, T.; Wanikawa, A.; Kono, K.; Shibata, K. Comparison of the Odor-Active Compounds in Unhopped Beer and Beers Hopped with Different Hop Varieties. *J. Agric. Food Chem.* **2006**, *54*, 8855–8861.

- (5) Kishimoto, T.; Morimoto, M.; Kobayashi, M.; Yako, N.; Wanikawa, A. Behaviors of 3-Mercaptohexan-1-ol and 3-Mercaptohexyl Acetate During Brewing Processes. *J. Am. Soc. Brew. Chem.* **2008**, *66*, 192–196.

- (6) Chen, L.; Capone, D. L.; Jeffery, D. W. Analysis of Potent Odour-Active Volatile Thiols in Foods and Beverages with a Focus on Wine. *Molecules* **2019**, *24*, 2472.

- (7) Vermeulen, C.; Lejeune, I.; Tran, T. T. H.; Collin, S. Occurrence of polyfunctional thiols in fresh lager beers. *J. Agric. Food Chem.* **2006**, *54*, 5061–5068.

- (8) Kishimoto, T.; Kobayashi, M.; Yako, N.; Iida, A.; Wanikawa, A. Comparison of 4-Mercapto-4-methylpentan-2-one Contents in Hop Cultivars from Different Growing Regions. *J. Agric. Food Chem.* **2008**, *56*, 1051–1057.

- (9) Reglitz, K.; Lemke, S.; Hanke, S.; Steinhaus, M. On the Behaviour of the Important Hop Odorant 4-Mercapto-4-methylpentan-2-one (4MMP) during Dry Hopping and during Storage of Dry Hopped Beer. *Brew. Sci.* **2018**, *71*, 96–99.

- (10) Takazumi, K.; Takoi, K.; Koie, K.; Tuchiya, Y. Quantitation Method for Polyfunctional Thiols in Hops (*Humulus lupulus* L.) and Beer Using Specific Extraction of Thiols and Gas Chromatography-Tandem Mass Spectrometry. *Anal. Chem.* **2017**, *89*, 11598–11604.

- (11) Ochiai, N.; Sasamoto, K.; Kishimoto, T. Development of a Method for the Quantitation of Three Thiols in Beer, Hop, and Wort Samples by Stir Bar Sorptive Extraction with in Situ Derivatization and Thermal Desorption-Gas Chromatography-Tandem Mass Spectrometry. *J. Agric. Food Chem.* **2015**, *63*, 6698–6706.

- (12) Vichi, S.; Cortés-Francisco, N.; Caixach, J. Analysis of volatile thiols in alcoholic beverages by simultaneous derivatization/extraction and liquid chromatography-high resolution mass spectrometry. *Food Chem.* **2015**, *175*, 401–408.

- (13) Tominaga, T.; Dubourdiou, D. A novel method for quantification of 2-methyl-3-furanthiol and 2-furanmethanethiol in wines made from *Vitis vinifera* grape varieties. *J. Agric. Food Chem.* **2006**, *54*, 29–33.

- (14) Herbst-Johnstone, M.; Piano, F.; Duhamel, N.; Barker, D.; Fedrizzi, B. Ethyl propiolate derivatization for the analysis of varietal thiols in wine. *J. Chromatogr. A.* **2013**, *1312*, 104–110.

- (15) Dagan, L.; Reillon, F.; Roland, A.; Schneider, R. Development of a routine analysis of 4-mercapto-4-methylpentan-2-one in wine by stable isotope dilution assay and mass tandem spectrometry. *Anal. Chim. Acta* **2014**, *821*, 48–53.

- (16) Pavez, C.; Agosin, E.; Steinhaus, M. Odorant Screening and Quantitation of Thiols in Carmenere Red Wine by Gas Chromatography-Olfactometry and Stable Isotope Dilution Assays. *J. Agric. Food Chem.* **2016**, *64*, 3417–3421.

- (17) Mateo-Vivaracho, L.; Ferreira, V.; Cacho, J. Automated analysis of 2-methyl-3-furanthiol and 3-mercaptohexyl acetate at ngL<sup>-1</sup> level by headspace solid-phase microextraction with on-fibre derivatization and gas chromatography-negative chemical ionization mass spectrometric determination. *J. Chromatogr. A.* **2006**, *1121*, 1–9.

- (18) Hofmann, T.; Schieberle, P.; Grosch, W. Model Studies on the Oxidative Stability of Odor-Active Thiols Occurring in Food Flavors. *J. Agric. Food Chem.* **1996**, *44*, 251–255.

- (19) Dennenlöhner, J.; Thörner, S.; Maxminer, J.; Rettberg, N. Analysis of Selected Staling Aldehydes in Wort and Beer by GC-EI-MS/MS Using HS-SPME with On-Fiber Derivatization. *J. Am. Soc. Brew. Chem.* **2020**, *78*, 284–298.

(20) Carrillo, G.; Bravo, A.; Zufall, C. Application of factorial designs to study factors involved in the determination of aldehydes present in beer by on-fiber derivatization in combination with gas chromatography and mass spectrometry. *J. Agric. Food Chem.* **2011**, *59*, 4403–4411.

(21) Nešpor, J.; Karabin, M.; Hanko, V.; Dostálek, P. Application of response surface design to optimise the chromatographic analysis of volatile compounds in beer. *J. Inst. Brew.* **2018**, *124*, 244–253.

(22) Reglitz, K.; Steinhaus, M. Quantitation of 4-Methyl-4-sulfanyl-pentan-2-one (4MSP) in Hops by a Stable Isotope Dilution Assay in Combination with GC×GC-TOFMS: Method Development and Application To Study the Influence of Variety, Provenance, Harvest Year, and Processing on 4MSP Concentrations. *J. Agric. Food Chem.* **2017**, *65*, 2364–2372.

(23) Capone, D. L.; Sefton, M. A.; Jeffery, D. W. Application of a modified method for 3-mercaptohexan-1-ol determination to investigate the relationship between free thiol and related conjugates in grape juice and wine. *J. Agric. Food Chem.* **2011**, *59*, 4649–4658.

(24) Funk, W.; Dammann, V.; Donnevert, G. *Qualitätssicherung in der Analytischen Chemie*, 2nd ed.; Wiley-VCH Verlag GmbH & Co. KGaA: Weinheim, 2005.

(25) American Society of Brewing Chemists. *Methods of Analysis*, 14th ed.; Statistical Analysis-2 Limits of Detection and Determination; ASBC: St. Paul, MN, 2011.

(26) United States Pharmacopoeial Convention. *United States Pharmacopoeia*, 29th ed., National Formulary, 24th ed.; United States Pharmacopoeial Convention: Rockville, MD, USA, 2006.

(27) Ng, K.-M.; Lau, Y.-T. R.; Weng, L.-T.; Yeung, K.-L.; Chan, C.-M. ToF-SIMS and computation analysis: Fragmentation mechanisms of polystyrene, polystyrene-d5, and polypentafluorostyrene. *Surf. Interface Anal.* **2018**, *50*, 220–233.

(28) Derringer, G.; Suich, R. Simultaneous Optimization of Several Response Variables. *J. Qual. Technol.* **1980**, *12*, 214–219.

(29) Beccaria, M.; Franchina, F. A.; Nasir, M.; Mellors, T.; Hill, J. E.; Purcaro, G. Investigation of mycobacteria fatty acid profile using different ionization energies in GC–MS. *Anal. Bioanal. Chem.* **2018**, *410*, 7987–7996.

(30) Dennenlöhner, J.; Thörner, S.; Manowski, A.; Rettberg, N. Analysis of Selected Hop Aroma Compounds in Commercial Lager and Craft Beers Using HS-SPME-GC-MS/MS. *J. Am. Soc. Brew. Chem.* **2020**, *78*, 16–31.

(31) Biendl, M.; Schmidt, C.; Smith, R. J. *New England IPA (NEIPA)—The Hop Aroma Champion*; ASBC Meeting: New Orleans, LA, 2019.

(32) Steinhaus, M.; Sinuco, D.; Polster, J.; Osorio, C.; Schieberle, P. Characterization of the key aroma compounds in pink guava (*Psidium guajava* L.) by means of aroma re-engineering experiments and omission tests. *J. Agric. Food Chem.* **2009**, *57*, 2882–2888.

(33) Engel, K. H.; Tressl, R. Identification of new sulfur-containing volatiles in yellow passionfruit (*Passiflora edulis* f. *flavicarpa*). *J. Agric. Food Chem.* **1991**, *39*, 2249–2252.

(34) Buettner, A.; Schieberle, P. Evaluation of key aroma compounds in hand-squeezed grapefruit juice (*Citrus paradisi* Macfayden) by quantitation and flavor reconstitution experiments. *J. Agric. Food Chem.* **2001**, *49*, 1358–1363.

(35) Lin, J.; Jella, P.; Rouseff, R. L. Gas Chromatography-Olfactometry and Chemiluminescence Characterization of Grapefruit Juice Volatile Sulfur Compounds. *Heteroatomic Aroma Compounds*; ACS Symposium Series; American Chemical Society, 2002; Vol. 826, pp 102–112.

(36) Swiegers, J. H.; Capone, D. L.; Pardon, K. H.; Elsey, G. M.; Sefton, M. A.; Francis, I. L.; Pretorius, I. S. Engineering volatile thiol release in *Saccharomyces cerevisiae* for improved wine aroma. *Yeast* **2007**, *24*, 561–574.

## Supporting information

Figure S1. Calibration curves of 4MMP (A), 3MH (B), and 3MHA (C) based on the raw data of Table S2 used for method validation.

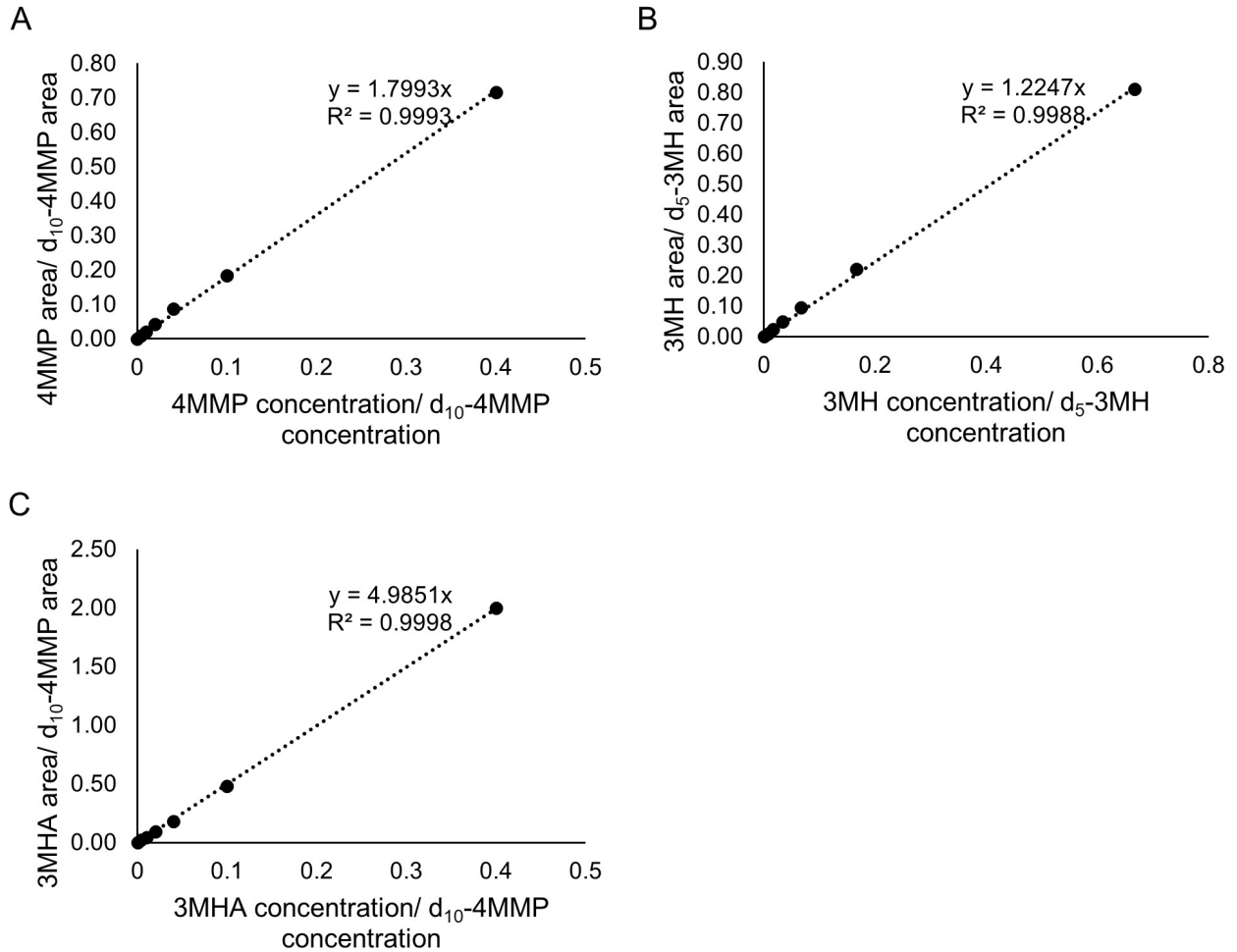


**Table S1. Response equations in terms of actual and coded factors. In the case that 0 was filled in the column, this factor is not contained in the equation.**

Factors	d <sub>10</sub> -4MMP				4MMP				d <sub>5</sub> -3MH				3MH				3MHA			
	109→46		322→46		99→43		312→43		138→85		319→87		133→81		314→82		115→81		115→73	
	actual	coded	actual	coded	actual	coded	actual	coded	actual	coded	actual	coded	actual	coded	actual	coded	actual	coded	actual	coded
Intercept	-113570	26694	-18085	4357	-79524	17282	-12254	3306	-1849	9158	2121	1435	-7657	14140	2565	1641	-637520	146400	-849346	198300
A	3321	-838,88	674	-287,18	1762	-1045,3	428	-162,89	-206	1337,01	-55	360,2	-224	2079,28	-67	445,88	17247	1961,49	25144	4032,46
B	0	0	0	0	5882	330,53	773	-20,06	2551	200,9	0	0	3763	240,48	0	0	0	0	0	0
C	1528	3227,46	198	892,64	1212	2427,8	142	590,75	-445	1386,88	-121	367,05	-693	2082,94	-150	452,84	4721	15735,7	7052	20770,2
D	24637	2049,48	3145	570,5	17628	175,74	2457	349,35	4774	955,18	814	232,79	12568	1306,03	322	297,37	114155	9449,14	168074	12817,5
E	0	0	-109	577,97	0	0	-87	422,67	1076	0	222	-16,65	1810	-355,18	299	-102,93	22763	-11094	19049	-1072,9
F	1050	5517,99	5	1840,41	932	4405,95	-1	1214,3	85	1815,42	-68	554,87	129	2698,45	-77	697,78	4500	22388,5	5050	30492,8
A*B	0	0	0	0	-39	-765,27	0	0	0	0	0	0	0	0	0	0	0	0	0	0
A*C	-10	-1126,3	-3	-332,41	-10	-1177,3	-1	-177,36	5	608,67	1	163,95	8	976,75	2	186,61	0	0	0	0
A*D	0	0	0	0	-102	-834,33	0	0	60	493,23	11	93,2	0	0	15	122,45	0	0	0	0
A*F	0	0	-1	-326,28	-4	-1181,1	-1	-197,3	4	1101,08	1	326,17	5	1668,72	1	405,77	0	0	0	0
C*D	0	0	51	302,56	0	0	29	171,77	97	573,61	20	119,36	135	799,94	32	187,39	0	0	0	0
C*E	0	0	4	230	0	0	3	179,36	0	0	0	0	0	0	0	0	-121	-7114,3	0	0
C*F	12	2634,23	4	847,59	10	2208,52	3	564,83	5	1123,95	1	331,95	8	1727,87	2	413,02	57	12623,8	77	17175,5
D*F	113	1725,86	36	558,31	0	0	22	331,39	55	841,08	15	228,02	80	1218,72	19	295,05	514	7865,8	704	10777,7
E*F	0	0	3	446,44	0	0	2	339,92	0	0	0	0	0	0	-1	-121,64	-79	-12003	0	0
A <sup>2</sup>	-32	-5289,3	-6	-983,67	-13	-2127,9	-4	-632,59	0	0	0	0	0	0	0	0	-171	-27914	-248	-40545
B <sup>2</sup>	0	0	0	0	-714	-1679,2	-151	-355,38	-465	-1094,4	0	0	-694	-1630,9	0	0	0	0	0	0
C <sup>2</sup>	-41	-3510,5	-8	-645,23	-30	-2561,5	-6	-507,66	0	0	0	0	0	0	0	0	-145	-12486	-274	-23494
D <sup>2</sup>	-13392	-5467,3	-2388	-975,09	-6122	-2499,2	-1694	-691,58	-5206	-2125,2	-1020	-416,5	-8200	-3347,6	-1006	-410,77	-61886	-25265	-90727	-37039
E <sup>2</sup>	0	0	0	0	0	0	0	0	-54	-2170,9	-11	-451	-93	-3751,6	-14	-558,35	-940	-37990	-956	-38645
F <sup>2</sup>	-12	-6749,4	0	0	-7	-4284,7	0	0	-3	-1949,6	0	0	-5	-2955,9	0	0	-44	-25191	-60	-34330

A-Temperature, B- Derivatization time, C- Extraction time, D- NaCl, E- Collision energy, F- Ionization energy

Table S2. Raw data for calibration curves used for method validation.

Level 1: Compound	Concentration [ng/L]	Quantitative transition [m/z]	Area	Qualitative transition [m/z]	Area
<b>d<sub>10</sub>-4MMP</b>	250.0	109→46	27213	322→46	10389
4MMP	0.0	99→43	0	312→43	0
<b>d<sub>5</sub>-3MH</b>	1500.0	138→85	17748	319→87	5863
3MH	0.0	133→81	0	314→82	0
3MHA	0.0	115→81	467	115→73	495
Level 2: Compound	Concentration [ng/L]	Quantitative transition [m/z]	Area	Qualitative transition [m/z]	Area
<b>d<sub>10</sub>-4MMP</b>	250.0	109→46	27664	322→46	10054
4MMP	1.0	99→43	238	312→43	59
<b>d<sub>5</sub>-3MH</b>	1500.0	138→85	19721	319→87	6450
3MH	10.0	133→81	192	314→82	41
3MHA	1.0	115→81	1150	115→73	1288
Level 3: Compound	Concentration [ng/L]	Quantitative transition [m/z]	Area	Qualitative transition [m/z]	Area
<b>d<sub>10</sub>-4MMP</b>	250.0	109→46	24613	322→46	9209
4MMP	2.5	99→43	493	312→43	126
<b>d<sub>5</sub>-3MH</b>	1500.0	138→85	15819	319→87	5218
3MH	25.0	133→81	378	314→82	86
3MHA	2.5	115→81	1484	115→73	1573
Level 4: Compound	Concentration [ng/L]	Quantitative transition [m/z]	Area	Qualitative transition [m/z]	Area
<b>d<sub>10</sub>-4MMP</b>	250.0	109→46	20727	322→46	7602
4MMP	5.0	99→43	884	312→43	220
<b>d<sub>5</sub>-3MH</b>	1500.0	138→85	12462	319→87	3994
3MH	50.0	133→81	620	314→82	144
3MHA	5.0	115→81	2354	115→73	2254
Level 5: Compound	Concentration [ng/L]	Quantitative transition [m/z]	Area	Qualitative transition [m/z]	Area
<b>d<sub>10</sub>-4MMP</b>	250.0	109→46	20226	322→46	7311
4MMP	10.0	99→43	1746	312→43	445
<b>d<sub>5</sub>-3MH</b>	1500.0	138→85	10986	319→87	3588
3MH	100.0	133→81	1059	314→82	249
3MHA	10.0	115→81	4036	115→73	4265
Level 6: Compound	Concentration [ng/L]	Quantitative transition [m/z]	Area	Qualitative transition [m/z]	Area
<b>d<sub>10</sub>-4MMP</b>	250.0	109→46	20444	322→46	7737
4MMP	25.0	99→43	3764	312→43	932
<b>d<sub>5</sub>-3MH</b>	1500.0	138→85	12100	319→87	3975
3MH	250.0	133→81	2669	314→82	600
3MHA	25.0	115→81	10161	115→73	10517
Level 7: Compound	Concentration [ng/L]	Quantitative transition [m/z]	Area	Qualitative transition [m/z]	Area
<b>d<sub>10</sub>-4MMP</b>	250.0	109→46	15080	322→46	5581
4MMP	100.0	99→43	10810	312→43	2753
<b>d<sub>5</sub>-3MH</b>	1500.0	138→85	12448	319→87	4039
3MH	1000.0	133→81	10087	314→82	2325
3MHA	100.0	115→81	30429	115→73	36078

Table S3. Raw data for recovery experiments used for method validation.

Measurement 1, not spiked:	<b>Compound</b>	<b>Concentration [ng/L]</b>	<b>Quantitative transition [m/z]</b>	<b>Area</b>	<b>Qualitative transition [m/z]</b>	<b>Area</b>
	d <sub>10</sub> -4MMP	250.0	109→46	35276	322→46	10166
	4MMP	0.0	99→43	1453	312→43	1557
	d <sub>5</sub> -3MH	1500.0	138→85	7963	319→87	1887
	3MH	0.0	133→81	1732	314→82	253
	3MHA	0.0	115→81	2457	115→73	1772
Measurement 2, not spiked:	<b>Compound</b>	<b>Concentration [ng/L]</b>	<b>Quantitative transition [m/z]</b>	<b>Area</b>	<b>Qualitative transition [m/z]</b>	<b>Area</b>
	d <sub>10</sub> -4MMP	250.0	109→46	27219	322→46	8388
	4MMP	0.0	99→43	1367	312→43	1407
	d <sub>5</sub> -3MH	1500.0	138→85	8104	319→87	2041
	3MH	0.0	133→81	1689	314→82	234
	3MHA	0.0	115→81	2333	115→73	1802
Measurement 3, not spiked:	<b>Compound</b>	<b>Concentration [ng/L]</b>	<b>Quantitative transition [m/z]</b>	<b>Area</b>	<b>Qualitative transition [m/z]</b>	<b>Area</b>
	d <sub>10</sub> -4MMP	250.0	109→46	24645	322→46	7535
	4MMP	0.0	99→43	1296	312→43	1312
	d <sub>5</sub> -3MH	1500.0	138→85	7128	319→87	1641
	3MH	0.0	133→81	1660	314→82	212
	3MHA	0.0	115→81	1849	115→73	1357
Measurement 1, spiked, level 1:	<b>Compound</b>	<b>Concentration [ng/L]</b>	<b>Quantitative transition [m/z]</b>	<b>Area</b>	<b>Qualitative transition [m/z]</b>	<b>Area</b>
	d <sub>10</sub> -4MMP	250.0	109→46	23884	322→46	7339
	4MMP	5.0	99→43	1891	312→43	1562
	d <sub>5</sub> -3MH	1500.0	138→85	6150	319→87	1582
	3MH	50.0	133→81	1720	314→82	257
	3MHA	25.0	115→81	10723	115→73	9371
Measurement 2, spiked, level 1:	<b>Compound</b>	<b>Concentration [ng/L]</b>	<b>Quantitative transition [m/z]</b>	<b>Area</b>	<b>Qualitative transition [m/z]</b>	<b>Area</b>
	d <sub>10</sub> -4MMP	250.0	109→46	23657	322→46	7176
	4MMP	5.0	99→43	1697	312→43	1233
	d <sub>5</sub> -3MH	1500.0	138→85	6714	319→87	1448
	3MH	50.0	133→81	1842	314→82	237
	3MHA	25.0	115→81	11156	115→73	9933
Measurement 3, spiked, level 1:	<b>Compound</b>	<b>Concentration [ng/L]</b>	<b>Quantitative transition [m/z]</b>	<b>Area</b>	<b>Qualitative transition [m/z]</b>	<b>Area</b>
	d <sub>10</sub> -4MMP	250.0	109→46	19705	322→46	5877
	4MMP	5.0	99→43	1877	312→43	1056
	d <sub>5</sub> -3MH	1500.0	138→85	7028	319→87	1381
	3MH	50.0	133→81	1665	314→82	326
	3MHA	25.0	115→81	11081	115→73	9917
Measurement 1, spiked, level 2:	<b>Compound</b>	<b>Concentration [ng/L]</b>	<b>Quantitative transition [m/z]</b>	<b>Area</b>	<b>Qualitative transition [m/z]</b>	<b>Area</b>
	d <sub>10</sub> -4MMP	250.0	109→46	16730	322→46	5660
	4MMP	25.0	99→43	3656	312→43	1760
	d <sub>5</sub> -3MH	1500.0	138→85	4893	319→87	1569
	3MH	250.0	133→81	2295	314→82	341
	3MHA	125.0	115→81	36950	115→73	33149
Measurement 2, spiked, level 2:	<b>Compound</b>	<b>Concentration [ng/L]</b>	<b>Quantitative transition [m/z]</b>	<b>Area</b>	<b>Qualitative transition [m/z]</b>	<b>Area</b>
	d <sub>10</sub> -4MMP	250.0	109→46	17789	322→46	5428
	4MMP	25.0	99→43	3559	312→43	1681
	d <sub>5</sub> -3MH	1500.0	138→85	5798	319→87	1100
	3MH	250.0	133→81	2251	314→82	347
	3MHA	125.0	115→81	41919	115→73	38758
Measurement 3, spiked, level 2:	<b>Compound</b>	<b>Concentration [ng/L]</b>	<b>Quantitative transition [m/z]</b>	<b>Area</b>	<b>Qualitative transition [m/z]</b>	<b>Area</b>
	d <sub>10</sub> -4MMP	250.0	109→46	15638	322→46	4851
	4MMP	25.0	99→43	3022	312→43	1562
	d <sub>5</sub> -3MH	1500.0	138→85	6503	319→87	1473
	3MH	250.0	133→81	2166	314→82	337
	3MHA	125.0	115→81	42924	115→73	39671

Table S4. Raw data for measurement precision used for method validation.

Measurement 1:	Compound	Quantitative transition [m/z]	Area	Qualitative transition [m/z]	Area
	<b>d<sub>10</sub>-4MMP</b>	109→46	17789	322→46	5428
	4MMP	99→43	3559	312→43	1681
	<b>d<sub>5</sub>-3MH</b>	138→85	5798	319→87	1100
	3MH	133→81	2251	314→82	347
	3MHA	115→81	41919	115→73	38758
Measurement 2:	Compound	Quantitative transition [m/z]	Area	Qualitative transition [m/z]	Area
	<b>d<sub>10</sub>-4MMP</b>	109→46	15638	322→46	4851
	4MMP	99→43	3022	312→43	1562
	<b>d<sub>5</sub>-3MH</b>	138→85	6503	319→87	1473
	3MH	133→81	2166	314→82	337
	3MHA	115→81	42924	115→73	39671
Measurement 3:	Compound	Quantitative transition [m/z]	Area	Qualitative transition [m/z]	Area
	<b>d<sub>10</sub>-4MMP</b>	109→46	14764	322→46	4336
	4MMP	99→43	2311	312→43	980
	<b>d<sub>5</sub>-3MH</b>	138→85	5136	319→87	1195
	3MH	133→81	2118	314→82	315
	3MHA	115→81	38112	115→73	34394
Measurement 4:	Compound	Quantitative transition [m/z]	Area	Qualitative transition [m/z]	Area
	<b>d<sub>10</sub>-4MMP</b>	109→46	11795	322→46	3776
	4MMP	99→43	2439	312→43	1283
	<b>d<sub>5</sub>-3MH</b>	138→85	4152	319→87	944
	3MH	133→81	1654	314→82	245
	3MHA	115→81	26805	115→73	25193
Measurement 5:	Compound	Quantitative transition [m/z]	Area	Qualitative transition [m/z]	Area
	<b>d<sub>10</sub>-4MMP</b>	109→46	10862	322→46	3541
	4MMP	99→43	2293	312→43	904
	<b>d<sub>5</sub>-3MH</b>	138→85	4418	319→87	840
	3MH	133→81	1552	314→82	234
	3MHA	115→81	27937	115→73	24505
Measurement 6:	Compound	Quantitative transition [m/z]	Area	Qualitative transition [m/z]	Area
	<b>d<sub>10</sub>-4MMP</b>	109→46	12064	322→46	3882
	4MMP	99→43	2475	312→43	1283
	<b>d<sub>5</sub>-3MH</b>	138→85	5392	319→87	1116
	3MH	133→81	1653	314→82	247
	3MHA	115→81	31609	115→73	28418

Table S5. Raw data for ruggedness regarding elapsed assay times used for method validation.

Beginning, measurement 1:	Compound	Quantitative transition [m/z]	Area	Qualitative transition [m/z]	Area
	<b>d<sub>10</sub>-4MMP</b>	109→46	17540	322→46	5505
4MMP	99→43	2933	312→43	1414	
<b>d<sub>5</sub>-3MH</b>	138→85	4880	319→87	1208	
3MH	133→81	1641	314→82	264	
3MHA	115→81	47214	115→73	43183	

Beginning, measurement 2:	Compound	Quantitative transition [m/z]	Area	Qualitative transition [m/z]	Area
	<b>d<sub>10</sub>-4MMP</b>	109→46	24448	322→46	7265
4MMP	99→43	4651	312→43	2618	
<b>d<sub>5</sub>-3MH</b>	138→85	8338	319→87	1916	
3MH	133→81	3101	314→82	489	
3MHA	115→81	70993	115→73	65668	

Middle, measurement 1:	Compound	Quantitative transition [m/z]	Area	Qualitative transition [m/z]	Area
	<b>d<sub>10</sub>-4MMP</b>	109→46	18483	322→46	5906
4MMP	99→43	3030	312→43	1673	
<b>d<sub>5</sub>-3MH</b>	138→85	6463	319→87	1557	
3MH	133→81	2580	314→82	397	
3MHA	115→81	55321	115→73	51934	

Middle, measurement 2:	Compound	Quantitative transition [m/z]	Area	Qualitative transition [m/z]	Area
	<b>d<sub>10</sub>-4MMP</b>	109→46	17653	322→46	5680
4MMP	99→43	2739	312→43	1585	
<b>d<sub>5</sub>-3MH</b>	138→85	6665	319→87	2009	
3MH	133→81	2733	314→82	421	
3MHA	115→81	52739	115→73	47149	

End, measurement 1:	Compound	Quantitative transition [m/z]	Area	Qualitative transition [m/z]	Area
	<b>d<sub>10</sub>-4MMP</b>	109→46	11573	322→46	3421
4MMP	99→43	2318	312→43	1024	
<b>d<sub>5</sub>-3MH</b>	138→85	4009	319→87	849	
3MH	133→81	1617	314→82	247	
3MHA	115→81	29399	115→73	26301	

End, measurement 2:	Compound	Quantitative transition [m/z]	Area	Qualitative transition [m/z]	Area
	<b>d<sub>10</sub>-4MMP</b>	109→46	13603	322→46	4030
4MMP	99→43	2572	312→43	1503	
<b>d<sub>5</sub>-3MH</b>	138→85	4352	319→87	1066	
3MH	133→81	1860	314→82	265	
3MHA	115→81	34137	115→73	30359	

Table S6. Raw data for ruggedness regarding different days used for method validation.

Day 1, measurement 1:	Compound	Quantitative transition [m/z]	Area	Qualitative transition [m/z]	Area
	<b>d<sub>10</sub>-4MMP</b>	109→46	17540	322→46	5505
	4MMP	99→43	2933	312→43	1414
	<b>d<sub>5</sub>-3MH</b>	138→85	4880	319→87	1208
	3MH	133→81	1641	314→82	264
	3MHA	115→81	47214	115→73	43183
Day 1, measurement 2:	Compound	Quantitative transition [m/z]	Area	Qualitative transition [m/z]	Area
	<b>d<sub>10</sub>-4MMP</b>	109→46	18483	322→46	5906
	4MMP	99→43	3030	312→43	1673
	<b>d<sub>5</sub>-3MH</b>	138→85	6463	319→87	1557
	3MH	133→81	2580	314→82	397
	3MHA	115→81	55321	115→73	51934
Day 1, measurement 3:	Compound	Quantitative transition [m/z]	Area	Qualitative transition [m/z]	Area
	<b>d<sub>10</sub>-4MMP</b>	109→46	17653	322→46	5680
	4MMP	99→43	2739	312→43	1585
	<b>d<sub>5</sub>-3MH</b>	138→85	6665	319→87	2009
	3MH	133→81	2733	314→82	421
	3MHA	115→81	52739	115→73	47149
Day 2, measurement 1:	Compound	Quantitative transition [m/z]	Area	Qualitative transition [m/z]	Area
	<b>d<sub>10</sub>-4MMP</b>	109→46	16730	322→46	5660
	4MMP	99→43	3656	312→43	1760
	<b>d<sub>5</sub>-3MH</b>	138→85	4893	319→87	1569
	3MH	133→81	2295	314→82	341
	3MHA	115→81	36950	115→73	33149
Day 2, measurement 2:	Compound	Quantitative transition [m/z]	Area	Qualitative transition [m/z]	Area
	<b>d<sub>10</sub>-4MMP</b>	109→46	17789	322→46	5428
	4MMP	99→43	3559	312→43	1681
	<b>d<sub>5</sub>-3MH</b>	138→85	5798	319→87	1100
	3MH	133→81	2251	314→82	347
	3MHA	115→81	41919	115→73	38758
Day 2, measurement 3:	Compound	Quantitative transition [m/z]	Area	Qualitative transition [m/z]	Area
	<b>d<sub>10</sub>-4MMP</b>	109→46	15638	322→46	4851
	4MMP	99→43	3022	312→43	1562
	<b>d<sub>5</sub>-3MH</b>	138→85	6503	319→87	1473
	3MH	133→81	2166	314→82	337
	3MHA	115→81	42924	115→73	39671

Table S7. Raw data for ruggedness regarding different analysts used for method validation.

Analyst 1, measurement 1:	<b>Compound</b>	<b>Quantitative transition [m/z]</b>	<b>Area</b>	<b>Qualitative transition [m/z]</b>	<b>Area</b>
	<b>d<sub>10</sub>-4MMP</b>	109→46	24417	322→46	7386
	4MMP	99→43	2610	312→43	1578
	<b>d<sub>5</sub>-3MH</b>	138→85	8258	319→87	2052
	3MH	133→81	1810	314→82	301
	3MHA	115→81	15977	115→73	14750
Analyst 1, measurement 2:	<b>Compound</b>	<b>Quantitative transition [m/z]</b>	<b>Area</b>	<b>Qualitative transition [m/z]</b>	<b>Area</b>
	<b>d<sub>10</sub>-4MMP</b>	109→46	25166	322→46	7205
	4MMP	99→43	2296	312→43	1119
	<b>d<sub>5</sub>-3MH</b>	138→85	8090	319→87	2002
	3MH	133→81	1905	314→82	293
	3MHA	115→81	15304	115→73	14281
Analyst 1, measurement 3:	<b>Compound</b>	<b>Quantitative transition [m/z]</b>	<b>Area</b>	<b>Qualitative transition [m/z]</b>	<b>Area</b>
	<b>d<sub>10</sub>-4MMP</b>	109→46	24312	322→46	7660
	4MMP	99→43	2297	312→43	1314
	<b>d<sub>5</sub>-3MH</b>	138→85	7789	319→87	2212
	3MH	133→81	1847	314→82	285
	3MHA	115→81	15711	115→73	14235
Analyst 2, measurement 1:	<b>Compound</b>	<b>Quantitative transition [m/z]</b>	<b>Area</b>	<b>Qualitative transition [m/z]</b>	<b>Area</b>
	<b>d<sub>10</sub>-4MMP</b>	109→46	23739	322→46	7215
	4MMP	99→43	2462	312→43	1749
	<b>d<sub>5</sub>-3MH</b>	138→85	6780	319→87	1462
	3MH	133→81	1654	314→82	235
	3MHA	115→81	15196	115→73	13618
Analyst 2, measurement 2:	<b>Compound</b>	<b>Quantitative transition [m/z]</b>	<b>Area</b>	<b>Qualitative transition [m/z]</b>	<b>Area</b>
	<b>d<sub>10</sub>-4MMP</b>	109→46	16128	322→46	5262
	4MMP	99→43	1166	312→43	1131
	<b>d<sub>5</sub>-3MH</b>	138→85	4888	319→87	1297
	3MH	133→81	1377	314→82	258
	3MHA	115→81	12562	115→73	13646
Analyst 2, measurement 3:	<b>Compound</b>	<b>Quantitative transition [m/z]</b>	<b>Area</b>	<b>Qualitative transition [m/z]</b>	<b>Area</b>
	<b>d<sub>10</sub>-4MMP</b>	109→46	10692	322→46	2866
	4MMP	99→43	1145	312→43	775
	<b>d<sub>5</sub>-3MH</b>	138→85	4240	319→87	903
	3MH	133→81	857	314→82	134
	3MHA	115→81	7281	115→73	6267



caused by the reactivity and lowered thresholds of the target analytes. While for the hop aroma compounds listed in *Publication A* concentration levels in the  $\mu\text{g/L}$  range are sufficient, for (*E*)-2-nonenal and (*E,E*)-2,4-decadienal a reliable quantification in the sub  $\mu\text{g/L}$  range is required. Through the successful implementation of OFD in *Publication B*, these low concentrations were reliably quantified in the complex beer matrix. Due to the need to reach the range of the lowest technically possible LOD and LOQ in *Publication C*, in addition to OFD, the matrix was diluted and an alkali was added to achieve the required sensitivity in the lower calibration range. Furthermore, a CCD was used for optimization in method development.

In the last part of the thesis, the aroma potential and analytical challenges of bound aroma compounds as well as further analytical aspects will be discussed that were beyond the scope of the three publications.

## 5.1 Bound Aroma Compounds

In many plant systems (e.g., roses, grapes, passion fruit)<sup>97-99</sup> aroma compounds are present both as free volatiles and in non-volatile bound forms. These odorless bound aroma compounds have been detected in hops.<sup>40,100</sup> Potentially, the most interesting bound aroma classes in hops and beer are glycosides as well as cysteinylated and glutathionylated conjugates. The binding behavior of the volatile aroma compounds to the non-volatile components are different depending on the reactivity of the aroma compound, the other beer ingredients (proteins, carbohydrates), and intracellular enzymatic processes. For example, while the reactivity of the thiol group of cysteines with the carbonyl function of aldehydes causes the formation of cysteinylated bound aldehydes,<sup>101</sup> enzymatic glycosylation are the reason for the glycosidic bond of terpenes to a carbohydrate moiety.<sup>102,103</sup>

When investigating flavor and flavor stability of beer, the potential of bound aroma compounds should be considered, since a subsequent release of aroma-active compounds can influence the beer aroma. In addition, an improved understanding of the release mechanisms allows more efficient hop dosage. Hence, a reliable quantification of these bound aroma substances is essential. For this reason, the objective of future work is to extend the assays so that they are capable of accurately detecting the bound aroma compounds after prior release. It has already been shown by sufficient sensitivity and stability that the presented assays are very promising to detect smallest concentration changes. In the following section, bound aroma compound in

form of glycosides as well as cysteinylated and glutathionylated conjugates and their relevance to beer flavor are introduced in more detail.

### 5.1.1 Glycosidic Aroma Compounds in Hops

The glycosides consist of a carbohydrate moiety (monosaccharide, disaccharide, or polysaccharide), which is bound to the aroma compound (aglycone) via a glycosidic bond. By means of glycosylation, hydrophobic compounds become water-soluble, which improves the transport and storage properties of these substances in the plant.<sup>102</sup> Many terpene compounds are present as glycosides.<sup>102</sup> The monoterpene glycosides (e.g., linalyl glycoside, geranyl glycoside) provide an additional source of aroma-active compounds and represent potential aroma reserves, since their corresponding free volatile components contribute significantly to the hop aroma. The glycoside content depends on the hop variety and the hop product used.<sup>104–106</sup> The glycosidically bound hop aroma compounds can be released by acidic, enzymatic, and thermal hydrolysis.<sup>22</sup> During fermentation and storage, yeast glycoside hydrolase activity liberate the volatile aglycones. However, their impact to the overall hop flavor in beer is smaller compared to the free hop-derived volatiles.<sup>105,107</sup> For an increased release of aroma-active compounds, a screening for brewing yeast strains with high glycoside hydrolase activity was performed. Certain *Saccharomyces* strains with high exo- $\beta$ -glucanase activity and *Brettanomyces* species with  $\beta$ -glucosidase activity enhance the hydrolysis of glycosidically bound hop aroma compounds.<sup>108</sup> A better understanding of the amount of bound and free aroma compounds in different hop varieties would offer another approach to use hops more efficiently.<sup>109</sup> Using the classification of Takoi et al.<sup>106</sup> into “free geraniol dominant hops” (e.g., Cascade, Citra, Mosaic) and “geraniol precursor dominant hops” (e.g., Amarillo, Hallertau Blanc, Summit) the selection of hop varieties can be optimized according to the different hopping regimes. In order to increase the yield of hop aroma, geraniol precursor dominant hops need to be added before or during fermentation to ensure that the yeast can liberate the bound aroma compounds. In contrast, to fully exploit the potential of free geraniol dominant hops, these hop varieties should be applied for dry hopping after fermentation.<sup>109</sup>

For this purpose, an analytical tool for determining the bound aroma precursors is beneficial. There are two possible procedures for the determination of bound aroma compounds: Either a direct analysis of the glycosidic aroma precursors or an indirect analysis after prior liberation of the aglycones. Options for a direct identification are LC or GC (analyzed as trifluoroacetylated

derivatives) approaches in combination with MS or MS/MS.<sup>110,111</sup> Near-infrared spectroscopy and chemometrics have also been used to determine the glycosidically bound aroma components in grapes.<sup>112</sup> Although spectroscopic methods have the advantage that they require minimal sample preparation and provide fast results, the overlapping of glycoside peaks hinders the identification and quantification of individual glycosides. As explained in the introduction, the isolation and separation steps are important for the method performance. The sample preparation of previously published direct LC and GC analysis methods<sup>110,111</sup> require a lot of manual handling (column chromatography, filtration) in order to obtain sufficient purified samples. In addition, the direct analysis of the precursors is more complex due to the large number of possible sugar combinations (mono-, di-, or polysaccharides) that are bound to the aglycone. This means that a multitude of different precursors have to be evaluated and calibrated for the same aglycone. Therefore, the direct analysis of precursors is recommended for qualitative purposes to investigate the detailed structure rather than for a quantitative approach.

For the indirect analysis of glycosidically bound aroma components it is essential to liberate the aglycones as gently as possible to make them accessible for analysis by GC. There are two possibilities for release: acidic and enzymatic hydrolysis. The hydrolysis under acidic conditions is simpler and cheaper than enzymatic hydrolysis, since the chemical process is not inhibited by the low pH or the high ethanol content in beer. However, there is a risk of structural rearrangement of monoterpenes during acid hydrolysis, as a result the analyzed aglycone composition may not reflect the original occurring in the sample.<sup>113</sup> In addition, increased  $\beta$ -damascenone levels during artificial aging of beers, which could be partially explained by acid hydrolysis of glycosides or other precursors, supports rearrangement processes at harsh conditions.<sup>114</sup> Therefore, variable hydrolysis conditions (pH, temperature, time) have to be evaluated not only with respect to efficient aglycone liberation but also carefully for possible rearrangements of the released aroma compounds. Hampel et al.<sup>115</sup> extensively compared the aroma compound stability and hydrolysis efficiency of acidic and enzymatic hydrolysis in a model mixture with free volatile and monoglycosidically bound aroma compounds. For this model mixture, enzymatic hydrolysis proved to be more efficient, but the hydrolysis method has to be selected based on the investigations for the respective matrix and the experimental objectives. Commercially available purified  $\beta$ -glucosidase from Almonds or *Aspergillus niger* has been widely used for hops and beer, but it is limited to the enzymatic-catalyzed cleavage of  $\beta$ -D-glucosides.<sup>100,105-107</sup> When selecting a crude enzyme mixture for a broader range of

glycosides, it is necessary to investigate whether additional enzyme activities are present that lead to a possible analyte degradation. For instance, Rapidase AR-2000, a pectolytic enzyme mixture used for grape homogenates, shows an increased esterase activity towards long straight-chain esters compared to shorter straight-chain, branched-chain, or phenolic esters.<sup>115</sup>

To assess the glycoside content, the developed HS-SMPE-GC-MS/MS assay for hop aroma (*Publication A*) could be performed for the liberated volatiles. By subtracting the concentration of each free aroma compound in a blank (control sample without hydrolysis) from the sample with released aglycones, the amount of bound aroma compounds is calculated. To add this application to the HS-SPME-GC-MS/MS method, further research is needed to optimize the still very time-consuming isolation procedure for the hop glycoside fraction achieving a high sample throughput.<sup>105</sup> First of all, the hydrolysis conditions (e.g., pH, amount of enzyme, temperature, time) should be optimized by an experimental design to evaluate the best conditions for aroma compound stability and hydrolysis efficiency in a minimum number of experiments. For the detection of glycosides in beer, Takoi et al.<sup>106</sup> directly enzymatically hydrolyzed the glycosides without prior isolation steps. Thus, in order to reduce the requirement for manual handling, the direct hydrolysis approach of Hampel et al.<sup>115</sup>, for example, could be adapted to hop samples. In combination with a high hydrolysis efficiency and a sensitive assay, additional enrichment and purification steps may no longer be necessary. Similar to the studies presented in this thesis, an extensive automation of the hydrolysis will be targeted, preferably to be performed by the autosampler. Finally, the efficiency and the quality of the existing isolation procedure and the direct hydrolyses on the released aroma compounds should be compared. The results of Kankolongo Cibaka et al.<sup>105</sup> additionally show that the enzymatic hydrolysis efficiency of  $\beta$ -glucosidase for the release of various aglycones differs significantly. Glycosidically bound octan-1-ol, serving as ISTD, was 2.8 times more liberated than glycosidically bound geraniol. To ensure a reliable quantification, the use of labeled isotopologue as ISTD for the glycosidically bound aroma compounds should be considered.

### 5.1.2 S-cysteinylated and S-glutathionylated Thiol Precursors

Similar to the monoterpenes, polyfunctional thiols (e.g., 4MMP, 3MH) can exist in hops as odor-active free volatiles and as odorless bound precursors.<sup>116,117</sup> Kishimoto et al.<sup>38</sup> suggested that, in addition to hops, malts also contain 3MH precursors, as 3MH was also identified in unhopped beer. By detecting the corresponding 3MH precursors in malted grains, Roland et al.<sup>118</sup> validate

this hypothesis. Due to their low thresholds (ng/L), changes caused by an increased liberation of bound thiols have a significant impact on the overall beer flavor.<sup>119</sup> In the past, mainly *S*-cysteinylated and *S*-glutathionylated conjugates have been investigated as thiol precursors in hops. Recently, other precursor structures (dipeptide conjugates) as already identified in grape must<sup>120,121</sup> were detected in hops and malts (e.g., 3-*S*-cysteinyl-glycine-hexan-1-ol, 3-*S*- $\gamma$ -glutamyl-cysteine-hexan-1-ol).<sup>122</sup> The amounts of bound and free thiols in hops as well the distribution of thiol precursors depend on the variety, the hop product used, and the harvest maturity.<sup>40,117,123,124</sup> When comparing the proportion of bound and free 3MH and 4MMP fractions, Roland et al.<sup>117</sup> demonstrated that more than 99% of 3MH occurred as precursors in hops. Among the hop varieties tested (Chinook, Saaz, Cascade, Mistral, Aramis Alsace, Strisselspat, and Mandarina), 3-*S*-glutathionyl-hexan-1-ol (G3MH) accounted for more than 80% of the total amount of precursor. Only in the Barbe Rouge hops was the distribution of 3-*S*-cysteinyl-hexan-1-ol (Cys3MH) and G3MH approximately equal. The G3MH concentrations (up to 19 mg/kg for Cascade hops) were higher than the free 3MH fraction ( $\mu\text{g}/\text{kg}$  levels) by a factor of 1000. The significant contribution of G3MH to the thiol fraction was also confirmed for Amarillo, Hallertau Blanc, and Mosaic hops.<sup>125</sup> In contrast, the proportion of bound 4MMP precursors (4-*S*-glutathionyl-4-methylpentan-2-one (G4MMP), 4-*S*-cysteinyl-4-methylpentan-2-one (Cys4MMP)) and the free 4MMP fraction were 23 and 95% for Chinook and Saaz hops, respectively.<sup>117</sup> However, Cys4MMP was the main precursor in the tested hop varieties, since G4MMP was only detected in Chinook hops. Chenot and Collin<sup>126</sup> recently investigated the transfer rate of 3MH from the Mandarina Bavaria variety into finished beers. In the late hopped beers, 33-50 ng/L of free 3MH was detected. However, based upon hopping rate, only a maximum of 1 ng/L free 3MH could have been transferred directly from the hops into the beers (assuming a 100% transfer rate). Consequently, the majority of the 3MH determined in the beers must originate from the release of bound precursors. For example, the Mandarina Bavaria hops tested need to release only 0.2% 3MH from G3MH to achieve the detected 3MH levels in the beers. Furthermore, Cys3MH and Cys4MMP were found to release 3MH and 4MMP by bottle refermentation promoted by yeast  $\beta$ -lyase activity (three weeks of storage in the dark at 27 °C).<sup>127</sup> These observations suggest that concentrations of polyfunctional thiols should progressively increase in (unpasteurized) beers with residual enzyme activity. Tran et al.<sup>119</sup> monitored the thiol release during one-year aging of Belgian beers (dark storage at 20 °C). They discovered two different trends for fresh beers with either high or low initial concentrations. For beers with already high initial concentrations, subsequent thiol synthesis in the bottle seems to be insignificant compared to the loss due to oxidation. In contrast, for some beers with initial

concentrations at trace level, thiol concentrations increased within the first three months. After one year, 4MMP and 3MH were absent in all beers tested. Since the increase occurred within the first three months in beers even in the absence of yeast, it was suspected that the *S*-cysteinylated conjugates were chemically degraded. In various storage tests in which the 4MMP, 3MH, and 3MHA concentrations were determined using the OFD-HS-SPME-GC-MS/MS thiol assay presented, no increase in concentration has yet been detected in any of the beers tested during the first few months. On the other hand, the significant decrease in concentrations in the first few months can be confirmed. In addition to oxidation reactions of the highly reactive thiols, the formation of disulfides and thioether compounds during aging could also contribute to the decrease.<sup>117,128</sup>

By understanding which hop varieties contain predominantly bound thiol precursors or have high levels of free thiols at which harvest maturity, brewers can maximize the thiol-derived flavor potential adapting hopping regimes to the composition of hops. The findings of Roland et al.<sup>129</sup> recommend the use of hops with higher thiol precursor concentrations (e.g., Hallertau Perle, Calypso, Saaz) for kettle hopping, since yeast releases the thiols by  $\beta$ -lyase activity during fermentation. In contrast, hops with a high amount of free thiols (e.g., Bravo, Eureka, Simcoe) are more suited for dry hopping, whereby the thermal degradation and the loss of volatile thiols is reduced. These recommendations are consistent with the observations of Lafontaine et al.<sup>40</sup> Depending on the thiol precursor content, early harvest Cascade hops (high thiol precursor content) should be added during wort boiling or whirlpool whereas later harvest Cascade hops (high free thiol content) should be used for dry hopping. In addition, this study indicated that it is more likely that 3MH may be released via an unknown enzymatic pathway in hops.<sup>40</sup>

In addition, a closer understanding of the influence of malt variety and roasting level on thiol precursors, can help brewers exploit the flavor potential of malt. Roland et al.<sup>118</sup> first investigated 3MH precursors in different types of malts (barley 3-1150 EBC, rice, sorghum, wheat). As in hops, G3MH (40-700  $\mu\text{g}/\text{kg}$  in barley malts) was more abundant than Cys3MH (1-7  $\mu\text{g}/\text{kg}$  in barley malts) whereas cysteinylated or glutathionylated 4MMP precursors were not detected. Barley malts have higher concentrations of 3MH precursors compared to the three specialty malts tested (<20  $\mu\text{g}/\text{kg}$ ). The degree of kilning also affects the amount of 3MH precursors, since no 3MH precursors were quantified in the most roasted barley malt sample. Even though the 3MH precursor levels in malts ( $\mu\text{g}/\text{kg}$  levels) appears more negligible compared to the concentrations in hops (mg/kg levels), it is useful for fruity aromas to choose a malt with higher 3MH precursor concentrations due to the fact that malt (kg/hL levels) is added

in much larger quantities than hops (g/hL levels). Roland et al.<sup>128</sup> calculated that 64% of 3MH in final beer originally originated from 3MH precursors from malt assuming a malt and hops addition of 25 kg/hL and 400 g/hL, respectively. In summary, the release of thiols in beers can be managed by choosing thiol precursor rich hops and malts as well as suitable mashing, hopping, and fermentation conditions.

As with the glycosidically bound hop aroma compounds, the thiol precursors in hops can be quantified either directly using LC-MS/MS<sup>117,125</sup> or indirectly after prior enzymatic release.<sup>123</sup> After prior liberation, the OFD-HS-SPME-GC-MS/MS assay for thiols (*Publication C*) presented in this thesis is also suited for the quantification of *S*-Cysteinylated and *S*-Glutathionylated thiol precursors. As in the study of Lafontaine et al.<sup>130</sup> shown, the presented OFD-HS-SPME-GC-MS/MS method has already been successfully adapted for the direct analysis of free thiols in hop samples. For the analysis of free thiols in hops, it was necessary to adjust the calibration range, since higher concentrations ( $\mu\text{g}/\text{kg}$ ) than in beer were expected. Furthermore, a fast sample preparation was targeted without a time-consuming extraction of the thiol fraction. Thus, 50 mg grinded hops or hop pellets were weighed out and the ISTD mixture as well as triethylamine (TEA) were added into 10 mL amber headspace vials containing 20 mg sand. For calibration, the analyte and ISTD mixtures were added to 70 mg sand. The function of the sand is to absorb the pipetted standards so that they do not interact with the glass. Compared to the assay developed by Reglitz et al.<sup>37</sup> using mercurated agarose gel followed by GC $\times$ GC-TOFMS analysis, the OFD-HS-SPME approach requires less manual handling with similar sensitivities.

### 5.1.3 Cysteinylated Aldehydes

The release of aldehydes from nonvolatile adducts (e.g., amino acids, proteins, sulfites) during beer aging is nowadays considered to be the primary source of increased aldehyde concentrations.<sup>131</sup> Gaining a deeper insight into the factors that influence the release of the bound staling aldehydes improve the flavor stability during aging. Therefore, as a first step, it is crucial to determine which bound precursors exist. However, the relevance of bound precursors, which were identified once, should also be critically considered and, if necessary, revised on the basis of more current research results.

In 2015, Baert et al.<sup>101</sup> first proposed a new type of bound aldehydes, namely 2-substituted 1,3-thiazolidine-4-carboxylic acids. In this study, a binding reaction between cysteine and (*E*)-2-nonenal as well as nonanal was observed in model solutions at pH values of 4.4, 5.2, and 6 and subsequent heat treatment at 50 °C for 1 hour. The binding behavior of (*E*)-2-nonenal to cysteine has been found to be pH dependent: Significantly more (*E*)-2-nonenal was bound to cysteine at pH 6. Based on the above results, this research group focused on 2-substituted 1,3-thiazolidine-4-carboxylic acids as aldehyde precursors in the following years.

Soon after, 2-(furan-2-yl)-1,3-thiazolidine-4-carboxylic acid (Cys-FUR) in fresh Pale Lager beers was identified and quantified for the first time by ultra performance LC coupled to photo diode array detector (UPLC-PDA) by Baert et al.<sup>132</sup> Although in the previous study<sup>101</sup> no significant decrease in the level of free furfural was detected in model solution at pH 4.4 after cysteine addition, which was also confirmed in the current study, an analytical assay was developed for this bound-state aldehyde in beer. Using external calibration in model solution (pH 4.4), 4.3-7.9 mg/L Cys-FUR was quantified in five fresh Pale Lager beers. This amount is relatively high considering that only about 20-60 µg/L of furfural was released from the same beers by 4-vinylpyridine (4VP) addition, although 4VP causes aldehyde release for both cysteine and bisulfide adducts. To achieve a more detailed insight into the quality of the UPLC-PDA assay used, it is worthwhile to take a critical look at the corresponding method validation, which, however, has only been published in the thesis of Baert.<sup>133</sup> According to the stated method validation results, the UPLC-PDA assay is valid with respect to the tested parameters such as linearity, sensitivity, limit of detection and quantification, repeatability precision, and trueness (%recovery). However, some aspects of calibration and method validation are worthy of critical consideration. For an external calibration procedure, as mentioned in the introduction, the composition of the sample and standard matrix must be as similar as possible for good accuracy.<sup>22</sup> The composition of the model solution (phosphate buffer, pH 4.4) and a complex matrix such as beer differ too much to exclude that matrix effects occur resulting in over- or underestimation. To prevent false results, a matrix-matched calibration or the standard addition method should be used. Unfortunately, the influence of possible matrix effects could not be excluded by the experimental design of the method validation. The %recovery was only determined in different spiked model solutions instead of spiked real beer samples. Furthermore, the calibration range used for method validation (0.1-46.2 mg/L) differs from that used later for quantification of beer samples (2-77 mg/L). It is not apparent why the calibration range was extended upward for results of 4.3-7.9 mg/L Cys-FUR, especially since the higher

concentrated calibration points have the greatest influence on the slope of calibration graphs and thus on the quantification. Due to the discrepancy between the determined Cys-FUR concentrations in the five beers and the amount of released furfural that was determined by OFD-HS-SPME-GC-MS and internal calibration with ISTDs in beer, it would have been advisable to verify the Cys-FUR quantification by a suitable calibration procedure as well as recovery testing and to examine more beers of different beer styles.

The next study by Baert et al.<sup>134</sup> showed that cysteine-spiked beer samples significantly reduce free furfural level in forced-aging beer samples, but at the same time 4VP addition to aged cysteine-spiked beers did not result in furfural release. Based upon the fact that the binding of free furfural to cysteine at pH 4.4 was also found to be almost non-existent<sup>132</sup> meant that cysteine had to react with other furfural precursors (e.g., Maillard intermediate reaction products) preventing furfural release. Therefore, it was hypothesized that during forced-aging furfural is formed mainly *de novo* from Maillard intermediates rather than being released from a bound state. This experiment therefore raises skepticism about the high impact of 2-substituted 1,3-thiazolidine-4-carboxylic acids on the release of some bound staling aldehydes during beer aging.

Bustillo Trueba et al.<sup>135</sup> followed up with a detailed investigation of the influence of pH 2, 4.4, 5.2, 6, and 9 in model solutions on the stability of various 2-substituted 1,3-thiazolidine-4-carboxylic acids using the same UPLC-PDA assay. The UPLC-PDA assay has been adapted to include besides Cys-FUR also cysteine-bound methional (2-(2-(methylthio)ethyl)thiazolidine-4-carboxylic acid, Cys-MET), benzaldehyde (2-phenylthiazolidine-4-carboxylic acid, Cys-BEN), 2-methylpropanal (2-isopropylthiazolidine-4-carboxylic acid, Cys-2MP), 2-methylbutanal (2-(secbutyl)thiazolidine-4-carboxylic acid, Cys-2MB), 3-methylbutanal (2-isobutylthiazolidine-4-carboxylic acid, Cys-3MB), phenylacetaldehyde (2-benzylthiazolidine-4-carboxylic acid, Cys-PAA), and hexanal (2-pentylthiazolidine-4-carboxylic acid, Cys-HEX). However, the sensitivity of the UPLC-PDA assay was found to be insufficient for some analytes (e.g., Cys-HEX), resulting in the investigation of only Cys-FUR, Cys-MET, and Cys-BEN. The pH dependence of the cysteine-bound state aldehydes was confirmed: In the model solution at pH 4.4, degradation of Cys-FUR, Cys-MET, and Cys-BEN to approximately 15%, 40%, and 5%, respectively, of the initial concentration of cysteine adducts was observed within 24 hours. Except at pH 9, the cysteine adducts were relatively stable (maximum 10% degradation over 24 h). The poor stability at pH 4.4 leads to further doubts

about the release of aldehydes from the cysteine-bound state over a longer period of time in the finished beer.

In 2019, with the development of a ultra high performance LC-MS (UHPLC-MS) assay, an analytical tool was created that has sufficient sensitivity to detect cysteine-bound aldehydes in the  $\mu\text{g/L}$  range.<sup>136</sup> Again, the external calibration was carried out in a buffer solution (Carmody) but this time at pH 9, due to the demonstrated good stability of the substances at alkaline pH.<sup>135</sup> Although the linear calibration range for Cys-FUR was 1-1000  $\mu\text{g/L}$ , being much lower compared to the UPLC-PDA assay (2-77 mg/L), Cys-FUR was not detected in the fresh beer samples. Cys-MET, Cys-2MP, Cys-2MB, Cys-3MB, Cys-PAA, and Cys-HEX were also determined in malt samples but not in finished beer. Considering the poor stability of cysteine-bound aldehydes at pH 4.4, this is in line with the expectations indicated by the previous studies. Of course, it would have been desirable that this method was applied to more than two beers. Even considering that in the study by Baert et al.<sup>132</sup> Pale Lager beers and in the current study top-fermented beers were analyzed, it is not probable that Cys-FUR concentrations in the mg/L are detected in the first beer selection and less than 1  $\mu\text{g/L}$  in the other.

In a recently published study by Bustillo Trueba et al.<sup>137</sup>, the evolution of free aldehydes and the corresponding cysteine-bound aldehydes was investigated from malt through mashing, wort boiling, fermentation, and maturation, to beer forced aged for three months. Results provided by the previously introduced UHPLC-MS assay show lower concentrations of cysteine-bound aldehydes in malt compared to samples taken at the beginning of mashing, which is contrary to the behavior of free aldehydes. These results indicate that free aldehydes are additionally bound to cysteine during mashing. A decrease of free and cysteinylated aldehydes was observed during the brewing process. Cys-2MP, Cys-3MB, and Cys-MET, for instance, were detected in concentrations up to 700 $\mu\text{g/L}$  in the first steps of wort production and decrease until the end of wort boiling at levels less than 10  $\mu\text{g/L}$ . Most of the cysteine-bound aldehydes were not detected during the following brewing steps until the fresh beer. In contrast to the free aldehydes, whose concentrations all increased in the forced aged beer samples, this behavior was observed only for Cys-2MB (up to 10  $\mu\text{g/L}$ ). The other cysteine-bound aldehydes remained constant or were below the LOD. This observation suggests that the increase of staling aldehydes during beer aging is not related to the release of the corresponding free aldehyde from 2-substituted 1,3-thiazolidine-4-carboxylic acids. Nevertheless, the formation of cysteine-bound aldehydes during malting is proven.

## 5.2 Analytical Aspects

### 5.2.1 Further Development of Hop-Derived Thiol Quantification

In *Publication C*, the conditions of six HS-SPME and MRM parameters were optimized to achieve a method sensitivity below the sensory threshold for 4MMP. For this purpose, GC-MS/MS had to be operated at the lowest technically achievable level of quantification. A conscious decision was made to develop a measurement method using the most widely used ionization mode, electron impact (EI). As already outlined in *Publication B*, the majority of volatile aroma compounds in brewery laboratories are analyzed in EI mode. Ion sources that can operate EI and negative chemical ionization (NCI) are not commonly available. In order to provide the presented method to a wider community without an ion source change being an obstacle for the use of the method, the performance of EI and NCI has not yet been compared. Although the OFD-HS-SPME-GC-NCI-MS approach of Mateo-Vivaracho et al.<sup>138</sup> does not meet the requirement for 4MMP analysis in beer, GC-NCI-MS/MS could be a promising further variant for the analysis of PFBBBr-derivatized thiols.

In contrast to EI, only negative ions are detected by NCI. Since not all sample compounds have high electron affinity, NCI offers a selective ionization. By introducing electron affinity using halogenated derivatization reagent, compounds without electronegative elements can benefit from this selective ionization. In NCI, low-energy electrons are formed by electron ionization of reagent gas molecules (e.g., methane, ammonia). By resonance electron capture, molecular ions are formed, while dissociative electron capture produces fragment ions. For NCI optimization, the impact of different reagent gases, ion source temperature, reagent gas flow rate, emission current, and ionization energy on the mass spectral pattern have to be evaluated.

The PFBBBr-derivatized thiols contain bromine atoms that are ideal for accepting electrons, thus becoming stable negative ions. Selective ionization of the analytes of interest can provide an improved signal-to-noise ratio, resulting in a higher sensitivity in the lower calibration range. For optimal method selectivity and sensitivity, characteristic and abundant fragment ions have to be selected for MRM transitions. As in the case of EI ionization, no common PFBBBr fragment ions should be selected for thiol identification and quantification. Since these ions are not only produced by the target thiols but also by all volatiles undergoing OFD with PFBBBr, possible overestimation by co-elution cannot be prevented. In a current research project, the factors

influencing the stability of thiols during beer aging in hoppy ales are being investigated. The goal is to achieve a better understanding of the causes of thiol degradation and to verify the effectiveness of appropriate countermeasures. Therefore, this research project will examine whether NCI can obtain an increase in sensitivity, which allows the smallest change in concentration (in the range around the LOQ) to be quantified. Even the smallest changes have a significant impact on the entire beer aroma due to the low odor thresholds. Especially with regard to the observed peak area decrease in the presented OFD-HS-SPME-GC-MS/MS method, the alternative ionization mode is well worth a detailed investigation.

### 5.2.2 HS-SPME – not the End of the Road yet

Microextraction techniques have great advantages over classical isolation methods such as SDE, SPE, LLE, or SAFE. They do not require large sample volumes or solvents, they could be automatable, and the sample preparation requires minimal manual handling and is less time consuming. Especially in view of the fact that aroma compounds are prone to possible oxidation processes and adduct formation during isolation and enrichment of the target analytes, fast sample preparations without long thermal exposure are to be preferred. HS-SPME approaches to chromatographic analysis have experienced rapid development and growth in many application areas since its introduction. Consequently, (OFD-)HS-SPME techniques have been also applied to the analysis of a wide range of malting and brewing related analytes.<sup>25,28,71,139</sup>

In *Publication A* and *B*, it was shown that common SPME-related drawbacks (e.g., short fiber-lifetimes, poor calibration consistency and long-term stability) have been overcome using MRM mode and suitable ISTDs. Nevertheless, there is no doubt that HS-SPME approaches will be replaced by improved automated microextraction techniques in the future. However, this requires that the newly developed techniques first be made available to a broad mass of scientists because the lack of technical equipment hinders a widespread use of new extraction techniques. Since there is no universal sample preparation, optimizations of the new analytical approaches have to be elaborated and published for each new application area in order to find broad acceptance among users. Therefore, the prerequisite is that the corresponding hardware and software is included in the portfolio of established instrument manufacturers. It often takes many years before a new technology can establish itself as state of the art over conventional techniques.

SPME Arrow, already available as an option when purchasing new GC-MS or GC-MS/MS systems, could be a promising improvement of SPME approaches in beer flavor analysis. Unfortunately, not all existing GC and autosampler systems can be equipped with a SPME Arrow unit, because a special SPME Arrow holder as well as the modification of the GC injection port is necessary due to the larger external diameter. As mentioned in the introduction, SPME Arrow with its higher sorption phase volume can provide an improvement for ultra-trace analysis (e.g., thiols). In addition, SPME Arrow could isolate and enrich target analytes to a level that can be detected by less sensitive instruments, so that, for instance, GC-MS could be used instead of GC-MS/MS. In the future, appropriate studies comparing the method performance of HS-SPME and SPME Arrow extraction have to be conducted to identify beneficial SPME Arrow application in beer flavor analysis. During these studies, it has also to be examined whether the currently twice as high acquisition costs compared to conventional SPME fibers are amortized by extended SPME Arrow lifetimes.

In conclusion, this thesis has presented powerful analytical tools to improve instrumental flavor stability analysis. Using the presented HS-SPME-GC-MS/MS assays, the required sensitivity for low analyte thresholds as well as for minor concentration changes in various beer matrices could be reliably quantified over a long period of time. By continued research using the analytical assays, unexplored factors or reactions regarding the decrease of desired hop aroma compounds or the increase of off-flavors could be identified. In addition, the assays expand the monitoring of beer flavor and flavor stability even further for improved batch-to-batch consistency. Finally, this work contributes with another small piece to the key quality feature, a consistent and stable beer flavor.

## References

1. Bamforth, CW. Beer: An Ancient Yet Modern Biotechnology. *Chem. Educator* 5(3), 102–112, 2000.
2. Lafontaine, S; Senn, K; Knoke, L; Schubert, C; Dennenlöhner, J; Maxminer, J; Cantu, A; Rettberg, N; Heymann, H. Evaluating the Chemical Components and Flavor Characteristics Responsible for Triggering the Perception of “Beer Flavor” in Non-Alcoholic Beer. *Foods* 9(12), 1914, 2020.
3. Hill, AE. Microbiological stability of beer. In: Bamforth CW, editor. Beer: A Quality Perspective, 1st edn. Burlington, MA, USA: Academic Press, 2009. pp. 163–183.
4. Sakamoto, K; Konings, WN. Beer spoilage bacteria and hop resistance. *Int. J. Food Microbiol.* 89, 105–124, 2003.
5. Hill, AE; Priest, FG. Microbiology and Microbiological Control in the Brewery. In: Stewart GG, Russel I, Anstruther A, editors. Handbook of Brewing, 3rd edn. Boca Raton, FL, USA: CRC Press, 2017. pp. 529–545.
6. Haikara, A; Mattila-Sandholm, T; Manninen, M. Rapid Detection of Contaminants in Pitching Yeast Using Automated Turbidometry. *J. Am. Soc. Brew. Chem.* 48(3), 92–95, 1990.
7. Suzuki, K; Iijima, K; Yamashita, H. Study on ATP Production of Lactic Acid Bacteria in Beer and Development of a Rapid Pre-Screening Method for Beer-Spoilage Bacteria. *J. Inst. Brew.* 111(3), 328–335, 2005.
8. Koivula, TT; Juvonen, R; Haikara, A; Suihko, M. Characterization of the brewery spoilage bacterium *Obesumbacterium proteus* by automated ribotyping and development of PCR methods for its biotype 1. *J. Appl. Microbiol.* 100(2), 398–406, 2006.
9. Leiper, KA; Miedl, M. Colloidal stability of beer. In: Bamforth CW, editor. Beer: A Quality Perspective, 1st edn. Burlington, MA, USA: Academic Press, 2009. pp. 111–161.
10. Gorinstein, S; Moshe, R; Wolfe, FH; Berliner, M; Rotenstreich, A; Tilis, K. Characterization of stabilized and unstabilized beers. *J. Food Biochem.* 14, 161–172, 1990.
11. Evans, DE; Robinson, LH; Sheehan, MC; Tolhurst, RL; Hill, A; Skerritt, JS; Barr, AR. Application of Immunological Methods to Differentiate between Foam-Positive and Haze-Active Proteins Originating from Malt. *J. Am. Soc. Brew. Chem.* 61(2), 55–62, 2003.
12. Evans, DE; Bamforth, CW. Beer foam: achieving a suitable head. In: Bamforth CW, editor. Beer: A Quality Perspective, 1st edn. Burlington, MA, USA: Academic Press, 2009. pp. 1–60.
13. Todd, PH; Held, RW; Guzinski, JG. The Development and Use of Modified Hop Extracts in the Art of Brewing. *Tech. Q. Master Brew. Assoc. Am.* 33(2), 91–95, 1996.
14. Asano, K; Hashimoto, N. Isolation and Characterization of Foaming Proteins of Beer. *J. Am. Soc. Brew. Chem.* 38(4), 129–137, 1980.

15. Biendl, M; Engelhard, B; Forster, A; Gahr, A; Lutz, A; Mitter, W; Schmidt, R; Schönberger, C. Hopfen: Vom Anbau bis zum Bier, 1st edn., Nürnberg, Germany: Fachverlag Hans Carl, 2012.
16. Hughes, P. Beer flavor. In: Bamforth CW, editor. Beer: A Quality Perspective, 1st edn. Burlington, MA, USA: Academic Press, 2009. pp. 61–83.
17. Narziß, L; Back, W. Die Bierbrauerei: Band 2: Die Technologie der Würzebereitung, 8th edn., Weinheim, Germany: Wiley-VCH Verlag GmbH & Co. KGaA, 2009.
18. Roberts, MT; Dufour, J; Lewis, AC. Application of comprehensive multidimensional gas chromatography combined with time-of-flight mass spectrometry (GC×GC-TOFMS) for high resolution analysis of hop essential oil. *J. Sep. Sci.* 27(5-6), 473–478, 2004.
19. Hanke, S; Herrmann, M; Back, W; Becker, T; Krottenthaler, M. Synergistic and Suppression Effects of Flavour Compounds in Beer. 32nd European Brewery Convention Congress, Hamburg, Germany, 2009.
20. Takoi, K; Itoga, Y; Koie, K; Kosugi, T; Shimase, M; Katayama, Y; Nakayama, Y; Watari, J. The Contribution of Geraniol Metabolism to the Citrus Flavour of Beer: Synergy of Geraniol and  $\beta$ -Citronellol Under Coexistence with Excess Linalool. *J. Inst. Brew.* 116(3), 251–260, 2010.
21. Sharpe, FR; Laws, DRJ. The essential oil of hops - A review. *J. Inst. Brew.* 87(2), 99–107, 1981.
22. Rettberg, N; Biendl, M; Garbe, L. Hop Aroma and Hoppy Beer Flavor: Chemical Backgrounds and Analytical Tools-A Review. *J. Am. Soc. Brew. Chem.* 76(1), 1–20, 2018.
23. Eyres, G; Dulfour, J. Hop essential oil: Analysis, chemical composition and odor characteristics. In: Preedy VR, editor. Beer in Health and Disease Prevention, 1st edn. London, UK: Academic Press, 2009. pp. 239–254.
24. Steinhaus, M; Schieberle, P. Comparison of the Most Odor-Active Compounds in Fresh and Dried Hop Cones (*Humulus lupulus* L. Variety Spalter Select) Based on GC-Olfactometry and Odor Dilution Techniques. *J. Agric. Food Chem.* 48(5), 1776–1783, 2000.
25. Takoi, K; Tokita, K; Sanekata, A; Usami, Y; Itoga, Y; Koie, K; Matsumoto, I; Nakayama, Y. Varietal Difference of Hop-Derived Flavour Compounds in Late-Hopped/Dry-Hopped Beers. *BrewingSci.* 69(1/2), 1–7, 2016.
26. Rettberg, N; Schubert, C; Dennenlöhner, J; Thörner, S; Knoke, L; Maxminer, J. Instability of Hop-Derived 2-Methylbutyl Isobutyrate during Aging of Commercial Pasteurized and Unpasteurized Ales. *J. Am. Soc. Brew. Chem.* 78(3), 175–184, 2020.
27. Lermusieau, G; Bulens, M; Collin, S. Use of GC-Olfactometry to Identify the Hop Aromatic Compounds in Beer. *J. Agric. Food Chem.* 49(8), 3867–3874, 2001.
28. Steinhaus, M; Fritsch, HT; Schieberle, P. Quantitation of (R)- and (S)-Linalool in Beer Using Solid Phase Microextraction (SPME) in Combination with a Stable Isotope Dilution Assay (SIDA). *J. Agric. Food Chem.* 51(24), 7100–7105, 2003.

29. Fritsch, HT; Schieberle, P. Identification Based on Quantitative Measurements and Aroma Recombination of the Character Impact Odorants in a Bavarian Pilsner-type Beer. *J. Agric. Food Chem.* 53(19), 7544–7551, 2005.
30. Sakuma, S; Hayashi, S; Kobayashi, K. Analytical Methods for Beer Flavor Control. *J. Am. Soc. Brew. Chem.* 49(1), 1–3, 1991.
31. Kaltner, D. Untersuchungen zur Ausbildung des Hopfenaromas und technologische Maßnahmen zur Erzeugung hopfenaromatischer Biere. Thesis. Technische Universität München, München, Germany, 2000.
32. Hanke, S; Becker, T. Influence of Hop Volatiles on Perception of Hop Aroma. 33rd European Brewery Convention Congress, Glasgow, UK, 2011.
33. King, AJ; Dickinson, R. Biotransformation of hop aroma terpenoids by ale and lager yeasts. *FEMS Yeast Res.* 3, 53–62, 2003.
34. Peppard, TL. Volatile organosulphur compounds in hops and hop oils: a review. *J. Inst. Brew.* 87(6), 376–385, 1981.
35. Kishimoto, T; Wanikawa, A; Kono, K; Shibata, K. Comparison of the Odor-Active Compounds in Unhopped Beer and Beers Hopped with Different Hop Varieties. *J. Agric. Food Chem.* 54(23), 8855–8861, 2006.
36. Kishimoto, T; Kobayashi, M; Yako, N; Iida, A; Wanikawa, A. Comparison of 4-Mercapto-4-methylpentan-2-one Contents in Hop Cultivars from Different Growing Regions. *J. Agric. Food Chem.* 56(3), 1051–1057, 2008.
37. Reglitz, K; Steinhaus, M. Quantitation of 4-Methyl-4-sulfanylpentan-2-one (4MSP) in Hops by a Stable Isotope Dilution Assay in Combination with GC×GC-TOFMS: Method Development and Application To Study the Influence of Variety, Provenance, Harvest Year, and Processing on 4MSP Concentrations. *J. Agric. Food Chem.* 65(11), 2364–2372, 2017.
38. Kishimoto, T; Morimoto, M; Kobayashi, M; Yako, N; Wanikawa, A. Behaviors of 3-Mercaptohexan-1-ol and 3-Mercaptohexyl Acetate During Brewing Processes. *J. Am. Soc. Brew. Chem.* 66(3), 192–196, 2008.
39. Swiegers, JH; Capone, DL; Pardon, KH; Elsey, GM; Sefton, MA; Francis, IL; Pretorius, IS. Engineering volatile thiol release in *Saccharomyces cerevisiae* for improved wine aroma. *Yeast* 24(7), 561–574, 2007.
40. Lafontaine, S; Varnum, S; Roland, A; Delpech, S; Dagan, L; Vollmer, DM; Kishimoto, T; Shellhammer, TH. Impact of harvest maturity on the aroma characteristics and chemistry of Cascade hops used for dry-hopping. *Food Chem.* 278, 228–239, 2019.
41. Bailey, B; Schönberger, C; Drexler, G; Gahr, A; Newman, R; Pöschl, M; Geiger, E. The Influence of Hop Harvest Date on Hop Aroma in Dry-Hopped Beers. *MBAA TQ* (online). doi: 10.1094/TQ-46-2-0409-01, 2009.
42. Sharp, DC; Qian, Y; Shellhammer, G; Shellhammer, TH. Contributions of Select Hopping Regimes to the Terpenoid Content and Hop Aroma Profile of Ale and Lager Beers. *J. Am. Soc. Brew. Chem.* 75(2), 93–100, 2017.

43. Haseleu, G; Intelmann, D; Hofmann, T. Identification and RP-HPLC-ESI-MS/MS Quantitation of Bitter-Tasting  $\beta$ -Acid Transformation Products in Beer. *J. Agric. Food Chem.* 57(16), 7480–7489, 2009.
44. Kishimoto, T; Wanikawa, A; Kagami, N; Kawatsura, K. Analysis of Hop-Derived Terpenoids in Beer and Evaluation of Their Behavior Using the Stir Bar-Sorptive Extraction Method with GC-MS. *J. Agric. Food Chem.* 53(12), 4701–4707, 2005.
45. Lafontaine, S; Shellhammer, TH. How Hoppy Beer Production Has Redefined Hop Quality and a Discussion of Agricultural and Processing Strategies to Promote It. *Tech. Q. Master Brew. Assoc. Am.* 56(1), 1–12, 2019.
46. Shellhammer, TH; Lafontaine, S; Sharp, DC; Wolfe, PH. Controlling Dry-Hop Aroma and Flavor in Beer. In: Shellhammer TH, Lafontaine S, editors. Hop Flavor and Aroma: Proceedings of the 2nd International Brewers Symposium, 1st edn. St. Paul, MN, USA: ASBC-MBAA, 2020. pp. 155–183.
47. Saison, D; Schutter, DP de; Uyttenhove, B; Delvaux, F; Delvaux, FR. Contribution of staling compounds to the aged flavour of lager beer by studying their flavour thresholds. *Food Chem.* 114(4), 1206–1215, 2009.
48. Schubert, C; Dennenlöhner, J; Thörner, S; Maxminer, J; Rettberg, N. The contribution of staling aldehydes to the flavor (in)stability of top fermented, hoppy beers. 37th Congress of the European Brewery Convention, Antwerp, Belgium, 2019.
49. Vanderhaegen, B; Neven, H; Verachtert, H; Derdelinckx, G. The chemistry of beer aging – a critical review. *Food Chem.* 95(3), 357–381, 2006.
50. Baert, JJ; Clippeleer, J de; Hughes, PS; Cooman, L de; Aerts, G. On the Origin of Free and Bound Staling Aldehydes in Beer. *J. Agric. Food Chem.* 60(46), 11449–11472, 2012.
51. Madigan, D; Perez, A; Clements, M. Furanic Aldehyde Analysis by HPLC as a Method to Determine Heat-Induced Flavor Damage to Beer. *J. Am. Soc. Brew. Chem.* 56(4), 146–151, 1998.
52. Bettenhausen, HM; Benson, A; Fisk, S; Herb, D; Hernandez, J; Lim, J; Queisser, SH; Shellhammer, TH; Vega, V; Yao, L; Heuberger, AL; Hayes, PM. Variation in Sensory Attributes and Volatile Compounds in Beers Brewed from Genetically Distinct Malts: An Integrated Sensory and Non-Targeted Metabolomics Approach. *J. Am. Soc. Brew. Chem.* 78(2), 136–152, 2020.
53. Heuberger, AL; Broeckling, CD; Lewis, MR; Salazar, L; Bouckaert, P; Prenni, JE. Metabolomic profiling of beer reveals effect of temperature on non-volatile small molecules during short-term storage. *Food Chem.* 135(3), 1284–1289, 2012.
54. Heuberger, AL; Broeckling, CD; Sedin, D; Holbrook, C; Barr, L; Kirkpatrick, K; Prenni, JE. Evaluation of non-volatile metabolites in beer stored at high temperature and utility as an accelerated method to predict flavour stability. *Food Chem.* 200, 301–307, 2016.

55. Spevacek, AR; Benson, KH; Bamforth, CW; Slupsky, CM. Beer metabolomics: molecular details of the brewing process and the differential effects of late and dry hopping on yeast purine metabolism. *J. Inst. Brew.* 122(1), 21–28, 2016.
56. Marin, AB; Acree, TE; Barnard, J. Variation in odor detection thresholds determined by charm analysis. *Chem. Senses* 13(3), 435–444, 1988.
57. Langos, D; Granvogl, M; Schieberle, P. Characterization of the Key Aroma Compounds in Two Bavarian Wheat Beers by Means of the Sensomics Approach. *J. Agric. Food Chem.* 61(47), 11303–11311, 2013.
58. Schieberle, P. Primary odorants of pale lager beer: Differences to other beers and changes during storage. *Z. Lebensm. Unters. Forsch.* 193, 558–565, 1991.
59. Meilgaard, MC. Flavor Chemistry of Beer: Part II: Flavour and Threshold of 239 Aroma Volatiles. *Tech. Q. Master Brew. Assoc. Am.* 12(3), 151–168, 1975.
60. Meilgaard, MC. Prediction of Flavor Differences between Beers from Their Chemical Composition. *J. Agric. Food Chem.* 30(6), 1009–1017, 1982.
61. Rettberg, N. Instrumental Analysis of Hop Aroma in Beer: The Challenges of Transforming a Research Application into a QC Tool. In: Shellhammer TH, Lafontaine S, editors. Hop Flavor and Aroma: Proceedings of the 2nd International Brewers Symposium, 1st edn. St. Paul, MN, USA: ASBC-MBAA, 2020. pp. 11–24.
62. Likens, ST; Nickerson, GB. Detection of Certain Hop Oil Constituents in Brewing Products. *Proc. Am. Soc. Brew. Chem.* 22(1), 5–13, 1964.
63. Irwin, AJ; Thompson, DJ. A rapid method for the extraction and analysis of beer flavour components. *J. Inst. Brew.* 93, 113–115, 1987.
64. Battistutta, F; Bulatti, S; Zenarola, C; Zironi, R. Rapid Analysis of Free Medium-Chain Fatty Acids and Related Ethyl Esters in Beer using SPE and HRGC. *J. High Resolut. Chromatogr.* 17(9), 662–664, 1994.
65. Buiatti, S; Battistutta, F; Celotti, E; Zironi, R. Evaluation of Beer Flavor Compounds by Liquid-Liquid Extraction and GC/MS Analysis. *Tech. Q. Master Brew. Assoc. Am.* 34(4), 243–245, 1997.
66. Engel, W; Bahr, W; Schieberle, P. Solvent assisted flavour evaporation – a new and versatile technique for the careful and direct isolation of aroma compounds from complex food matrices. *Eur. Food Res. Technol.* 209, 237–241, 1999.
67. Kremser, A. Advances in Automated Sample Preparation for Gas Chromatography: Solid-Phase Microextraction, Headspace-Analysis, Solid-Phase Extraction. Thesis. Universität Duisburg-Essen, Duisburg/Essen, Germany, 2016.
68. Schmidt, C; Biendl, M. Headspace Trap GC-MS analysis of hop aroma compounds in beer. *BrewingSci.* 69(1/2), 9–15, 2016.
69. Vanderhaegen, B; Derdelinckx, G. Characterization of flavour compounds in fresh and aged beer by purge and trap-gas chromatography-mass spectrometry. *BrewingSci.* 58(11/12), 1–9, 2005.

70. Saison, D; Schutter, DP de; Delvaux, F; Delvaux, FR. Optimisation of a complete method for the analysis of volatiles involved in the flavour stability of beer by solid-phase microextraction in combination with gas chromatography and mass spectrometry. *J. Chromatogr. A* 1190(1-2), 342–349, 2008.
71. Ortiz, RM. Analysis of Selected Aldehydes in Packaged Beer by Solid-Phase Microextraction (SPME)–Gas Chromatography (GC)–Negative Chemical Ionization Mass Spectrometry (NCIMS). *J. Am. Soc. Brew. Chem.* 73(3), 266–274, 2015.
72. Belardi, RP; Pawliszyn, JB. The Application of Chemically Modified Fused Silica Fibers in the Extraction of Organics from Water Matrix Samples and their Rapid Transfer to Capillary Columns. *Water Qual. Res. J. Can.* 24(1), 179–191, 1989.
73. Hao, J; Dong, J; Yin, H; Yan, P; Ting, PL; Li, Q; Tao, X; Yu, J; Chen, H; Li, M. Optimum Method of Analyzing Hop Derived Aroma Compounds in Beer by Headspace Solid-Phase Microextraction (SPME) with GC/MS and Their Evolutions during Chinese Lager Brewing Process. *J. Am. Soc. Brew. Chem.* 72(4), 261–270, 2014.
74. Gonçalves, J; Figueira, J; Rodrigues, F; Câmara, JS. Headspace solid-phase microextraction combined with mass spectrometry as a powerful analytical tool for profiling the terpenoid metabolomic pattern of hop-essential oil derived from Saaz variety. *J. Sep. Sci.* 35, 2282–2296, 2012.
75. Stashenko, EE; Martínez, JR. Sampling volatile compounds from natural products with headspace/solid-phase micro-extraction. *J. Biochem. Biophys. Methods.* 70(2), 235–242, 2007.
76. Risticvic, S; Lord, H; Górecki, T; Arthur, CL; Pawliszyn, JB. Protocol for solid-phase microextraction method development. *Nat. Protoc.* 5(1), 122–139, 2010.
77. Baltussen, E; Sandra, P; David, F; Cramers, C. Stir Bar Sorptive Extraction (SBSE), a Novel Extraction Technique for Aqueous Samples: Theory and Principles. *J. Microcolumn Sep.* 11(10), 737–747, 1999.
78. Ochiai, N; Sasamoto, K; Kishimoto, T. Development of a Method for the Quantitation of Three Thiols in Beer, Hop, and Wort Samples by Stir Bar Sorptive Extraction with in Situ Derivatization and Thermal Desorption–Gas Chromatography–Tandem Mass Spectrometry. *J. Agric. Food Chem.* 63(30), 6698–6706, 2015.
79. Eisert, R; Pawliszyn, JB. Automated In-Tube Solid-Phase Microextraction Coupled to High-Performance Liquid Chromatography. *Anal. Chem.* 69(16), 3140–3147, 1997.
80. Lipinski, J. Automated solid phase dynamic extraction – Extraction of organics using a wall coated syringe needle. *Fresenius J. Anal. Chem.* 369, 57–62, 2001.
81. Jochmann, MA; Yuan, X; Schilling, B; Schmidt, TC. In-tube extraction for enrichment of volatile organic hydrocarbons from aqueous samples. *J. Chromatogr. A* 1179(2), 96–105, 2008.

82. Kremser, A; Jochmann, MA; Schmidt, TC. PAL SPME Arrow—evaluation of a novel solid-phase microextraction device for freely dissolved PAHs in water. *Anal. Bioanal. Chem.* 408, 943–952, 2016.
83. Castro, LF; Ross, CF; Vixie, KR. Optimization of a Solid Phase Dynamic Extraction (SPDE) Method for Beer Volatile Profiling. *Food Anal. Methods* 8, 2115–2124, 2015.
84. Zapata, J; Mateo-Vivaracho, L; Lopez, R; Ferreira, V. Automated and quantitative headspace in-tube extraction for the accurate determination of highly volatile compounds from wines and beers. *J. Chromatogr. A* 1230, 1–7, 2012.
85. Herrington, JS; Gómez-Ríos, GA; Myers, C; Stidsen, G; Bell, DS. Hunting Molecules in Complex Matrices with SPME Arrows: A Review. *Separations* 7, 12, 2020.
86. Westland, J. SPME Arrow Sampling of Terpenes in Cannabis Plant Material, 2019. <https://www.agilent.com/cs/library/applications/application-spme-arrow-sampling-of-terpenes-in-cannabis-plant-material-5994-1046en-agilent.pdf>. Accessed 6 November 2020.
87. Lee, J; Kim, WS; Lee, Y; Choi, Y; Choi, H; Jang, HW. Solid-phase microextraction Arrow for the volatile organic compounds in soy sauce. *J. Sep. Sci.* 42(18), 2942–2948, 2019.
88. Nam, TG; Lee, J; Kim, B; Song, N; Jang, HW. Analyzing volatiles in brown rice vinegar by headspace solid-phase microextraction (SPME)–Arrow: Optimizing the extraction conditions and comparisons with conventional SPME. *Int. J. Food Prop.* 22(1), 1195–1204, 2019.
89. Song, N; Lee, J; Lee, Y; Park, J; Jang, HW. Comparison of headspace–SPME and SPME–Arrow–GC–MS methods for the determination of volatile compounds in Korean salt–fermented fish sauce. *Appl. Biol. Chem.* 62(16), 2019.
90. Vichi, S; Cortés-Francisco, N; Caixach, J. Analysis of volatile thiols in alcoholic beverages by simultaneous derivatization/extraction and liquid chromatography-high resolution mass spectrometry. *Food Chem.* 175, 401–408, 2015.
91. Jiang, W; Wang, D; Wu, Y; Lin, Z; Wang, L; Wang, L; Huangfu, J; Pavlovic, M; Dostalek, P. Analysis of Monoterpenol Isomers in Hops and Beers: Comparison of Methods with a Chiral Column and a Nonchiral Column. *J. Am. Soc. Brew. Chem.* 75(2), 149–155, 2017.
92. Silva, GC da; Silva, AAS da; Silva, LSN da; Godoy, Ronoel Luiz de O; Nogueira, LC; Quitério, SL; Raices, Renata S L. Method development by GC-ECD and HS-SPME-GC-MS for beer volatile analysis. *Food Chem.* 167, 71–77, 2015.
93. Hengel, MJ; Miller, M. Analysis of Pesticides in Dried Hops by Liquid Chromatography–Tandem Mass Spectrometry. *J. Agric. Food Chem.* 56(16), 6851–6856, 2008.
94. Schmidt, C; Biendl, M; Lagemann, A; Stettner, G; Vogt, C; Dunkel, A; Hofmann, T. Influence of Different Hop Products on the cis/trans Ratio of Iso- $\alpha$ -Acids in Beer and Changes in Key Aroma and Bitter Taste Molecules during Beer Ageing. *J. Am. Soc. Brew. Chem.* 72(2), 116–125, 2014.

95. Reglitz, K; Lemke, S; Hanke, S; Steinhaus, M. On the Behaviour of the Important Hop Odorant 4-Mercapto-4-methylpentan-2-one (4MMP) during Dry Hopping and during Storage of Dry Hopped Beer. *BrewingSci.* 71(11/12), 96–99, 2018.
96. Garbe, L; Rettberg, N. The Power of Stable Isotope Dilution Assays in Brewing. *BrewingSci.* 64(11/12), 140–150, 2011.
97. Francis, MJO; Allcock, C. Geraniol  $\beta$ -d-glucoside: Occurrence and synthesis in rose flowers. *Phytochemistry* 8(8), 1339–1347, 1969.
98. Williams, PJ; Cynkar, W; Francis, IL; Gray, JD; Iland, PG; Coombe, BG. Quantification of Glycosides in Grapes, Juices, and Wines through a Determination of Glycosyl Glucose. *J. Agric. Food Chem.* 43(1), 121–128, 1995.
99. Tominaga, T; Dubourdieu, D. Identification of Cysteinylated Aroma Precursors of Certain Volatile Thiols in Passion Fruit Juice. *J. Agric. Food Chem.* 48(7), 2874–2876, 2000.
100. Goldstein, H; Ting, P; Navarro, A; Ryder, D. Water-soluble hop flavor precursors and their role in beer flavor. *Proc. Congr. Eur. Brew. Conv.* 27, 53–62, 1999.
101. Baert, JJ; Clippeleer, J de; Cooman, L de; Aerts, G. Exploring the Binding Behavior of Beer Staling Aldehydes in Model Systems. *J. Am. Soc. Brew. Chem.* 73(1), 100–108, 2015.
102. Rivas, F; Parra, A; Martinez, A; Garcia-Granados, A. Enzymatic glycosylation of terpenoids. *Phytochem. Rev.* 12(2), 327–339, 2013.
103. Schwab, W; Fischer, T; Wüst, M. Terpene glucoside production: Improved biocatalytic processes using glycosyltransferases. *Eng. Life Sci.* 15(4), 376–386, 2015.
104. Kollmannsberger, H; Biendl, M; Nitz, S. Occurrence of glycosidically bound flavour compounds in hops, hop products and beer. *BrewingSci.* 59(5/6), 83–89, 2006.
105. Kankolongo Cibaka, ML; Ferreira, CS; Decourrière, L; Lorenzo-Alonso, CJ; Bodart, E; Collin, S. Dry Hopping with the Dual-Purpose Varieties Amarillo, Citra, Hallertau Blanc, Mosaic, and Sorachi Ace: Minor Contribution of Hop Terpenol Glucosides to Beer Flavors. *J. Am. Soc. Brew. Chem.* 75(2), 122–129, 2017.
106. Takoi, K; Itoga, Y; Koie, K; Takayanagi, J; Kaneko, T; Watanabe, T; Matsumoto, I; Nomura, M. Systematic Analysis of Behaviour of Hop-Derived Monoterpene Alcohols During Fermentation and New Classification of Geraniol-Rich Flavour Hops. *BrewingSci.* 70(11/12), 177–186, 2017.
107. Sharp, DC; Vollmer, DM; Qian, Y; Shellhammer, TH. Examination of Glycoside Hydrolysis Methods for the Determination of Terpenyl Glycoside Contents of Different Hop Cultivars. *J. Am. Soc. Brew. Chem.* 75(2), 101–108, 2017.
108. Daenen, L; Saison, D; Sterckx, F; Delvaux, FR; Verachtert, H; Derdelinckx, G. Screening and evaluation of the glucoside hydrolase activity in *Saccharomyces* and *Brettanomyces* brewing yeasts. *J. Appl. Microbiol.* 104(2), 478–488, 2008.
109. Lafontaine, S; Shellhammer, TH. Investigating the Factors Impacting Aroma, Flavor, and Stability in Dry-Hopped Beers. *Tech. Q. Master Brew. Assoc. Am.* 56(1), 13–23, 2019.

110. Morcol, TB; Negrin, A; Matthews, PD; Kennelly, EJ. Hop (*Humulus lupulus* L.) terroir has large effect on a glycosylated green leaf volatile but not on other aroma glycosides. *Food Chem.* 321, 126644, 2020.
111. Ugliano, M; Bartowsky, EJ; McCarthy, J; Moio, L; Henschke, PA. Hydrolysis and Transformation of Grape Glycosidically Bound Volatile Compounds during Fermentation with Three *Saccharomyces* Yeast Strains. *J. Agric. Food Chem.* 54(17), 6322–6331, 2006.
112. Boido, E; Fariña, L; Carrau, F; Dellacassa, E; Cozzolino, D. Characterization of Glycosylated Aroma Compounds in Tannat Grapes and Feasibility of the Near Infrared Spectroscopy Application for Their Prediction. *Food Anal. Methods* 6(1), 100–111, 2013.
113. Williams, PJ; Strauss, CR; Wilson, B; Massy-Westropp, RA. Use of C18 reversed-phase liquid chromatography for the isolation of monoterpene glycosides and nor-isoprenoid precursors from grape juice and wines. *J. Chromatogr. A* 235(2), 471–480, 1982.
114. Chevance, F; Guyot-Declerck, C; Dupont, J; Collin, S. Investigation of the  $\beta$ -Damascenone Level in Fresh and Aged Commercial Beers. *J. Agric. Food Chem.* 50(13), 3818–3821, 2002.
115. Hampel, D; Robinson, AL; Johnson, AJ; Ebeler, SE. Direct hydrolysis and analysis of glycosidically bound aroma compounds in grapes and wines: comparison of hydrolysis conditions and sample preparation methods. *Aust. J. Grape Wine Res.* 20(3), 361–377, 2014.
116. Gros, J; Peeters, F; Collin, S. Occurrence of Odorant Polyfunctional Thiols in Beers Hopped with Different Cultivars. First Evidence of an S-Cysteine Conjugate in Hop (*Humulus lupulus* L.). *J. Agric. Food Chem.* 60(32), 7805–7816, 2012.
117. Roland, A; Viel, C; Reillon, F; Delpech, S; Boivin, P; Schneider, R; Dagan, L. First identification and quantification of glutathionylated and cysteinylated precursors of 3-mercaptohexan-1-ol and 4-methyl-4-mercaptopentan-2-one in hops (*Humulus lupulus*). *Flavour Fragr. J.* 31(6), 455–463, 2016.
118. Roland, A; Delpech, S; Viel, C; Reillon, F; Schneider, R; Dagan, L. First evidence of cysteinylated and glutathionylated precursors of 3-mercaptohexan-1-ol in malts: Toward a better aromatic potential management? World Brewing Congress, Denver, CO, USA, 2016.
119. Tran, TTH; Kankolongo Cibaka, ML; Collin, S. Polyfunctional Thiols in Fresh and Aged Belgian Special Beers: Fate of Hop S-Cysteine Conjugates. *J. Am. Soc. Brew. Chem.* 73(1), 61–70, 2015.
120. Capone, DL; Pardon, KH; Cordente, AG; Jeffery, DW. Identification and Quantitation of 3-S-Cysteinylglycinehexan-1-ol (Cysgly-3-MH) in Sauvignon blanc Grape Juice by HPLC-MS/MS. *J. Agric. Food Chem.* 59(20), 11204–11210, 2011.
121. Bonnaffoux, H; Roland, A; Rémond, E; Delpech, S; Schneider, R; Cavelier, F. First identification and quantification of S-3-(hexan-1-ol)- $\gamma$ -glutamyl-cysteine in grape must as a potential thiol precursor, using UPLC-MS/MS analysis and stable isotope dilution assay. *Food Chem.* 237, 877–886, 2017.
122. Delpech, S; Bonnaffoux, H; Cavelier, F; Dagan, L. Identification of new odorless thiol precursors in hops and malts. Brewing Summit, San Diego, CA, USA, 2018.

123. Gros, J; Tran, TTH; Collin, S. Enzymatic release of odourant polyfunctional thiols from cysteine conjugates in hop. *J. Inst. Brew.* 119(4), 221–227, 2013.
124. Kankolongo Cibaka, ML; Gros, J; Nizet, S; Collin, S. Quantitation of Selected Terpenoids and Mercaptans in the Dual-Purpose Hop Varieties Amarillo, Citra, Hallertau Blanc, Mosaic, and Sorachi Ace. *J. Agric. Food Chem.* 63(11), 3022–3030, 2015.
125. Kankolongo Cibaka, ML; Decourrière, L; Lorenzo-Alonso, C; Bodart, E; Robiette, R; Collin, S. 3-Sulfanyl-4-methylpentan-1-ol in Dry-Hopped Beers: First Evidence of Glutathione S - Conjugates in Hop (*Humulus lupulus* L.). *J. Agric. Food Chem.* 64(45), 8572–8582, 2016.
126. Chenot, C; Collin, S. Ability of the Mandarina Bavaria hop variety to release free odorant polyfunctional thiols in late-hopped beers. *J. Inst. Brew.* 127(2), 140–148, 2021.
127. Nizet, S; Gros, J; Peeters, F; Chaumont, S; Robiette, R; Collin, S. First Evidence of the Production of Odorant Polyfunctional Thiols by Bottle Refermentation. *J. Am. Soc. Brew. Chem.* 71(1), 15–22, 2013.
128. Roland, A; Delpech, S; Dagan, L. How to Monitor Positive Aromatic Thiols During Winemaking and Brewing. In: Shellhammer TH, Lafontaine S, editors. Hop Flavor and Aroma: Proceedings of the 2nd International Brewers Symposium, 1st edn. St. Paul, MN, USA: ASBC-MBAA, 2020. pp. 49–70.
129. Roland, A; Delpech, S; Dagan, L. A Powerful Analytical Indicator to Drive Varietal Thiols Release in Beers: The “Thiol Potency”. *BrewingSci.* 70(11/12), 170–175, 2017.
130. Lafontaine, S; Caffrey, A; Dailey, J; Varnum, S; Hale, A; Eichler, B; Dennenlöhner, J; Schubert, C; Knoke, L; Lerno, L; Rettberg, N; Heymann, H; Ebeler, S. Evaluation of Variety, Maturity, and Farm on the Concentrations of Monoterpene Diglycosides and Hop Volatile/Nonvolatile Composition in Five *Humulus lupulus* Cultivars. *J. Agric. Food Chem.* 69(15), 4356–4370, 2021.
131. Suda, T; Yasuda, Y; Imai, T; Ogawa, Y. Mechanisms for the development of Strecker aldehydes during beer aging. 31st European Brewery Convention Congress, Venice, Italy, 2007.
132. Baert, JJ; Clippeleer, J de; Jaskula-Goiris, B; Opstaele, F van; Rouck, G de; Aerts, G; Cooman, L de. Further Elucidation of Beer Flavor Instability: The Potential Role of Cysteine-Bound Aldehydes. *J. Am. Soc. Brew. Chem.* 73(3), 243–252, 2015.
133. Baert, JJ. Unravelling the Role of Free and Bound-state Aldehydes in Beer Flavour Instability. Thesis. Katholieke Universiteit Leuven, Leuven, Belgium, 2015.
134. Baert, JJ; Clippeleer, J de; Bustillo Trueba, P; Jaskula-Goiris, B; Rouck, G de; Aerts, G; Cooman, L de. Exploring Aldehyde Release in Beer by 4-Vinylpyridine and the Effect of Cysteine Addition on the Beer’s Pool of Bound Aldehydes. *J. Am. Soc. Brew. Chem.* 76(4), 257–271, 2018.

135. Bustillo Trueba, P; Clippeeler, J de; Van der Eycken, Erik; Guevara Romero, Juan Sebastian; Rouck, G de; Aerts, G; Cooman, L de. Influence of pH on the Stability of 2-Substituted 1,3-Thiazolidine-4-Carboxylic Acids in Model Solutions. *J. Am. Soc. Brew. Chem.* 76(4), 272–280, 2018.
136. Bustillo Trueba, P; Jaskula-Goiris, B; Clippeeler, J de; Goiris, K; Praet, T; Sharma, UK; Van der Eycken, Erik; Sanders, MG; Vincken, J; Brabanter, J de; Rouck, G de; Aerts, G; Cooman, L de. Validation of an ultra-high-performance liquid chromatography-mass spectrometry method for the quantification of cysteinylated aldehydes and application to malt and beer samples. *J. Chromatogr. A* 1604, 460467, 2019.
137. Bustillo Trueba, P; Jaskula-Goiris, B; Ditych, M; Filipowska, W; Brabanter, J de; Rouck, G de; Aerts, G; Cooman, L de; Clippeeler, J de. Monitoring the evolution of free and cysteinylated aldehydes from malt to fresh and forced aged beer. *Food Res. Int.* 140, 110049, 2021.
138. Mateo-Vivaracho, L; Ferreira, V; Cacho, J. Automated analysis of 2-methyl-3-furanthiol and 3-mercaptohexyl acetate at ng L<sup>-1</sup> level by headspace solid-phase microextracion with on-fibre derivatisation and gas chromatography–negative chemical ionization mass spectrometric determination. *J. Chromatogr. A* 1121(1), 1–9, 2006.
139. Ditych, M; Filipowska, W; Rouck, G de; Jaskula-Goiris, B; Aerts, G; Andersen; M. L; Cooman, L de. Investigating the evolution of free staling aldehydes throughout the wort production process. *BrewingSci.* 72(1/2), 10–17, 2019.

# Appendix

## List of Publications

\* Publications that are part of this thesis

Lafontaine, S; Caffrey, A; Dailey, J; Varnum, S; Hale, A; Eichler, B; Dennenlöhr, J; Schubert, C; Knoke, L; Lerno, L; Rettberg, N; Heymann, H; Ebeler, S. Evaluation of Variety, Maturity, and Farm on the Concentrations of Monoterpene Diglycosides and Hop Volatile/Nonvolatile Composition in Five *Humulus lupulus* Cultivars. *J. Agric. Food Chem.* 69(15), 4356–4370, 2021. DOI: 10.1021/acs.jafc.0c07146

Lafontaine, S; Senn, K; Knoke, L; Schubert, C; Dennenlöhr, J; Maxminer, J; Cantu, A; Rettberg, N; Heymann, H. Evaluating the Chemical Components and Flavor Characteristics Responsible for Triggering the Perception of “Beer Flavor” in Non-Alcoholic Beer. *Foods* 9(12), 1914, 2020. DOI: 10.3390/foods9121914

\* Dennenlöhr, J; Thörner, S; Rettberg, N. Analysis of Hop-Derived Thiols in Beer Using On-Fiber Derivatization in Combination with HS-SPME and GC-MS/MS. *J. Agric. Food Chem.* 68(50), 15036–15047, 2020. <https://doi.org/10.1021/acs.jafc.0c06305> (chapter 4, Version of Record)

Lafontaine, S; Senn, K; Dennenlöhr, J; Schubert, C; Knoke, L; Maxminer, J; Cantu, A; Rettberg, N; Heymann, H. Characterizing Volatile and Nonvolatile Factors Influencing Flavor and American Consumer Preference toward Nonalcoholic Beer. *ACS Omega* 2020. DOI: 10.1021/acsomega.0c03168

\* Dennenlöhr, J; Thörner, S; Maxminer, J; Rettberg, N. Analysis of Selected Staling Aldehydes in Wort and Beer by GC-EI-MS/MS Using HS-SPME with On-Fiber Derivatization. *J. Am. Soc. Brew. Chem.* 78(4), 284–298, 2020. <https://doi.org/10.1080/03610470.2020.1795478> (chapter 3, Accepted Manuscript)

Rettberg, N; Schubert, C; Dennenlöhr, J; Thörner, S; Knoke, L; Maxminer, J. Instability of Hop-Derived 2-Methylbutyl Isobutyrate during Aging of Commercial Pasteurized and Unpasteurized Ales. *J. Am. Soc. Brew. Chem.* 78(3), 175–184, 2020. DOI: 10.1080/03610470.2020.1738742

\* Dennenlöhr, J; Thörner, S; Manowski, A; Rettberg, N. Analysis of Selected Hop Aroma Compounds in Commercial Lager and Craft Beers Using HS-SPME-GC-MS/MS. *J. Am. Soc. Brew. Chem.* 78(1), 16–31, 2020. <https://doi.org/10.1080/03610470.2019.1668223> (chapter 2, Accepted Manuscript)

## Conference Contributions

Schubert, C; Dennenlöhr, J; Knoke, L; Thörner, S; Rettberg, N. The contribution of staling aldehydes to the flavor (in)stability of hoppy ales. ASBC Annual Meeting, New Orleans, LA, USA, 2019.

Thörner, S; Dennenlöhr, J; Rettberg, N. Critical assessment of calibration strategies for effective beer flavor analysis by solid-phase microextraction (SPME). 37th Congress of the European Brewery Convention, Antwerp, Belgium, 2019.

Schubert, C; Dennenlöhr, J; Thörner, S; Maxminer, J; Rettberg, N. The contribution of staling aldehydes to the flavor (in)stability of top fermented, hoppy ales. 37th Congress of the European Brewery Convention, Antwerp, Belgium 2019.

Dennenlöhr, J; Thörner, S; Rettberg, N. Rapid and solventless analysis of thiols in brewing samples. 6th International Young Scientists Symposium on Malting, Brewing and Distilling, Bitburg/Trier, Germany, 2018.

Rettberg, N; Koserske, J; Thörner, S. Rapid and solventless analysis of thiols in brewing samples. Brewing Summit, San Diego, CA, USA, 2018.

Thörner, S; Koserske, J; SPME Anwendungen in der Bieranalytik. 105. Brau- und maschinentechnische Arbeitstagung, Dortmund, Germany, 2018.

Koserske, J; Thörner, S; Rettberg, N. Rapid quantification of major hop aroma compounds in beer by static headspace GC-MS. ASBC Annual Meeting, Fort Myers, FL, USA, 2017.

Maxminer, J; Koserske, J; Rettberg, N; Thörner, S. Chasing staling aldehydes—A unique application of HS-SPME-GC-MS/MS in brewing. World Brewing Congress, Denver, CO, USA, 2016.

Koserske, J. Chasing volatiles - gas chromatography tandem mass spectrometry (GC-MS/MS) in beer flavor analysis. 5th International Young Scientists Symposium on Malting, Brewing and Distilling, Chico, CA, USA, 2016.